

---

# ***Degradation characterisation of various geo-chemical matrices during leaching***

*by*

***Jacoline Pienaar***

Thesis submitted in partial fulfilment of the requirements  
for the degree of

**MASTER OF SCIENCE IN ENGINEERING**

**(MINERAL PROCESSING)**

in the Department of Chemical Engineering

at the University of Stellenbosch



Supervisor: **Prof. L. Lorenzen**

*Stellenbosch, December 1999.*

---

## **Declaration**

I, the undersigned, hereby declare that the work contained in this thesis is my own work and has not been submitted previously in its entirety or part for a degree at any university.

J. Pienaar



## SUMMARY

Immobilisation is currently a well-known and cost-effective method in which solid waste can be treated to render hazardous elements less harmful to the environment, by converting the contaminants into their least soluble, mobile or toxic form. The stabilising interaction between the wastes and the solidifying reagents may be either chemical or mechanical. In the latter case, the elements are encapsulated into a monolithic solid. This would evidently require a material of high structural integrity, able to withstand long-term exposure to water infiltration in disposal sites conditions, while continuing to limit the leaching of contaminants into ground or surface waters.

Laboratory scale leaching tests are generally used for testing the stability of such materials. Characterisation of these tests is of major importance in clarifying the leaching phenomena, for valid extrapolations of leaching behaviour in a few years time (ageing). The impetus of this study was on characterising the degradation behaviour of immobilised matrices during leaching tests.

Two specific waste forms (fly ash and jarosite) were stabilised and additives were added to produce two geo-chemical matrix types: (a) a pozzolanic and (b) a geopolymeric matrix. A 5% acetic acid solution was used during batch leaching tests, where the pH was held constant throughout the tests.

Regarding crack patterns, the physical degradation appeared somewhat different for the two matrix types. Larger cracks were found in some pozzolanic samples, and the outer layers (of about 5mm) of some samples, appeared detached from the rest of the blocks after leaching. The geopolymeric matrix exhibited smaller cracks and the layers rather flaked off, compared to the larger layers that cracked off the pozzolanic samples. The main degradation mechanisms emerged to be acid attack and the alkali silica reaction for both matrices. The leaching of the main matrix elements was further considered as an indication of the degradation performance. These elements were primarily Si, Al, Fe, Na and Ca. Typically during leaching tests the behaviour is governed by an initial fast surface reaction, followed by much slower diffusion and a slow mobilising chemical reaction and/or corrosion or structural breakdown of the waste matrix. However, a substantial percentage of the elements that leached into the leaching solution were precipitated. A simple semi-empirical model, that considered the effect of degradation, was used to characterise these typical reactions that govern the leaching behaviour of each element.

In both matrix types, Ca and Na (and some of the other minor elements) showed a clear reaction front in the leaching phenomenon (difference in leaching rate from the deeper layers of the samples than from surface samples). This is contradictory to the leaching of Si, Fe, Al and Ti. The leaching behaviour of Ca, Na, Mn, Mg and P were very closely related, while in

turn, Si, Fe, Al and Ti showed similar behaviour. These similarities in performance indicate that they might be bound into the matrix structure in the same way. The percentages that were leached out after 600 hours were in the same order of magnitude for both matrices, but Si, Al, Ca, and Fe were slightly more stable in the geopolymeric matrix, while Na and Mg were more stable in the pozzolanic matrix. Overall, the geopolymeric matrix seemed to be more structurally stable at extended leaching times.

## OPSOMMING

Immobilisasie is tans 'n welbekende en ekonomies vatbare behandelingsmetode om die besoedelingspotensiaal van soliede afval te verminder. Die skadelike elemente word sodoende omgesit in hulle mees onoplosbare, stabiele en nie-toksiese vorms. Dit kan geskied deur of chemiese-, of meganiese interaksie met die matriksbestandele. In laasgenoemde geval word die toksiese elemente vasgevang in 'n monolitiese vastestof. Dit vereis 'n stewige materiaal wat selfs na langtermyn-blootstelling aan stortingsterreinkondisies, steeds voldoende stremming sal plaas op die logging van toksiese elemente na grond- en oppervlak waters.

Laboratorium-skaal toetse, bekend as loggingstoetse, word as 'n reël aangewend om die stabiliteit van hierdie geïmmobiliseerde afval te toets. Vir aanvaarbare ekstrapolasies van toetsdata, om langtermyn gedrag te voorspel, is dit dus van belang om die algemene logingsmeganismes te kan verklaar en dit noodsaak gevolglik die karakterisering van logings toetse. Hierdie studie het spesifiek gefokus op die degradasie-karakterisering van geo-chemiese matrikse gedurende logging.

Twee spesifieke afvalstowwe; jarosiet en vlieg-as, is gestabiliseer en deur die bymiddels te varieër kon verskillende geo-chemiese matrikstipes berei word. Eksperimente is gedoen op twee van hierdie matrikstipes: (a) matrikse van pozzolaniese- en (b) geopolimeriese aard.

Wanneer die aard van die kraakpatrone van die verskillende matrikse vergelyk word, vertoon die pozzolaniese matriks groter krake en die buitenste lae (van omtrent 5mm) is geneig om los te kraak van die blok gedurende die loggingstydperk. Die geopolimeer vertoon egter kleiner krakies en die oppervlak is meer geneig om af te flok as die breër (5mm) lae wat van sommige pozzolaanblokke losgekraak het.

Die hoof meganismes van degradasie is oënskynlik die suur-aanval- en alkali-silika-reaksies. As verdere degradasie-karakteriseringsmetode, is die logingsgedrag van die hoofmatrikselemente ook beskou. Hierdie elemente is, hoofsaaklik Si, Al, Fe, Na en Ca. Tydens loggingstoetse word die gedragtipes gekenmerk deur 'n vinnige oppervlakreaksie by die aanvang van logging, wat gevolg word deur 'n stadiger diffusiereaksie en dan ook derdens 'n stadige mobiliseringsreaksie of degradasie (die fisiese verweer van die matriks struktuur). Vanuit die toetse was dit duidelik dat 'n substansiële deel van die geloogde elemente nie in die oplossing teenwoordig is na logging nie, maar eerder presipiteer en uitsak na die bodem van die logingsbak. 'n Eenvoudige semi-empiriese model, is gebruik om die bydrae van elk van hierdie logingsmeganismes te beskryf vir die logging van elke element. Die effek van presipitasie op die konsentrasies van die logingsoplossing, word egter ook in ag neem.

In beide matrikstipes loog Ca en Na uit met 'n duidelike reaksiefront wat van die oppervlak na die dieper dele van die vastestof-monster beweeg, maar Si, Fe, Al and Ti vertoon nie dieselfde gedrag nie. Verder was dit duidelik dat daar 'n ooreenkoms is in die logingsgedrag van Ca, Na, Mn, Mg and P, terwyl Si, Fe, Al and Ti weer eenders uitgeloog het. Hierdie soortgelyke logingsgedrag wys op moontlike ooreenstemmende maniere van gebondenheid in die matriksstruktuur. Die persentasies wat in beide gevalle na 600 uur uitgeloog is, is in dieselfde grootte-orde vir spesifieke elemente van albei matrikstipes, maar Si, Al, Ca, and Fe het wel effens meer stabiel vertoon in die geopolimeriese matriks, terwyl Na en Mg meer stabiel in die pozzolaniese materiaal was. In geheel het die geopolymeriese matriks, tot 'n mate, 'n groter stabiliteit as die pozzolaniese matriks na langer logings tye.

# **ACKNOWLEDGEMENTS**

The work contained in this thesis was carried out in the Department of Chemical Engineering at the University of Stellenbosch between January 1998 and January 2000.

I would like to express sincere gratitude to:

- My supervisor, Prof. Leon Lorenzen for his leadership during my research work as well as his financial support throughout the project;
- The FRD for financial support;
- Mr. Freddie Greeff for his enthusiastic help during my experimental work and also the rest of the personnel of the Department of Chemical Engineering who helped me in the course of my project;
- All my friends, family and fellow students who encouraged and helped me greatly throughout my project;
- And lastly, but mostly I want to acknowledge my heavenly Father, for His continuous guidance through the last two years.

---

To my parents and grandmother.

---

# THESIS CONTENTS

	<u>PAGE</u>
<b>DECLARATION</b>	i
<b>SUMMARY</b>	ii
<b>OPSOMMING</b>	iv
<b>ACKNOWLEDGEMENTS</b>	vi
<b>LIST OF FIGURES</b>	
<b>LIST OF TABLES</b>	
<b>LIST OF ABBREVIATIONS AND SYMBOLS</b>	
<b>1. INTRODUCTION</b>	1
1.1. INTRODUCTION	1
1.2. CHEMICAL FIXATION AND STABILISATION (CFS)	2
1.3. THE STABILITY OF THE MATRIX	3
1.4. OBJECTIVES OF THIS THESIS	5
<b>2. LITERATURE SURVEY</b>	6
2.1. INTRODUCTION	6
2.2. IMMOBILISATION	8
2.2.1. Definitions	8
2.2.2. Classification	9
2.2.3. Choosing an immobilisation system	9

2.2.4. Chemistry involved	11
2.2.5. Waste materials under consideration Fly ash and Jarosite	12
2.2.5.1. <i>Jarosite</i>	12
2.2.5.2. <i>Fly ash</i>	15
2.2.6. Different geochemical matrices	17
2.2.6.1. <i>Cementitious matrix</i>	17
2.2.6.2. <i>Pozzolanic matrix</i>	18
2.2.6.3. <i>Geopolymeric matrix</i>	19
2.2.6.4. <i>Zeolites</i>	20
2.3. LEACHING	21
2.3.1. Definitions	21
2.3.2. Leaching tests	21
2.3.3. Expected leaching test results	24
2.4. DEGRADATION	25
2.4.1. Different mechanisms of concrete degradation (microscopic behaviour)	25
2.4.1.1. <i>Alkali silica reaction (ASR)</i>	26
2.4.1.2. <i>Sulphate attack</i>	27
2.4.1.3. <i>Delayed ettringite formation (DEF)</i>	28
2.4.1.4. <i>Acid attack</i>	29



2.4.2. Destruction of C-S-H	30
2.5. MODELLING	31
2.5.1. Bulk diffusion model	31
2.5.2. Leaching model based on bulk diffusion and chemical reaction	33
2.5.3. Leaching model based on interface mass resistance	35
2.5.4. Semi-empirical leaching model for the cumulative amount leached	37
2.5.5. Shrinking unreacted core model	37
2.6. CONCLUSIONS	42
3. MATERIALS AND METHOD	44
3.1. INTRODUCTION	44
3.2. SAMPLE PREPARATION	44
3.3. LEACHING TESTS	48
3.4. LEACHING TESTS	48
3.4.1. Parameters kept constant	50
3.5. SAMPLING AND ANALYSIS	52
3.5.1. Solution analysis	52
3.5.2. Solid analysis	52
3.5.3. Mass and Density determination	52
3.5.3.1. <i>Mass determination</i>	52
3.5.3.2. <i>Density determination</i>	54

3.6.	CONCLUSIONS AND RECOMMENDATIONS ON THE MATERIALS USED	54
4.	PHYSICAL AND MICROCRYSTALLINE BEHAVIOUR	56
4.1.	INTRODUCTION	56
4.2.	OBSERVATIONS DURING LEACHING TESTS	56
4.2.1.	Pozzolanic matrix	56
4.2.2.	Geopolymeric matrix	60
4.3.	MICROCRYSTALLINE BEHAVIOUR	63
4.3.2.	Alkali Silica Reaction (ASR)	63
4.3.3.	Sulphate Attack	64
4.3.4.	Delayed Ettringite Formation	64
4.3.5.	Conclusion on mechanisms of degradation	64
4.4.	MASS LOSS AND POROSITY CHANGES	70
4.4.1.	Mass loss during leaching	70
4.4.2.	Porosity changes during leaching	72
4.4.3.	Conclusions on the mass loss and porosity changes during leaching	75
4.5.	CONCLUSIONS ON THE PHYSICAL DEGRADATION OF POZZOLANIC AND GEOPOLYMERIC SAMPLES	75
4.5.1.	Observed leaching behaviour of pozzolanic and geopolymeric samples	75

### Degradation characterisation of various geo-chemical matrices during leaching.

6.2.1	Pozzolanic matrix	117
6.2.2.	Geopolymeric matrix	118
6.3.	LEACHING RESULTS	119
6.3.1	Pozzolanic matrix results	119
6.3.2	Geopolymeric matrix results	134
6.3.3.	Comparison between different elements	147
6.3.3.1.	<i>Pozzolanic matrix</i>	147
6.3.3.2.	<i>Geopolymeric matrix</i>	149
6.4.	DISCUSSION OF RESULTS (AS GIVEN IN 6.3)	150
6.4.1.	Pozzolanic matrix	150
6.4.2.	Geopolymeric matrix	159
6.4.3.	Comparison between the leaching behaviour of different elements	163
6.4.3.1.	<i>Pozzolanic matrix</i>	163
6.4.3.2.	<i>Geopolymeric matrix</i>	165
6.4.3.3.	<i>Comparison between the leaching behaviour and mechanisms of Pozzolanic and Geopolymeric matrices</i>	167
7.	CONCLUSIONS	171

<b>REFERENCES</b>	176
<b>APPENDIX A</b>	181
<b>APPENDIX B</b>	183

# LIST OF FIGURES

## CHAPTER 2

- Figure 2.1. *The compositions of most of the primary chemical binders used in inorganic S/S systems. The combinations of these five oxides express the essential composition of most S/S materials, even though the actual compounds are not all simple oxides, but are often complex silicates and aluminates (Conner, 1993).*
- Figure 2.2. *Schematic illustration of the principles of the shrinking unreacted core (SUC) model (Baker and Bishop, 1997).*

## CHAPTER 3

- Figure 3.1. *X-ray fluorescence analysis of Jarosite (major elements, expressed as oxides).*
- Figure 3.2. *X-ray fluorescence analysis of Jarosite (minor elements, in ppm).*
- Figure 3.3. *X-ray fluorescence analysis of fly ash (major elements, expressed as oxides).*
- Figure 3.4. *X-ray fluorescence analysis of fly ash (minor elements, in ppm).*
- Figure 3.5. *Leaching experiment set-up.*
- Figure 3.6. *Layers in which samples were cut for XRF analysis.*

## CHAPTER 4

- Figure 4.1. *Sample of the Pozzolan matrix before the leaching test (L#17).*
- Figure 4.2. *The pozzolan sample above after it has been subjected to a leaching test lasting 4 days (L#17).*
- Figure 4.3. *A pozzolan sample prior to leaching tests (L#18).*
- Figure 4.4. *The sample in figure 4a after a leaching time of 6 days (L#18).*
- Figure 4.5. *Pozzolan sample in the leaching vessel, after leached for 6 days (L#19).*

- Figure 4.6. Geopolymeric sample in the leaching vessel, after leached for 6 days (G7).
- Figure 4.7. The crystals found inside of a crack formed in the degraded pozzolanic matrix after a leaching test of 150 hours. The SEM showed that these crystals mostly consist of calcium, secondly some P and also some silica. Another small peak could be identified as some aluminium, but no S was found in these crystals [magnification = 2000x].
- Figure 4.8. SEM photograph of the remainder of the pozzolanic matrix after a leaching test L#18 [magnification = 1000x].
- Figure 4.9. Another part of the pozzolanic matrix after a leaching test of 144 hrs (L#18) [magnification = 1000x].
- Figure 4.10. Grooves in the side of the sample after L#18 [magnification = 100x].
- Figure 4.11. Sample of the geopolymeric matrix leached for 240 hours (G4) [magnification = 1000x].
- Figure 4.12. Sample of the second layer of the geopolymeric matrix leached for 24 hrs (G6) [magnification = 1000x].
- Figure 4.13. The same part of the geopolymeric matrix sample as in figure 4.13 above, but only magnified 250x, showing that it is in actual fact inside of a pore.
- Figure 4.14. 100x magnification of a sample from the second layer of the sample leached for 240 hrs (G4). (Note the pore of about 10  $\mu\text{m}$  on the right).
- Figure 4.15. 2000x magnification of a sample from the first layer of the sample leached for 72 hrs (G2) (The spheres seem to be mostly Al and Si. Apart from Si and Al, Fe and some P are also present in this sample, but Ca seemed to have leached out).
- Figure 4.16. 2000x magnification of a sample from the first layer of the sample leached for 144 hrs (G3).
- Figure 4.17. 100x magnification of the sample above (144 hours leach, G3).
- Figure 4.18. 1000x magnification of a piece of a geopolymeric sample, which was not subjected to a leaching test yet. (The lighter parts of the photograph are mostly silica).

- Figure 4.19. 500x magnification of the same part of a geopolymeric sample as in figure 4.18.
- Figure 4.20. 500x magnification of a pore (8-9  $\mu\text{m}$  diameter) in the first layer of a sample leached for 24 hrs (G6) – Consists mostly of Si and P, no Ca, Mg, Al or Fe were found.
- Figure 4.21. 105x magnification of a pore from the second layer of the sample of G6 (about 40  $\mu\text{m}$ ).
- Figure 4.22. 100x magnification of another piece from the second layer of the geopolymeric matrix, leached for 24 hrs (G6) (The pore on the bottom, right, is about 10  $\mu\text{m}$  wide).
- Figure 4.23. Mass loss during various acetic acid leaching tests on the pozzolanic matrix.
- Figure 4.24. Mass loss during leaching tests on the geopolymeric matrix.
- Figure 4.25. Porosities of matrices after leaching tests as calculated for the leached pozzolanic matrix.
- Figure 4.26. Porosity of matrices after leaching tests as calculated for the leached geopolymeric matrix.

## CHAPTER 5

- Figure 5.1. XRD graph of the outer layers of a pozzolanic sample leached for 7 days with 5% acetic acid.
- Figure 5.2. XRD graph of the outer layers of a pozzolanic sample leached for 32 days with 5% acetic acid.
- Figure 5.3. Different elements initially in the pozzolanic matrix.
- Figure 5.4. Silica speciation at different depths in the pozzolanic matrix-structure after exposure to acetic acid leaching solution for various times.
- Figure 5.5. Fraction of silica left in the entire pozzolanic matrix-structure after 0-32 days of intensive leaching with acetic acid.



- Figure 5.6. *The extent of decalcification speciation at different depths in the pozzolanic matrix-structure due to exposure to acetic acid leaching solution for various times.*
- Figure 5.7. *Fraction of calcium left in the entire pozzolanic matrix-structure after 0-32 days of intensive leaching with acetic acid.*
- Figure 5.8. *Aluminium left at different depths in the pozzolanic matrix-structure after exposure to acetic acid leaching solution for various times.*
- Figure 5.9. *Aluminium fraction left in the entire pozzolanic matrix-structure after 0-32 days of intensive leaching with acetic acid.*
- Figure 5.10. *Iron left at different depths in the pozzolanic matrix-structure after exposure to acetic acid leaching solution for various times.*
- Figure 5.11. *Iron fractions left in the entire pozzolanic matrix-structure after 0-32 days of intensive leaching with acetic acid.*
- Figure 5.12. *Sodium speciation at different depths in the pozzolanic matrix-structure after exposure to acetic acid leaching solution for various times.*
- Figure 5.13. *Na fractions left in the entire pozzolanic matrix-structure after 0-32 days of intensive leaching with acetic acid.*
- Figure 5.14. *Titanium left at different depths in the pozzolanic matrix-structure after exposure to acetic acid leaching solution for various times.*
- Figure 5.15. *Titanium left in the entire pozzolanic matrix-structure after 0-32 days of intensive leaching with acetic acid.*
- Figure 5.16. *Manganese left at different depths in the pozzolanic matrix-structure after exposure to acetic acid leaching solution for various times.*
- Figure 5.17. *Fraction of Manganese left in the entire pozzolanic matrix-structure after 0-32 days of intensive leaching with acetic acid.*
- Figure 5.18. *Magnesium speciation at different depths in the pozzolanic matrix-structure after exposure to acetic acid leaching solution for various times.*

- Figure 5.19. *Magnesium fraction left in the entire pozzolanic matrix-structure after 0-32 days of intensive leaching with acetic acid.*
- Figure 5.20. *Potassium left in the speciation at different depths in the pozzolanic matrix-structure after exposure to acetic acid leaching solution for various times.*
- Figure 5.21. *K fraction left in the entire pozzolanic matrix-structure after 0-32 days of intensive leaching with acetic acid.*
- Figure 5.22. *P left at different depths in the pozzolanic matrix-structure after exposure to acetic acid leaching solution for various times.*
- Figure 5.23. *P fraction left in the entire pozzolanic matrix-structure after 0-32 days of intensive leaching with acetic acid.*
- Figure 5.24. *Different elements initially in the geopolymeric matrix.*
- Figure 5.25. *Silica speciation at different depths in the matrix-structure after exposure to leaching solution for various times.*
- Figure 5.26. *Total fraction of silica left in the matrix at different times during the leaching test.*
- Figure 5.27. *The calcium left in the layers after different leaching times shows the extent of decalcification.*
- Figure 5.28. *Fraction of calcium left in the geopolymeric matrix as leaching time increases.*
- Figure 5.29. *Aluminium left in different layers after leaching tests.*
- Figure 5.30. *Aluminium fraction left in the entire sample after different leaching times.*
- Figure 5.31. *Iron left in the different layers after different leaching times.*
- Figure 5.32. *Iron fractions left in the entire sample after different leaching times.*
- Figure 5.33. *Sodium left in different layers after the leaching tests.*
- Figure 5.34. *Na fractions left in the whole sample after tests*

Figure 5.35. *Titanium left in the pozzolanic matrix after acetic acid leaching tests.*

Figure 5.36. *Fraction of Titanium left in the solid matrix after leaching tests.*

Figure 5.37. *Manganese left in the pozzolanic matrix after acetic acid leaching tests.*

Figure 5.38. *Fraction of Manganese left in the solid matrix after leaching tests.*

Figure 5.39. *Magnesium left in the pozzolanic matrix after acetic acid leaching tests.*

Figure 5.40. *Magnesium fraction left in the sample after different leaching time.*

Figure 5.41. *Potassium left in the pozzolanic matrix after acetic acid leaching tests.*

Figure 5.42. *Potassium (K) fraction left in the sample after different leaching times.*

Figure 5.43. *P left in pozzolanic matrix after acetic acid leaching tests.*

Figure 5.44. *P fraction left in the whole sample after different leaching times*

## CHAPTER 6

Figure 6.1(a). *Leaching solution data and leaching curve for silica (pozzolanic matrix)[0-700 hours].*

Figure 6.1(b). *Leaching solution data and leaching curve for silica (pozzolanic matrix)[0-150 hours].*

Figure 6.2(a). *Leaching solution data and leaching curve for aluminium (pozzolanic matrix)[0-700 hours].*

Figure 6.2(b). *Leaching solution data and leaching curve for aluminium (pozzolanic matrix)[0-150 hours].*

Figure 6.3(a). *Leaching solution data and leaching curve for calcium (pozzolanic matrix)[0-700 hours].*

Figure 6.3(b). *Leaching solution data and leaching curve for calcium (pozzolanic matrix)[0-150 hours].*

Figure 6.4(a). Leaching solution data and leaching curve for iron (pozzolanic matrix)[0-700 hours].

Figure 6.4(b). Leaching solution data and leaching curve for iron (pozzolanic matrix)[0-150 hours].

Figure 6.5(a). Leaching solution data and leaching curve for sodium (pozzolanic matrix)[0-700 hours].

Figure 6.5(b). Leaching solution data and leaching curve for sodium (pozzolanic matrix)[0-150 hours].

Figure 6.6(a). Leaching solution data and leaching curve for magnesium (pozzolanic matrix)[0-700 hours].

Figure 6.7(a). Leaching solution data and leaching curve for potassium (pozzolanic matrix)[0-700 hours].

Figure 6.7(b). Leaching solution data and leaching curve for potassium (pozzolanic matrix)[0-150 hours].

Figure 6.8. Leaching solution data and leaching curve for lead (pozzolanic matrix)[0-150 hours]- assuming no precipitation.

Figure 6.9. Leaching solution data and leaching curve for copper (pozzolanic matrix)[0-150 hours] – assuming no precipitation.

Figure 6.10. % Contributions of each mechanism for silica.

Figure 6.11. % Contributions of each mechanism for aluminium.

Figure 6.12. % Contributions of each mechanism for calcium.

Figure 6.13. % Contributions of each mechanism for iron.

Figure 6.14. % Contributions of each mechanism for sodium.

Figure 6.15. % Contributions of each mechanism for magnesium.

Figure 6.16(a) % Contributions of each mechanism for potassium (K) [0-48 hours].

*Figure 6.16(b) % Contributions of each mechanism for potassium (K) [48-600 hours].*

*Figure 6.17. % Contributions of each mechanism for lead (Pb).*

*Figure 6.18. % Contributions of each mechanism for copper (Cu).*

*Figure 6.19. Silica leaching trends [0-48 hours].*

*Figure 6.20. Aluminium leaching trends [0-48 hours].*

*Figure 6.21. Calcium leaching trends [0-600 hours].*

*Figure 6.22. Iron leaching trends [0-60 hours].*

*Figure 6.23. Sodium leaching trends [0-40 hours].*

*Figure 6.24. Magnesium leaching trends [0-60 hours].*

*Figure 6.25. K leaching trends [0-48 hours].*

*Figure 6.26. Lead leaching trends [0-48 hours].*

*Figure 6.27. Zinc leaching trends [0-48 hours].*

*Figure 6.28. % Contributions of each mechanism for silica [0-600 hours] – Geopolymeric matrix.*

*Figure 6.29. % Contributions of each mechanism for aluminium [0-600 hours] – Geopolymeric matrix.*

*Figure 6.30. % Contributions of each mechanism for calcium [0-600 hours] – Geopolymeric matrix.*

*Figure 6.31. % Contributions of each mechanism for iron (Fe) [0-600 hours] – Geopolymeric matrix.*

*Figure 6.32. % Contributions of each mechanism for sodium (Na) [0-40 hours] – Geopolymeric matrix.*

Figure 6.33. % Contributions of each mechanism for magnesium (Mg) [0-600 hours] – Geopolymeric matrix

Figure 6.34. % Contributions of each mechanism for potassium (K) [0-600 hours] – Geopolymeric matrix.

Figure 6.35. Solution concentrations for the different elements in solution (pozzolanic matrix).

Figure 6.36. Concentrations of the different elements that leached from the (pozzolanic) solids.

Figure 6.37. Solution concentrations for the different elements (geopolymeric matrix).

Figure 6.38. Percentages that leached from the (geopolymeric) solids for different elements.

#### **BYLAE A**

Figure A1. Correction factors for the concentrations of the leaching solutions (L#17 and L#18 of the pozzolanic matrix).

Figure A2. Correction factors for the concentrations of the leaching solutions G1 to G6 (Geopolymeric matrix).

#### **BYLAE B**

Figure B1. Trends followed by silica when leached from the solid as well as leaching trends of solution (pozzolanic matrix).

Figure B2. Trends followed by aluminium when leached from the solid as well as leaching trends of solution (pozzolanic matrix).

Figure B3. Trends followed by calcium when leached from the solid as well as leaching trends of solution (pozzolanic matrix).

Figure B4. Trends followed by Fe when leached from the solid as well as leaching trends of solution (pozzolanic matrix).

Figure B5. Trends followed by Na when leached from the solid as well as leaching trends of solution (pozzolanic matrix).

- Figure B6. Trends followed by Mg when leached from the solid as well as leaching trends of solution (pozzolanic matrix).
- Figure B7. Trends followed by K when leached from the solid as well as leaching trends of solution (pozzolanic matrix).
- Figure B8. Trends of leaching from the solid for silica [0-600 hours] – Geopolymeric matrix.
- Figure B9. Trends of leaching from the solid for aluminium [0-600 hours] – Geopolymeric matrix
- Figure B10. Trends of leaching from the solid for calcium [0-600 hours] – Geopolymeric matrix.
- Figure B11. Trends of leaching from the solid for iron [0-600 hours] – Geopolymeric matrix.
- Figure B12. Trends of leaching from the solid for sodium (Na) [0-600 hours] – Geopolymeric matrix.
- Figure B13. Trends of leaching from the solid for magnesium [0-600 hours] – Geopolymeric matrix.
- Figure B14. Trends of leaching from the solid for potassium (K) [0-600 hours] – Geopolymeric matrix.

# LIST OF TABLES

## CHAPTER 2

*Table 2.1. Basic hydration reactions of Portland cement (Conner, 1993).*

## CHAPTER 3

*Table 3.1. Ingredients of the pozzolanic matrix.*

*Table 3.2. Ingredients of the geopolymeric matrix.*

## CHAPTER 4

*Table 4.1. Physical observations during leaching tests on the pozzolanic material.*

*Table 4.2. Physical observations during leaching tests on the geopolymeric material.*

## CHAPTER 5

*Table 5.1. Summary of the leaching behaviour of different elements of the pozzolanic and geopolymeric matrix (leaching times > 600 hours).*

## CHAPTER 6

*Table 6.1. Leaching tests done and used in analysis for to evaluate the leaching of a pozzolanic as well as a geopolymeric matrix.*

*Table 6.2. Table with the mean square differences between the fitted semi-empirical model (equations 6.2 or 6.3) and the data of L#18, for the different elements.*

*Table 6.3. Values of constants ( $K_1$  to  $K_6$ ) after regression analysis of either equation 6.2 or 6.3, depending on formation of precipitate with time.*

*Table 6.4. Table with the mean square differences between the fitted semi-empirical model (equations 6.2 or 6.3) and the data of G5, for the different elements.*



*Table 6.5. Values of constants ( $K_1$  to  $K_6$ ) for the leaching test run G5 (on the geopolymeric matrix) after regression analysis of either equation 6.2 or 6.3, depending on formation of precipitate with time.*

# ***LIST OF ABBREVIATIONS AND SYMBOLS***

## **ABBREVIATIONS:**

ANC	Acid neutralisation capacity of the solid.
ANS/ANSI 16.1	American Nuclear Society test procedure.
ANSR	American National Standard Tests.
APD	Acid penetration depth (APD) of the leached shell.
ASR	Alkali silica reaction
C <sub>3</sub> A	Tricalcium aluminates
C <sub>3</sub> S <sub>2</sub> H <sub>3</sub>	Tobermorite
CAL	Cumulative Amount Leached of a contaminant in a stabilising matrix (eq. 2.32)
CERCLA	Comprehensive Environmental Response, and the Compensation and Liability Act
CFS	Chemical Fixation and Stabilisation
CH	Calcium oxide and water compound
C-S-H	Calcium silicate hydrate
DEF	Delayed Ettringite Formation
DWAF	Department of Water Affairs and Forestry
EDS	Energy Dispersive Spectrometer
EPA	Environmental Protection Agency

EPT	Extraction Procedure Toxicity (EPT) test
Ettringite	$3\text{CaO} \cdot \text{Al}_2\text{O}_3 \cdot 3\text{CaSO}_4 \cdot 32\text{H}_2\text{O}$
Gypsum	$(\text{CaSO}_4 \cdot 2\text{H}_2\text{O})$
ICP	Inductively Coupled Plasma Spectroscopy
LX	Leachability index
OPC	Ordinary Portland Cement
PC	Portland cement
PRF	The potential release factor
RCA	Resource Conservation and Recovery Act
Rsquare*	Mean square statistical comparison of predicted values with actual values
S/S	Chemical stabilisation/solidification
SEM	Scanning electron microscopy
SQI	Analogous to the leachability index (LX) values obtained in the ANS 16.1 test procedure ( $= -\log(\text{PFR})$ (eq. 2.40))
SUC	Shrinking unreacted core model
TCLP	Toxicity Characteristic Leaching Procedure
WILT	Waste Interface Leaching Tests
XRD and XRF	X-ray diffraction and X-ray fluorescence

---


$$* R^2 = 1 - \frac{\sum (\hat{y} - \bar{y})^2}{\sum (y - \bar{y})^2}$$

**SYMBOLS:**

- $\beta_c$  Acid neutralisation capacity [ $\text{kmol eq. m}^{-3}$ ] or quantitative capacity of cement to react with a strong acid (eq.2.34)
- $\overline{c_T}$  Average acid concentration (eq. 2.33)
- $\zeta$  Conversion (amount of leached shell to the original amount of material)
- $A$  Geometrical surface area of the waste specimen (eq. 2.12)
- $a_{\text{Fe}^{3+}}$  Activity term for the iron ions (eq. 2.2).
- $a_{\text{H}^+}$  Activity term for the hydrogen ions (eq. 2.2).
- $C$  concentration of the contaminant ( $\text{g.cm}^{-3}$ ) (eq 2.10)
- $C^{(w)}(t)$  the concentration of the species in the aqueous solution
- $c(x,t)$  concentration profiles (eq.2.14)
- $c_0$  Initial contaminant concentration in the solid (eq.2.14)
- $C_e$  the equilibrium concentration (eq. 2.19)
- $c_{\text{H},c}$  Hydrogen ion concentration at the core boundary [ $\text{kmol m}^{-3}$ ]
- $C_{\text{H},i}$  Hydrogen ion concentration at the liquid interface [ $\text{kmol m}^{-3}$ ]
- $C_{\text{im}}$  Species present in immobile form in a state of chemical equilibrium (eq. 2.15)
- $C_m$  Solid contaminant concentration [ $\text{mol cm}^{-3}$ ] (eq. 2.37)
- $C_{\text{mo}}$  Initial concentration in the matrix (eq. 2.11)
- $C_{\text{mo}}$  species present in mobile forms in a state of chemical equilibrium (eq. 2.15)
- $C_{\text{sat}}^{(w)}$  Saturation concentration
- $C_T$  the total initial concentration in the matrix (eq. 2.11)

- $D_e$  Effective diffusion coefficient, corrected for porosity and tortuosity ( $\text{cm}^2\text{s}^{-1}$ ) (eq 2.10)
- $D_{e,s}$  Effective diffusion coefficient (for acid species) [ $\text{cm}^2 \text{s}^{-1}$ ] (eq. 2.34)
- $D_e'$  Effective diffusion coefficient =  $\frac{D_e}{(1-k_d)}$  in (eq. 2.18)
- $D_e''$  Effective diffusion coefficient =  $\frac{D_e}{\Phi^2}$  (eq. 2.21)
- $(E_h)$  Redox-potential
- erf Standard error function (eq.2.14)
- $F(t)$  Cumulative fraction leached
- $f_{mo}$  Dimensionless leachable fraction (eq. 2.37)
- $I(t)$  Acid exposure (eq. 2.35) or acid exposure integral (eq. 2.33) or acid equivalents x time/volume [ $\text{mol min l}^{-1}$ ]
- $K$  Leaching constant (eq. 2.35)
- $K$  Overall mass-transfer coefficient (eq. 2.26)
- $K'$  Conditional stability constant (eq.2.2) for jarosite formation
- $K_1, K_2, K_3, K_4, K_5$  and  $K_6$  Constants for the cumulative amount leached according to equations 6.2 and 6.3
- $K_1, K_2, K_3, K_4$  Constants for (eq. 2.32)
- $K_d$  Linear adsorption isotherm constant ( eq. 2.15)
- $k_1, k_d$  Phenomenological rate constant coefficients describing the kinetics of all elementary processes involved in releasing or attaching species “j” from or to the surface
- $L$  Leaching function (eq. 2.35)
- $L(t)$  Leaching rate:

$L_0$	Leach rate maximum value (eq. 2.27)
$L_2$	Leaching function for leached shell diffusion limitation (eq. 2.36)
$l_s$	Thickness of the leached shell [cm] (eq. 2.37)
$M^p(t)$	Contaminant release per unit surface area [ $\text{mol cm}^{-2}$ ] (eq. 2.37)
$M_{mo}$	Initial amount of the mobile species in the specimen (eq. 2.12)
$t$	Leaching time (eq 2.14)
$t$	Time (s) (eq. 2.10)
$u(t)$	Network dissolution velocity (eq. 2.29)
$V$	Volume of the waste specimen (eq. 2.13)
$x$	Distance (cm) into the solid (eq.2.10) and (eq.2.14)
$y$	Actual value in Rsquare
$\bar{y}$	Average of actual values Rsquare
$\hat{y}$	Predicted value Rsquare

# CHAPTER 1

## INTRODUCTION

*This chapter discusses industrial waste disposal problems and stabilisation as a possible treatment for wastes, prior to landfilling, to immobilise hazardous components and thereby prevent potentially harmful interaction with the biosphere. The effects of long-term leaching on such deposits are considered, and form the basis of the work presented in this thesis.*

---

### 1.1. INTRODUCTION

Waste disposal is an icon of the latter half of the 20th century, as it has left no inhabitant of the planet unaffected. The escalating requirement for consumables is an obvious indicator of a widespread problem affecting residential, commercial and industrial sectors, of which the latter is under continual scrutiny regarding waste disposal practices. Historically, the easiest means of waste disposal has been dumping either into a river or onto land. Although the easiest and least expensive, it is not necessarily the most desirable option, because this can lead to undesirable changes, directly or indirectly, to the existing environmental system.

Reducing, reusing and recycling is now firmly implanted in our conventional wisdom. However, industrial waste minimisation practise is limited by economical constraints and consequently, disposal methods such as landfilling and incineration becomes the only viable options. Landfills unfortunately have the disadvantage of being infiltrated by rainfall and surface water. This water, coupled with biochemical and physical breakdown of wastes, produces a leachate liquor, high in suspended solids with a high organic and inorganic content. Inevitably, the leachate enters into surface or groundwater before sufficient attenuation has occurred, and results in a pollution problem.

To reduce the contaminant concentration in the leachate, and thus the potential hazard, a stabilisation process can be employed. This involves additives being mixed with wastes prior to landfilling, resulting in a product where the hazardous elements/compounds are trapped inside a stable matrix. This entrapment reduces the rate of contaminant migration, but long-term weathering and random wetting patterns due to intermittent rainfall on a landfill, will inevitably cause degradation of these stable matrices, resulting in the release of potentially harmful elements.

Fly ash and jarosite are examples of two industrial waste forms that are considered to be hazardous to humans and other forms of life. Fly ash is a by-product of the combustion of coal at high temperatures and jarosite is formed during the recovery of zinc. The two waste forms, which are produced in large quantities, are considered to be hazardous due to traces of heavy metal ions that can be found in both substances. By applying stabilisation processes the metal ions can be immobilised and rendered less available for release into the environment, and can subsequently be used in landfills. Despite the success of stabilisation in the short term (Van Zyl, 1997), little research has been done on the effects of long-term leaching on such deposits.

The focus of this thesis will be to investigate the degradation of immobilised matrices (consisting of fly ash and jarosite) and characterise the modified leaching behaviour of contaminants from stabilised waste. By identification and modelling of leaching mechanisms, this study may contribute to a better understanding of the very complex, but unknown, physico-chemical phenomena involved in pollutant release.

## **1.2. CHEMICAL FIXATION AND STABILISATION (CFS)**

Stabilisation is a process where additives are mixed with wastes to minimise the rate of contaminant migration from the waste and to reduce toxicity. This may also reduce inherent reactivity, incompatibility with other wastes or handling difficulties, due to, for example, a too high liquid content. Stabilisation can be used to prevent hazardous contaminants from interacting with the biosphere for an indefinite time (Jansen van Rensburg, 1997). This involves the physical entrapment and/or chemical binding of the toxic elements or compounds in a stable matrix, thereby converting the contaminants into their least soluble, mobile, or toxic form. The exposed surface of the waste and the leachability of toxic elements into the groundwater and surface waters are therefore reduced, and the immobilised material can be used for landfilling.

Solidification processes are particularly suited to the treatment of inorganic wastes and may be the preferred route when significant quantities of toxic metals such as mercury, cadmium, arsenic, lead and antimony are present in the waste, as can be found in the two waste forms under consideration (jarosite and fly ash). According to previous work done by Van Zyl (1997), contaminants in jarosite and fly ash can be adequately stabilised by preparing matrices containing these two ingredients. A review of technologies by Rosato and Agnew (1993) identified chemical fixation and stabilisation with Portland cement, a process known as Jarofix, as the only practical option to dispose of zinc plant iron residues (i.e. jarosite) based on a list of four criteria, including (i) environmental acceptance, (ii) extent of development of the technology, (iii) impact of integration into the plant and (iv) economic viability. (This criteria were subsequently accepted in 1993 by the Quebec Ministry of the Environment.) In the work of Van Zyl (1997), fly ash was used instead of Portland cement. Apart from possessing excellent pozzolanic qualities that can result in the formation of pozzolanic concrete, fly ash, being a waste product, has the advantage of being available in vast quantities at minimal costs.



characterise most leaching processes. Smaller particle sizes will render more surface area available for the surface reaction, which explains the expected higher leaching rates during the initial stage (Jansen van Rensburg, 1997).

As of yet, the long-term leaching behaviour has not been successfully quantified mainly due to the very complex nature of the mechanisms. Degradation occurring in a landfill and the resulting effects on leaching from solidified waste are still to be studied extensively for the development of a model, representing stability predictions.

#### **1.4. OBJECTIVES OF THIS THESIS**

The objectives of this thesis are to study and characterise matrix degradation during leaching tests. Samples containing fly ash, jarosite and other additives in different proportions will be prepared in order to represent possible matrices of the solidified and stabilised waste material, as it would be prepared prior to landfilling. It is already known through previous work (Van Zyl, 1997) that the solidification/stabilisation of jarosite and fly ash produced matrices that proved adequate in both structural strength and immobilisation characteristics. By investigating and characterising this degradation phenomenon the aim is to understand and to possibly model the leaching behaviour, which includes:

1. the kinetics of the exchanges of species between the surface of the waste and the aqueous solution,
2. the transport of the species by diffusion, as well as
3. the leaching due to the slow mobilising chemical reaction and/or to corrosion or structural breakdown of the waste matrix.

## CHAPTER 2

# LITERATURE SURVEY

*In this chapter a review of available literature on some issues, involving the history and development of the immobilisation technology, will be presented. Furthermore different immobilised matrices and their expected leaching and degradation behaviour, during leaching tests, will also be discussed.*

---

### 2.1. INTRODUCTION

As the awareness of the vulnerability of our environment increases, the search for better waste disposal methods are under continuous consideration and is expected to still increase in the near future. Reducing, reusing, and recycling of the unwanted residues are generally applied by most industries as far as economic circumstances permit, still leaving them with material to dispose of. Many of these are often classified as hazardous and pose a serious threat to the environment, should it be deposited into water or onto land. Today, immobilisation (or stabilisation) of toxic or hazardous components of a waste, as a treatment prior to general disposal methods, is a widely acceptable technology and a solution to many waste disposal problems. However, this was not the case a few years ago, when this technology experienced serious growing pains.

With a few exceptions, the history of the development of stabilisation systems for general use on waste residues, dates only from about 1970, but the roots of most present-day commercial stabilisation systems go back to four primary areas of technology that were practised long before 1970. These are:

- ☐ radioactive waste solidification and disposal,
- ☐ mine backfilling,
- ☐ soil stabilisation and grouting, and
- ☐ production of stabilised base courses for road construction.

Of these, only radioactive waste treatment is an immobilisation process in the present sense. The other three applications had other utilitarian purposes, although waste, such as fly ash,

was frequently used in the processes. Portland cement, fly ash, or both were used in mine backfilling. Sodium silicate plus setting agents, cement and organic polymerising systems were used for grouting and soil stabilisation, while lime and fly ash were mostly used for road-base construction. There are many isolated instances where waste residue generators, especially waste disposal site operators, used cement, fly-ash, lime, soil and various combinations of these materials to solidify liquids for disposal in landfills where some stability was required in the fill material. Nearly all of this early work involved a need for solidification only, and rarely, if ever, were leaching or other performance tests, as an indication of the stability, conducted or required.

Other than internal studies at various nuclear installations and government nuclear regulatory agencies, where radioactive wastes were considered, there was no published work done on leachability, environmental degradation, or any other performance characteristics of solidified waste until the early 1970's. At this time, a few organisations began applying scientific principles to solidification of various waste materials, using among others lime/fly-ash processes and soluble silicates and silicate setting agents (usually sodium silicate solution and Portland cement). From a business point of view, this was not the most propitious period for anyone to enter the waste residual field. Few laws and regulations concerning the disposal of waste residues, existed and cheaper methods of waste disposal were obviously preferred (sea dumping or inland landfilling), leaving no market for the chemical fixation and stabilisation (CFS) technology. Therefore, it might come as no surprise that the hazardous waste treatment industry was, until the passage of the Resource Conservation and Recovery Act (RCA), characterised by undercapitalisation, overcapacity, and financial losses.

Only in about 1975 did industries begin to take interest in this field in anticipation of the coming of the RCA. With the increase in environmental awareness and regulations, solid waste disposal companies increasingly took interest in the hazardous waste treatment technology and a number of vendors started to offer processes, chemicals, and services. Vendors, especially those who started prior to the coming of the RCA have done considerable technical development. However, little detail has been published and most of this is only found in patent literature and vendors are now reluctant to share their knowledge in this field, especially to those who previously paid no attention to the CFS technology.

Today, regulations define the technology. Apart from the already mentioned RCA and the subsequent 1984 Hazardous and Solid Waste Amendments, the Comprehensive Environmental Response, and the Compensation and Liability Act (CERCLA), as well as its 1986 amendments, also provided some impetus (Conner, 1990). South Africa is undergoing the same war-on-waste tendency. At present the Department of Water Affairs and Forestry (DWAF) is entrusted to ensure that waste disposal is carried out in a responsible manner. Ignoring of legislation regarding this issue, can lead to severe penalties, and industries are more and more forced to invest in better disposal methods.

Protection Agency (EPA), stabilisation and solidification can be defined as follows:

- **Stabilisation** reduces the hazard potential of a waste by converting the contaminants into their least soluble, mobile or toxic form. The physical nature and handling characteristics of the waste are not necessarily changed.
- **Solidification** encapsulates the waste in a monolithic solid of high structural integrity. The encapsulation may be of fine particles (micro encapsulation) or of a large block container (macro encapsulation). It does not necessarily involve a chemical interaction between the wastes and the solidifying reagents but may mechanically bind the waste into the monolith. Contaminant migration is restricted by vastly decreasing the surface area exposed to leaching or by isolating the wastes within an impervious capsule.

The technology is also known as CFS, i.e. chemical fixation and stabilisation (Conner, 1990), which is the same as what the EPA generally calls stabilisation.

### 2.2.2. Classification

CFS systems are often categorised according to the nature of the solidification chemicals in two main groups; organic systems and inorganic systems. The first is processes primarily used for radioactive material and involves thermoplastic and polymerisation techniques. The systems to be studied in this thesis will be inorganic processes, which can be further classified according to whether or not bulking agents were added. In the work that follows fly ash as a bulking agent, will be used in immobilised systems developed by Van Zyl (1997) to stabilise a hazardous waste, jarosite, which is a waste product from a zinc recovery process.

### 2.2.3. Choosing an immobilisation system

According to a detailed discussion by Conner (1990), the most popular binder systems are Portland cement, Portland cement-fly ash, Portland cement- soluble silicate, lime-fly ash, and cement or lime kiln dust. Many other combinations as well as different additives have been used of which many have been patented. When considering the quantity of waste treated, the lime-fly-ash processes can be considered as the mostly used systems, primarily on flue gas desulphurisation sludge. Whereas kiln dust and Portland cement-based processes as well as cement-soluble silicate and cement-fly ash processes are more widely used on other kinds of waste.

Choosing a S/S system does not merely involve picking one of the most popular systems and treating the waste in such a manner. The problem are somewhat complicated by the fact that no two waste/regulatory/disposal scenarios are ever exactly the same. Even the testing methods might change for different cases, causing standards to rapidly change from one place



$\text{SiO}_2$ ,  $\text{CaO} + \text{MgO}$ , and  $\text{Al}_2\text{O}_3 + \text{Fe}_2\text{O}_3$

The actual components will not consist of only these simple oxides, but more often of complex silicates and aluminates. Different combinations of these five oxides can express the essential compositions of different binder systems. These combinations can be visualised on a ternary diagram as in figure 2.1.

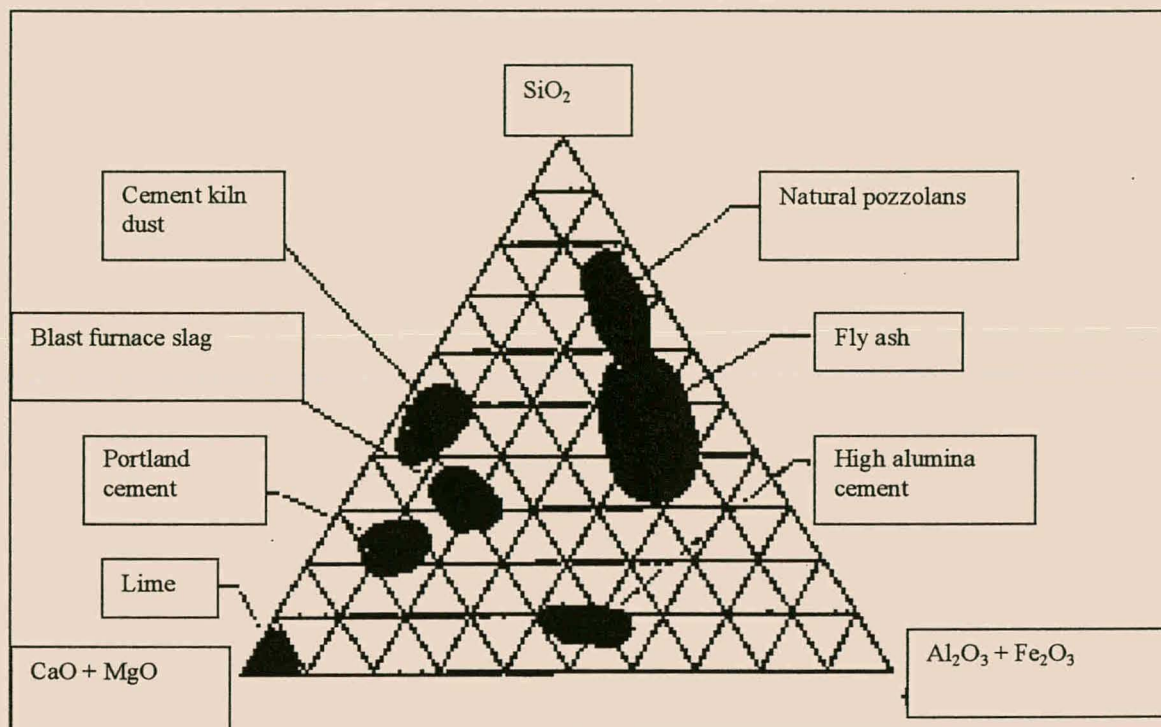


Figure 2.1: The compositions of most of the primary chemical binders used in inorganic S/S systems. The combinations of these five oxides express the essential composition of most S/S materials, even though the actual compounds are not all simple oxides, but are often complex silicates and aluminates (Conner, 1993).

## 2.2.5. Waste materials under consideration: Jarosite and Fly ash

### 2.2.5.1. Jarosite

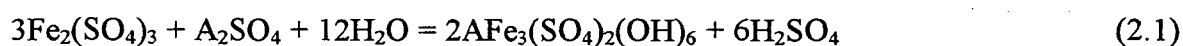
According to a review of jarosites by Das et.al. (1996), the Jarosite Process was developed as an important solution purification technique for the removal of iron at 90-100°C in the zinc industries during the mid-sixties. Due to good solid characteristics, the process was widely accepted for commercial application. Other processes, such as Goethite- and Hematite-formation, were also developed, but more than 60% of the zinc plants operate on the Jarosite Process. Despite a considerable amount of efforts to understand jarosites, not much information is available, particularly information related to processes being developed at elevated temperatures.

Jarosites are known to be potential compounds for the Fe(III),  $\text{SO}_4^{2-}$  and impurities control, in hydrometallurgical processes. Due to inherent association of Na, K, Fe and Al with the oxidic and sulphidic ores, these metal ions dissolve during sulphuric acid leaching and subsequently reprecipitate as varieties of ferric hydroxysulphates. The presence of mono- and tri-valent cations and suitable counter anions such as sulphate, arsenate, phosphate, silicates, etc. stabilise these compounds even at very high acid concentrations, and temperatures  $> 200^\circ\text{C}$ .

Mineralogically, jarosites belong to a broad mineral family of general formula  $\text{AB}_3(\text{XO}_4)_2(\text{OH})_n \cdot m\text{H}_2\text{O}$ , with various substitutions for A, B and X and corresponding mineral families. When half of the X is substituted by sulphur, the mineral groups are known as beudantites and crandallites with general formula  $\text{AB}_3(\text{XO}_4)(\text{SO}_4)(\text{OH})_5 \cdot \text{H}_2\text{O}$ , where A and B are the bivalent and trivalent cations respectively, and X is a non-metal such as As, P or Si. Alunites and jarosites are obtained by substituting both the X by sulphur and B by  $\text{Al}^{3+}$  for alunites and  $\text{Fe}^{3+}$  for jarosites. Other metal ions such as  $\text{Cu}^{2+}$ ,  $\text{Sn}^{2+}$ ,  $\text{Cr}^{3+}$ , etc., are also known to substitute B in alunites. When A, B, X, n and m are defined, typical compounds with exact chemical formulae are obtained and characteristic names are assigned to such compounds, e.g., beudantite,  $\text{PbFe}_3(\text{AsO}_4)(\text{SO}_4)(\text{OH})_6$ , natrojarosite  $\text{NaFe}_3(\text{SO}_4)_2(\text{OH})_6$ , beaverite,  $\text{Pb}(\text{Cu, Fe, Al})(\text{SO}_4)_2(\text{OH})_6$ , etc. More than one hundred and fifty of such compounds are known to exist. The jarosites,  $\text{AFe}_3(\text{SO}_4)_2(\text{OH})_6$  have six naturally occurring minerals. These are carphosiderite or hydronium jarosite, jarosite, natrojarosite, ammoniojarosite, argentojarosite and plumbojarosite where  $\text{H}_3\text{O}^+$ ,  $\text{K}^+$ ,  $\text{Na}^+$ ,  $\text{NH}_4^+$ ,  $\text{Ag}^+$  and  $0.5\text{Pb}^{2+}$  are respectively, substituted for  $\text{A}^+$  in the formula. The very narrow range of characteristic peaks for various jarosites, complicates the identification of a mixture of jarosites through XRD-analysis.

Jarosite possesses the R3M structure and consist of sheets of hydroxyl- and sulphate bridged  $\text{Fe}^{3+}$  distorted octahedra.  $\text{Fe}^{3+}$  is co-ordinated by four OH<sup>-</sup> groups and two oxygen atoms from two separate  $\text{SO}_4^{2-}$  groups. Each distorted octahedra is linked to its neighbours by four OH<sup>-</sup> groups and three oxygen ions of each  $\text{SO}_4^{2-}$  group that are bound with three  $\text{Fe}(\text{OH})_4^-$  units. One oxygen in the  $\text{SO}_4^{2-}$  is free and is doubly bonded to sulphur. This accounts basically to a structure, made up of layers of tilted  $\text{Fe}(\text{OH})_4\text{O}_2$  octahedra, joining layers of combined sulphate tetrahedra and alkali co-ordination icosahedra.

The formation of jarosite takes place in sulphate solution in the presence of an appropriate salt and low pH as:



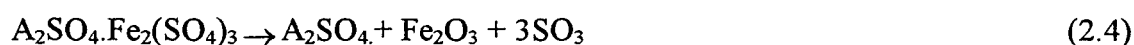
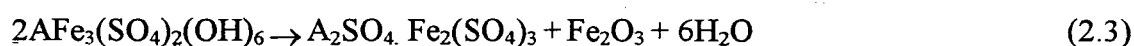
The equilibrium constant indicates that low acid, high  $\text{Fe}^{3+}$ ,  $\text{SO}_4^{2-}$  and  $\text{A}^+$  concentration favour jarosite formation. At high  $\text{SO}_4^{2-}$  and  $\text{A}^+$  concentrations, the conditional stability constant,  $K'$  can be given as:

$$K' = (a_{H^+})^2 / a_{Fe^{3+}} \quad (2.2)$$

Where  $a$  is the activity term for the hydrogen and iron ions, respectively in equation 2.2. Increase in temperature narrows down the stability domain and causes a shift towards the more acidic region. At lower temperatures the kinetics of the precipitation process is very slow, whereas the process can become rather rapid above 80°C.

Decomposition of jarosites has been reported to be carried out by two different methods, (1) thermal decomposition, and (2) hydrothermal decomposition. In both, jarosite decomposes to the most stable phase of iron, i.e. hematite.

□ Thermal decomposition of jarosite would take place as:



And the total decomposition reaction as suggested by XRD analysis of the product is given by:



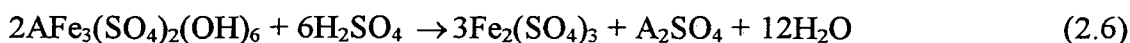
□ Hydrothermal decomposition can be carried out in two different ways: (a) alkali decomposition, and (b) acid decomposition.

➤ Alkali decomposition:

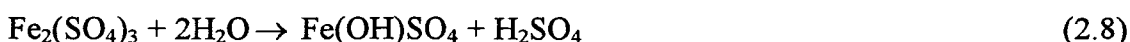
In the presence of ammonia the aqueous decomposition of ammoniojarosite was found to produce hematite or magnetite and ammonium sulphate. A temperature between 50 –100 °C is sufficient for the conversion of jarosite to hematite, but it has also been reported that decomposition starts as low as 25 °C, where after one hour approximately 88% of the decomposition were completed. In the presence of  $Fe^{2+}$  in ammoniacal media, jarosite can also be converted to magnetite. The alkaline decomposition process is characterised by the liberation of sulphate ions from the lattice and their rapid diffusion through the bulk solution. This decomposition occurs with an induction period and the end of the period is identified by a change in the surface colour of the solid. The lime treatment of jarosite produces the corresponding metal hydroxides. Silver hydroxides, formed during the decomposition of argentojarosite, will undergo the formation of crystalline silver ferrite with longer residence time.

➤ Acid decomposition:

Pure solutions of ferric sulphate in sulphuric acid at 200 °C give a hematite precipitate at low acidity and ferric-hydroxy sulphate at higher acidity. The conversion of hydronium-, sodium- and potassium jarosite to hematite at elevated temperatures (>200 °C), in weakly acidic media, takes place through dissolution and reprecipitation reactions, i.e.;



At higher initial acid concentration (> 0.5 M  $\text{H}_2\text{SO}_4$ ), hematite formation is suppressed and the precipitation of  $\text{Fe}(\text{OH})\text{SO}_4$  is favoured.



In recent studies on the hydrothermal decomposition of ammoniojarosite at elevated temperatures and in the presence of ammonium sulphate the main parameters have been found to be temperature, acid and ammonium sulphate concentrations.

The jarosites can become a potential leaching reagent and solutions to the environmental problems arising due to piling of large amounts of jarosite need to be established. This calls for treatment and alternate uses of jarosite containing residues. Though some research is done in this direction, a suitable techno-economic evaluation would be required. Many alternate applications of jarosites such as filling materials, iron-sul and pigment, etc. have been suggested. In the use as a filling material neutralising and solidifying with 20% excess CaO did the conversion of the sulphate in the jarosite to gypsum. The process is known as the 'Jarochaux Process'. Van Zyl (1997) used a similar process and tested various combinations of jarosite, fly ash and additives to produce matrices in which the hazardous components were stabilised.

#### 2.2.5.2. *Fly ash*

At present an enormous amount of fly ash is being produced by thermal power plants throughout the world and the problem of accumulation of unmanageable quantities of fly ash is reaching serious proportions in some parts. Fly ash requires a huge disposal area and is commonly used as a landfill in many parts of the world (Subbarao and Ghosh, 1997). However, depending on the sources of coal, uncontrolled disposal of fly ash may pose a significant risk to the environment due to possible leaching of toxic substances, such as heavy metals and polynuclear aromatic hydrocarbons. In dry state, fly ash also creates a dusting problem. Typical CFA consists of oxides of silicon, aluminium, iron, calcium and magnesium, and it usually contains trace elements such as (Co, Cr, V, Cu, Pb, Cd, Ni, Mo and Zn). The potential leaching of the major elements from CFA, under different conditions and ambient



conditions in particular, was investigated extensively in the last two decades (Seidell et. al., 1998). Stabilisation of the fly ash is one of the promising methods to manage environmental problems of fly ash disposal. When the ash contains lime it is known to have self-hardening properties and gains strength with time. But low lime fly ash needs special attention for its applications and management. Apart from presenting a solution to environmental problems by preventing leaching of hazardous elements from the landfill into the environment, stabilised fly ash achieved higher strengths and can be used as construction materials (Drakonaki, et. al., 1998).

The self-hardening properties depend on the availability of free lime. There are fly ashes available throughout the world called 'low lime fly ashes' which contain very little lime. Low lime fly ash cannot give much strength, rather in the dry state it creates dusting problems that may increase the concentration of solid suspended particulate material in air. This presents an important problem in solid waste management, but solidification or stabilisation with lime might present a solution to this problem.

Assessment of environmental risk due to fly ash is usually performed by means of standard leaching tests. These tests are either batch or column lab-scale studies or field lysimeter studies. The liquid-to-solid ratio is a significant operating variable, since it relates to the time scale of the leaching process. Based on this approach various scenarios for long-term environmental assessment can be devised considering diffusion effects and hydrogeochemical conditions.

In studies of Al-Amoudi, et. al. (1996), on the performance of fly ash cement concrete specimens, with various replacement levels (parameters such as the compressive strength, pulse velocity, porosity, and water permeability) indicated a better performance by 20% fly ash cement concrete than by plain cement concrete and those made with other cement replacement levels. The reason could be attributed to the test techniques used or the marginal improvement in the properties of fly ash cement concrete may be related to their mineralogical and physical properties. These properties, which invariably result from the industrial processes related to their production and the properties of the raw materials, significantly influence the final properties of pozzolanic concrete.

Al -Amoudi et.al. (1996) concluded that the marginal improvement in the pulse velocity and compressive strength, due to 20% replacement of cement with fly ash, compared to a significant reduction in the porosity and permeability, can be attributed to the pozzolanic reaction. The reaction between the pozzolanic silica and calcium hydroxide results in the formation of secondary calcium silicate hydrate (C-S-H). This leads to the transformation of large pores into small pores that significantly contribute to a reduction in the permeability and porosity.

On the other hand, the secondary C-S-H, although being capable of blocking and segmenting

the large pores and thereby lowering the permeability and porosity, is weaker than the primary C-S-H and does not significantly contribute to the improvement in the strength and pulse velocity. The increased permeability and porosity, and decreased compressive strength and pulse velocity in the 30 and 40 % fly ash cement concrete, compared to the 20% fly ash cement concrete, may be related to a reduction in the cement content which leads to a decrease in both the primary and secondary C-S-H. Recent studies also showed that the CFA could be used as a primary component in solidified mixtures containing cement and fixed heavy metals.

## 2.2.6. Different geo-chemical matrices

A porous matrix is usually obtained as the immobilised product. Depending on the materials and additives, different reactions occur and result in matrices with different geo-chemical consistencies.

### 2.2.6.1. *Cementitious matrix*

Conner (1990) described how ordinary Portland Cement (OPC) reacts with water, sets, and produces a rigid structure, which can be used in various applications. The reactions start when the cement powder and water are mixed together. Despite the rather simple composition (limestone and clay) and long history of use, scientists still do not agree upon this reaction mechanism. Basically, each of the major crystalline compounds hydrates, but the products, and their contributions to the final waste form, are different:

OPC(lime stone and clay) + water  $\rightarrow$  C<sub>3</sub>A hydrates  $\rightarrow$  rapid setting  $\rightarrow$  rigid structure

Tricalcium aluminates and sulphates react almost immediately to form hydrates. If sufficient sulphate is present, the reaction product is hydrated calcium aluminate-sulphate, which coats the surfaces of the particles, preventing rapid further hydration. This is why gypsum retards setting. If no gypsum is present, calcium aluminium hydrates form immediately and the system sets. The strength development after setting is primarily due to C<sub>3</sub>S and *b*-C<sub>2</sub>S, both of which give the same reaction products, that is, Ca(OH)<sub>2</sub> and calcium silicate hydrate, or tobermorite gel (CSH). All of the reaction products, with the exception of lime, have low solubility in the lime-saturated medium of the cement paste compared to anhydrous minerals in the original cement. Ettringite that forms does not contribute to setting, but coats the cement particles and retards the setting reactions. Large amounts of gypsum would result in secondary gypsum precipitation, causing quick setting. Hydration of C<sub>3</sub>S and C<sub>2</sub>S, which account for approximately 75 percent of the cement by weight, is responsible for strength development after the initial set. The reaction products in both cases are the same – C<sub>3</sub>S<sub>2</sub>H<sub>3</sub>, or tobermorite, and crystalline calcium hydroxide.

There are two basic models to explain the setting reactions; the crystalline and the osmotic- or gel- model. The crystalline model pictures the cement grains to be dispersed in water at the start of hydration, after which calcium-aluminate-hydrates begin to form on the surfaces of the grains in about 2 minutes. Two hours later the sulphoaluminate-hydrates, and possibly other hydrates, begin forming an intermeshing network that causes setting. After two days, the network has developed further due to the hydration of calcium silicates, forming tobermorite and causing hardening. In the crystal model, initial hydration proceeds by nucleation and growth of hexagonal crystals of calcium hydroxides that eventually fill up all the spaces between the cement grains, leaving a silicate-rich layer on the surfaces of the grains. This layer slows the movement of water to the cement surface and the release of calcium and silicate ions from the cement. Meanwhile, particles of calcium silicate hydrate grow outward from the cement grains in the form of needles or spines followed by a different crystalline morphology of the same chemical nature that pushes the spines outward. As they come into contact with other spines on neighbouring cement grains, the spines crumple into sheets of tobermorite, which accounts for the final strength and durability of cement.

According to the osmotic model, calcium silicate in the cement hydrates in the presence of water, coat each grain with a hydrate gel and develops into protuberances, which become tubular (hollow) fibrils. At the same time, calcium hydroxide (called "Portlandite") precipitates and forms large crystals between the grains. The membrane initially formed around the grain acts as an osmotic pump, the salt solution flowing up the tube and precipitating at the tip by an almost steady-state process. This is due to the semi-permeable membrane that allows inward flow of water and the outward flow of small ions-  $\text{Ca}^{2+}$  and  $\text{OH}^-$  - by diffusion, but prevents the outward diffusion of the large hydrated silicate ions. The result is an excess of  $\text{Ca}(\text{OH})_2$  on the fluid side of the membrane, producing an osmotic pressure differential across the membrane. The latter results in fibril growth as the membrane alternately ruptures and reforms by extruding concentrated silicate solution into the saturated  $\text{Ca}(\text{OH})_2$  pore solution where it reacts to form a new CSH gel membrane. Both models end in the same result; the cement grains become interlocked, first setting the cement and finally hardening it (Connor, 1990).

#### 2.2.6.2. *Pozzolan matrix*

Pozzolan concrete is a concrete-like product resulting from the reaction between the alumina-siliceous material of a pozzolan, lime and water. A pozzolan is a siliceous or aluminosiliceous compound that inherently has minimal or no cementitious properties, but will, in the finely divided form react with lime ( $\text{Ca}(\text{OH})_2$ ) at ambient temperatures in the presence of water, to produce a cementitious compound (Van Zyl, 1997).

Fly ash is an excellent example of such a material and has successfully been used as a cement replacement material because of this pozzolanic activity. Van Zyl (1997), used fly ash as a pozzolan to stabilise jarosite to produce a solidified pozzolanic matrix (by adding  $\text{CaO}$ ,  $\text{NaOH}$ , silica sand and water to fly ash and jarosite). The resulting matrix was microcrystalline in

nature (according to an XRD analysis). The identified peaks were low in intensity, but the absence of their raised base line was an indication of less amorphous material than in another matrix, that was produced with the same waste forms and which was considered to be geopolymeric.

The main difference between the cementitious and pozzolanic matrices, is the fact that a cementitious matrix has large amounts of portlandite, which forms as a reaction product. In the case of a pozzolanic matrix this portlandite is used in the formation of other reaction products. Since the reaction products of the two reactions are the same, the absence or presence of portlandite is the only way the two reactions can be distinguished. The absence of a large amorphous phase as well as the reaction components and conditions lead us to expect a pozzolanic matrix and sufficient proof of the matrix type would be the presence of reaction products of a cementitious reaction, but the absence of portlandite (Van Zyl, 1997).

#### 2.2.6.3. *Geopolymeric matrix*

Geopolymeric binders according to a discussion by Van Zyl (1997), are the synthetic analogues of natural zeolitic materials and require much the same hydrothermal conditions for synthesis. Reaction times, however, are substantially faster than that of the comparable zeolite, resulting in an amorphous to semi-crystalline product with some zeolitic properties. These inorganic binders consist of two components – a very fine and dry powder and a syrup-like, highly alkaline liquid. Liquid and powder portions are combined to produce a mixture of molasses-like consistency, which then reacts with the desired waste aggregate. The geopolymeric reaction occurs as a result of the reaction of alumino-silicate oxides with alkali's, such as NaOH, KOH and soluble alkali polysilicates. Resulting from this reaction is the formation of  $\text{SiO}_4^-$  and  $\text{AlO}_4^-$  tetrahedra, linked by shared oxygen ions. Hardening and polycondensation accompany a mildly exothermic reaction in the alkali-activated mixture. A polymeric structure of Al-O-Si bonds is thus formed that constitutes the main building blocks of the geopolymeric structure. Due to thermodynamic considerations, Al-O-Al bonds do not preferentially form while it is expected that some Si-O-Si bonding occur. Because of aluminium's fourfold co-ordination, other cations must be present in the structure in order to keep structure neutrality, and  $\text{Na}^+$ ,  $\text{K}^+$ ,  $\text{Ca}^+$ , as well as other metallic cations usually do this. Whether these ions simply play a charge-balancing role or are actively bonded into the matrix, is still unclear, and it is expected that both scenarios may take place. This characteristic offers a solution for the immobilisation of heavy metal ions in industrial wastes (Van Jaarsveld et. al., 1998).

The mechanism of immobilisation is expected to be a combination of both chemical and physical interactions. By chemical means, the metal cation is either bonded into the matrix via an Al-O or Si-O bond or is present in the framework cavities to maintain electrical charge balance. A physically encapsulated metal cation could be substituted by another cation if its surroundings allowed the diffusion process to occur. By physical immobilisation, the cation

will be prevented from diffusing either by total encapsulation, pores being too small, or pores being present but not connected to the outside. The exact mechanism by which geopolymer hardening occurs is still not fully understood, and most proposals in this regard consist of a dissolution, transportation or orientation, as well as reprecipitation(condensation) steps (Van Jaarsveld et. al., 1998).

Geopolymeric matrices are usually homogeneous in nature, which contributes to the high compressive strength and resistance to chemical attack, which are qualities of geopolymeric concrete. The concrete do not rely on lime for structural integrity and can therefore not easily be dissolved by acidic solutions. Shrinkage is very low, which prevents the formation of cracks during setting and drying. Geopolymers can be blended with hydraulic binders (geopolymeric/portland), resulting in a conjugation of the properties of both systems, offering a combination of high strength, durability and ultra-rapid curing (Van Zyl, 1997).

Van Jaarsveld, et.al., (1996), regarded most waste materials containing sources of silica and alumina as capable of taking part in a geopolymerisation reaction and subsequently used fly ash as a reactant to immobilise process water containing Cu and Pb cations.

There are certain characteristics to be associated with geopolymeric matrices that mainly involve the presence of large quantities of amorphous material due to the semi-amorphous nature of geopolymers. Although XRD cannot evaluate amorphous material, the presence thereof can be seen in the form of a raised background baseline. The texture of the matrices (seen from a SEM micrograph) can be compared to that of toffee, which is also compatible with the perception that a geopolymeric binder is an amorphous gel.

#### 2.2.6.4. *Zeolites*

Zeolites are essentially hydrated alumino silicates of alkali and alkali-earth cations, and have infinite, three-dimensional structures. In these structures some of the tetravalent Si is replaced by trivalent Al, giving rise to a deficiency of positive charge that is balanced by the presence of  $\text{Na}^+$ ,  $\text{K}^+$ ,  $\text{Ca}^+$  and  $\text{Mg}^{2+}$  cations. The resulting structure, which can be pictured as cages that contain these exchangeable ions, lends this group of minerals useful properties for the stabilisation of soluble components that threaten the environment. This crystalline alumino-silicate with 4-connected tetrahedral framework structure is characteristic of zeolites. The enclosing cavities are occupied by large ions and water molecules, both, which have considerable freedom of movement, permitting ion exchange and reversible dehydration (Van Zyl, 1997).

Natural zeolite minerals have been used in pollution control, for the clean up and remediation of contaminated sites, in agriculture and other industrial applications and synthetic zeolites used as molecular sieves and catalyst supports. Many of the synthetic zeolith materials do not meet the mineralogical criteria for a zeolite, but do exhibit zeolitic properties (Giesekke,



1998).

## **2.3. LEACHING**

### **2.3.1. Definitions**

As Conner (1990) stated - there is no such thing as a completely insoluble material, wherever water penetrates, some of the waste dissolves. Therefore, when a waste (treated or not) is exposed to water a RATE of dissolution can be measured. We call this process LEACHING, the water with which we start is called a LEACHANT, and the contaminated water that has passed through the waste, the LEACHATE. The capacity of the waste material to leach is called its LEACHABILITY.

Leaching, being a rate phenomenon, is usually described as a rate or in some cases as a cumulative fraction. Our interest, environmentally, is in the rate at which hazardous or other undesirable constituents are removed from the waste and passed into the environment via the leachate. This rate is usually measured and expressed, in terms of concentration of the constituent in the leachate (that is, milligrams of constituent per litre of leachant after completion of the test). This is because concentration determines the constituent's effects on living organisms, especially humans. Concentration is the primary basis for water quality standards, and water quality standards, especially drinking water standards, are normally the basis for leaching standards. Thus, we speak of the leaching rate of the constituent, but usually measure it as concentration in the leachate. When evaluating a material for leachability, we usually compare the concentration of the hazardous constituent in the leachate to that in the original waste. This tells us what proportion of the constituent dissolved out during the test, which becomes a measure of the leachability of the material. If the test conditions can be expressed in terms of a time-related number, such as equivalent years of field exposure to rainfall, then we can state leachability in true rate terms; for example, pounds of constituent per year or percent of the original of the original content per year. Multiplying the hazardous constituent's concentration in the original waste by the total quantity of the waste, gives us the total amount of the constituent, and thus the hazard potential posed by that quantity of waste. Interestingly, as the hazardous constituents leach, the hazard potential gradually diminishes. Thus, if the leaching rate is controlled so as not to exceed the allowable environmental standards in the ground- or surface water, leaching should really be a beneficial process in the long term. This assumes, of course, that the leaching rate remains constant at an acceptable level, or decreases with time. As we shall see later, a number of scenarios are possible, depending on the disposal conditions.

### **2.3.2. Leaching tests**

Ideally, as far as contaminant release from the waste is concerned, a leaching test must be able to determine the following characteristics:

- the compounds that can be released from the waste;
- the maximum concentration of these compounds in the leachate;
- the quantities released per unit mass of waste;
- the release rate of these compounds;
- the effects of co-disposal of the waste.

The aspect regarding concentration is relevant because the toxic effects of a number of elements, like most chemical reactions, depend on concentration. As far as the amount of release is concerned, the necessity to evaluate the maximum amount of hazardous compounds leachable from a waste under different environmental conditions is evident; moreover, it would be important to determine the possibility of accumulation of toxic compounds due to biological and chemical reactions.

As with the testing of any other product requiring long-term stability, we must make judgements and reach decisions based on information that is available or can be obtained rather quickly. Usually, the primary forms of such information, consists of actual field data, laboratory test results, some understanding of the chemistry of the system, and models that tie everything else together. A large body of information has been built up in this fashion, primarily for the metal constituents specified by the EPA, i.e. arsenic, barium, cadmium, chromium, lead, mercury, selenium and silver. Test methods for CFS-treated wastes must address needs at four levels of control (Connor, 1990):

- research,
- regulatory,
- treatability study, and
- operational quality assurance and quality control.

This is also true for other test methods, but especially applicable and more difficult to implement in leachability testing. The difficulty arises primarily at the operational quality assurance and control level because of the time necessary to carry out regulatory test procedures. This prevents their use on a real-time basis in process control.

In most cases the Toxicity Characteristic Leaching Procedure (TCLP) and Extraction Procedure Toxicity (EPT) test methods are being used for leachability testing, but neither the

TCLP nor its predecessor the EPT, actually simulate any real-world set of conditions. Arguably, however, they do perhaps create a worst-case environment for leaching. Attempts to correlate laboratory-scale leaching tests with field data have not been successful. Nevertheless, these procedures are so widely used and required as specification tests that arguments over their validity are largely academic today. It is also not unusual to use several tests or a whole test battery for specific disposal situations (Conner, 1990).

Still, as Peterson et al. (1996) concluded, the TCLP test provides no indication of the rate of leachate generation and is of little use as an indicator of long-term landfill stability. It is thus necessary to develop a procedure to model the leachate generation at different variables that would predict the long-term effects on the waste.

All of the test methods currently used for regulatory purposes are batch procedures in which the waste is contacted with a leachant for a specific period of time, agitating the mixture to achieve continuous mixing. Chemical equilibrium is often obtained, especially when the solidified waste is crushed before extraction. After extraction and separation of the fluid from the solids, the leachate is analysed for specific constituents. It should be noted that most of these tests use a leachant-to-waste ratio of 20:1, so that the maximum concentration of constituent that can be attained in the leachate is 5 percent of that in the original solid. The leachant in most cases is dilute acetic acid, buffered in some procedures. The total amount of acid added varies with the test and/or with the alkalinity of the waste. The final pH of the leachate at the end of the test is controlled by the alkalinity of the waste in most cases where the leachant is deionised water or dilute acid. As we will see, final pH is one of the prime controlling factors in metal leaching. The TCLP test is designed to simulate the leaching potential of a waste in a so-called "mismanagement" scenario, where it is disposed in a landfill designed for municipal refuse. Such landfills are known to generate organic acids during decomposition of organic matter in the refuse. The purpose of acetic acid in the leachate is to simulate those acids.

It has been found that the acetic acid leaching medium is the most aggressive leaching medium due to its ability to form complexes with the extracted material. Most of the variables in the acetic acid leaching tests are kept constant during experimentation, such as pH, temperature, stirring rate and particle size and may have a significant influence on the leaching phenomena. However, this medium does not accurately reflect environmental leaching processes to which immobilised wastes might be exposed to in landfills. This is because the leaching of heavy metals from waste in a high alkaline environment was not accounted for, and does not differentiate between the different chemical environments found in an ash monofill and a conventional municipal solid waste landfill (Jansen van Rensburg, 1997). Albino et al. (1995) used an acetic acid test, the ANS 16.1, but found that it did not predict reliable long term results due to a constant value of cumulative amount released, which is reached after a time (672 hours), and also because it never exceeds a few units per cent of the initial quantity added. The use of the leaching test with an acetic buffer at pH = 4.74, was a step forward in



understanding the actual efficiency of stabilisation. When using acetic acid alone, the free acidity might be neutralised when stabilisation systems are alkaline. This would obviously avoid that metals are leached, which explains why the buffer leaching medium is preferred.

Apart from acetic acid, acid rain or water is also sometimes considered as leaching media for test purposes. A drawback of most acid rain procedures is that the leaching results can also not be used as an indication of long term leaching effects because the pH is not kept constant, resulting in an alkaline environment which slows down leaching and does not necessarily represents the effect of acid rain over long periods.

Leaching by water provides a simulation of the actual quality of the percolate that may be generated as a result of the contact between water and waste, but due to the length of the existing tests, these tests are impractical as standard leaching techniques. Furthermore, these tests do not include the worst environmental conditions in a landfill, such as acid rain or ground acid, which may penetrate the waste resulting in an increased leaching of the chemical species.

In conclusion, we must agree with Albino et. al. (1995), that only a set of tests, properly designed, can help understanding the entire range of interactions that occur between the matrix and the waste in a solidification/stabilisation process. A single leaching test cannot give full information on the prevailing entrapment mechanism and on the long-term release behaviour.

### **2.3.3. Expected leaching test results**

Results of leaching tests by Albino et. al. (1995) are found to be widely variable and dependant on (a) the nature of the metal; (b) the nature of the stabilising matrix, and (c) the initial metal concentration. These three variables do not always act all together. The leaching of lead proofed to be only dependant on the matrix nature, whereas this was not true for copper.

It was concluded that in cases where the cumulative weight % quantities released are constant, and the absolute quantities are proportional to the initial quantities (as for lead), stabilisation relies on physical micro-entrapment of the metal in the matrix. On the other hand, it might also be concluded that when the cumulative absolute quantities are almost constant (as for copper), chemical factors such as solubility of respeciated metal compounds limit leachability. Generally two sources of leaching from immobilised material exists, i.e. (a) the surface exposed as a result of size reduction, and (b) from inside the solids resulting from crack formation and/or existing pores. The latter mechanism will contribute to pore diffusion, which is a kinetic phenomenon. This analysis will be totally based on an equilibrium approach, which means that the total amount of material (metal) leachable from the matrix will be considered. Evidently, the amount leachable from the surface (external) is dependent on the concentration of metal in the matrix, the amount of matrix, and the particle size.

For a better understanding of the release mechanism the initial part of each release curve should be examined. When the amount released is plotted on a log-log scale different leaching mechanisms can be identified. The possible mechanisms are surface wash off (slope of 0), pore matrix diffusion (slope equal to 0.5) and dissolution (slope equal to 1). Evidently in very complex systems it cannot be excluded that parallel mechanisms play a role, although less relevant. Furthermore, the possibility of matrix morphology changes, during leaching, must also be taken into account (Albino, et.al., 1995).

## 2.4. DEGRADATION

Degradation of the immobilised materials also needs to be accounted for, especially, when considering the long-term stability of such a material. Chemical and physical attacks occur due to environmental conditions and may cause a subsequent increase in the leaching rate of components from the stabilised waste form. According to Conner (1990), the chemical attacks are interfacial phenomena that take place through complex mechanisms, which include ion exchange, dissolution of hydrated solids or formation of new insoluble compounds. Sulphates are the most destructive compounds normally present in the environment because they react with aluminates in the cement structure to form the expansive sulfo-aluminate, ettringite, as well as acids. The former, break down the physical structure of the waste forms. Acids leach lime from the waste form, until 10 to 15 percent of the original weight of the wet cement has dissolved. However, these weak acids will have little effect on the strength of the waste form, because the Portland cement matrix, for example, will resist attack from solutions with pH as low as 5 and the high-alumina cement as low as pH 4. Strong acids, though, can completely dissolve the matrix.

Ageing can also influence the degradation process. The initial hydration products of high alumina cements (decahydrate  $\text{CAH}_{10}$ , smaller amounts of  $\text{C}_2\text{AH}_8$  and alumina gel) tend to be unstable and eventually age to the more stable  $\text{C}_3\text{AH}_6$  and gibbsite,  $\text{AH}_3$ . This ageing is accompanied by a substantial reduction in volume due to the different crystal structures and may result in the loss of long-term strength and sensitivity to corrosive attack in high-alumina cements. High temperatures and water/cement ratio facilitate these ageing effects.

### 2.4.1. Different mechanisms of concrete degradation (microscopic behaviour)

Different types of microscopic behaviour can perhaps explain the causes of physical defects and/or chemical deterioration. Mainly four mechanisms are common in the degradation of most concretes and cements (Thaulow and Jakobsen, 1997):

- Alkali Silica Reaction,
- Sulphate Attack,

- Delayed Ettringite Formation(DEF), and
- Acid Attack.

#### 2.4.1.1. *Alkali silica reaction (ASR)*

This is a heterogeneous chemical reaction that takes place in aggregate particles between the alkaline pore solution of the cement paste and silica in the aggregate particles. Hydroxyl ions penetrate the surface regions of the aggregate and break the silicon-oxygen bonds. Positive sodium, potassium and calcium ions in the pore liquid follow the hydroxyl ions so that electro neutrality is maintained. Water is absorbed into the reaction sites and eventually alkali-calcium silica gel is formed. The reaction products occupy more space than the original silica and puts pressure on the surface reaction sites. The surface pressure is balanced by tensile stresses in the centre of the aggregate particle and in the ambient cement paste. At a certain stage the tensile stresses may exceed the surface pressure and brittle cracks propagate. The cracks radiate from the interior of the aggregate out into the surrounding paste. The cracks are empty (not gel-filled) when formed, but small or large amounts of gel may subsequently exude into the cracks, whereas small particles may undergo complete reaction without cracking. Formation of the alkali silica gel does not cause expansion of the aggregate and observation of gel in concrete is therefore no indication that the aggregate or concrete will crack.

The reaction is primarily diagnosed by the presence of cracks in *reactive aggregates* radiating out into the cement paste. Reactive aggregates contain amorphous or microcrystalline silica,  $\text{SiO}_2$ . Frequently, alkali silica gel is also observed, however, the amount of gel is not a measure of the extensiveness of the reaction, but dependent on the type of reactive aggregate. Aggregates, containing reactive silica, such as porous flint, will react rapidly to form alkali silica gel both at the surface and inside the aggregate. Denser polymineralic particles, such as mylonitised granites, which contain microcrystalline quartz, will react more slowly and the reaction initiates primarily at pre-existing cracks, inhomogeneities and grain boundaries and leads to expansion and cracking of the aggregate.

The crack pattern observed depends on the type of reactive aggregate. Aggregates without preferred orientation of the mineral grains, such as porous flint, crack and create a triple junction with angles of ideally  $120^\circ$ . In aggregates with oriented minerals, such as mylonites, cracks are often parallel to the mineral orientation and in aggregates, like sandstone, the cracks may run along grain boundaries.

Typically for all types of aggregates the cracks are wide in the centre and narrow towards the rim of the aggregates. Locally the cracks tend to be perpendicular to the surface of the reactive particle (radial cracks).

If a certain number of reactive particles are present in the concrete a continuous crack pattern is present in the paste. Usually, the cracks follow the line of least resistance perpendicular to the tensile stresses of the concrete. At the surface of the concrete, cracks perpendicular to the surface are commonly observed. Beneath the surface, a large number of cracks tend to be parallel to the surface. These cracks usually run through the cement paste and reactive aggregates, and in rare cases even sound aggregates may be cracked. Another diagnostic feature of the alkali silica reaction, is the presence of alkali silica gel; a clear isotropic material with low refractive index and a typical shrinkage crack pattern. Alkali silica gel may, however, be partly crystallised and gel, replacing the outer part of particles (e.g. porous flint particles), can sometimes be observed situated in cracks and/or voids. Ettringite in pores and cracks is commonly found in ASR-affected concrete. The trained petrographer can, however, distinguish alkali silica gel from massive ettringite formation by the slight birefringence of ettringite. Furthermore, ettringite exhibits a different crack pattern consisting of almost parallel micro cracks. In the cases of intensive ASR the  $\text{Ca}(\text{OH})_2$  of the paste can be dissolved leaving a black and opaline shining paste when observed in crossed polarised light. Generally, the dark paste areas are found in a narrow zone around reactive aggregates, but are also observed along cracks containing gel.

Primarily four main features diagnose alkali silica reaction:

- Presence of alkali silica reactive aggregates,
- Crack pattern,
- Presence of alkali silica gel in cracks and/or voids, and
- $\text{Ca}(\text{OH})_2$  depleted paste.

2.4.1.2. *Sulphate attack*

Sulphate ions may attack components of cement paste. According to Thaulow and Jakobsen (1995), such attacks can occur when concrete is in contact with sulphate containing water e.g. sea water, swamp water, ground water or sewage water. The often massive formation of gypsum ( $\text{CaSO}_4 \cdot 2\text{H}_2\text{O}$ ) and/or ettringite ( $3\text{CaO} \cdot \text{Al}_2\text{O}_3 \cdot 3\text{CaSO}_4 \cdot 32\text{H}_2\text{O}$ ) formed during the sulphate attack, may cause the concrete to crack.

The formation of gypsum requires a high concentration of sulphate in the ambient water in contact with the concrete. The formation of ettringite occurs by a transformation of the calcium and aluminium containing components in the cement paste. Formation of sulphate phases takes place through dissolution of the cement paste as the sulphate ions consume calcium ions from calcium hydroxide.

Primarily four main features of the microscopic appearance diagnose sulphate attack:

- Cracks parallel to the surface of the concrete,
- Presence of gypsum and/or excessive amounts of ettringite in voids, cracks and paste,
- Dissolution of cement paste, and
- External sulphate source.

Concrete subjected to sulphate attack contains parallel cracks filled or partly filled with gypsum. The cracks occur parallel to and near the surface of the concrete. The orientation depends on the possible expansion direction of the concrete. The cracks traverse the cement paste and follow aggregate surfaces. Gypsum is diagnosed by its fibrous texture when observed in crossed polarised light and is typically observed in parallel cracks and in voids near the surface. Gypsum is not always recognisable in the optical microscope and using an energy dispersive spectrometer (EDS) during scanning electron microscopy (SEM) can positively identify gypsum precipitates in the cement paste.

Ettringite is identified as needle shaped crystals with low birefringence. It has to be emphasised that the occurrence of ettringite in voids and cracks is common for every mature water-exposed concrete; ettringite by itself is not a diagnostic feature of sulphate attack (or delayed ettringite formation). To diagnose sulphate attack, near-surface paste expansion forming surface parallel cracks in the cement paste must be present. Chemical analyses of the sulphate content in the surface and the interior may be helpful. Furthermore, in order to distinguish sulphate attack from delayed ettringite formation an outside sulphate source must be identified. The crack patterns observed by Taylor and Gollop (1997), in cement pastes that have been attacked by  $\text{Na}_2\text{SO}_4$  solutions suggest that expansion has taken place in a surface layer, which tended to become detached. The cracking occurred in the zone of gypsum formation and thus nearer the surface than the zone in which the ettringite was formed. Consideration of the formation of gypsum, rather than ettringite, as the source of expansion, was consistent with some findings, but the extensive evidence that expansion is related to the content of available  $\text{Al}_2\text{O}_3$  from  $\text{C}_3\text{A}$  or other sources did not support this and Taylor and Gollop (1997) concluded that the damage can rather be associated with ettringite formation. It may be an indirect instead of direct result of ettringite, with the immediate cause of the expansion possibly being water uptake.

#### 2.4.1.3. *Delayed ettringite formation (DEF)*

Generally DEF is seen as a form of internal sulphate attack. A number of factors such as concrete composition, curing conditions and exposure conditions influence the potential for



DEF. Although the fundamental reaction mechanism is still debated among researchers, DEF is believed to be a result of improper heat curing of the concrete where the normal ettringite formation is suppressed. The sulphate concentration in the pore liquid is high for an unusually long period of time in the hardened concrete. Eventually, the sulphate reacts with calcium- and aluminium- containing phases, and the cement paste expands. Due to this expansion empty cracks (gaps) are formed around aggregates. The cracks may remain empty or later be partly or totally filled with ettringite.

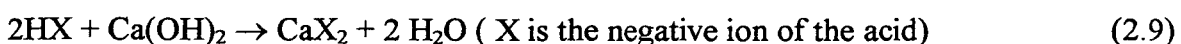
Microscopically the DEF are diagnosed by four main features in the appearance:

- Presence of gaps completely surrounding aggregates,
- Wider gaps around large aggregates than around small aggregates,
- Absence of external sulphate source, and
- High temperature heat curing history.

In diagnosing DEF, cracks or gaps have to be observed around the aggregate particles. The gaps may be empty, partly filled by needle shaped ettringite or filled with a more massive type of ettringite. Some researchers believe that the crystal growth of ettringite is the cause of the gaps, but others do not agree with this. The width of the cracks is directly proportional to the diameter of the aggregates, resulting in wide cracks around coarse aggregates and narrow cracks around fine aggregates. Under ideal circumstances gaps are only seen around the aggregates. However, in field concrete narrow cracks are also observed perpendicular to the aggregate surfaces. Usually aggregate particles are not cracked by DEF. DEF is distinguished from external sulphate attack because gypsum is normally not formed. Furthermore, the paste expansion in DEF is not limited to the surface regions of the concrete. It is useful to know the curing conditions of the concrete, as high temperature heat curing is a prerequisite for delayed ettringite formation (Thaulow and Jakobsen, 1997).

#### 2.4.1.4. *Acid attack*

Concrete is susceptible to acid attack because of its alkaline nature. The components of the cement paste break down during contact with acids. Most pronounced is the dissolution of calcium hydroxide, which occurs according to the following reaction:



The decomposition of the concrete depends on the porosity of the cement paste, on the concentration of the acid, the solubility of the acid calcium salts ( $\text{CaX}_2$ ) and on the fluid

transport through the concrete. Insoluble calcium salts may precipitate in the voids and can slow down the attack. Acids such as nitric acid, hydrochloric acid and acetic acid are very aggressive as their calcium salts are readily soluble and removed from the attack front. Other acids such as phosphoric acid and humic acid are less harmful. Their calcium salts, due to their low solubility, inhibit the attack, by blocking the pathways within the concrete, such as interconnected cracks, voids and porosity. Sulphuric acid is very damaging to concrete as it combines an acid attack and a sulphate attack.

Primarily two main features diagnose an acid attack:

- Absence of calcium hydroxide in the cement paste, and
- Surface dissolution of cement paste exposing aggregates.

Acid attack is usually the diagnosis when dissolution of calcium hydroxide is observed. Dissolution of  $\text{Ca(OH)}_2$  makes the cement phase totally black and opaline shiny when observed in crossed polarised light. Dissolution of the calcium hydroxide is observed in the surface of the concrete and around the cracks in contact with the surface. The depth of the dissolution depends on the porosity of the concrete (water/cement ratio) and the type of acid. Generally, cracks are not produced by the acid attack itself, but instead the exposed aggregates are observed on the surface, due to the disintegration of the cement paste (Thaulow and Jakobsen, 1997).

#### **2.4.2. Destruction of C-S-H**

Taylor and Gollop (1997) studied the durability of some concrete and mentioned that several processes that can damage concrete take place through the inward movement of a reaction front. Studies on external sulphate attack illustrated, among other findings, that expansion and cracking are probably caused, directly or indirectly, by ettringite formation, while softening and disintegration are caused by destruction of C-S-H. The latter process appears to be at least as important in practice as expansion and cracking and is probably of greater relative importance with slag blends than with plain Portland cements. This could explain observations that slag blends often fail in laboratory tests by weakening or disintegration before much expansion has occurred.

During sulphate attack, the destruction of C-S-H is usually favoured by low or zero contents of CH and, very strongly, by the presence of  $\text{Mg}^{2+}$  ions. CH contents are low or even zero with blended cements of all kinds, and this may be why slag cement pastes or mortars tend to fail by weakening and disintegration. There may be other relevant effects. Pastes of slag blends are less permeable than those of plain PC's, and this possibly enhances the ability of the microstructure to accommodate an increase in solid volume due to ettringite formation

without undergoing damage. On the other hand, if  $\text{MgSO}_4$  attacks Portland cement (PC) pastes, a composite layer of gypsum and brucite is formed on the surface, and may have a protective effect. Such layers are not formed in blends containing slag, and this may lower their resistance to attack by  $\text{MgSO}_4$  solutions.

Decalcification of C-S-H begins when the CH has been depleted, or, perhaps, when CH from this source is no longer readily available. In decalcification, the Si/Ca ratio of the C-S-H increases due to removal of  $\text{Ca}^{2+}$  and  $\text{OH}^-$ , and this causes the amount of C-S-H to decrease. This contrasts with the increase in Si/Ca that occurs through pozzolanic action, which occurs through addition of  $\text{SiO}_2$  and thus causes the quantity of C-S-H to increase.

## 2.5. MODELLING

The degree of mobilisation of the contaminants in the matrix is evidently of great importance due to the hazardous implications to the environment, if these elements should leach into ground or surface waters. This motivates the need to be able to predict the leaching from such a material when subjected to an aggressive medium. For this purpose various mathematical models have been developed and proposed for certain conditions. Current practice in predicting leaching behaviour is generally based upon the concept of bulk diffusion of contaminants, from the waste into solution. The driving force is in this case the bulk contaminant concentration in the waste. Although these models cannot accurately predict long-term leaching behaviour, they are considered accepted practice in the environmental realm. Attempts have been made to predict long-term behaviour by curve fitting experimental results and extrapolating over time, although bulk diffusion may not always represent the main driving force for contaminant release (Hinsenveld, 1992). In the following chapter we will discuss a few proposed models:

- the bulk diffusion model,
- a leaching model based on bulk diffusion and chemical reaction,
- a model based on interface mass resistance,
- a semi-empirical model, which is a combination of the above mentioned models, and
- the shrinking unreacted core model (SUC).

### 2.5.1. Bulk diffusion model

According to Baker and Bishop (1997), the basic premise behind the bulk diffusion model is that contaminant release is a result of the concentration within the monolith. The rationale



behind this model is that in a disposal environment, diffusion through a solid represents a maximum contaminant loss rate when the waste permeability is less than  $10^{-3}$  times that of the surrounding geologic media.

The model is based on Fickian diffusion and was originally developed according to the following equation:

$$\frac{\partial C}{\partial t} = D_e \frac{\partial^2 C}{\partial x^2} \quad (2.10)$$

Where:  $D_e$  = effective diffusion coefficient, corrected for porosity and tortuosity ( $\text{cm}^2\text{s}^{-1}$ ),  $C$  = concentration of the contaminant ( $\text{g}\cdot\text{cm}^{-3}$ ),  $t$  = time (s) and  $x$  = distance (cm).

In applying this equation a zero surface concentration (and associated zero leachant concentration) is assumed, to maintain a dynamic leaching environment. The ANS/ANSI 16.1 test procedure is a commonly used semi-dynamic leach test that incorporates the bulk diffusion model into interpretation of leach test results (American Nuclear Society, 1986). In this test the specimens are leached in deionised water with periodic leachant replacement. Assuming that the groundwater velocity is high enough to maintain zero surface concentration, then equation (2.10) can be simplified to:

$$L(t) = C_T \left[ \frac{D_e}{\pi t} \right]^{\frac{1}{2}} \quad (2.11)$$

Where,  $C_T$  is the total initial concentration ( $C_{\text{mo}}$ ) throughout the matrix. The release can be expressed as a cumulative fraction leached by substitution (2.12) into the general equation for the leaching rate:

$$L(t) = \frac{M_{\text{mo}}}{A} \frac{dF(t)}{dt} \quad (2.12)$$

Where  $A$  is the geometrical surface area of the waste specimen and  $M_{\text{mo}}$  the initial amount of the mobile species in the specimen. After integration the cumulative fraction is:

$$F(t) = 2 \frac{A}{V} \left[ \frac{D_e t}{\pi} \right]^{\frac{1}{2}} \quad (2.13)$$

Where  $V$  is the volume of the waste specimen.

Hinselveld and Bishop (1994) presented a theoretical, bulk-diffusion based, concentration-profile for contaminants in a specimen, as a function of the dimensionless time (equation 2.14).

These concentration profiles, as in equation (2.14) can be used to determine leaching rates.

$$c(x,t) = 3c_0 \operatorname{erf} \left[ \frac{x}{4D_e t} \right] \quad (2.14)$$

Where,  $c_0$  = initial contaminant concentration in the solid, erf = standard error function,  $x$  = distance into the solid,  $t$  = leaching time.

This theoretical concentration profile for bulk diffusion, does, unfortunately, not necessarily agree with various experimental results, including those obtained from leaching in neutral leachants. As already mentioned, the main driving force in the bulk diffusion model is the bulk contaminant concentration and a proportional increase in this concentration would theoretically yield a proportional increase in the leaching rate, but this is often not the case. In addition, the model does not recognise the acidity dependence of contaminant leaching. This implies that increasing of the acidity of the leachant would have no impact on the observed leaching rate (see equation 2.11), which has been demonstrated to be false (Hinsenveld and Bishop, 1994, Cheng, 1991).

The primary failure of the bulk diffusion models is, in fact, that the effect of acidity on the leaching process is not addressed. This model was originally developed to study the leaching behaviour of radionuclides from stabilised wastes. The chemistry of these metals, and subsequent stabilisation mechanisms, are much different than those for typical priority pollutant metals (Poon, 1989). One important component of stabilisation for example, is the degree of chemical interaction between the waste and the cement and for heavy metals, pH dependent precipitation reactions (i.e., hydroxides, carbonates, sulphides) are often an important stabilisation mechanism. The subsequent dissolution of these precipitates is like-wise dependent upon pH; and their availability, generally much greater under acidic conditions. It is thus evident, that this model is not exactly suitable for the prediction of leaching from most immobilised matrices, and another model, which incorporates the pH-dependency of the leaching behaviour, needs to be considered.

### 2.5.2. Leaching model based on bulk diffusion and chemical reaction

Species can be present in both immobile ( $C_{im}$ ) and mobile ( $C_{mo}$ ) forms in a state of chemical equilibrium. Leaching of the mobile species will lead to a difference in chemical potential, thereby driving the reaction to transform the immobile form of the species into a mobile form. If the reaction is fast compared to the diffusion rate, the two forms of the species could be considered to be in a state of constant chemical equilibrium. But if the reaction is slow, the kinetics of production of the mobile species has to be taken into account.

#### ➤ *Instantaneous chemical reaction*

A simple analytical solution to the mass balance equation can be obtained if the chemical reaction is represented by a linear adsorption isotherm, i.e.:

$$K_d = \frac{C_{im}}{C_{mo}} \quad (2.15)$$

A mass balance across a differential section leads to:

$$\frac{\delta C_{mo}}{\delta t} = D_e \left( \frac{\delta^2 C_{mo}}{\delta x^2} \right) + \frac{\delta C_{im}}{\delta t} \quad (2.16)$$

Substitution  $C_{im}$  with  $K_d C_{mo}$ , obtained from eq. (2.14) gives:

$$\frac{\delta C_{mo}}{\delta t} = \frac{D_e}{(1 - k_d)} \frac{\delta^2 C_{mo}}{\delta x^2} \quad (2.17)$$

The effect of the chemical equilibrium is to slow down the leaching process. The solutions to equation (2.17) are given by equations (2.13) and (2.14), where  $C_T = C_{mo} + C_{im}$  and  $D_e$  is replaced by  $D_e'$  which is defined as:

$$D_e' = \frac{D_e}{(1 - k_d)} \quad (2.18)$$

#### ➤ *Kinetically controlled chemical reaction*

If a mobile species of initial concentration  $C_{mo}(0,x)$  is being produced at a rate  $k[C_{mo}(0,x) - C_{mo}(t,x)]$ , a mass balance across a differential section leads to:

$$\frac{\delta C}{\delta t} = D_e \left( \frac{\delta^2 C}{\delta x^2} \right) + k(C_e - C) \quad (2.19)$$

Here  $C$  represents  $C_{mo}(t,x)$  and  $C_e$ , the equilibrium concentration, represents  $C_{mo}(0,x)$ . A solution to this differential equation for a semi-infinite medium of uniform initial concentration  $C_e$  and zero surface concentration can be expressed as a leaching rate (Jansen van Rensburg, 1997):

$$L(t) = C_T (D_e' k)^{\frac{1}{2}} \left[ \text{erf}(kt)^{\frac{1}{2}} + \frac{e^{-kt}}{(\pi kt)^{\frac{1}{2}}} \right] \quad (2.20)$$

Where  $C_T$  is the total initial concentration ( $C_{im} + C_{mo}$ ), erf is the error function and the effective diffusion coefficient,  $D_e''$  is defined as:

$$D_e'' = \frac{D_e}{\Phi^2} \quad (2.21)$$

Where  $\phi$  is defined by  $C_T/C_e$ . An expression for the cumulative fraction leached is obtained by substituting eq. 2.5.11 into equation 2.5.4 and then integrating:

$$F(t) = \frac{A}{V} (D_e'' k)^{\frac{1}{2}} \left[ \left( t + \frac{1}{2} k \right) \text{erf}(kt)^{\frac{1}{2}} + (t/\pi k)^{\frac{1}{2}} e^{-kt} \right] \quad (2.22)$$

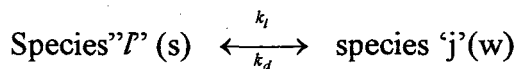
Equations 2.21 and 2.22 can be simplified for short and long periods of time by asymptotic analysis. For small values of  $kt$  ( $k \rightarrow 0$ ), equation 2.20 reduces to the simple diffusion model represented by equation 2.12. For large values of  $kt$ ,  $\text{erf}(kt)$  approaches unity and the leach rate as defined by equation 2.10, reaches steady state:

$$L(t) = C_T (D_e'' k)^{\frac{1}{2}} \quad (2.23)$$

### 2.5.3. Leaching model based on interface mass resistance.

#### ➤ *Using a chemical kinetics approach*

A kinetics approach was used in a complex leaching model, for glass waste forms, where the surface phenomenon were described based on the kinetics of exchanges of a species between the surface of the solid(s) and the aqueous solution (w) (Jansen van Rensburg, 1997).



Where  $k_i$  and  $k_d$  are phenomenological rate constant coefficients. They describe the kinetics of all elementary processes involved in releasing or attaching species "j" from or to the surface respectively. These coefficients may be complex functions of the physical and chemical properties of the surface and the aqueous solution. The resulting model indicates that, at short leaching time, the surface processes dominate leaching, rather than bulk diffusion, regardless of the leachant flow conditions. It is possible to demonstrate that the leach rate is an exponential function of the rate constants by using assumptions, which apply at short leaching times, and is given by,

$$L(t) = f[e^{-(k_i + \beta k_d)t}] \quad (2.24)$$

where the constant  $\beta$  is equal to the ratio of the solid surface area to the aqueous solution volume. The initial rapid decrease of the leach rate is due to the rapid release of surface species into the aqueous solution. Integrating the leach rate expression leads to an equation for the cumulative fraction leached.

$$F(t) = k_1[1 - e^{-(k_1 + \beta k_d)t}] \quad (2.25)$$

➤ *Using a mass transfer coefficient*

The surface phenomenon can be expressed in terms of an overall mass-transfer coefficient,  $K$  (Jansen van Rensburg, 1997). The leaching equation is given by

$$L(t) = K[C_{\text{sat}}^{(w)} - C^{(w)}(t)] \quad (2.26)$$

Where  $C_{\text{sat}}^{(w)}$  and  $C^{(w)}(t)$  are the saturation concentration and the concentration of the species in the aqueous solution, respectively. Since  $C_{\text{sat}}^{(w)}$  is the aqueous concentration when the system is at equilibrium, it represents the chemical potential of the surface species. The leach rate will reach a maximum value  $L_0$  when  $C^{(w)}(t)$  tends toward zero, i.e.

$$L_0 = KC_{\text{sat}}^{(w)} \quad (2.27)$$

Replacing the value of  $K$  obtained from equation (2.27) into equation (2.26) gives:

$$L(t) = L_0[1 - C^{(w)}(t) \frac{C^{(w)}(t)}{C_{\text{sat}}^{(w)}}] \quad (2.28)$$

If the leaching species is a major structural component of the waste, its release into the aqueous solution leads to a structural breakdown of the matrix. This process is referred to as corrosion. The kinetics of the process can be represented by a network dissolution velocity,

$u \left\{ \frac{L}{T} \right\}$ , given by:

$$u(t) = L(t) \frac{L(t)}{C_T} \quad (2.29)$$

Where  $C_T$  is the total initial concentration of chemical species throughout the matrix. Substituting equation (2.28) into (2.29) and defining the maximum network velocity as,  $u_0 = L_0/C_T$ , gives:

$$u(t) = u_0 \left[ 1 - C^{(w)}(t) \frac{C^{(w)}(t)}{C_{sat}^{(w)}} \right] \quad 2.30$$

For the simple case where  $C_{sat}^{(w)} \gg C^{(w)}(t)$  and  $u(t) = u_0$ , the following expression is obtained after substituting the time dependencies of  $C^{(w)}(t)$  in equation (2.13) and (2.14) into equation (2.30):

$$F(t) = \frac{A}{V} u_0 t \quad (2.31)$$

This implies that the cumulative fraction leached, is independent of the concentration of that species in the waste, if the concentration in the aqueous solution is much less than the saturation concentration (Jansen van Rensburg, 1997).

#### 2.5.4. Semi-empirical leaching model for the cumulative amount leached

A combination of the general forms of the models based on bulk diffusion, interface mass resistance and the bulk diffusion and chemical reaction presented a semi-empirical expression to describe the cumulative amount leached (CAL) of a contaminant in a stabilising matrix, as was used by Jansen van Rensburg (1997) and is used later on in Chapter 6 of this thesis.

The equation is given by:

$$CAL(t) = K_1(1 - e^{-k_2 t}) + K_3 t^{\frac{1}{2}} + K_4 t \quad (2.32)$$

However, although empirical models can be used to mathematically describe observed leach rates, these models do not yield information on the controlling leach mechanisms (Medici, et al., 1992). By using equation 2.32 we can determine the percentage contribution of each term to the cumulative amount leached at a certain time and the assumption was made in chapter 6, that the governing term were controlling the leaching rate at that specific time.

#### 2.5.5. Shrinking unreacted core model

As was already mentioned and discussed by Baker and Bishop (1997), most studies of leaching behaviour of cement based systems have assumed that bulk diffusion from the monolith is the main driving force for contaminant release, but recent research has shown that leaching of contaminants is actually a result of the dissolution of the outer shell of the waste form, which results in a solubilisation and release of contaminants from the leached shell and several studies have identified the presence of an inward moving dissolution front in specimens subjected to acidic and alkaline conditions.



This behaviour has been shown by Hinsenveld (1992) to follow a shrinking core model (SUC). This model incorporates the concept of acid exposure, rather than time, as the master variable in evaluating leaching behaviour. The rate of contaminant leaching is controlled by the inward diffusion of acid species into the alkaline depleted leached shell. Baker and Bishop (1997) observed the behaviour of 'real-world' solidified wastes in order to verify that previously observed behaviour in synthesised waste forms applied equally as well to real world wastes and metal leaching behaviour was evaluated as a function of the exposure.

In the bulk diffusion model, contaminant leaching is considered a result of diffusion from the monolith, into the leachant. Under the SUC model, contaminant leaching results from acidic species diffusing into the solid matrix. As acid penetrates into the monolith, a leached 'shell', depleted of free calcium and contaminants, is formed. Solubilised species are subsequently released into the leachant, or diffuse inward, where they are reprecipitated at the higher pH conditions of the unreacted matrix. The leached shell is clearly delineated by this region of demineralisation, while the inner 'core' of the monolith is assumed to remain unaltered. Figure 2.2 presents a schematic illustration of the SUC model.

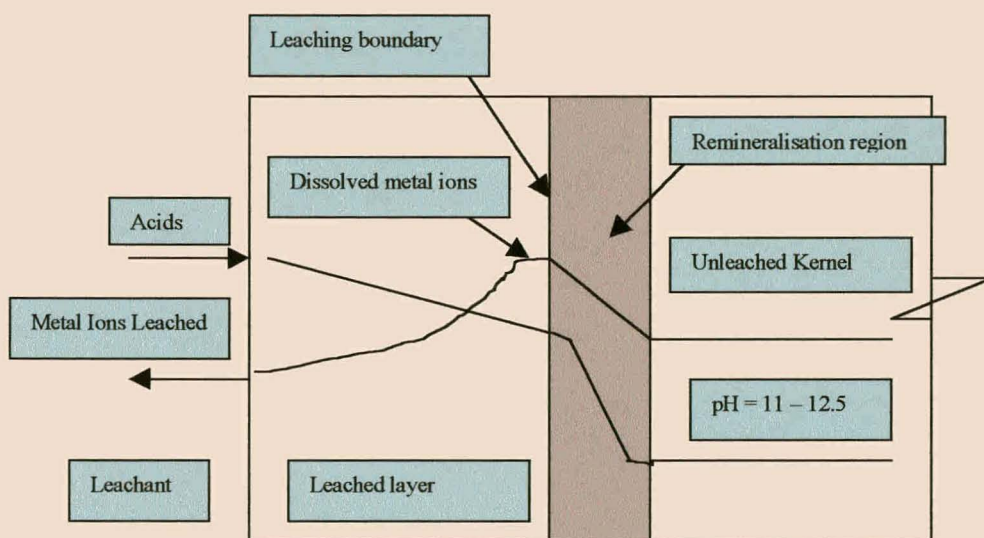


Figure 2.2. Schematic illustration of the principles of the shrinking unreacted core (SUC) model (Baker and Bishop, 1997)

In this model development, three possible limitations in the kinetics were evaluated:

- Diffusion through the concentration boundary layer,
- Diffusion through the leached shell, and
- Chemical reactions at the leached shell-core interface.

It was originally postulated that the limiting leaching mechanism is the diffusion controlled fast reaction of the acid species into the leached shell. Further evaluation of this data by Hinsenveld more clearly defined hydrogen ion diffusion into the leached shell as the limiting mechanism. For this reason, the shell diffusion limitation was the only limitation discussed by Hinsenveld and the following concepts associated with the derivation of the SUC model were developed:

- *Conversion ( $\zeta$ )*

This term relates the amount of leached shell to the original amount of material. With flat samples this would simply be the acid penetration depth (APD) of the leached shell. With specimens of cylindrical or spherical geometry, the conversion is a dimensionless number relating the original specimen radius to the core radius.

- *Exposure*

The amount of acid a specimen is exposed to under acidic conditions is defined as the acid exposure, which is equivalent to the acid concentration multiplied by the leaching time ( $c \times t$ ), measured in units of acid equivalents  $\times$  time/volume [ $\text{mol} \cdot \text{min} \cdot \text{l}^{-1}$ ]. During testing, the acid concentration is a function of leaching time; the pH increases as the alkalinity of the solid is consumed and compensation for the change in acid concentration over time was needed and presented in the form of the exposure integral,  $I(t)$ . When the pH is held constant, this term would not need to be integrated.

$$I(t) = \int_0^t \overline{c_T} \delta t \quad (2.33)$$

Where  $\overline{c_T}$  is the average acid concentration.

- *Solid acid neutralisation capacity (ANC)*

The solid acid neutralisation capacity,  $\beta_c$ , is defined as the quantitative capacity of cement to react with a strong acid to a pre-determined pH. Under leached shell diffusion limitation, the conversion, as measured by acid penetration depth (cm), follows the following relationship for strong acids:

$$\zeta = \sqrt{\frac{2D_{e,s}(c_{H,i} - v_{H,c})}{\beta_c}} t \quad (2.34)$$

Where  $D_{e,s}$  is the effective diffusion coefficient (for acid species) [ $\text{cm}^2 \text{s}^{-1}$ ],  $c_{H,i}$  is the hydrogen ion concentration at the liquid interface [ $\text{kmol} \cdot \text{m}^{-3}$ ],  $v_{H,c}$  the hydrogen ion concentration at the



core boundary [ $\text{kmol.m}^{-3}$ ] and  $\beta_c$  the acid neutralisation capacity [ $\text{kmol.eq.m}^{-3}$ ].

The driving force is provided by the bulk hydrogen ion concentration in the leachant. By assuming the  $\text{H}^+$  concentration at the leaching front is much less than that in the bulk liquid, the exposure integral can be substituted into this equation to give:

$$\zeta = \frac{2D_{e,s}I(t)}{\beta_c} \quad (2.35)$$

This relationship can be applied to predicting the conversion under a certain set of leaching conditions. (Note that this is not to acid concentration or time alone)

Hinselveld (1992) broke this equation into three basic components. The left-hand side is a function of the conversion, and can be defined as the leaching function,  $L$ . The right hand side can be broken down to a leaching constant,  $K$ , and the acid exposure,  $I(t)$ , yielding the following relationship:

$$L_2 = K_2 I(t) \quad (2.36)$$

Where  $L_2$  is the leaching function for leached shell diffusion limitation.

One basic premise of the SUC model is that contaminant release is directly related to the conversion, or acid penetration depth,

$$M''(t) = l_s C_m f_{mo} \quad (2.37)$$

where  $M''(t)$  is the contaminant release per unit surface area [ $\text{mol.cm}^{-2}$ ],  $l_s$  are the thickness of the leached shell [cm],  $C_m$  the solid contaminant concentration [ $\text{mol.cm}^{-3}$ ] and  $f_{mo}$  the dimensionless leachable fraction.

The contaminant release per unit surface can be determined by:

$$M''(t) = \sqrt{\frac{2D_{e,s}f_{mo}^2 C_m^2 I(t)}{\beta_c}} \quad (2.38)$$

As can be seen from the above equation the predicted contaminant release per unit surface (for a given exposure integral) is a function of a few basic parameters: the bulk contaminant concentration ( $C_m$ ) and availability ( $f_{mo}$ ) in the S/S specimen, the porosity and tortuosity of the leached shell and their effect on the diffusivity of the acid species ( $D_{e,s}$ ), and the solid ANC of the S/S specimen ( $\beta_c$ ).

The potential release factor (PRF) was introduced as a means of ranking the S/S specimens according to their leach resistance:

$$\text{PRF} = \sqrt{\frac{2D_{e,s} f_{mo}^2 C_m^2}{\beta_c}} \quad (2.39)$$

Lower PRF values are desirable, in that they yield a lower potential for leaching. The PRF should be independent of the conditions under which leaching occurs, provided diffusion of acid into the leached shell is the limiting mechanism and  $f_{mo}$  does not change. Due to the low PRF values a stabilisation quality index (the negative logarithm of the PRF), was also introduced by Hinselveld (1992):

$$\text{SQI} = -\log(\text{PRF}) \quad (2.40)$$

The SQI is analogous to the leachability index (LX) values obtained in the ANS 16.1 test procedure (only with an acidity dependence correlation). A good correlation between the theoretical and experimental SQI values would indicate that acid penetration is the controlling mechanism. Based upon leached shell diffusion, the experimental SQI is calculated as follows:

$$\text{SQI} = -\log\left(\frac{M''(t)}{I(t)^{0.5}}\right) \quad (2.41)$$

- *ANC release*

Hinselveld illustrated linearity between the release of calcium and acid neutralisation capacity (ANC) of the solid. According to the SUC model, contaminant leaching from cement-stabilised wastes results from the inward penetration of acid species, followed by dissolution and release of solid ANC from the specimen. The ANC provides buffering capacity and the high pH environment under which chemical precipitation occurs, primarily as hydroxides. The dissolution reaction for alkalinity can be represented by:



When the shell diffusion leaching function,  $L_2$ , is plotted against exposure, a linear fit indicates that leached shell diffusion is the controlling mechanism (Hinselveld, 1992).

By linking a model that typically represents the true behaviour of immobilised contaminants during leaching to the results we obtain from leaching solution concentrations, during leaching tests, we may be able to predict typical leaching behaviour after long times of exposure to leaching conditions in solid waste disposal sites.

## 2.6. CONCLUSIONS

When examining the chemistry behind geo-chemical immobilised matrices, it becomes evident that the binding and setting mechanisms are rather complex, and exact determination of the reaction products in these materials is virtually impossible. This complicates the characterisation of the leaching behaviour of such immobilised matrices even further. From this chapter it can be concluded that there are a few popular binder systems for the immobilisation of wastes, but each disposal situation seems to be unique and require it's own system for optimum immobilisation, by controlling the pH and redox-potential ( $E_h$ ) of the material. In the end, the most cost-effective system will usually be selected. Different geo-chemical matrices can be produced according to the additives added to the wastes and with the specific wastes under consideration, matrices of cementitious-, pozzolanic- or geopolymeric-structure or a combination of these, showed viable immobilisation and strength results, for the stabilisation of fly ash and jarosite samples.

Most of the matrix structures are assumed to have basically the same general types of active solidification components. They are essentially  $\text{SiO}_2$ ,  $\text{CaO} + \text{MgO}$ , and  $\text{Al}_2\text{O}_3 + \text{Fe}_2\text{O}_3$  of which the combinations would differ for different binder systems and the solidification reactions are expected to be similar to the hydration reactions experienced by Portland cement. The latter entails the formation of tobermorite gel from calcium silicates.

Standard leaching tests which are done to test the stability of immobilised materials, an acetic acid leaching test in which the pH was held constant, seemed to best simulate leaching conditions that would typically be experienced when these wastes are disposed of as landfills. Characterisation of the tests is of major importance in clarifying the leaching phenomena, for educated extrapolations of leaching behaviour in a few years time. The leachate compositions, obtained during tests, depend on the stability of the waste after immobilisation treatment is performed on it. However, the gradual breakdown of the matrix can lead to further mobilisation of some of the contaminants, causing an increased concentration of hazardous components in the leachate. The occurrence might be more pronounced for some cases, depending, for example, on the method in which the component was immobilised in the first place or the leaching test conditions.

A few models regarding the general behaviour of wastes during leaching tests have been proposed to characterise leaching from matrices. Current practice in predicting leaching behaviour is generally based upon the concept of bulk diffusion of contaminants, from the waste into solution. The driving force is in this case the bulk contaminant concentration in the waste. These models cannot accurately predict long-term leaching behaviour, and particularly fail to predict the pH dependence during the leaching of contaminants into solution, but they are still considered accepted practice in the environmental realm. Other models were developed to improve this model, and incorporate the pH effect on leaching. Examples of these models, such as the leaching model based on bulk diffusion and chemical reactions and

leaching models based on interface mass resistance were discussed in more detail in chapter 2. A combination of some of the different models presented a semi-empirical leaching model for the cumulative amount of contaminant/matrix component leached. This combined the derived effects of surface reaction, diffusion and degradation during leaching tests. A shrinking unreacted core model also seemed to be a suitable way to express the leaching behaviour. This model incorporated the concept of acid exposure, rather than time, as the master variable in evaluating leaching behaviour and the rate of contaminant leaching was controlled by the inward diffusion of acid species into the alkaline depleted leached shell.

## CHAPTER 3

# MATERIALS AND METHODS

*In this chapter, the different variables and methods in the preparation and testing of the pozzolanic and geopolymeric matrices are discussed.*

---

### 3.1. INTRODUCTION

It is necessary to conduct laboratory scale tests to see how an immobilised material would react when subjected to long-term exposure to the environment. A real environment leaching medium would be ideal if we wanted to see exactly what would happen under natural conditions, but this would obviously take too long and more aggressive reaction conditions are necessary to speed up the process during the tests. In this study the aim was to characterise the degradation that the stabilised materials will experience due to long-term corrosion. When considering the degradation of the samples in a worst-case scenario, knowledge of the basic degradation mechanisms can be obtained. This can form a basis for predictions of the degradation behaviour that would occur in a landfill in a few years time, and the subsequent impact on the environment. The different samples, the test methods and the analysis methods are discussed in the following chapter.

### 3.2. MATERIALS

The two waste materials that had to be stabilised were:

- Jarosite, and
- Fly ash.

The origin and significance of these materials were already discussed in chapter 2. Of primary importance, though, is that they contain contaminants, which can be immobilised when we combine the wastes with specific additives.

From X-ray fluorescence (XRF) – analysis, figures 3.1, 3.2, 3.3 and 3.4 were obtained. These charts give an indication of the average consistencies of the jarosite and fly ash that were used for the samples.



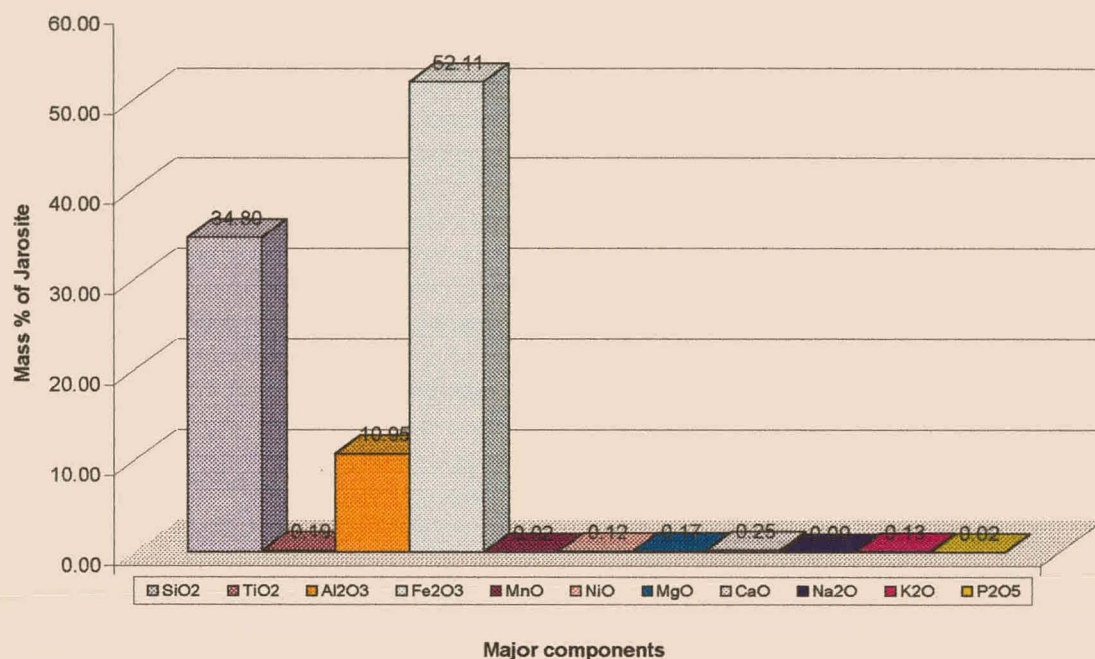


Figure 3.1: X-ray fluorescence analysis of Jarosite (major elements, expressed as oxides)

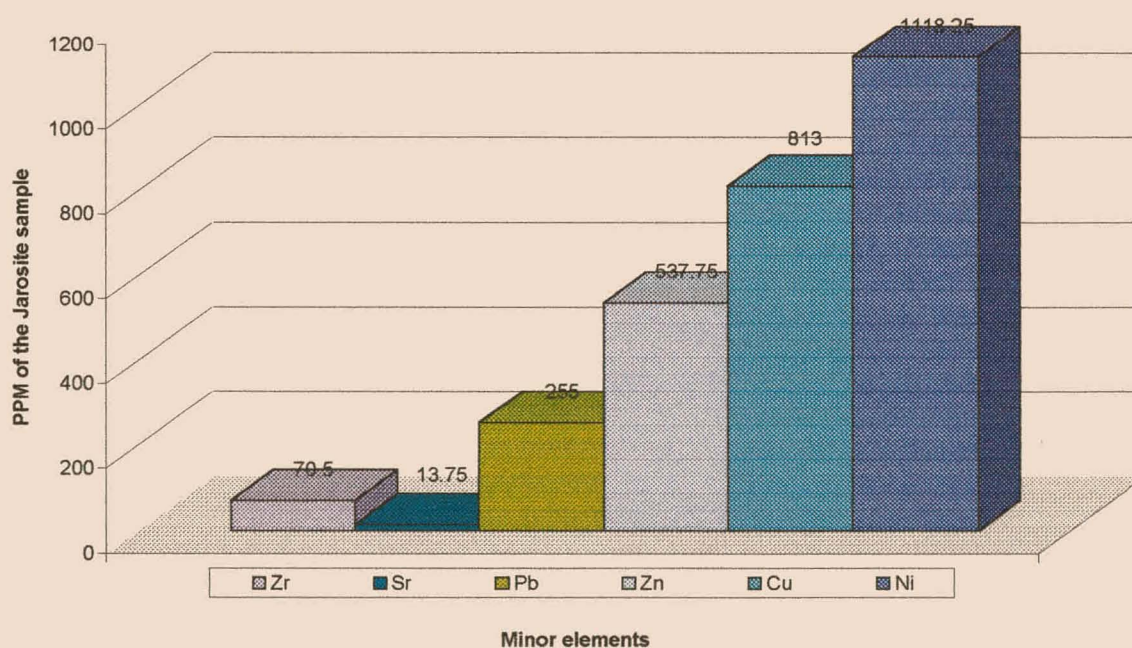


Figure 3.2: X-ray fluorescence analysis of Jarosite minor elements (in ppm)

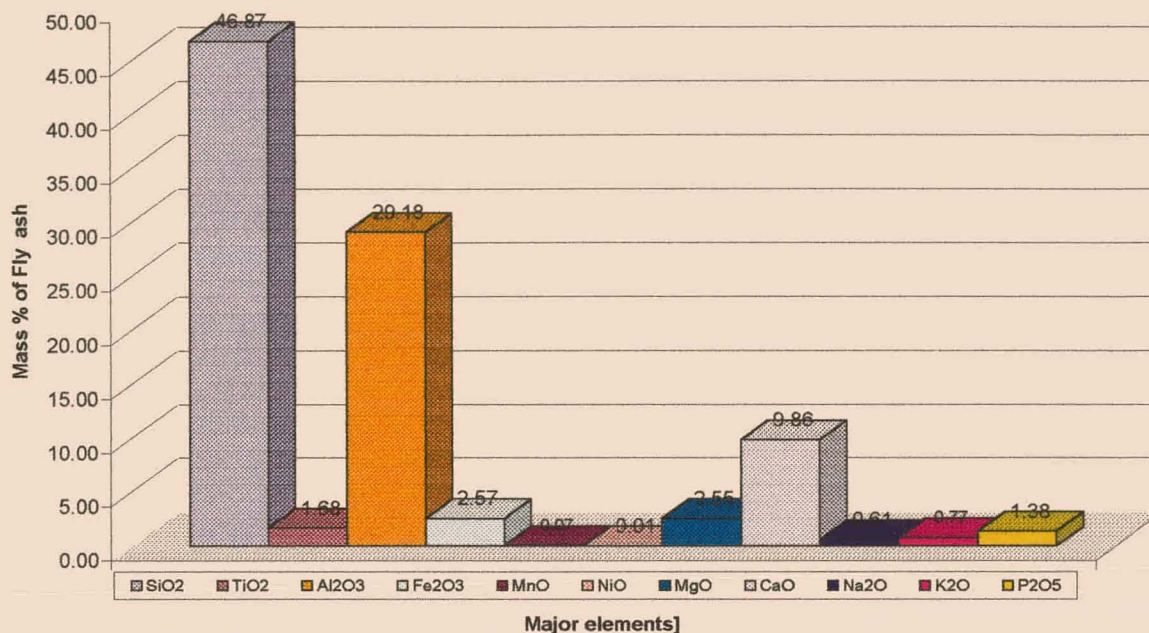


Figure 3.3. X-ray fluorescence analysis of fly ash (major elements, expressed as oxides)

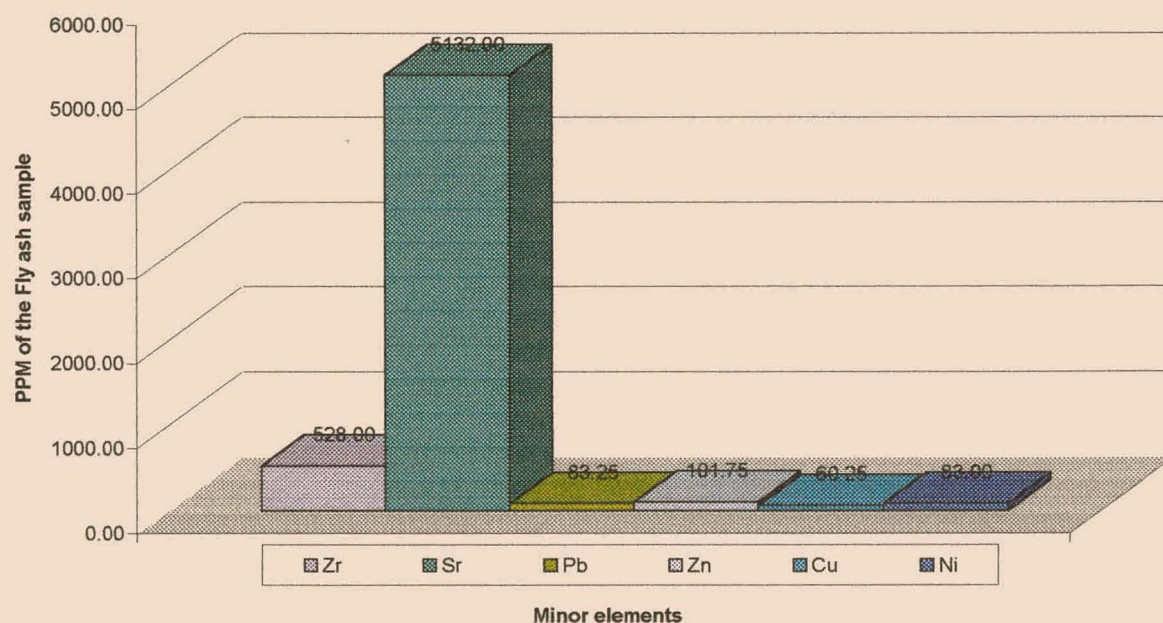


Figure 3.4. X-ray fluorescence analysis of fly ash (minor elements, in ppm)

Van Zyl (1997) mixed these wastes with various additives and established which additives and curing conditions gave the optimum stability results. Two of these developed matrices that exhibited the best stability behaviour, will be considered. The materials of these two



samples are tabulated in tables 3.1 and 3.2. Van Zyl(1997) found them to be of pozzolanic and of geopolymeric nature, respectively.

*Table 3.1 Ingredients of the pozzolanic matrix*

REAGENT	MASS PERCENTAGE [%]
Fly-ash	55
Jarosite	20
NaOH	10
CaO	15
Silica Sand	2:1
Water	~ 40 (mass percentage of dry ingredients)

*Table 3.2: Ingredients of the geopolymeric matrix*

REAGENT	MASS PERCENTAGE [%]
Fly-ash	50
Jarosite	20
NaOH	10
Sodium silicate solution	20

Silica sand	2:1
Water	~ 33 (mass percentage of all ingredients, including silica sand)

### 3.3. SAMPLE PREPARATION

The elements in tables 3.1 and 3.2 respectively, were combined and mixed with an ordinary electric hand-mixer to obtain in both cases a concrete-like material, which sets and hardens with time.

In both cases the Jarosite and NaOH was mixed with about half of the water and left for 2 hours, before any further additions. This step in the preparation process is essential to create sufficient opportunity for the conversion of jarosite to hematite. Thereafter, the rest of the ingredients were added, with silica sand added last of all. The sand is the bulking agent and the large volume causes difficulty during mixing.

After mixing, the material was poured into 5x5x5 cm<sup>3</sup> iron moulds, which were coated with an inert layer. For each test that was done, a few identical blocks were prepared to have reference samples that could be analysed to determine the average consistencies prior to any tests. From this, the average porosity could also be determined.

Curing of all the samples was performed in exactly the same way, because this could have a significant influence on the reaction products present inside of each sample. Van Zyl (1997) found that curing in a humid atmosphere lead to faster strength development and in our experiments the samples in their moulds were put into a room of 100% humidity for 8 days. After this time, the samples were removed from the moulds and the solid blocks were weighed and either used for the leaching tests or dried to determine the average mass of water present in the samples.

### 3.4. LEACHING TESTS

Standard leaching tests differ from country to country and the allowable contaminant concentrations of the elements in the leachate vary from one regulatory body to the next. It is therefore difficult to choose a specific leaching test that would characterise the degradation experienced by the immobilised matrices. Up to date, very little work has been done on the

long term leaching behaviour that such a material will have in the environment. Similar leaching tests, as were used by Jansen van Rensburg (1997) and Van Zyl (1997) were done. However, to give an indication of the longer term leaching behaviour, the tests were continued for longer times (a maximum of 670 hours for the pozzolanic case and 600 hours for the geopolymeric case). The same test was done for different samples of both the matrix types, and the tests varied from 0 to 600 hours, for the geopolymeric samples, and 0 to 670 hours, for the pozzolanic samples. It was necessary to stop the test at certain stages, to be able to see what is left of the solids after this period. Due to the destructiveness of the solid analysis method, new tests need to be performed for the analysis of the solid remainder after each leaching period.

A 5% acetic acid medium was chosen as the leaching solution for the tests. Jansen van Rensburg (1997) stated that acetic acid simulates ground acids and is a very aggressive leaching medium due to its buffering effect as well as complex formation. Acid rain was not used in these experiments, but future experiments with acid rain medium are advised, because this would simulate acid rain precipitation on landfill areas. Although the acetic acid tests would be more aggressive and present the worst case scenario, the acid rain might combine the effects of an acid attack and a sulphate attack, which is a slightly different degradation mechanism and could have different effects on the long-term stability.

The test set-up (figure 3.5) was also similar to the set-up used by Jansen van Rensburg(1997). She found that a batch test, with a stirred vessel was the most practical set-up. This was preferred to column leaching tests where problems with channelling of liquid through the samples, clogging of the sinter glass, rising of liquid levels and inaccurate pH and temperature control, were experienced. Van Zyl (1997) also used the stirred vessel set-up, due to practical problems experienced in other set-ups.

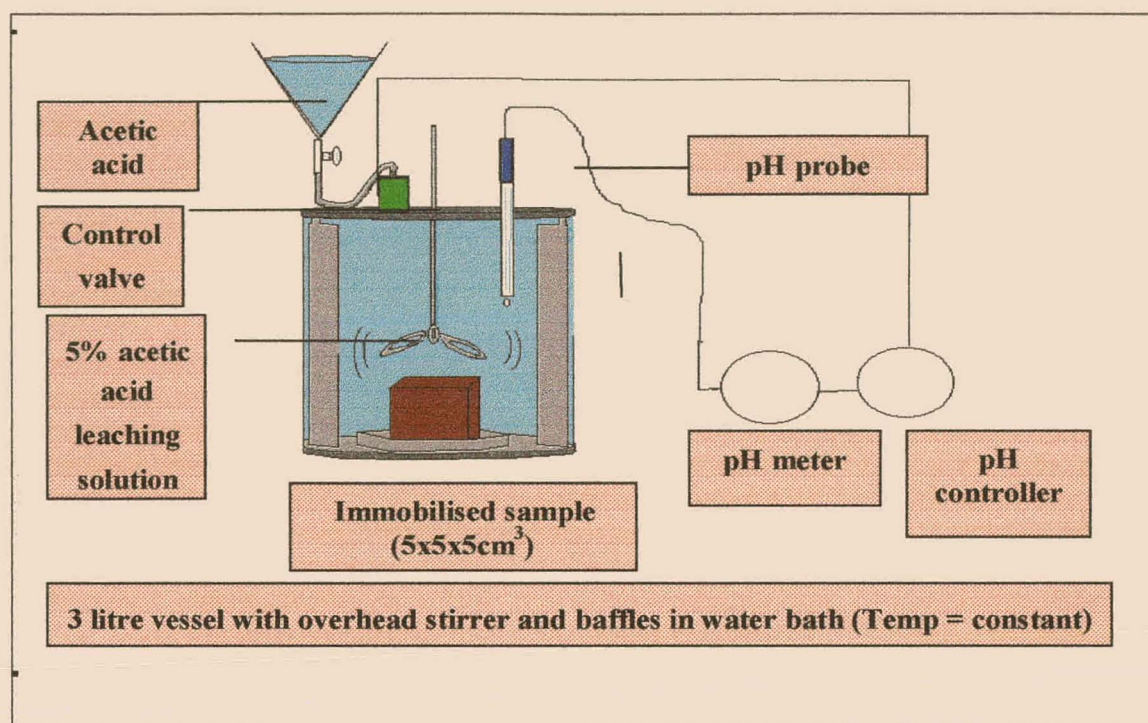


Figure 3.5: Leaching experiment set-up

The leaching vessel in figure 3.5 was situated inside a water bath with a temperature controller. The sample was placed inside of the 3 litre glass vessel, with overhead stirrer as seen in the figure and a pH-probe, coupled to a pH meter and –controller, was used to keep the pH constant, by adding concentrated acetic acid through the control valve, as soon as the pH rose above 2.45.

#### 3.4.1. Parameters kept constant

- Preparation and curing time of samples were kept as constant as experimentally possible. All the samples were cured for exactly 8 days under the same humid conditions, but slight variation in the sample sizes occurred due to slight differences in the mould sizes (supposedly 5x5x5 cm<sup>3</sup>).
- Only one leaching medium, acetic acid, was considered during the testwork. The solution was made up with 5% of acetic acid and distilled water, for all the tests.
- During these tests it was of great importance to keep the pH of the leaching solution constant, in order to minimise precipitation of suspensions as the pH increases. This adds to the aggressiveness of the leaching solution, because leaching is expected to decrease as soon as the solution pH rises. In all experiments the pH was regulated to be about 2.45.



- The leaching temperature was also kept constant during the tests at about 29°C. The standard temperature of 25°C was initially considered, but during the hot summer the atmospheric temperatures rose above this and to keep all experimental conditions as constant as possible, the higher temperatures were used in all the tests. Jansen van Rensburg found that the temperature only has an influence on the leaching behaviour in the first 500 minutes (i.e. 8 hours).
- A constant stirring rate for the different test runs were used. This rate was about 300 rpm. Work by Jansen van Rensburg (1997), indicated that the stirring rate might have a more pronounced effect in the initial phase of leaching, when the surface reaction has a dominant effect and could directly influence the physical degradation of the material, due to the effect of leaching of main matrix components such as aluminium and silica. However, the stirring rate did not show a significant effect on the leaching rate after leaching times > 500 min. Van Zyl (1997) considered a stirring rate of 70 rpm as a gentle, but adequate agitation of the leaching solution, but in this testwork, 300 rpm, as was used in most experiments by Jansen van Rensburg (1997), was selected as the constant stirring speed. Higher agitation rates was not feasible due to the resulting splashing and spillage of the solution from the leaching vessels, but the optimum rate was required for maximum degradation.
- Sample sizes were more or less constant. The average weight of the prepared pozzolanic samples accounted to 153 g (dry mass), with an average deviation of 5.82. For the geopolymeric case this average mass (dry) was 152 g, and the average deviation 7.67. The deviation could be due to differences in the moulds, which were not all exactly the same sizes.
- Liquid to solid ratios were kept more or less constant, but this could be influenced by, firstly the differences in mass of the different prepared samples as was just mentioned and secondly, due to volume changes during sampling and acid addition as the tests proceeds. Overall the volume stayed more or less the same and only samples that leached for longer times, where more samples were taken, had a mentionable volume decrease in the solution. The average sample mass was 152 [g] (geopolymeric and pozzolanic) accounts to a solid to liquid ratio of 1:20 [g(solid)/g(liquid)].
- The effects of the volume changes of the solution on the true concentrations of the samples were compensated for, by calculating a correction fraction for the volumes of the solution at the time of sampling (see later in chapter 6). For the calculation of this factor the acid added and samples subtracted from the solution were recorded throughout the tests. These factors were mostly 1 (no change in concentration), but did vary during the test up to 1.5. When expressing the overall volume change of the solution as a percentage of the original 3 litres, the volume changes seemed to be mostly below 15%, except for

the longer leaching tests such as L#11 (pozzolanic matrix leached for 670 hours) and G4 (geopolymeric matrix leached for 240 hours).

### **3.5. SAMPLING AND ANALYSIS**

#### **3.5.1. Solution analysis**

Samples of about 25 ml of the leaching solution were drawn from the leaching vessel at intervals throughout the testing procedure. These samples were then analysed by means of Inductively Coupled Plasma Spectroscopy (ICP), to determine the concentrations of the different elements in solution.

There was unfortunately in some cases a delay before the samples were analysed. This is not advisable, because in later experiments, it showed that the concentrations of some of the sample elements seemed to lower, while other element concentrations increased, after the samples were left for a few hours and these concentrations could not be considered in the results. From tests it was observed that the concentrations of samples that had just been leached for 24 hours, were similar after 168 hours (almost 3 days), but after 400 hours, it was clear that the major element concentrations decreased substantially, while the minor element concentrations increased. For samples that were leached for 48 hours and higher, the samples need to be analysed a little sooner after the test (less than 168 hours), because precipitation seemed to occur earlier at the higher concentrations. The best would have been to directly analyse each sample after it was taken from the solution. This was unfortunately not practically possible in this case and the sample concentrations were assumed to be the samples that were analysed within the shortest possible time (1 day).

#### **3.5.2. Solid analysis**

The samples were taken from the solution at different time intervals to analyse the element concentrations that were left in the solids at these stages. As was already mentioned, a new test needs to be performed for each different leaching time. Samples after each leaching time were cut into layers (figure 3.6) and each layer was analysed for major and minor components by means of X-ray fluorescence (XRF). From these results the remainder of each element in each layer could be seen as the leaching time increases. This was specifically done to determine how the leaching behaviour varies with depth into the block. Each layer was about 5 mm and the top 5 layers that were used, represented half of the block.

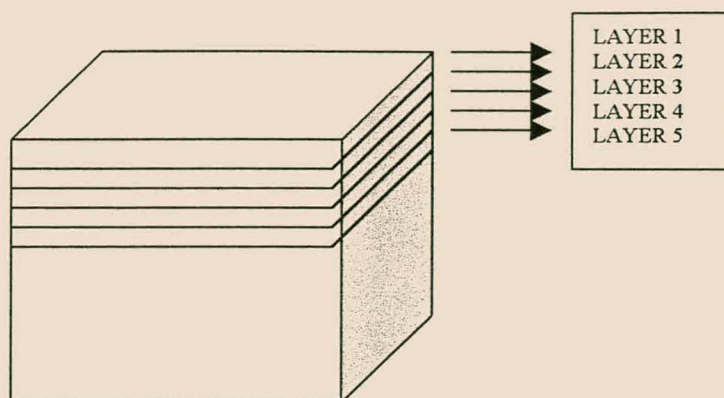


Figure 3.6: Layers in which samples were cut for XRF analysis.

- X-ray diffraction (XRD) was used on a few samples of the pozzolanic matrix to see what products were present after leaching. During this analysis the prepared samples were scanned and produced a series of peaks with different intensities. To determine the composition of the sample, peaks that fit on this pattern need to be searched from a database, that contains typical peak distributions of a magnitude of crystalline products. It is very difficult to identify exactly the composition of the products in the matrix, because only the crystalline components produce XRD peaks and the fit of possible products to the sample results needs to be done manually. This method was very time consuming and although the results gave an indication of what products might have been present in the matrix, no significant conclusions could be made of the degradation behaviour. This is possibly because the compounds that leached out were of amorphous nature, which cannot be analysed by this method. No XRD was done on the geopolymeric matrix, because this structure is supposed to have even less crystalline components, due to its semi-amorphous nature.
- A few samples of both the pozzolanic and geopolymeric matrices were viewed with the Scanning Electron-microscope, to clarify some of the behaviour of the matrix, by looking at typical samples of the structures when it is magnified between 100 and 2000 times.

### 3.5.3. Mass and Density determination

#### 3.5.3.1. Mass determination

This simply involved weighing of the samples as accurately as possible, directly after it was taken from the moulds (humid mass), then again after the samples were leached (wet leached mass) and then again after these same samples were dried. The prepared samples that are not used for the leaching tests are directly dried and from these samples an average water fraction in the humid samples (before leach) could be determined.



The scale that was used could weigh accurately to 1 decimal. It was important to weigh the sample as soon as it was taken from the solution or the moulds or after the dried samples cooled down, because evaporation and absorption of the vapour from the wet samples or onto the dried samples, seemed to be rather fast.

The samples were dried until the mass stayed constant, when it was assumed to be completely dry. The determination of the water content of the samples was used to express the porosity of the samples (i.e volume water in humid samples/volume of samples).

### 3.5.3.2. *Density determination*

The volumes of samples of the leached or unleached materials could be weighed accurately to 3 decimals, and the volumes of these samples were determined by using a densitometer. From the volumes and the mass measurements, it was therefore possible to determine the densities of the solid samples.

An average density for the pozzolanic matrix (leached) accounted to  $2.94 \text{ [g/m}^3\text{]}$  and for the geopolymeric sample the average was  $2.74 \text{ [g/m}^3\text{]}$ . These values were determined for use in the calculations of the porosity of the matrices. By weighing the samples and multiplying the values by the density, we could obtain the volumes of the solid mass, before or after leaching.

## 3.6. CONCLUSIONS AND RECOMMENDATIONS ON THE MATERIALS USED

In conclusion, two geo-chemical types of matrices were prepared, the pozzolanic and geopolymeric matrices, and leached with an acetic acid, batch leaching test in which the pH and most other variables was kept constant. This was done for different time intervals, after which the remainders of the solids were analysed by means of XRF, to determine the amounts of the different elements that were extracted from the solid during different leaching times. The blocks were also cut into layers, to determine the effect of depth into the block on the rate of leaching.

Samples of the solution were taken during each test and analysed with ICP. This should present more or less similar leaching curves for each case, unless the samples were kept for too long prior to analysis, or some of the reaction constants differed due to experimental problems or natural variation (e.g. sample concentrations and reaction products, might differ slightly due to the complex formation mechanisms).

As was already mentioned, it is advised that, apart from the acetic acid test, tests with an acid rain medium, should also be done on these samples, as a different degradation behaviour is expected in such a medium, especially regarding possible differences in crack formation.

Van Zyl (1997) prepared more matrices with jarosite and fly ash, and among the other matrices with optimum strength and immobilisation conditions, was a matrix with a cementitious consistency and a matrix in which the different geo-chemical types (pozzolanic-, geopolymeric-, and cementitious-) were combined. The degradation in these two types should also be investigated in further tests to determine how their long-term stability (and degradation, for that matter) compares to that of the pozzolanic and geopolymeric samples.

## CHAPTER 4

# PHYSICAL AND MICROCRYSTALLINE BEHAVIOUR

*In this chapter the observations of the physical degradation during acetic acid leaching tests on samples of the pozzolanic and geopolymeric matrices are discussed. Also, some microcrystalline observations were obtained from scanning electron microgram (SEM) photographs in order to give an indication of possible degradation mechanisms.*

---

### 4.1. INTRODUCTION

Samples of the pozzolanic and geopolymeric matrices were prepared, cured and subjected to acetic acid leaching tests, as discussed in chapter 3. Physical factors which can influence the leaching behaviour, such as pH, stirring speed, sample composition, liquid to solid ratio, curing time of the samples etc., were kept as constant as possible throughout the tests. The only variable in the following experiments, is the time of exposure of the samples to the leaching solution, to enable us to characterise the degree of degradation at different times during the tests.

### 4.2. OBSERVATIONS DURING LEACHING TESTS

#### 4.2.1. Pozzolanic matrix

In general, severely degraded samples appear to come apart due to cracks forming (more or less 5mm from the surface), followed by the outer 5 mm layer becoming detached from the main block sample. With further leaching, this also happened to a second layer in some of the samples. The effect was that these blocks partially fell apart. The effect can be visualised as an onion being peeled. The outer layers peel off, while the core stays intact. Apart from cracking, the matrix also slowly corrodes away from the outside, leaving an uneven surface.

The observed results are summarised in table 4.1

*Table 4.1: Physical observations during leaching tests on the pozzolanic material*

<u>Leaching test run number:</u>	<u>Total leaching time</u>	<u>Observation:</u>
L#9	17 days [404 hours]	The surface is clearly corroded and small cracks can be seen all over the top surface of the sample. The outer layers of the block seem to be on the verge of becoming detached from the block and the bigger cracks seems to be parallel to the surfaces. Smaller cracks on the top surface of the block appear to start at the outer rim of the block and move inwards towards the centre.
L#11	36 days [868 hours]	The block broke up into slices after about 68 hours, i.e. the outer layers became detached from the block due to cracking, giving the same effect as when an onion is peeled. Severe corrosion of the surface is also detected.
L#12	4 days [96 hours]	The same peeling phenomena as in L#11 were observed, where 5-6mm layers of the sides cracked and became detached from the sample.
L#15	1.2 days [29 hours]	Wear on the surface, especially the upper surface, with a multitude of small cracks all over.
L#16	7 days [161 hours]	Degraded and cracked inside.
L#17	4 days [52 hours]	No significant cracking patterns were observed. The surface showed signs of corrosion. See figure 4.2
L#18	6 days [141 hrs]	No significant cracking were observed. Corrosion of the surface seems to be more than after L#17. See figure 4.4
L#19	6 days [144 hrs]	No significant cracking were observed apart from surface corrosion. See figure 4.5.

Various leaching tests were conducted in the same fashion, on this kind of matrix. The only variable was supposed to be the time of exposure to the leaching medium, but a great degree of variability seemed to reign in the degradation behaviour of the different samples. No crack formation was, for example found in L#18 and L#17, where the samples were exposed to the



leaching solution for 6 and 4 days respectively, although cracking was observed in L#12 where the test also lasted for 4 days. Clearly, the leaching time was not the only variable as assumed, and other possible variables in the preparation, immobilisation reaction and leaching of the samples needs to be considered as the cause for the different degradation results of the tests.

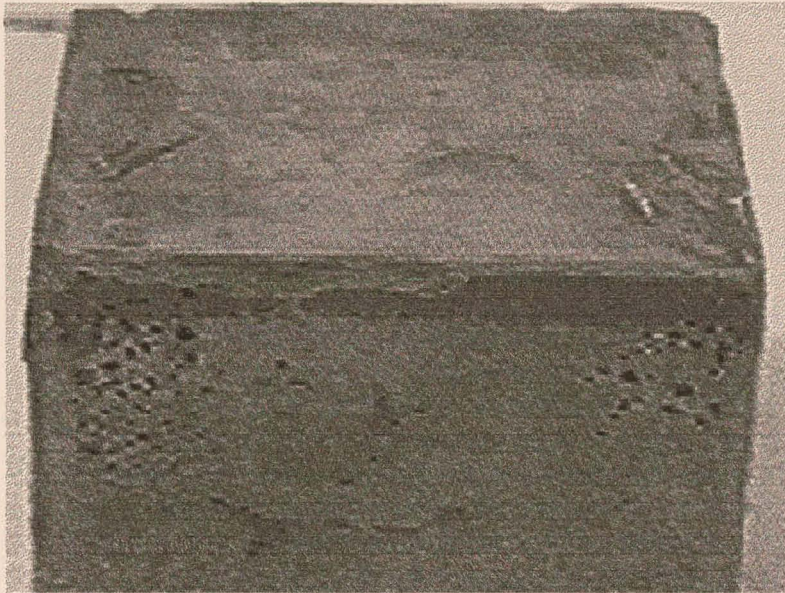


*Figure 4.1: Sample of the Pozzolanic matrix before the leaching test (L#17)*

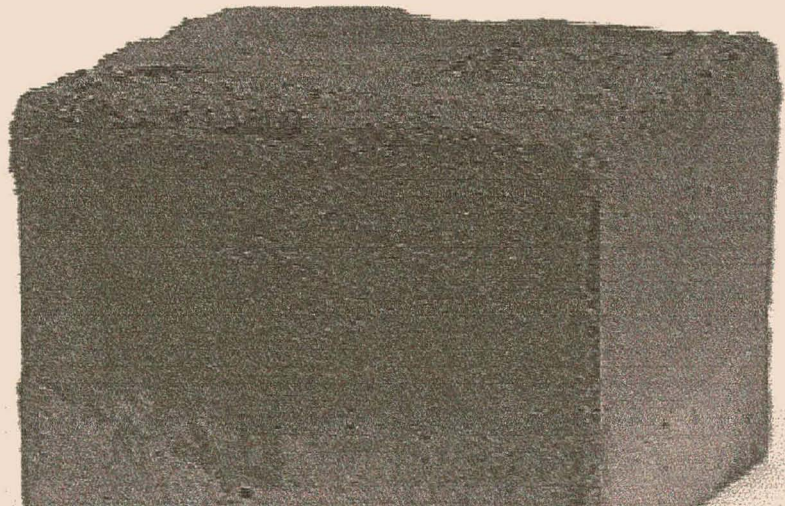


*Figure 4.2: The pozzolanic sample above after it has been subjected to a leaching test lasting 4 days (L#17)*



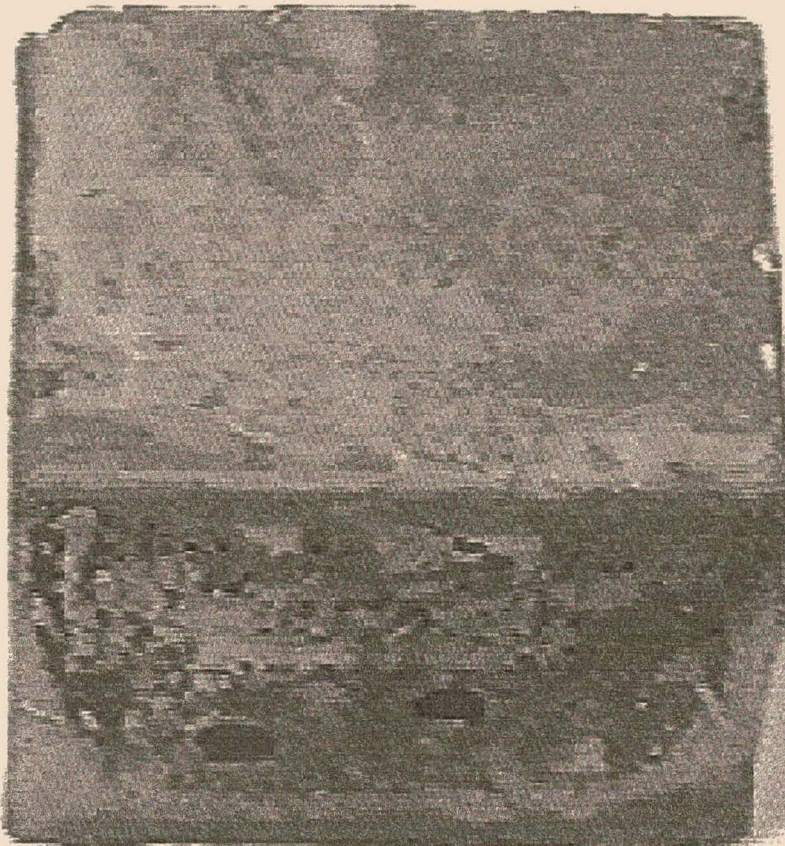


*Figure 4.3: A pozzolanic sample prior to leaching test (L#18)*



*Figure 4.4: The sample in figure 4a after a leaching time of 6 days (L#18)*





*Figure 4.5: Pozzolanic sample in the leaching vessel, after leached for 6 days (L#19)*

From these observations, one must conclude that there was some variation in the leaching behaviour even though the tests were done in the same way. Some samples were severely cracked, while others were just corroded on the surfaces, even though they were leached for longer. These dissimilarities can most likely be accounted for, by the very complex stabilisation reactions. Changes in reaction products of the different samples could lead to dissimilarities in structure, possibly inducing different stresses and weaknesses inside of the matrix.

Slight variation in the acid concentration during the different leaching tests is also possible, due to faulty readings by the pH probes and subsequent additions of too little or too much acid. However, it is expected that crack formation inside of the matrix attributed most significantly to the observed degradation (the peeling effect in some of the samples). Therefore, slight changes in the leaching solution pH, might not have such a noteworthy effect on the crack formation as would be expected from the matrix composition itself.

#### **4.2.2. Geopolymeric matrix**

The observations during acetic acid leaching tests on different samples of the geopolymeric matrix are summarised in table 4.2.

The degradation of the geopolymeric matrix appeared somewhat different from that of the pozzolanic matrix. The samples were softer than the pozzolanic samples directly after curing in a humid atmosphere and the crack formation when leached was also different. It is, however difficult to say which of the geopolymeric or pozzolanic samples degrades the most, at this stage.



The same ingredients were used for the different samples of each matrix, but slight variation in the distribution of elements after mixing, might have led to differences in the binding reactions of the matrix. Overall, the cracks that formed in this matrix were finer, and the wider spaced cracks (layers of 5mm) were not observed for the geopolymeric matrix, as was the case with the pozzolanic matrix.

The exposure to the acid solution leads to a flakiness in texture, which was different for the pozzolanic matrix, where the acid rather seemed to corrode away some of the material, than leaving flakes on the sample. In figures 4.6 the sample leached during G7 (test run of 6days) are photographed, just after the test.

*Table 4.2: Physical observations during leaching tests on the geopolymeric material*

<u>Leaching test run number:</u>	<u>Total leaching time</u>	<u>Observation:</u>
G1	25 days [600 hours]	Severe cracking after 12 days (more or less after 296 hours) was observed. Thin slivers peeled off from the surface.
G3	6 days [144 hours]	No major cracks were observed, throughout the test.
G4	10 days [240 hours]	After day 4, fine cracks were seen on the sides of the sample.
G5	1 day [24 hours]	The surface was slightly worn, but no cracks appeared.
G6	1 day [24 hours]	No severe cracks, only degradation of the surface.
G7	6 days [144 hrs]	Shortly after the sample was put into the solution (after about 9 hours) a heap of loose material were found on the surface of the block. The material came loose in little flakes and was dispersed on the block and on the bottom of the leaching vessel. After 4 days cracks were also observed on the sample.

Generally, cracks are not produced by the acid attack itself, but instead the exposed aggregates are observed on the surface, due to the disintegration of the cement paste. During the evaluation of the degraded samples, this kind of deterioration seems very likely to have taken place during the acetic acid leaching tests on both the pozzolanic and geopolymeric samples. This was probably in conjunction with other mechanisms that were responsible for the formation of cracks. The gradual depletion of calcium in the outer layers of this pozzolanic material (as seen from the XRF analysis in chapter 5), as well as the corrosion of the surfaces, as observed in all the sample surfaces, might be explained by this reaction.

#### 4.3.2. Alkali Silica Reaction (ASR)

The alkali silica reaction causes degradation due to the swelling of gel inside of the matrix. This gel is formed by the reaction of alkali's in the pore solution with reactive silica in aggregates, which, in the presence of water, leads to expansion and cracks. Some of the samples did show cracks, and the alkali silica reaction might well be the mechanism responsible for internal swelling inside of the samples and subsequently, crack formation. However, not all samples displayed cracks and those that did, cracked to different degrees, which could not be directly related to leaching time. Fine cracks all over the surface, bigger cracks parallel to the surfaces, which caused the layers to become detached, and also a combination of the two, were revealed during different leaching test runs (see table 4.2). In the geopolymeric samples smaller cracks that were closer to each other were observed. This was somewhat different with the pozzolanic samples, where larger cracks seemed to detach the outer layers of the block. It is possible that ASR occurred in all of these samples, but to a lesser extent in some samples than in others, causing severe cracks in some samples and no substantial visible damage in others. This can be attributed to the complex nature of the formation reactions of the matrix, possibly causing less reactive silica in the outer layers of some blocks, or perhaps slower hydration, due to lower permeability. The last two effects might cause a decreasing rate of ASR and less crack formation.

However, contradictory to the gel-like materials expected to form during the alkali silica reaction, crystals can clearly be observed inside of the cracks on the pozzolanic matrix. The latter might instead or additionally to ASR, be responsible for the cracking of the pozzolanic material. In figure 4.7 the SEM shows that the crystals are needle shaped (as ettringite is expected to be). However, from analysis the crystals consisted of mainly Ca, but also P, and thirdly some Si (in order of strongest to weakest peak intensities). Aluminium peaks were also present although at rather low intensities. No S was found in the crystals and the observed crystals are therefore not likely to be gypsum ( $\text{CaSO}_4 \cdot \text{H}_2\text{O}$ ) or ettringite ( $3\text{CaO} \cdot \text{Al}_2\text{O}_3 \cdot 3\text{CaSO}_4 \cdot 32\text{H}_2\text{O}$ ), which are also known to bring about cracks.

In figures 4.11 to 4.22, the SEM photographs showed that a more amorphous texture is present in the geopolymer. These pictures were taken of some of the layers of the geopolymers of different leaching times.

#### 4.3.3. Sulphate attack

This kind of deterioration is not likely to occur in either of the matrices, due to the absence of an external sulphate source. Also no sure signs of ettringite or gypsum were found during X-ray diffraction analysis of the samples. During a leaching test with sulphuric acid, this attack can be expected.

#### 4.3.4. Delayed ettringite formation

This formation is also ruled out as the primary degradation mechanism, mainly due to the absence of heat curing history in the samples (prerequisite for delayed ettringite formation).

#### 4.3.5. Conclusion on mechanisms of degradation

##### □ *Pozzolanic matrix*

In conclusion, when considering the scanning electron microscope (SEM) -analysis and crack patterns, the main mechanisms of degradation for the pozzolanic matrix seemed to be acid attack and also possibly the alkali silica reaction. Cracking due to the alkali silica reaction is caused by the hydration of gels. However, crystals were found in the cracks in this material. It is therefore very likely that these crystals (or the hydration and swelling of these crystals) initiated the cracks instead or additional to the ASR. The crystals contained Ca, P, Si, and some Al according to the SEM analysis of figure 4.7. and is not considered to be ettringite crystals.

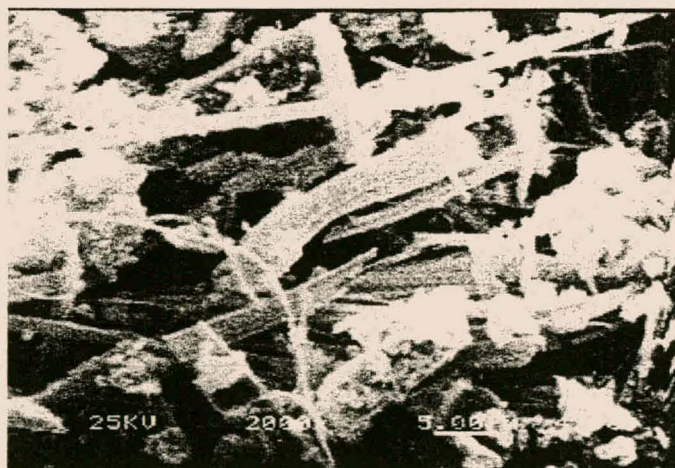


Figure 4.7. The crystals found inside of a crack formed in the degraded pozzolanic matrix after a leaching test of 150 hours. The SEM showed that these crystals consist mostly of calcium, secondly some phosphor and also some silica. Another small peak could be identified as some aluminium, but no sulphur was found in these crystals [magnification = 2000x.



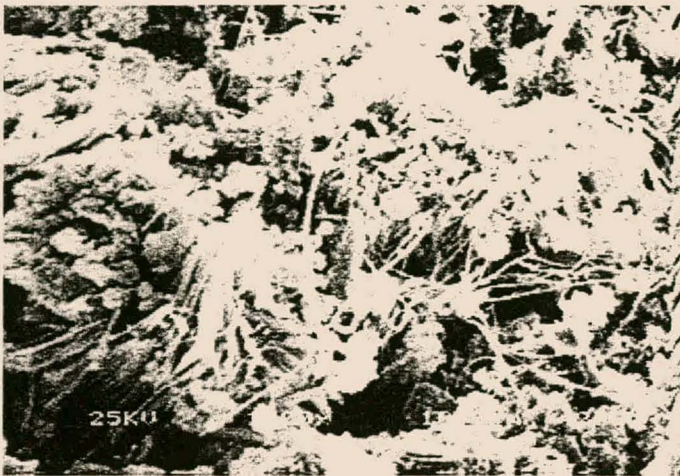


Figure 4.8 SEM photograph of the remainder of the pozzolanic matrix after a leaching test L#18 [magnification = 1000x].

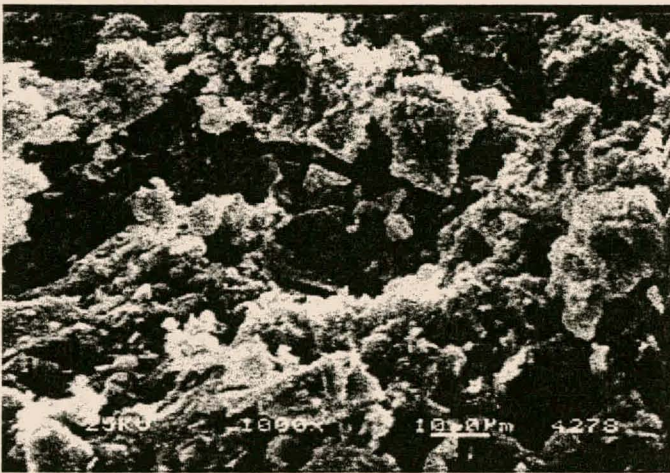


Figure 4.9: Another part of the pozzolanic matrix after a leaching test of 144 hrs (L#18) [magnification = 1000x].



Figure 4.10: Grooves in the side of the sample after L#18 [magnification = 100x].



#### □ *Geopolymeric matrix*

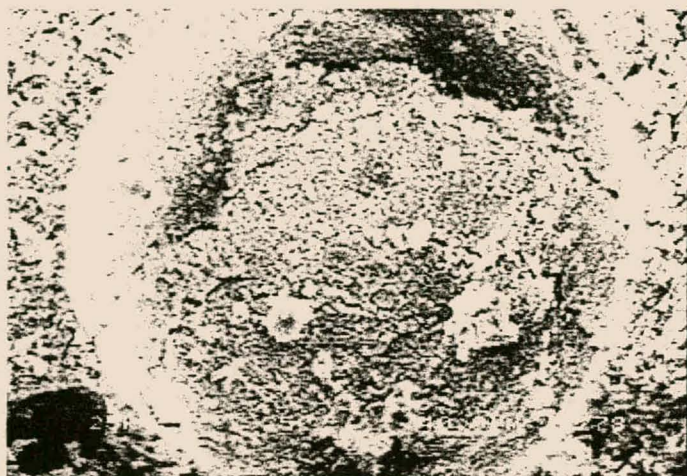
The geopolymeric matrix is less crystalline in nature and consists primarily of gel phases. The formation of crystals in the pozzolanic matrix, might be the cause for the wider spaced cracks which loosen 5 mm layers from the pozzolanic block, and the absence of these crystals might explain why these large cracks do not occur in the geopolymeric samples. The main mechanisms for this matrix type are also assumed to be acid attack and the alkali silica reaction.



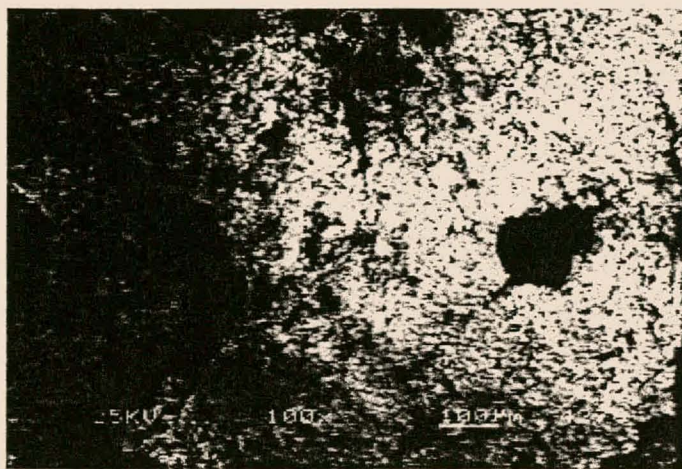
Figure 4.11: Sample of the geopolymeric matrix leached for 240 hours (G4) [magnification = 1000x].



Figure 4.12: Sample of the second layer of the geopolymeric matrix leached for 24 hrs (G6) [magnification = 1000x].



*Figure 4.13: The same part of the geopolymeric matrix sample as in figure 4.13 above, but only magnified 250x, showing that it is in actual fact inside of a pore.*



*Figure 4.14: 100x magnification of a sample from the second layer of the sample leached for 240 hrs (G4). (Note the pore of about 10 $\mu$ m on the right).*



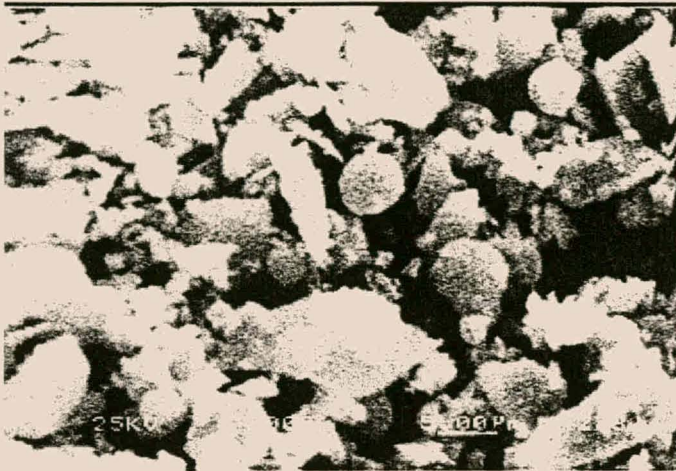


*Figure 4.15: 2000x magnification of a sample from the first layer of the sample leached for 72 hrs (G2) (The spheres seem to be mostly Al and Si. Apart from Si and Al, Fe and some P are also present in this sample, but Ca seemed to have leached out).*

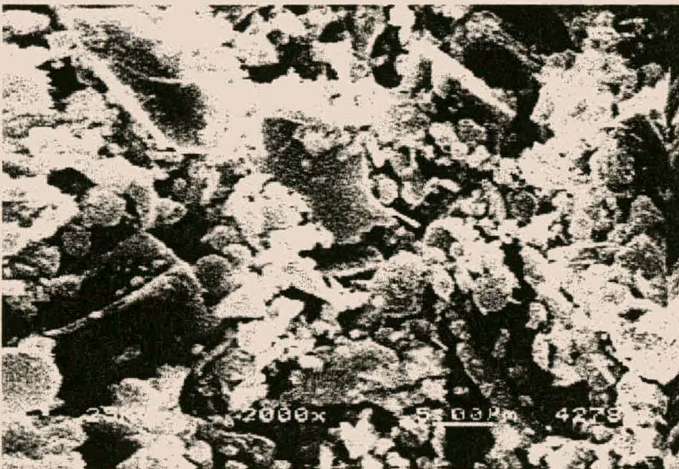


*Figure 4.16: 2000x magnification of a sample from the first layer of the sample leached for 144 hrs (G3).*

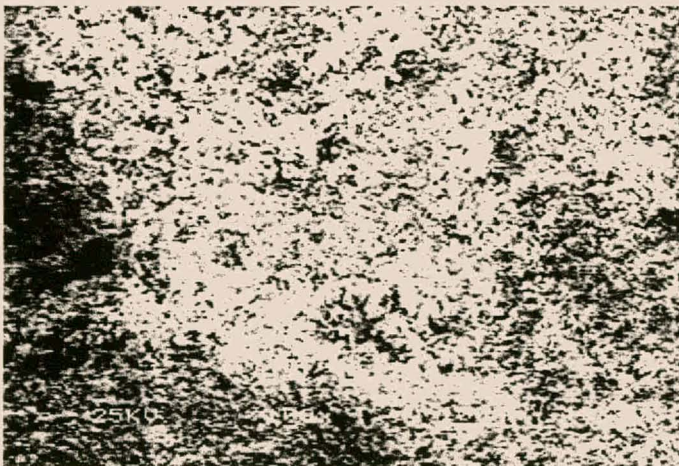


*Figure 4.17: 100x magnification of the sample above (144 hours leach, G3).*



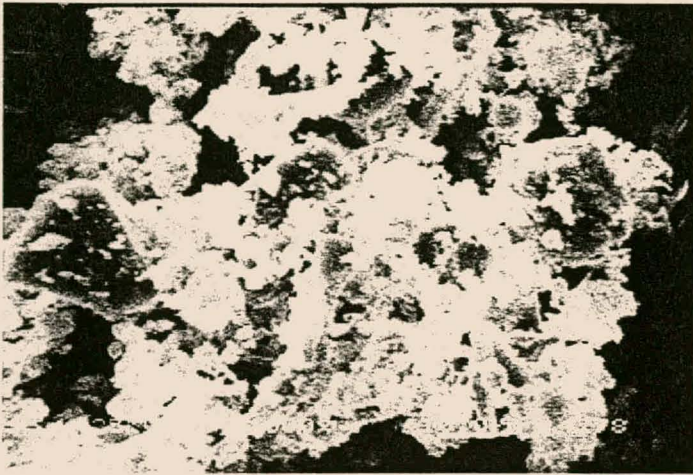


Figure 4.18: 1000x magnification of a piece of a geopolymeric sample, which was not subjected to a leaching test yet. (The lighter parts of the photograph are mostly silica).

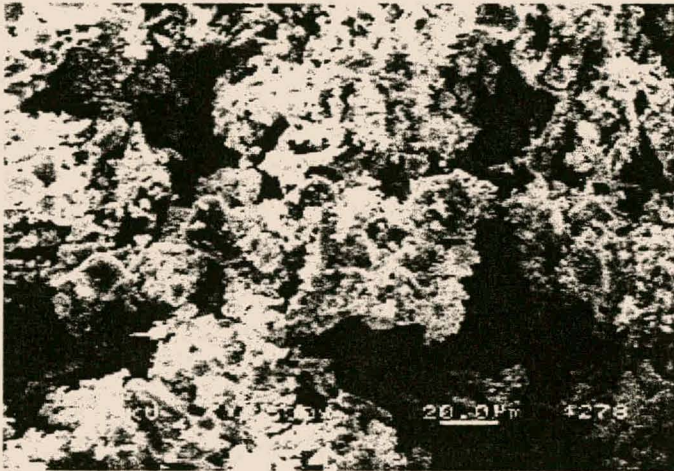


Figure 4.19: 500x magnification of the same part of a geopolymeric sample as in figure 4.18.

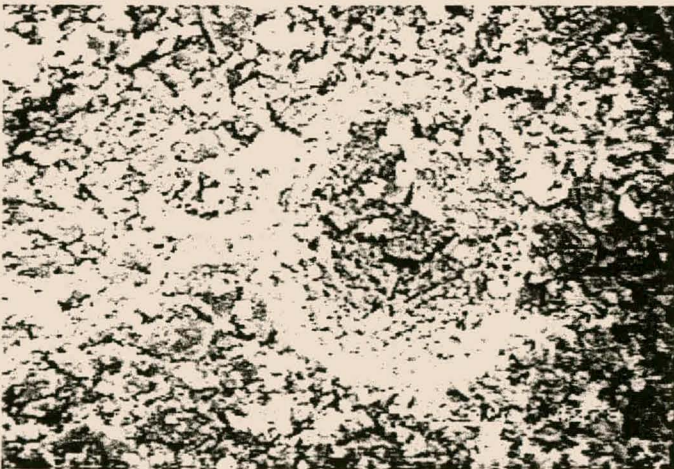
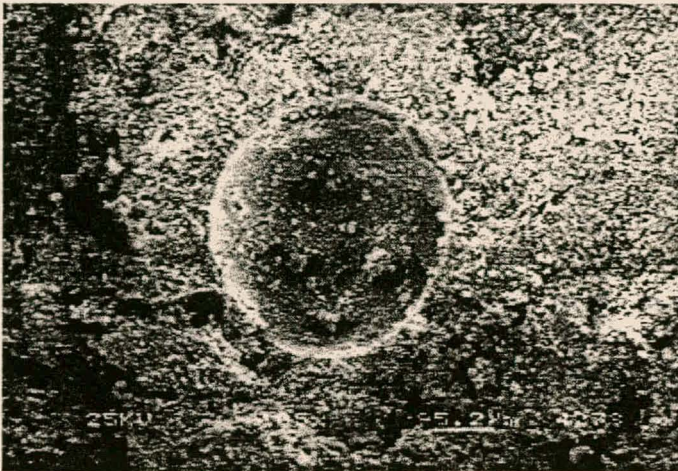
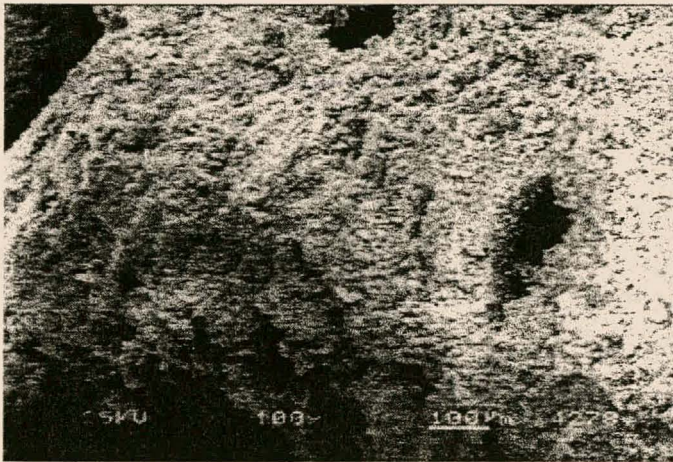


Figure 4.20: 500x magnification of a pore (8-9  $\mu\text{m}$  diameter) in the first layer of a sample leached for 24 hrs (G6) – Consists mostly of Si and P, no Ca, Mg, Al or Fe were found.





*Figure 4.21: 105x magnification of a pore from the second layer of the sample of G6 (about 40  $\mu\text{m}$ ).*



*Figure 4.22: 100x magnification of another piece from the second layer of the geopolymeric matrix, leached for 24 hrs (G6) (The pore on the bottom, right, is about 10  $\mu\text{m}$  wide).*

In conclusion, when considering the scanning electron microscopic (SEM) analysis and crack patterns, the main mechanisms of degradation seem to be acid attack and also possibly the alkali silica reaction for both the pozzolanic and geopolymeric cases. Still additional mechanisms, especially in the pozzolanic samples, might contribute to the degradation phenomena.

#### **4.4. MASS LOSS AND POROSITY CHANGES**

##### **4.4.1 Mass loss during leaching**

The mass loss of matrices during leaching, might also give an indication of the degree of degradation that was experienced during each test. The values in figures 4.23 and 4.24, was calculated, by weighing the samples, just after curing and drying some of the samples to determine the average water content of the humid samples. After the leaching tests, the

samples were dried again and the dry mass of the leached samples could be determined before and after each leach. The differences between these masses were plotted for the leaching tests on the pozzolanic matrix in figure 4.23 and for the geopolymeric tests in figure 4.24.

#### □ *Pozzolanic mass loss*

From figure 4.23 it is evident that considerable variation in the data occurred and the degradation of the pozzolanic samples did not happen strictly according to any particular trend. The sample that was leached for 96 hours seemed particularly out of place and less stable than the others. This could be due to differences in the exact reaction products inside of the material, which would influence the way in which elements are bound to the matrix structure and might be responsible for a more sound structure in one case than another.

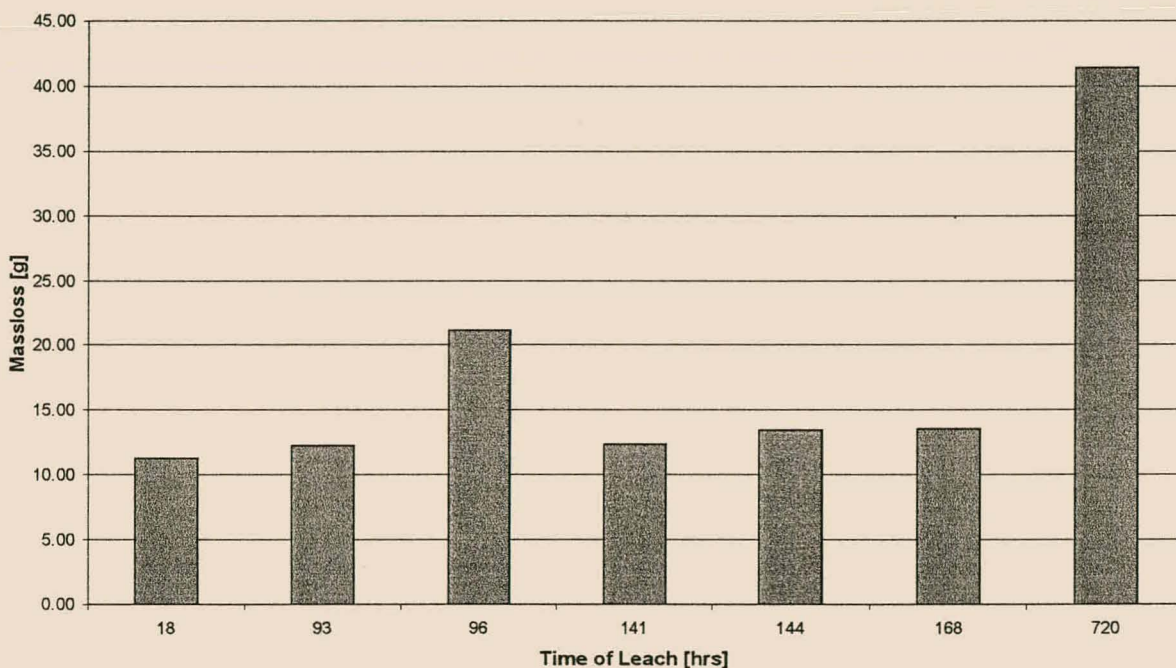


*Figure 4.23: Mass loss during various acetic acid leaching tests on the pozzolanic matrix.*

An exponential curve could be fitted on the data (with an R-square-value of 0.86). This gives an indication that the mass loss of the pozzolanic matrix might increase exponentially with increase in leaching time. More experiments is necessary to verify this, though.



### □ Geopolymeric mass loss

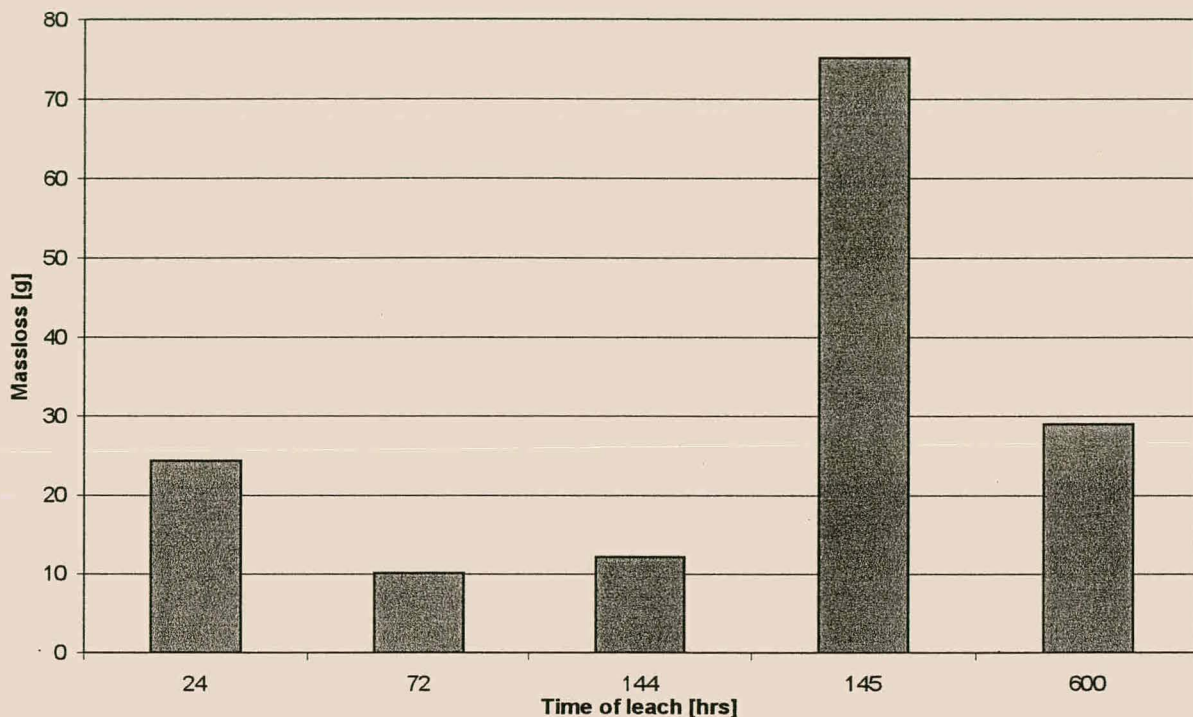


*Figure 4.24: Mass loss during leaching tests on the geopolymeric matrix*

In figure 4.24 the mass loss in the leaching of the geopolymeric samples also exhibited considerable fluctuations in degradation behaviour and the blocks seemed to behave differently during each leaching run, even though the same reaction conditions were maintained. The mass loss after 72 hours and after 144 hours seemed to be less than the loss experienced after 24 hours and after 145 hours the loss seemed much greater than after 600 hours. This cannot readily be explained and the variation in sample structure seemed to be even more than in the pozzolanic case, so that some samples are more stable and less prone to break up than others.

#### 4.4.2 Porosity changes during leaching

An average initial porosity (before leaching) was calculated for each batch of samples that we prepared (by drying a few samples and determining the average mass of water present). From this we could obtain the volume of water in a sample just after preparation (100% humid). After the leaching tests, the wet samples were also weighed and dried, and the volume of water in the leached samples was determined from these values. These samples have, however, been submerged in the leaching solution, in contrast to the initial samples that were just exposed to a humid atmosphere, and the pores might possibly be completely filled, or at least to a greater extent filled, with vapour than the samples that was not submerged in liquid. To compensate for this, tests were performed to determine a correction factor. The initial water

volumes were multiplied with an average calculated correction factor of 1.1 for the pozzolanic samples, and 1.04 for the geopolymeric samples. And the equations used for the porosity calculations before and after the leaching runs are given in equation 4.2. and 4.3., respectively.

$$\text{Porosity(before)} = V_{\text{water1}} / (V_{\text{water1}} + V_{\text{block1}}) \quad (4.2)$$

$$\text{Porosity(after)} = V_{\text{water2}} / (V_{\text{water2}} + V_{\text{block21}}) \quad (4.3)$$

Where:

- $V_{\text{water1}}$  = the volume of the water in the 100% humid samples (straight from moulds) x correction factor
- $V_{\text{water2}}$  = the volume of the water in the leached sample (straight from leaching solution)
- $V_{\text{block1}}$  = the volume of the block as calculated from the dry mass of the samples before any leaching divided by the average densities of the samples (as obtained from densitometer measurements)
- $V_{\text{block2}}$  = the volume of the block as calculated from the dry mass of the samples after the different leaching tests (divided by average density of the solid)

#### □ *Pozzolanic matrix porosity*

It is clear from figure 4.25 that, as in the cases of the mass loss during leaching, no particular trend were followed in the porosity behaviour of the samples. A better porosity determination method could have influenced the data and possibly produced more reliable data, but the fluctuations are assumed to be due to the differences in leaching behaviour during the tests rather than the determination method. The porosity do seem to increase as the leaching time increases, but substantially more data points is necessary to produce an average trend for the porosity increase.



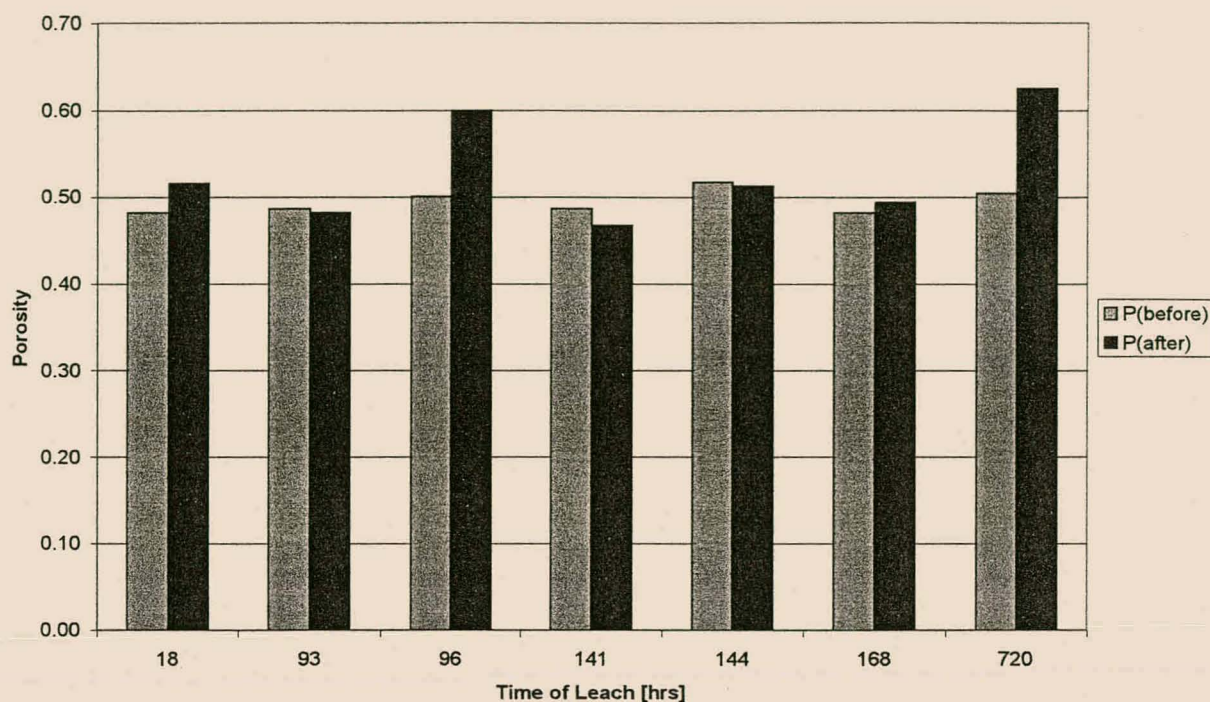


Figure 4.26: Porosities of matrices after leaching tests as calculated for the leached pozzolanic matrix

□ Geopolymeric matrix porosity

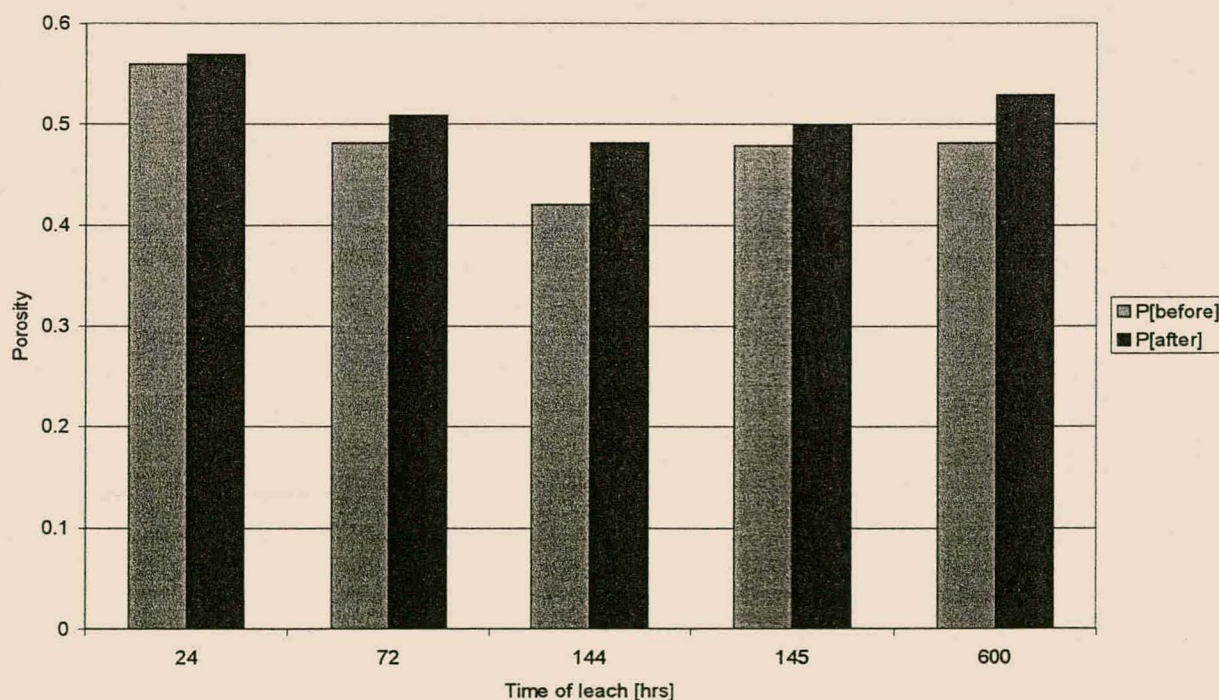


Figure 4.27: Porosity of matrices after leaching tests as calculated for the leached geopolymeric matrix



The porosity of the geopolymeric sample (figure 4.27) seems to generally increase as the leaching time increases and more of the major matrix components are being leached out, but as in the case for the pozzolanic matrix, no specific trend could be deducted from these data points. More tests need to be done to find a sure curve that would fit on this data. More data points are expected to exhibit either an exponential or logarithmic curve for the porosity when plotted against leaching times. For exact comparison of porosity after different leaching times, the initial porosity should be equal, which is difficult to achieve experimentally.

#### **4.4.3 Conclusions on the mass loss and porosity changes during leaching**

There are signs that the mass loss of the pozzolanic matrix might in fact exhibit exponential behaviour and that the porosity of the geopolymeric matrix might increase exponentially or logarithmically with leaching time, but the data produced from these leaching tests were not sufficient to verify this suspicion. More repetitions of these tests need to be done to determine if the mass loss and porosity changes, during the leaching of pozzolanic and geopolymeric matrices, will in fact, follow these trends.

### **4.5. CONCLUSIONS ON THE PHYSICAL DEGRADATION OF POZZOLANIC AND GEOPOLYMERIC SAMPLES**

#### **4.5.1. Observed leaching behaviour of pozzolanic and geopolymeric samples**

A specific crack pattern, similar to the effect of peeling an onion, was observed in leaching of some of the pozzolanic samples. Large cracks seem to form about 5mm from the sample surfaces and the whole layer seem to become detached from the sample, due to these large cracks, and with longer exposure to the leachate, this also happened to a second layer. This was not observed for all the samples, due to evident variation in behaviour during the different tests, which can be attributed to differences during the complex reactions in the samples, which lead to samples that slightly vary in strength and would degrade to different degrees.

The same reasons can be given for the variation in the degradation behaviour of the geopolymeric samples. The “onion effect” as in the leaching of the pozzolanic matrix, was not observed in this case and the outer layers seemed to rather flake off and small cracks were observed compared to the large cracks that were seen in the pozzolanic samples.

#### **4.5.2. Microcrystallinity and primary degradation mechanisms of the pozzolanic and geopolymeric matrices**

When considering the scanning electron microscopic (SEM) analysis and crack patterns, the main mechanisms of degradation seem to be acid attack and also possibly the alkali silica reaction for both the pozzolanic and geopolymeric matrices. The acid attack is most likely

responsible for the corrosion of the surfaces as were observed for both the matrices during the tests. The alkali silica reaction, in turn, might be the source of cracks due to the hydration and subsequent swelling of the alkali-silica gels that are likely to form in both structures.

Additional to these reactions, larger cracks in the pozzolanic matrix, might also be due to crystals (containing Ca, P, Si, and little Al), which could expand and crack off layers of the samples.

Other general degradation mechanisms such as delayed ettringite formation and sulphate attack do not seem to occur during these tests. When leaching with acid rain, however, the sulphate attack is likely to contribute to degradation.

#### **4.5.3. Mass loss and porosity changes of the pozzolanic and geopolymeric matrices**

No trends could be fitted with great accuracy onto either the porosity changes or the mass loss during leaching of the pozzolanic and the geopolymeric samples. The variation in the calculated values, are assumed to be due to natural variation in sample consistencies, which would lead them to degrade more substantially in some cases than in others.

As was mentioned before, if some of the fluctuations are ignored, and regarded as errors, there are signs that the mass loss of the pozzolanic matrix might increase exponentially as the leaching time increases. An exponential curve fitted on the porosity against leaching time data of both the geopolymeric and pozzolanic matrices, did not produce good correlations, but more leaching tests (done in the same way) might determine whether there are in fact a trend followed in both the mass loss and porosity increases, during leaching of pozzolanic and geopolymeric structures.

## CHAPTER 5

# RESULTS OF SOLID ANALYSIS AFTER LEACHING TESTS

*In this chapter the results of leaching tests conducted on samples of the pozzolanic as well as geopolymetric matrices are presented and discussed.*

*The results are obtained from analysing the remains of the solid matrices after each leaching test (after different leaching times). XRF was mainly used for an elemental analysis of the different layers of the solids that were left after each leaching test run. A few samples were also analysed with XRD to identify crystalline components.*

---

### 5.1. ANALYSIS OF CRYSTALLINE COMPONENTS (XRD)

X-ray diffraction analysis was performed on the pozzolanic samples in order to identify the crystalline components of the matrix. Each crystalline substance possesses an unique diffraction pattern and by comparing the diffraction pattern of our material with known patterns from a database, it might be possible to identify some of the matrix constituents. There are however, also amorphous phases present in this matrix, which cannot be recognised by this method. The presence of a raised background in the analysis graphs is an indication of a large amorphous phase.

From the graphs presented in figures 5.1 and 5.2, not much of a difference can be detected, between the peaks of the matrix leached for 7 days and the matrix leached for 32 days. The method is not quantitative, but should a crystalline component be sufficiently leached out, the peaks of the components would not be shown on the graph. None of the peaks seems to be present in the one graph and absent in the other and it can be readily assumed that most crystalline components would stay in the matrix even in a corrosive environment.

It was difficult to exactly determine the reaction products present in these materials, because a rather wide range of peak distributions is available and the latter should be manually fitted on this mixture of different products. The largest peak on all the graphs was caused by quartz (33-1161), that was evidently present in the matrix and other products such as hematite (33-0664), originating from the jarosite, CSH (34-0002) and clino-tobermorite (45-1479) seemed to be represented by the peaks in the figures 5.1 and 5.2. No ettringite was found in these

samples and other possible products could also have been hydroniumjarosite (31-0650) and possibly some gypsum (33-0311). If the last two products are present, they will only attribute to a very small percentage of the matrix, because these peaks are very small.

XRD analysis was stopped after these samples were analysed, as no additional informations was obtained about the degradation during leaching tests. For the geopolymeric matrix, these graphs are similar, only with a higher background, due to the larger amorphous phase present in the matrix.

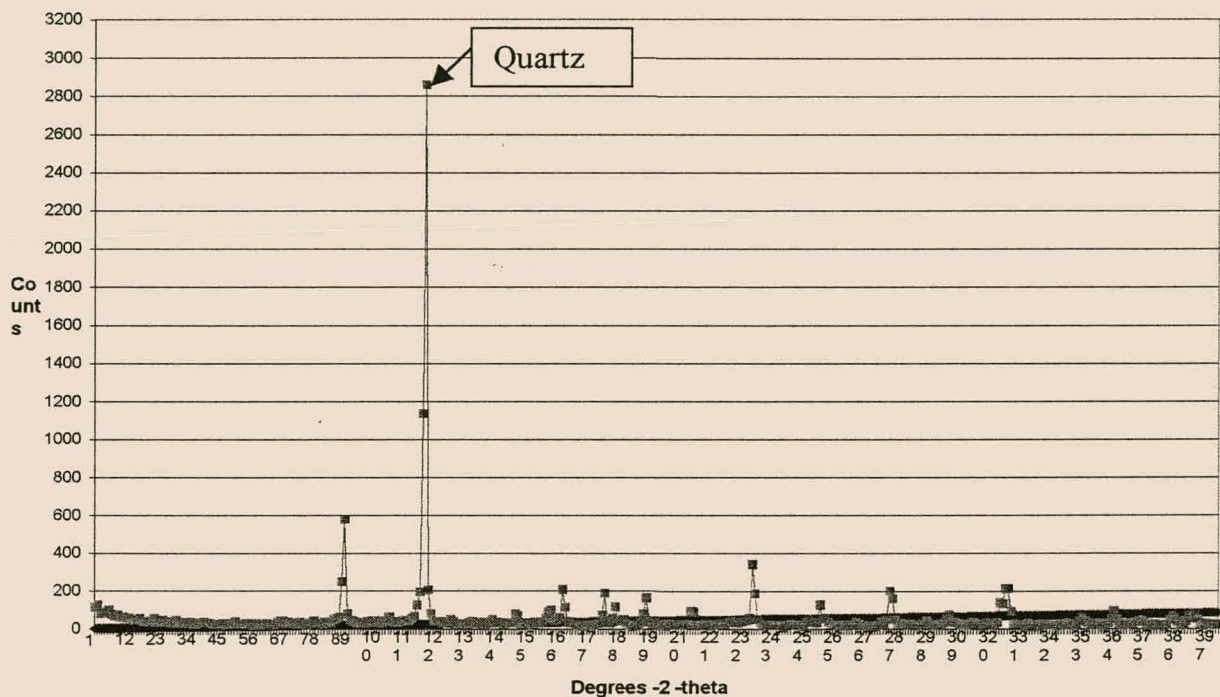


*Figure 5.1: XRD graph of the outer layers of a pozzolanic sample leached for 7 days with 5% acetic acid (L#16).*



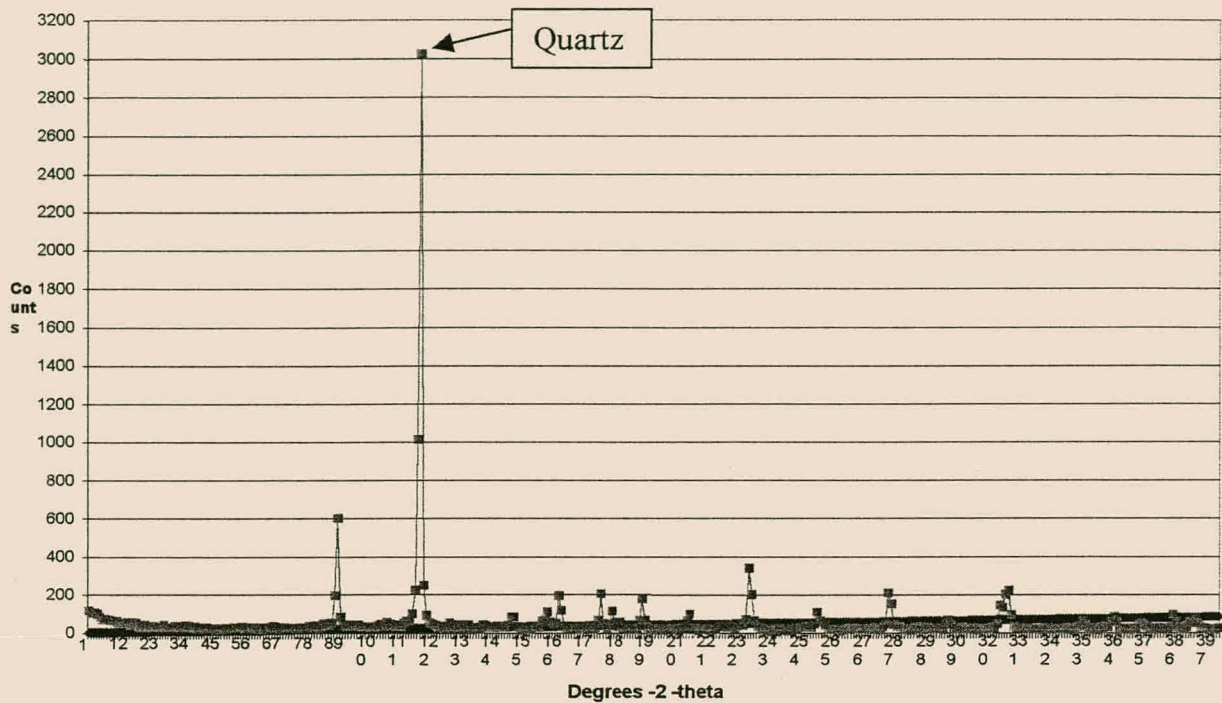


Figure 5.2: XRD graph of the outer layers of a pozzolanic sample leached for 32 days with 5% acetic acid (L#11).

## 5.2. ELEMENTAL ANALYSIS (XRF)

### 5.2.1. Pozzolanic matrix

The different layers of samples were evaluated by means of X-ray fluorescence analysis (XRF), as was explained in more detail in chapter 3. This gave an indication of the concentration of the elements left in the samples, after they had been leached for various times. The following graphs show how different elements leached from the matrix.

From the pie chart in figure 5.3 an idea can be formed of the initial concentrations of the different elements in a pozzolanic sample. The XRF analysis results are expressed as oxides of the elements.

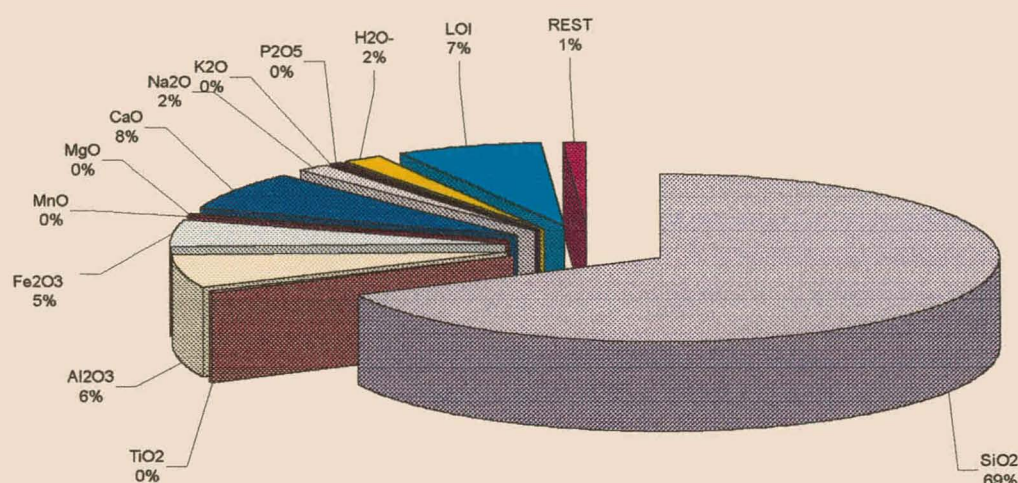


Figure 5.3: Different elements initially in the pozzolanic matrix (where H<sub>2</sub>O represents the vapour loss when drying the sample and LOI (loss on ignition at  $T > 800\text{ }^{\circ}\text{C}$ ) represents the crystal water bound into the matrix structure).

#### 5.2.1.1. Major matrix components

We can firstly consider the main matrix constituents, which is assumed to be Si, Ca, Al, Fe and Na.

##### □ Silica

As seen from the pie chart in figure 5.3, it is evident that Si takes up the largest portion of the prepared matrix, about 69%. Therefore, if a substantial amount of silica should leach out, a large part of the matrix would be degraded and the matrix might become less stable. It seems reasonable to link the physical degradation to the leaching of the main matrix components.

In figure 5.4 the maximum amount of silica leached from the matrix is about 20% (i.e. 100% - 80%), which would be about 15% of the total matrix. This was achieved after an acetic acid leaching test of about 31 days (672 hours). When evaluating long-term stability, silica appears rather stable in the matrix. Other acids such as nitric acid, hydrochloric acid and sulphuric acid are also very aggressive as their calcium salts are readily soluble and removed from the attack front, but acetic acid is considered to be the most aggressive in dissolution of the matrix, due to the acetate complexes that can form with the dissolved ions. However, sulphuric acid might damage the matrix by combining an acid attack and a sulphate attack, two degradation mechanisms. The latter would lead to crack formation in the matrix and,



subsequently a possible increase in leaching of matrix constituents during leaching tests. It is perhaps advisable to also conduct sulphuric acid tests on the matrix, in order to determine the long-term leaching behaviour when combining a sulphate- and acid attack.

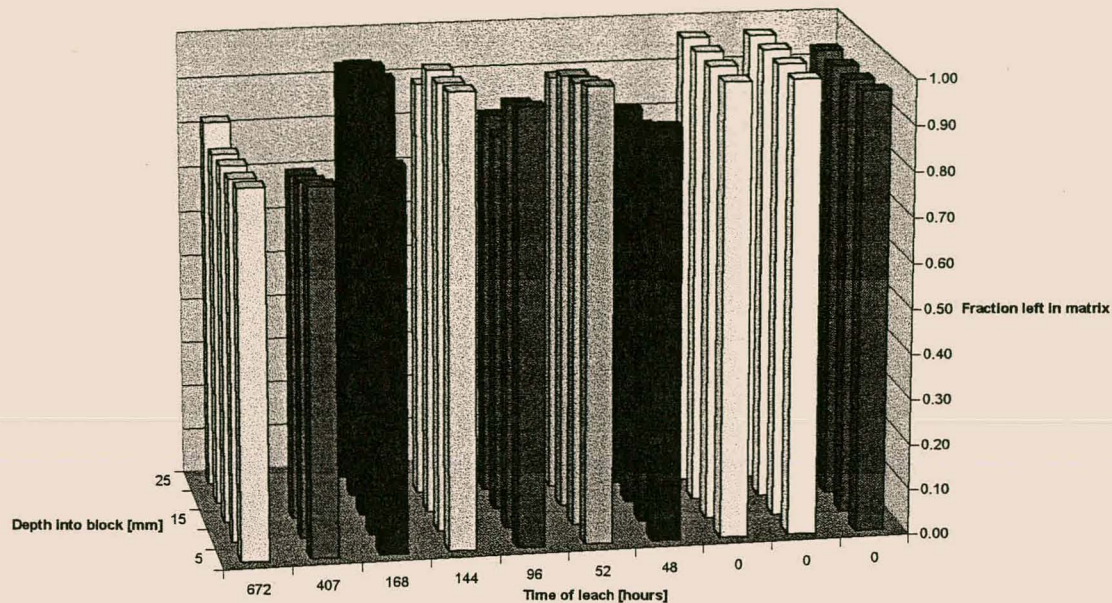


Figure 5.4: Silica speciation at different depths in the pozzolanic matrix-structure after exposure to acetic acid leaching solution for various times.

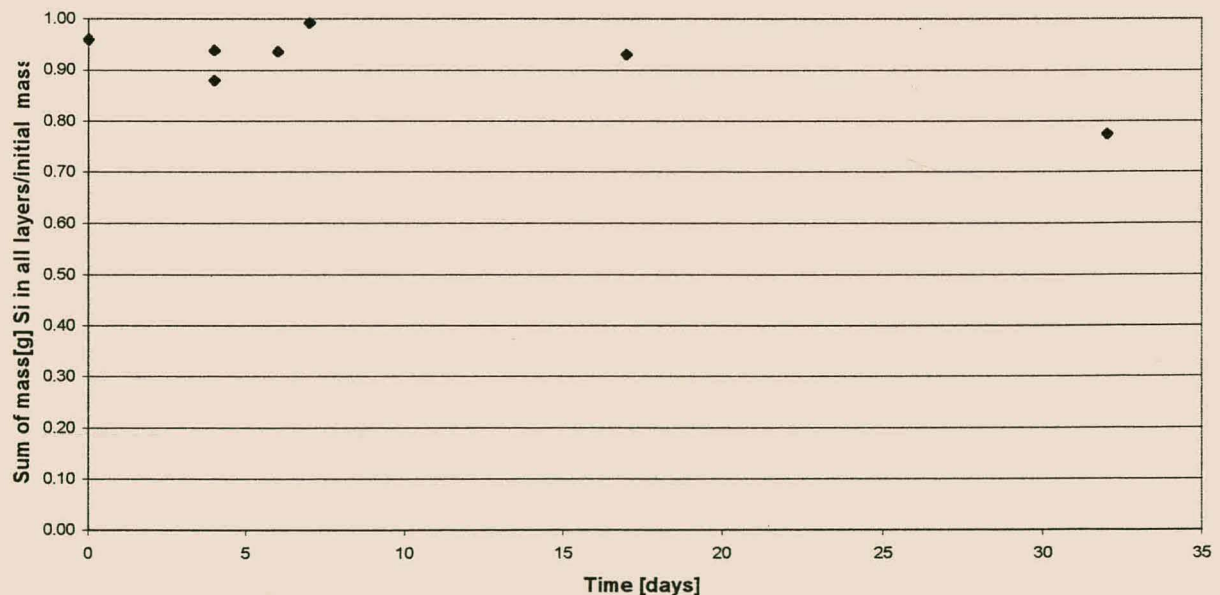


Figure 5.5: Fraction of silica left in the entire pozzolanic matrix-structure after 0-32 days of intensive leaching with acetic acid.

The silica are rather equally distributed between the different layers, which leads to speculation that the rate of dissolution of the silica is the rate limiting step, rather than diffusion through the matrix. From figure 5.4 no particular trends in concentration profiles were observed in the different layers. Uneven distribution of silica in the start-off samples might explain why there are less silica left in some samples, than in other samples that were leached for longer periods of time.

Variation from the general trend (in figure 5.5) in the fractions leached at different times, might be caused by the use of different samples for each leaching test, which is required due to the destructive analysis method. This variation is also expected for the rest of the elements and even more scattered data points are expected for elements present in very low concentrations.

#### □ Calcium

From figures 5.6 and 5.7, it is clear that more calcium leach from the matrix when it is exposed to the leaching solution for longer leaching times. After 31 days, almost all the calcium was leached from the sample (that is about 5% of the matrix). This decalcification seem to occur by means of a reaction front moving from the outside towards the inside of the sample with time (see figure 5.6). Calcium is very soluble and the rate of dissolution is not expected to limit the rate of leaching, but diffusion might have an influence on the rate at which the calcium reaches the bulk solution. Diffusion rates are mostly determined by permeability and porosity of the material.

The exceptionally high concentration in the surface layer of the third sample (leached for 168 hours) might once again be due to uneven distribution of the calcium in the initial sample, prior to leaching, or it might be due to the precipitation of an insoluble salt on the surface. This high concentration is not considered characteristic and could even be due to faulty analysis. Therefore, the analysis results of this specific layer should be ignored for all the following elements.

When considering the graph in figure 5.7 it can be assumed that all calcium would eventually leach from the matrix with sufficient exposure time. This can influence the long-term stability of the matrix, as the structure partially consists of C-S-H. The influence of calcium depletion on the structure and on other elements should hence be considered.



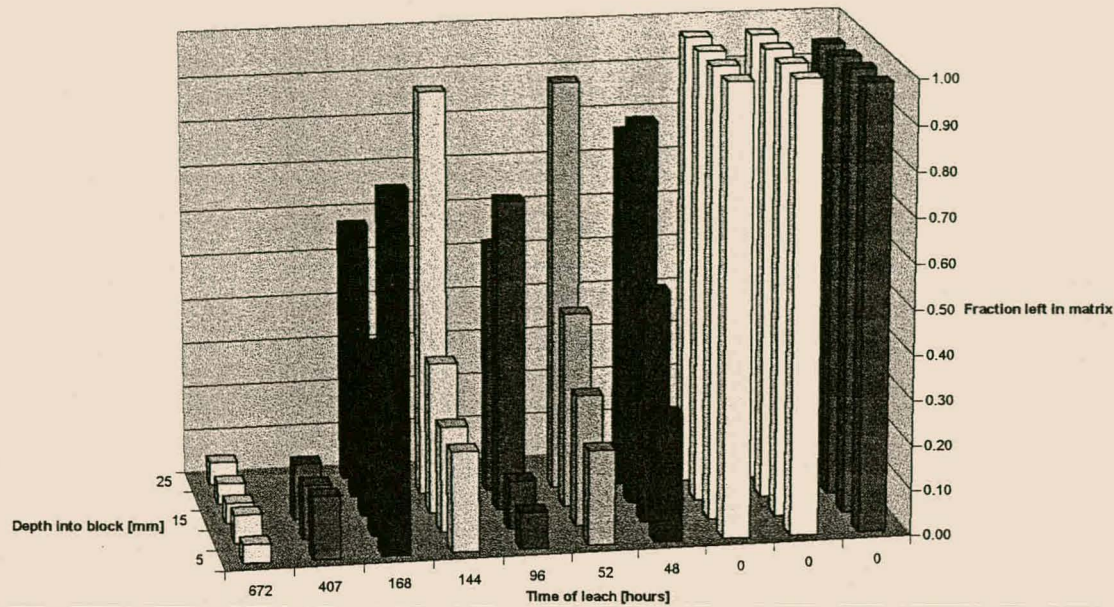


Figure 5.6: The extent of decalcification speciation at different depths in the pozzolanic matrix-structure due to exposure to acetic acid leaching solution for various times.

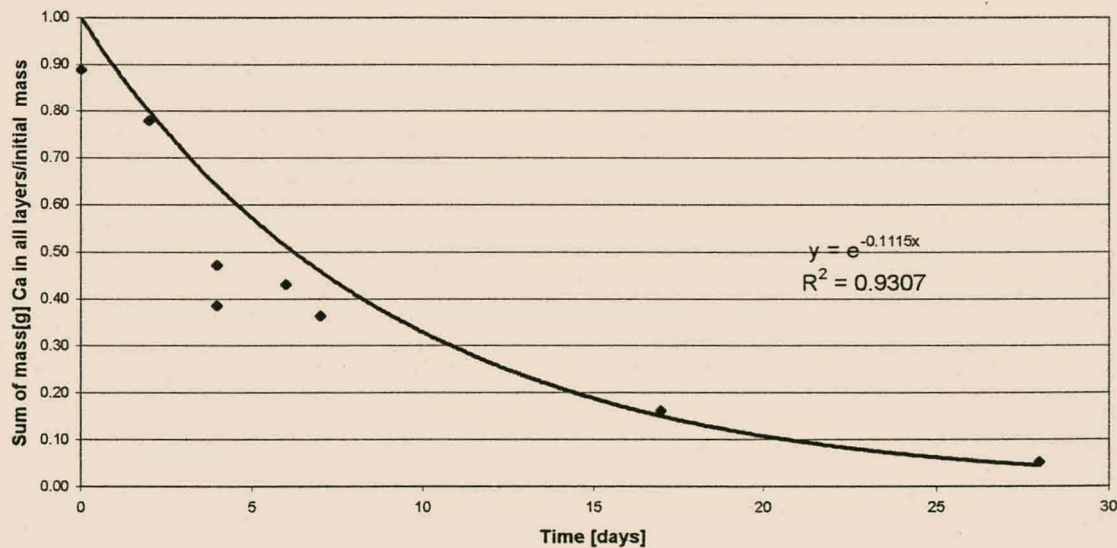


Figure 5.7: Fraction of calcium left in the entire pozzolanic matrix-structure after 0-32 days of intensive leaching with acetic acid.

#### □ Aluminium

Aluminium gradually leached from the matrix, but at a definite slower rate than calcium. About 27% of the aluminium was leached out after 28 days (see figure 5.9) with an initial fast leaching rate, decreasing with time. No specific reaction front can be identified in the layers (figure 5.8), although the leaching behaviour of aluminium are possibly linked to the leaching

of calcium, due to the disintegration of calcium alumina hydrates, as the calcium is leached from the samples.

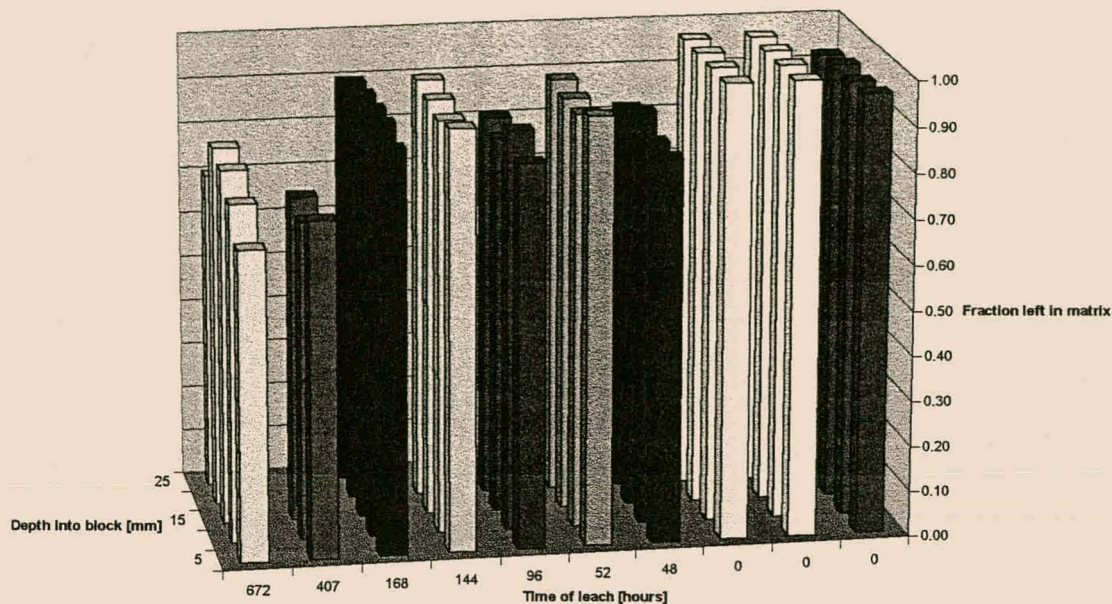


Figure 5.8: Aluminium left at different depths in the pozzolanic matrix-structure after exposure to acetic acid leaching solution for various times.

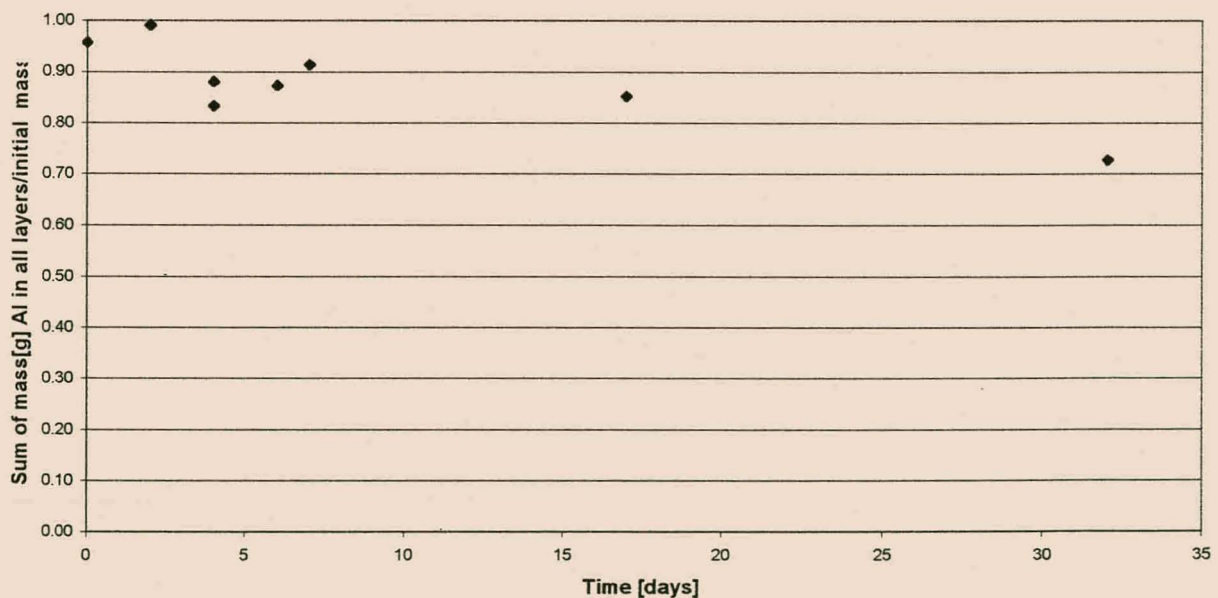
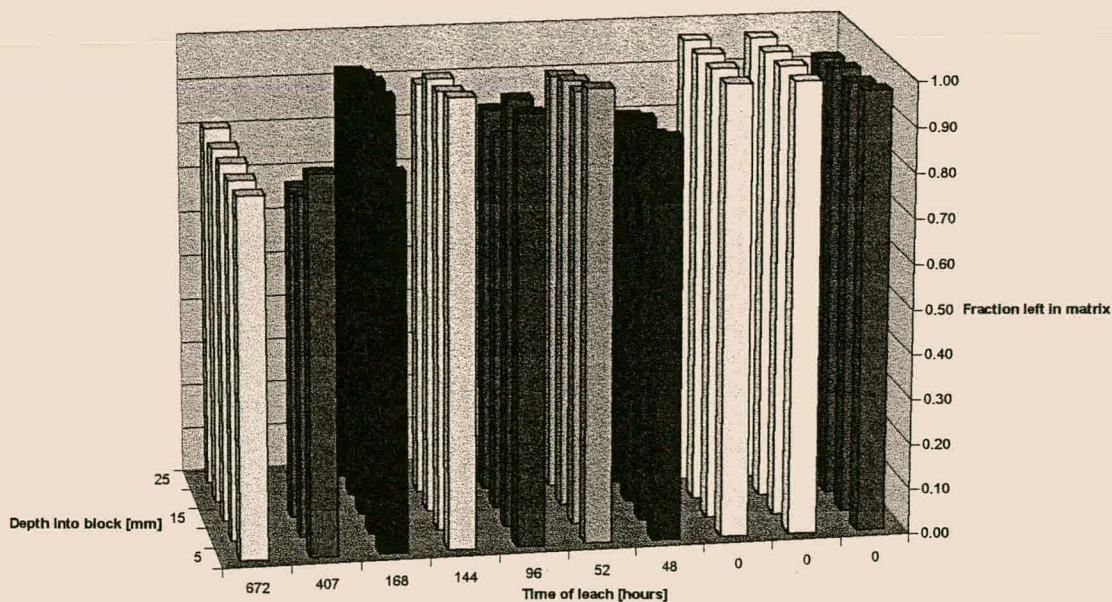


Figure 5.9: Aluminium fraction left in the entire pozzolanic matrix-structure after 0-32 days of intensive leaching with acetic acid.



## □ Iron

About 22% of the iron leach from the matrix after a leaching time of 760 hours and iron is also rather stable in the matrix (see figure 5.11). The leaching behaviour of aluminium and iron is very similar (figures 5.8 and 5.10) and these two elements are likely to be bound into the matrix in the same way. They might, for example both be part of the hematite crystals and as these compounds are attacked by the aggressive leaching solution, both the iron and aluminium will be released into the pore solution or directly into the bulk solution. Hematite is expected to be present in the material, as a reaction product of jarosite and sodium hydroxide. The leaching rate at the different depths in the sample did not form a recognisable trend in the obtained data, and no moving reaction front, as in the leaching of calcium, was identified.



*Figure 5.10: Iron left at different depths in the pozzolanic matrix-structure after exposure to acetic acid leaching solution for various times.*



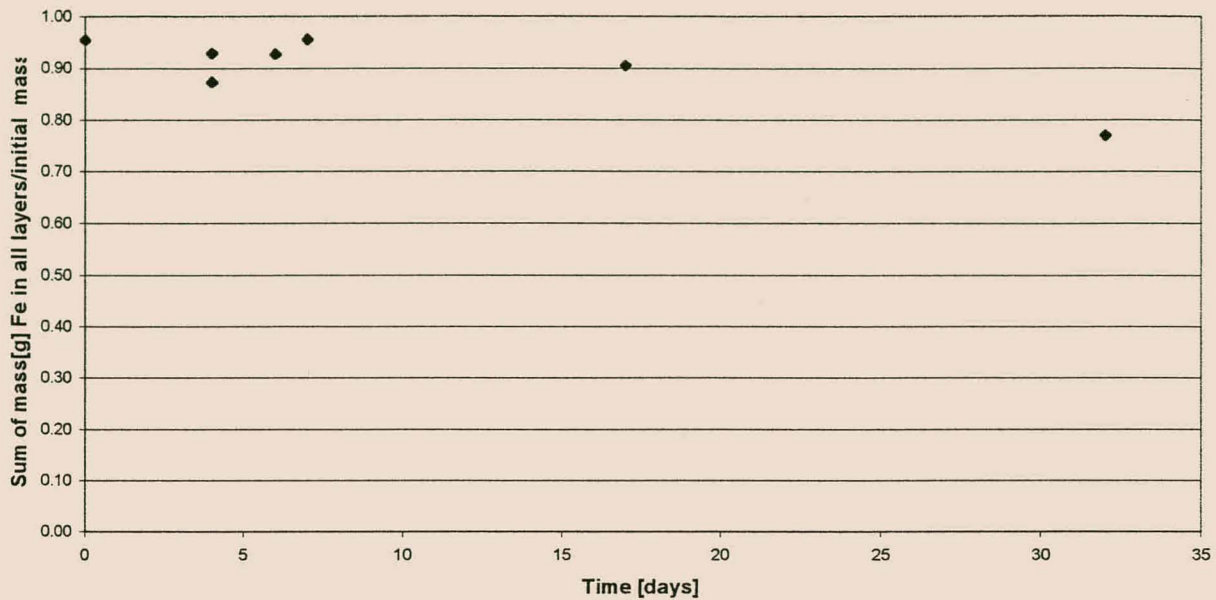


Figure 5.11: Iron fractions left in the entire pozzolanic matrix-structure after 0-32 days of intensive leaching with acetic acid.

#### □ Sodium

It is evident that virtually all sodium leaches from the matrix and this would probably also happen when the matrix would be left in the environment for a very long time. This is due to the high solubility of this element. A sodium dissolution reaction front moves from the surface inwards, towards the core of the sample and after 24 hours it is clear that the surface layer is completely depleted of Na, whereas the core still has almost all of the initial Na left (figure 5.12). With further exposure to the leaching solution Na seems to increase again in the surface layers. The sodium appears to start leaching from the surface layers into the sample, and as sodium from the inner layers diffuses outwards it partially settles in the adjoining layers closer to the surface, until also this sodium is eventually leached out. These adjoining layers were already depleted of all Na and the reason for the increase needs to be due to sites on the matrix that became vacant and bound with the Na in solution, as it diffused through the pore solution of the sodium depleted layers. This could also be due to Na salts that precipitate on the layers, but this is not likely, due to the high solubility of Na. Salts on the sample itself, would probably not even be picked up during the analysis.

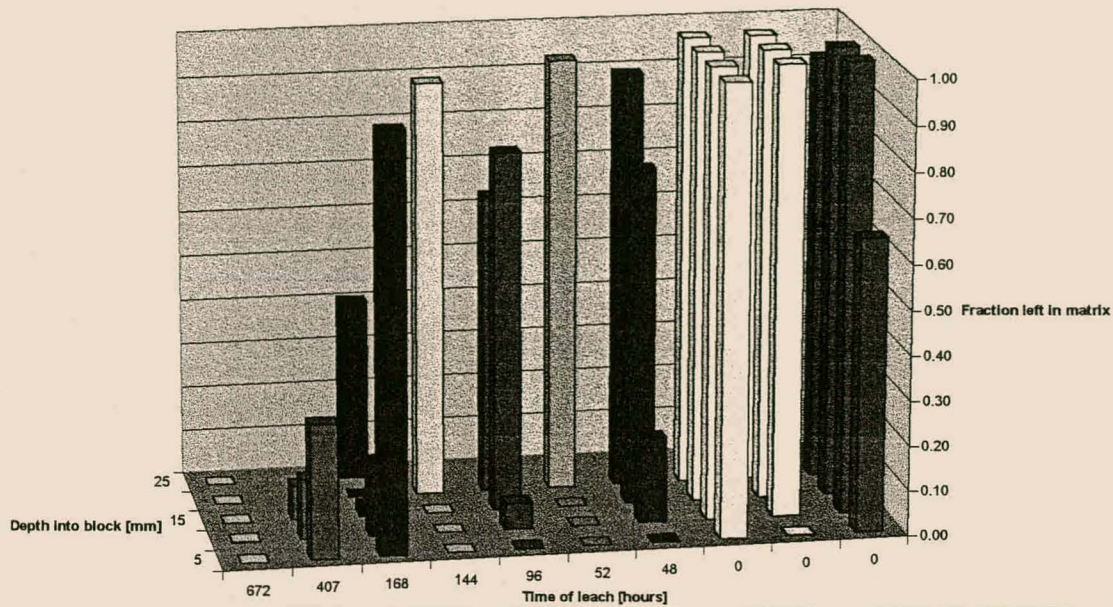


Figure 5.12: Sodium speciation at different depths in the pozzolanic matrix-structure after exposure to acetic acid leaching solution for various times.

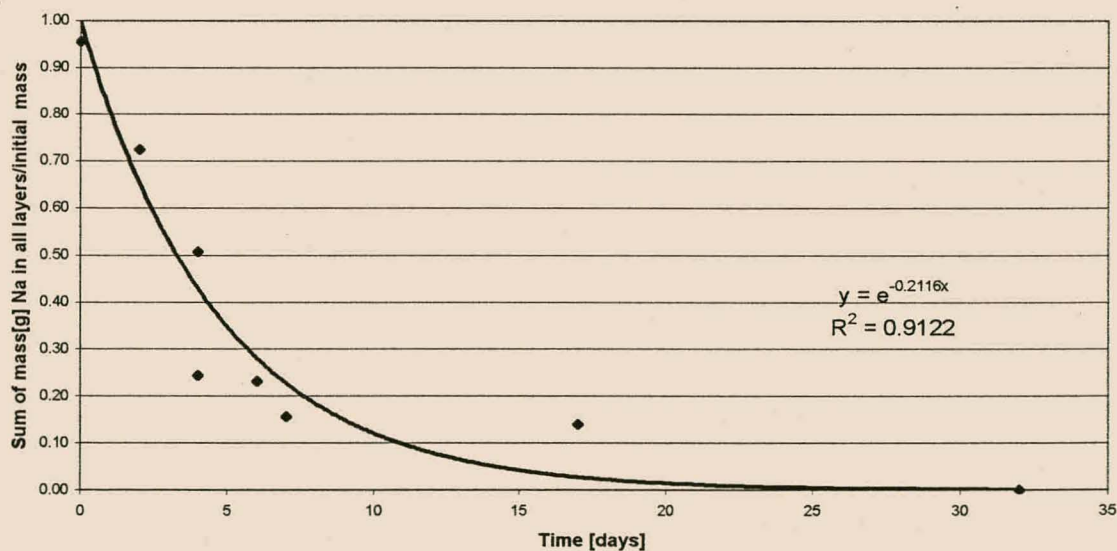


Figure 5.13: Na fractions left in the entire pozzolanic matrix-structure after 0-32 days of intensive leaching with acetic acid.

#### 5.2.1.2. Minor components left in matrix after leaching tests.

Some of the minor elements in the matrix were also analysed and the mass of each element was calculated after the different leaching times. From this, the fraction of the original mass of each element in each layer was calculated.



## □ Titanium

Titanium is also rather stable in the matrix and the behaviour in figures 5.14 and 5.15 show a resemblance with the leaching behaviour of aluminium and in particular iron. Once again, no clear reaction front for the leaching of titanium could be identified. A maximum of 25% of the titanium leached from the solid matrix after 32 days.

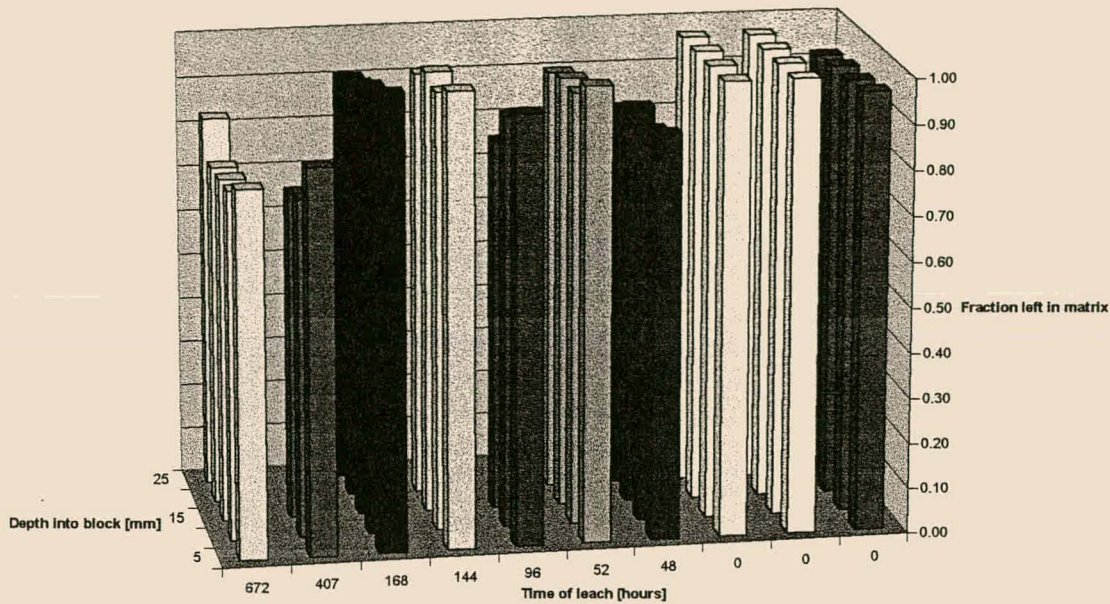


Figure 5.14: Titanium left at different depths in the pozzolanic matrix-structure after exposure to acetic acid leaching solution for various times.

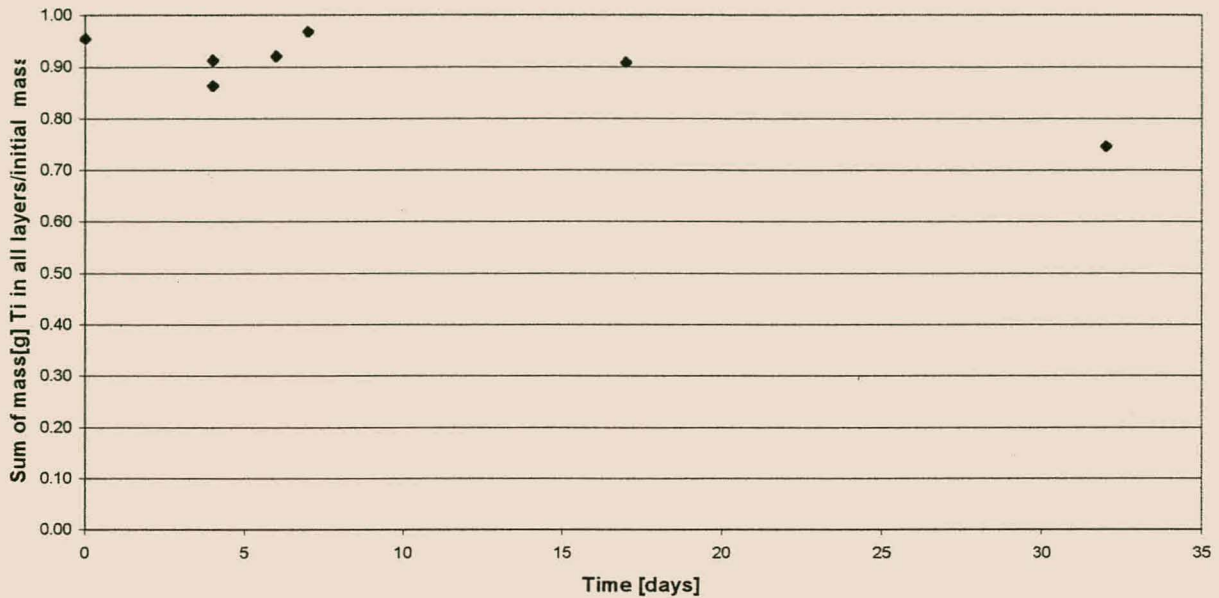


Figure 5.15: Titanium left in the entire pozzolanic matrix-structure after 0-32 days of intensive leaching with acetic acid.

#### □ Manganese

Most of the manganese (95%) seems to leach from the matrix after 32 days, as can be seen in figure 5.17. From figure 5.16, the moving reaction front leaching behaviour is once again observed and the leaching behaviour shows great similarity to the leaching of calcium in figures 5.6 and 5.7. This suggests that calcium and manganese might be bound in the matrix in the same way. The two elements also appear equally leachable, and all calcium and manganese might eventually leach from the solid, with sufficient exposure time to the acid solution.



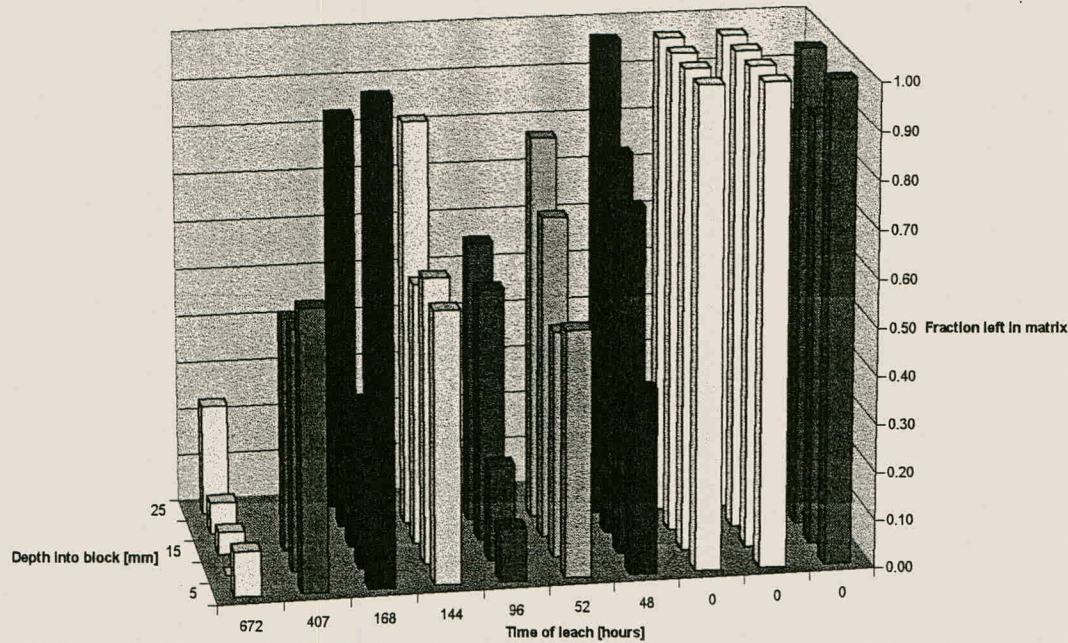


Figure 5.16: Manganese left at different depths in the pozzolanic matrix-structure after exposure to acetic acid leaching solution for various times.

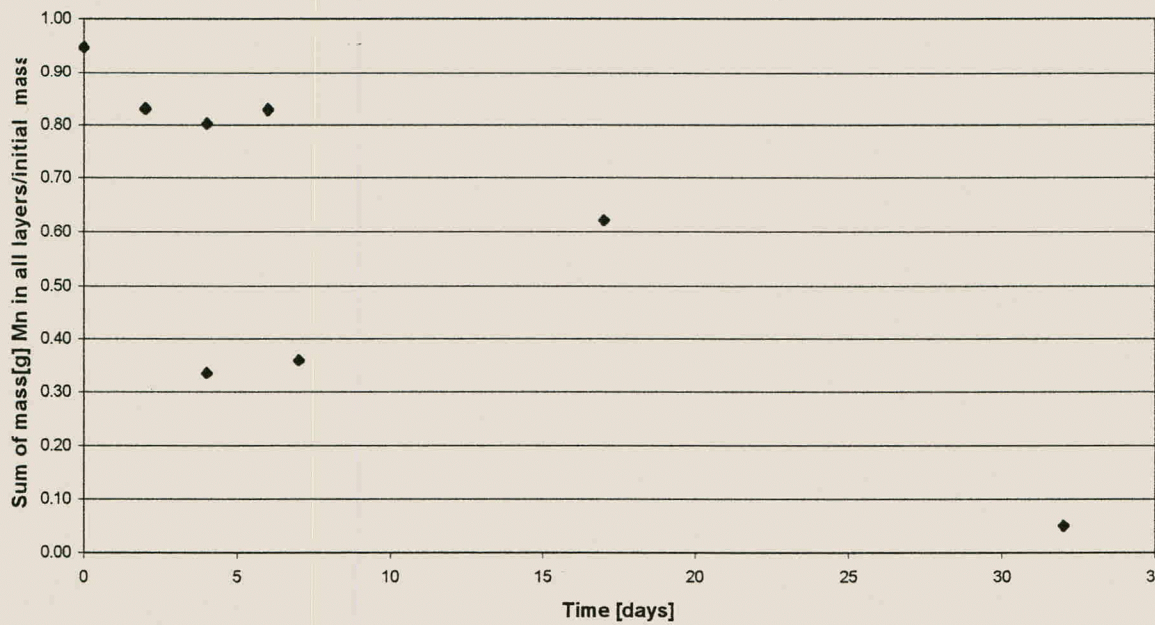


Figure 5.17: Fraction of Manganese left in the entire pozzolanic matrix-structure after 0-32 days of intensive leaching with acetic acid.

□ Magnesium

Magnesium decreases until about 20% of the initial amount is left in the solid matrix. A clear reaction front can be seen here, as the magnesium from the outer layer leached out first, followed by the second layer as the reaction front moved into the matrix. The diffusion of



acid into the matrix might be the limiting factor, which controls the leaching rate (figures 5.18 and 5.19).

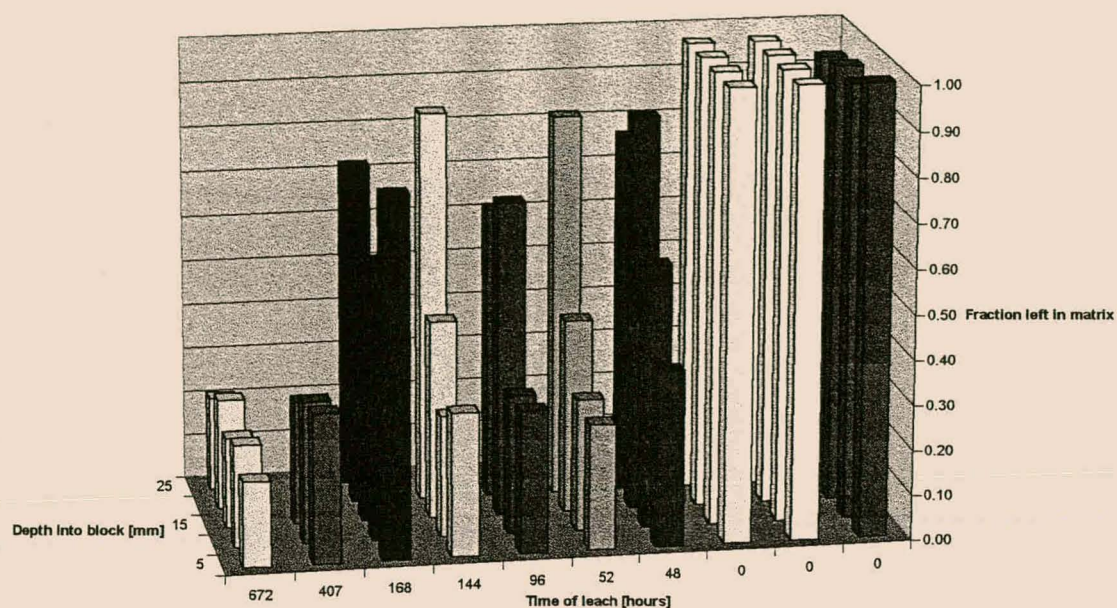


Figure 5.18: Magnesium speciation at different depths in the pozzolanic matrix-structure after exposure to acetic acid leaching solution for various times.

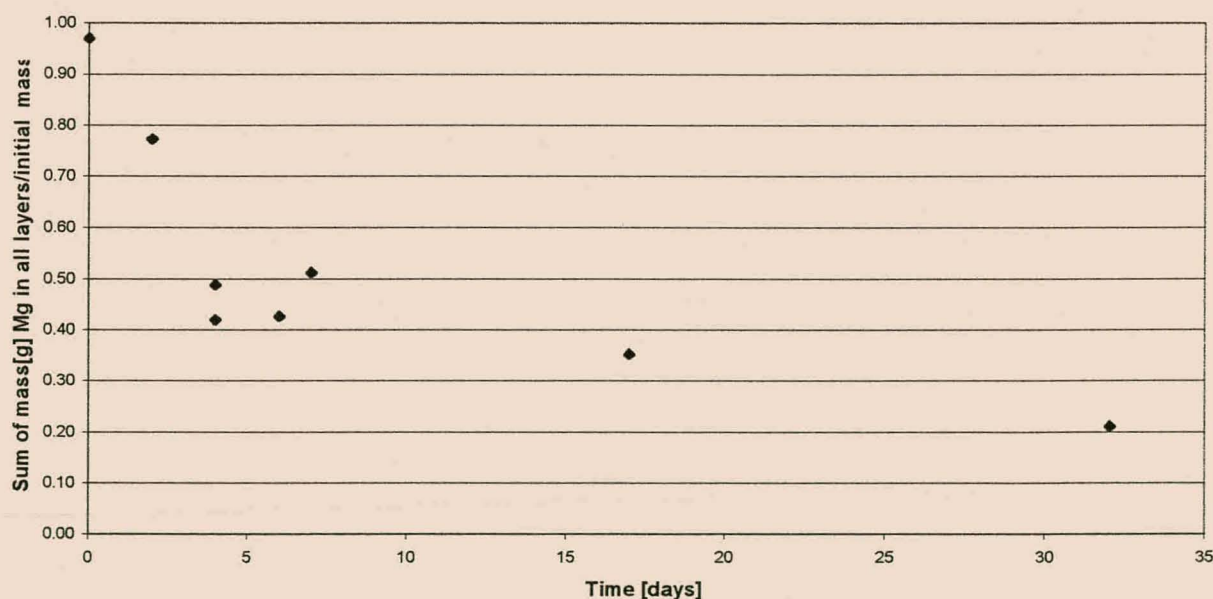
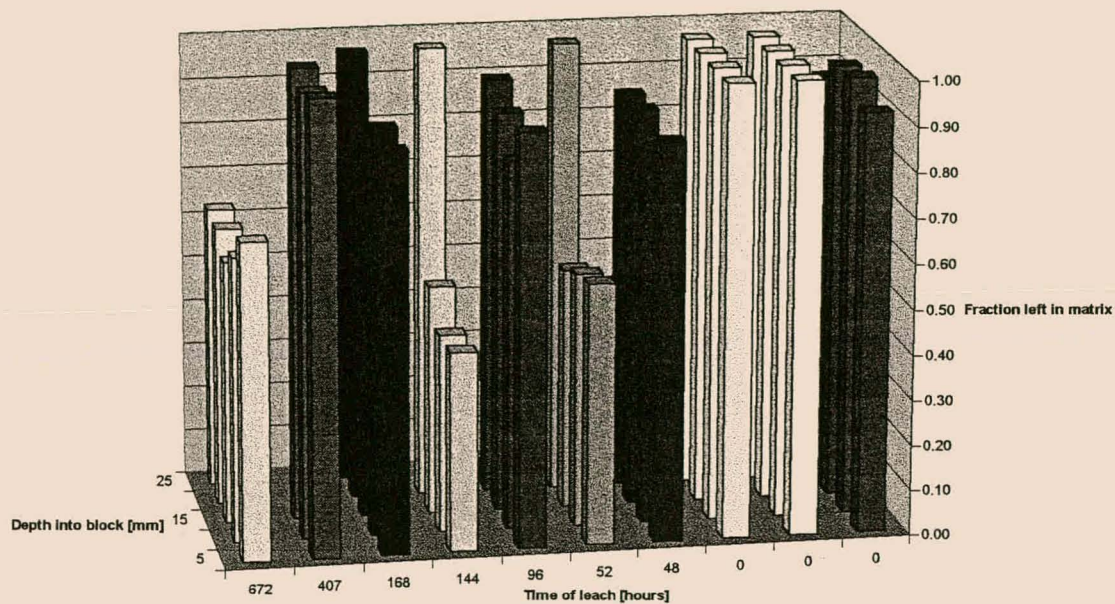


Figure 5.19: Magnesium fraction left in the entire pozzolanic matrix-structure after 0-32 days of intensive leaching with acetic acid.

### □ Potassium

Potassium did not leach according to a specific pattern in these tests and the fluctuations in data might largely due to insensitivity of the analysis of the very low K concentrations. About 40% leached out after 32 days and no specific leaching pattern were observed (figures 5.20 and 5.21).



*Figure 5.20: Potassium left in the pozzolanic matrix-structure after exposure to acetic acid leaching solution for various times.*



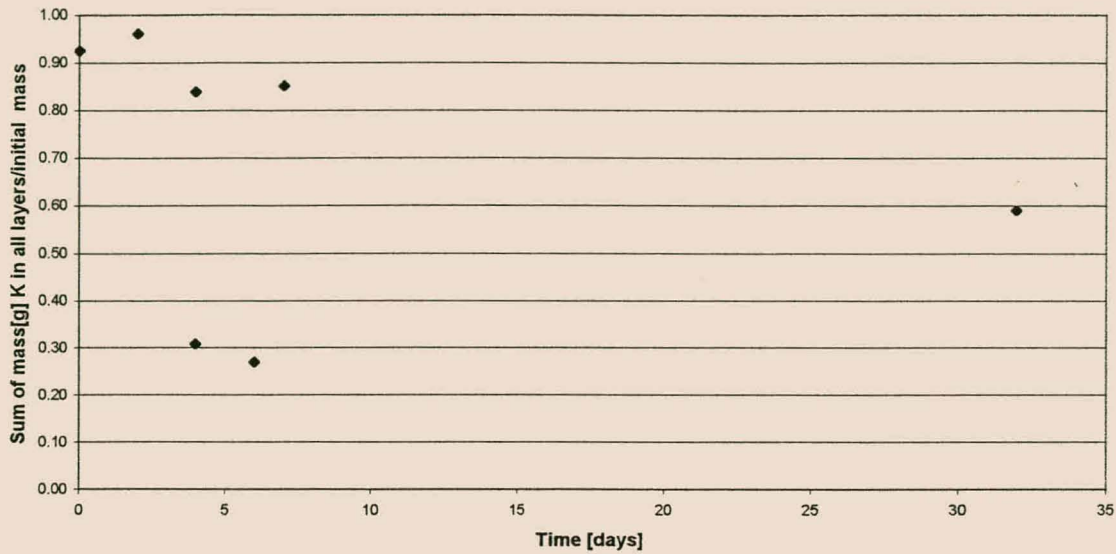


Figure 5.21: Potassium fraction left in the entire pozzolanic matrix-structure after 0-32 days of intensive leaching with acetic acid.

#### □ Phosphor

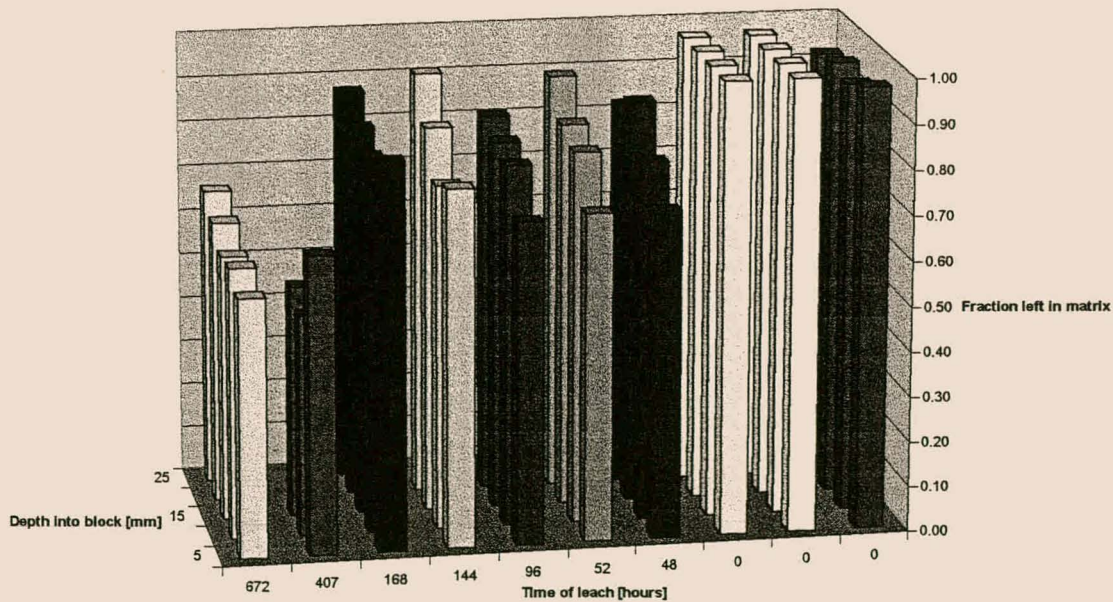
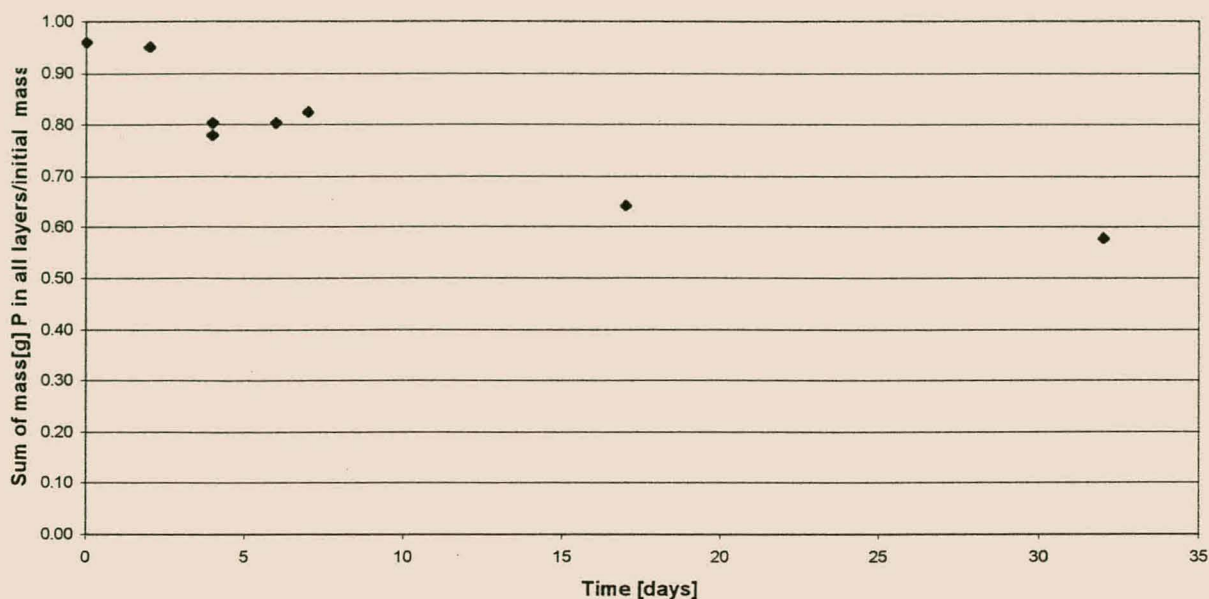


Figure 5.22: Phosphor left at different depths in the pozzolanic matrix-structure after exposure to acetic acid leaching solution for various times.





*Figure 5.23: Phosphor fraction left in the entire pozzolanic matrix-structure after 0-32 days of intensive leaching with acetic acid.*

Leaching occurred in a more or less logarithmic fashion, if considering the concentrations in figure 5.23. The leaching rate is initially higher, but slows down later on until the concentration stabilises. After 32 days about 40% of the P was leached from the matrix. Figure 5.22 shows that the moving reaction front behaviour exhibited by calcium was also observed in this case, where phosphor evidently left the outer layers faster than the inner layers. This might imply that phosphor is also bound to the matrix in the same way as calcium, or that the leaching of calcium is a direct cause for the leaching of phosphor.

### 5.2.2 Geopolymeric matrix

The XRF analysis of a geopolymeric sample (before leaching) presented the mass percentages in figure 5.24. These initial concentrations of the different elements were used to calculate the percentages of the elements that were leached out at different times during the tests. Slight variations from this initial percentage distribution might occur in some samples, which would lead to higher or lower calculated leached percentages, depending on the initial amounts truly present in the specific sample.

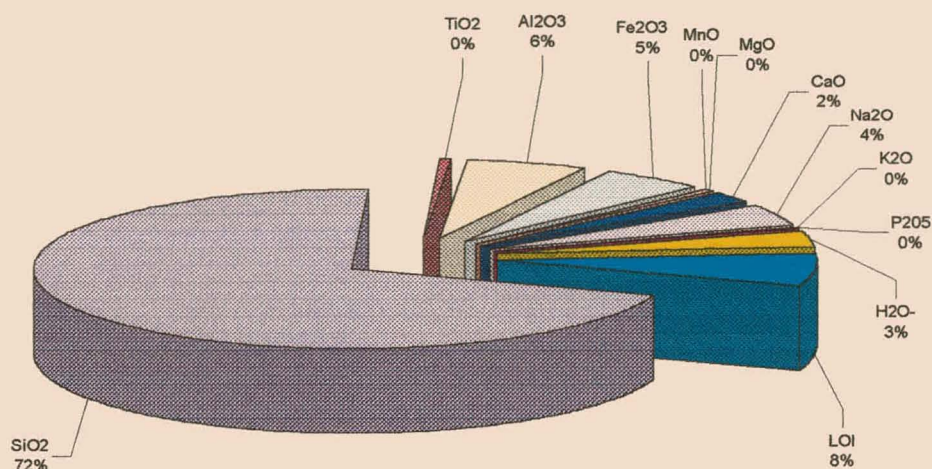


Figure 5.24 Different elements initially in the geopolymeric matrix (where H<sub>2</sub>O represents the vapour loss when drying the sample and LOI (loss on ignition at  $T > 800\text{ }^{\circ}\text{C}$ ) represents the crystal water bound into the matrix structure)

#### 5.2.2.1. Major matrix components

We can firstly consider the main matrix constituents, which is assumed to be Si, Ca, Al, Fe and Na.

##### □ Silica

According to figure 5.24, it is evident that Si once again takes up the largest portion of the prepared matrix, about 72%. Due to this large amount initially present and the low solubility of most silica substances in the matrix, the leached percentages are generally very low. In figure 5.26 the maximum amount of silica leached from the matrix are also about 20% as in the case of the pozzolanic matrix, which is about 14.5% of the total matrix. This implies that, after about 600 hours of leaching with 5% acetic acid, more than about 14% of the matrix are expected to degrade. The lower concentrations at 24 hours, in figure 5.26, are probably merely due to fluctuations in the experimental conditions or analysis, and are not considered to be typical of the leaching behaviour.

The silica is relatively randomly distributed between the different layers, but the surface layers do appear to have less silica left after leaching, than the inner layers (figure 5.25).



A moving reaction front mechanism might also be present during the leaching of silica in the geopolymeric matrix, but is not as clear as for calcium leaching. More silica in the surface layers in some experiments can once again be due to insoluble silica salts that precipitate in the surface layers, or merely due to natural variation in results. Protective silica oxide layers might also inhibit further leaching and add to the stability of silica after about 20% of all the silica are leached out.

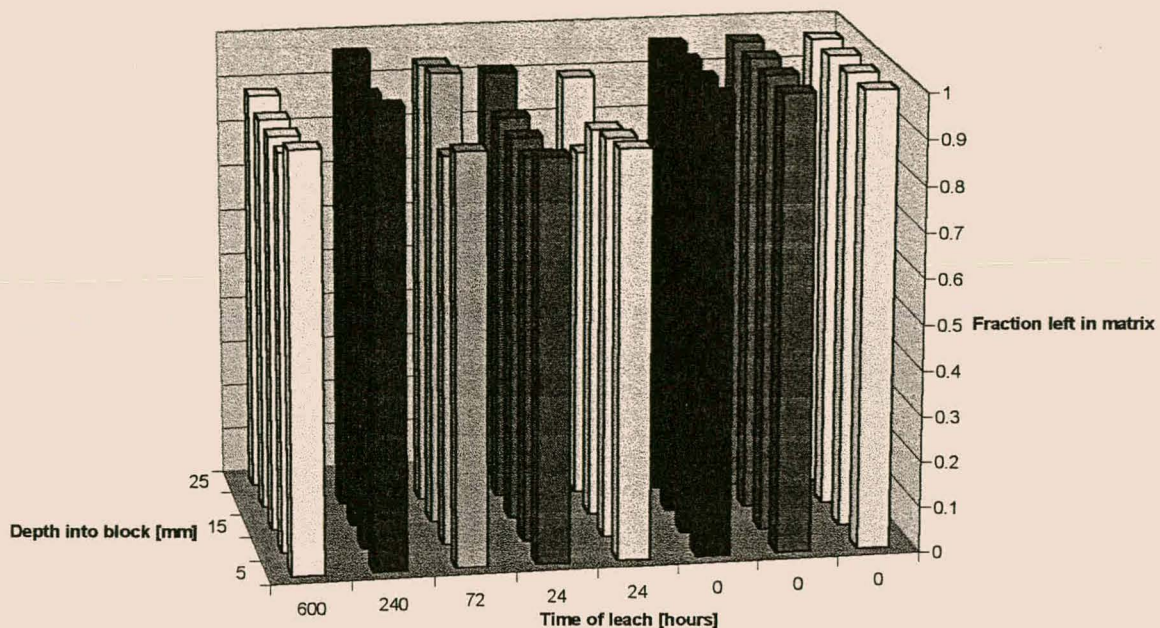
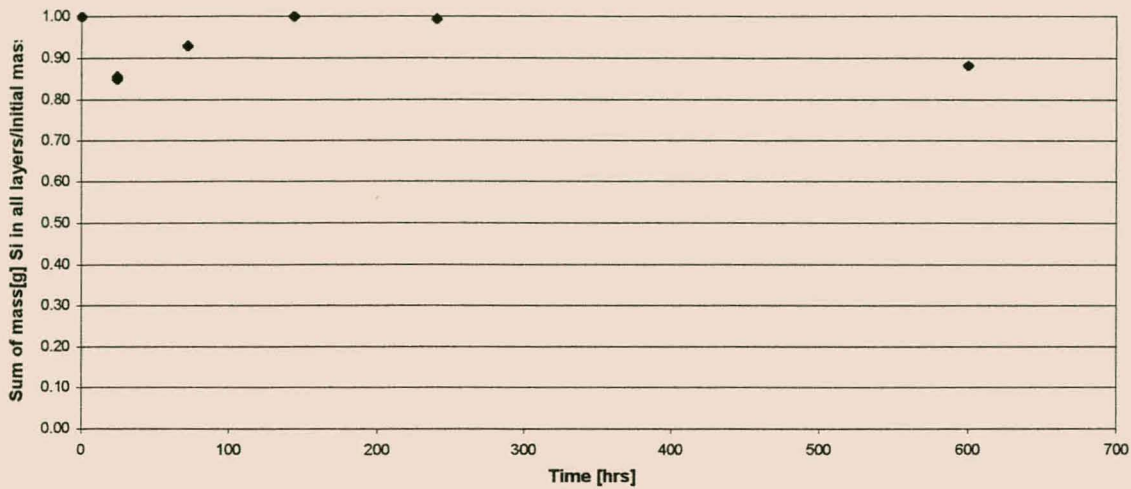


Figure 5.25: Silica speciation at different depths in the matrix-structure after exposure to leaching solution for various times.



*Figure 5.26: Total fraction of silica left in the matrix at different times during the leaching test.*

#### □ Calcium

From figure 5.27, it is evident that calcium leaching increases with increasing leaching times. After 600 hours, about 85% of the calcium was leached from the sample (that is about 1.7% of the matrix). As for the pozzolanic matrix, this decalcification also takes place by means of a reaction front moving from the outside towards the inside of the sample. This leads to the faster depletion of calcium from the surface layers, than from the inner layers. The leaching of calcium is not expected to be limited by dissolution, and the rate of leaching is more likely to be controlled by diffusion, which is limited by the permeability and porosity of the material.

When considering the graph in figure 5.28 it can be assumed that most calcium would eventually leach from the matrix with sufficient exposure time. This can influence the long-term stability of the matrix, as all silica compounds, for example C-S-H, would disintegrate. This would leave a porous matrix, with less structural stability, and could have an influence on the mobilisation of other elements.

On average the calcium seem to be more firmly bound into the geopolymeric matrix than in the pozzolanic matrix. In the latter case the calcium completely leaches out, much earlier than in the geopolymer. This could imply that slower degradation and mobilisation of the geopolymeric matrix can be expected.



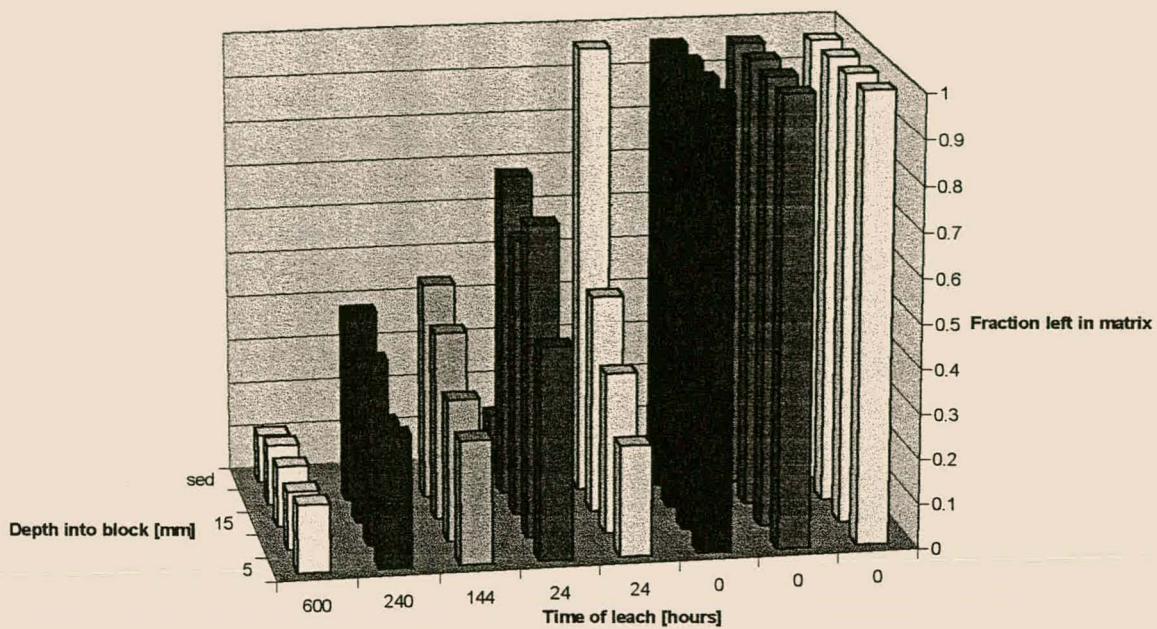


Figure 5.27: The calcium left in the layers after different leaching times shows the extent of decalcification.

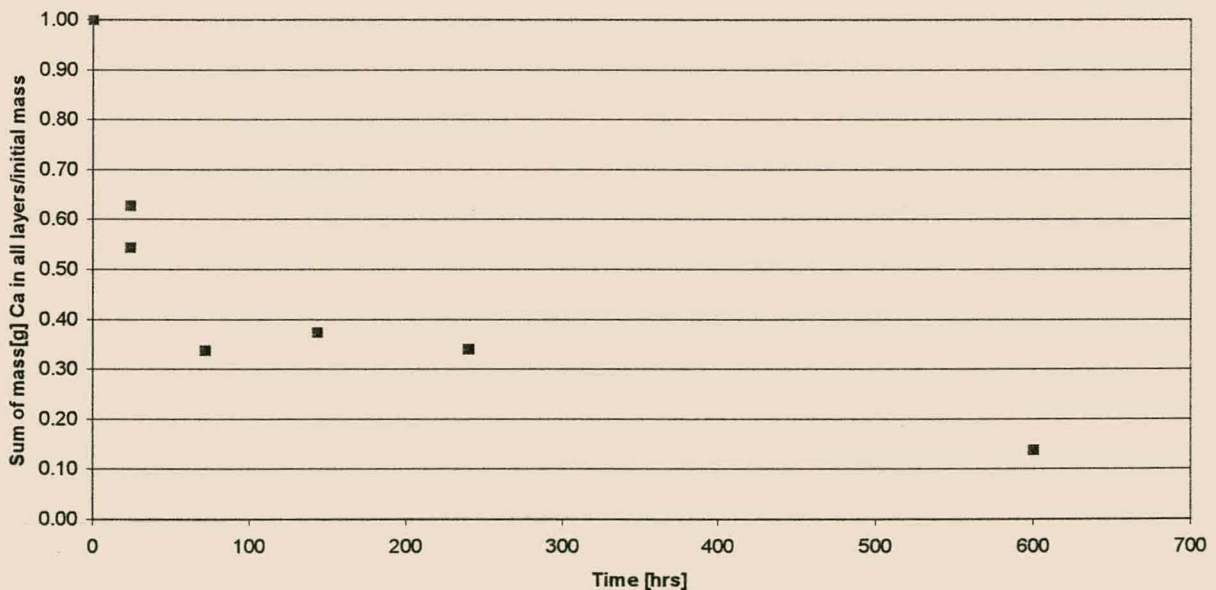


Figure 5.28: Fraction of calcium left in the geopolymeric matrix as leaching time increases.

## □ Aluminium

Aluminium, gradually leach from the matrix, and a maximum of about 20% was leached after 600 hours. In figure 5.30 a power trend line could be fitted to the data representing the leaching from the block, but this trend did not give a good R-square value, due to the large fluctuation in data. This behaviour closely relates that of the silica as in figure 5.26. Data fluctuations from the expected trend are possibly due to variation in the sample consistency or due to analysis insensitivity. The aluminium seems to be randomly distributed inside of the matrix (figure 5.29) and the outer layers do not appear to leach before the inner layers, leaving no indication of a reaction front that moves into or out of the matrix. The similar behaviour of silica and aluminium indicates that these substances could be similarly bound in the matrix. They are possibly both bound to calcium and might consequently leach from the matrix as the calcium is released. They might also be bound to each other as silica aluminates, which is not very soluble.

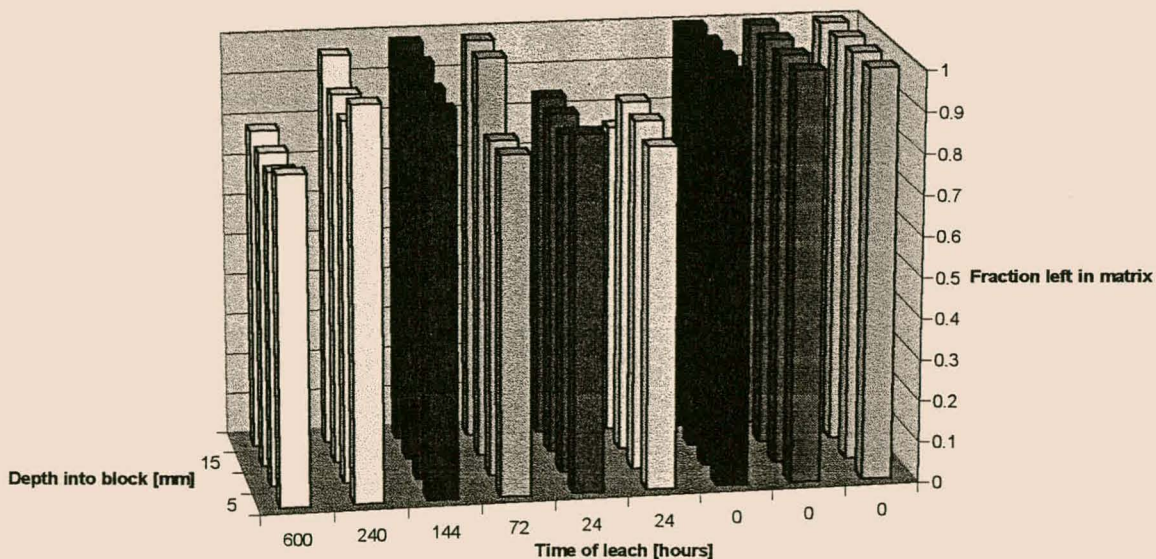


Figure 5.29: Aluminium left in different layers after leaching tests.



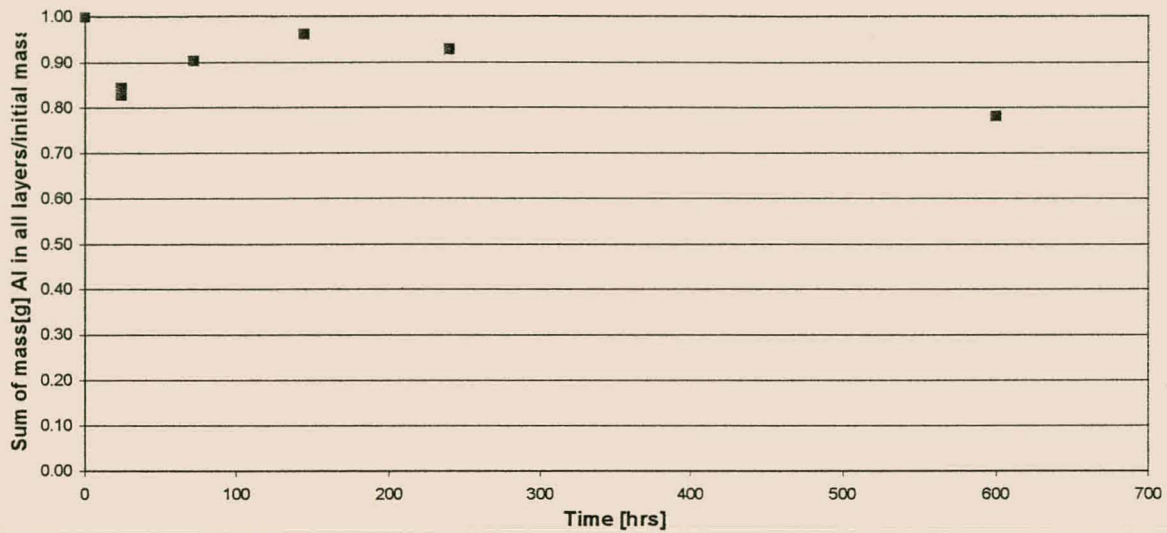


Figure 5.30: Aluminium fraction left in the entire sample after different leaching times.

□ Iron

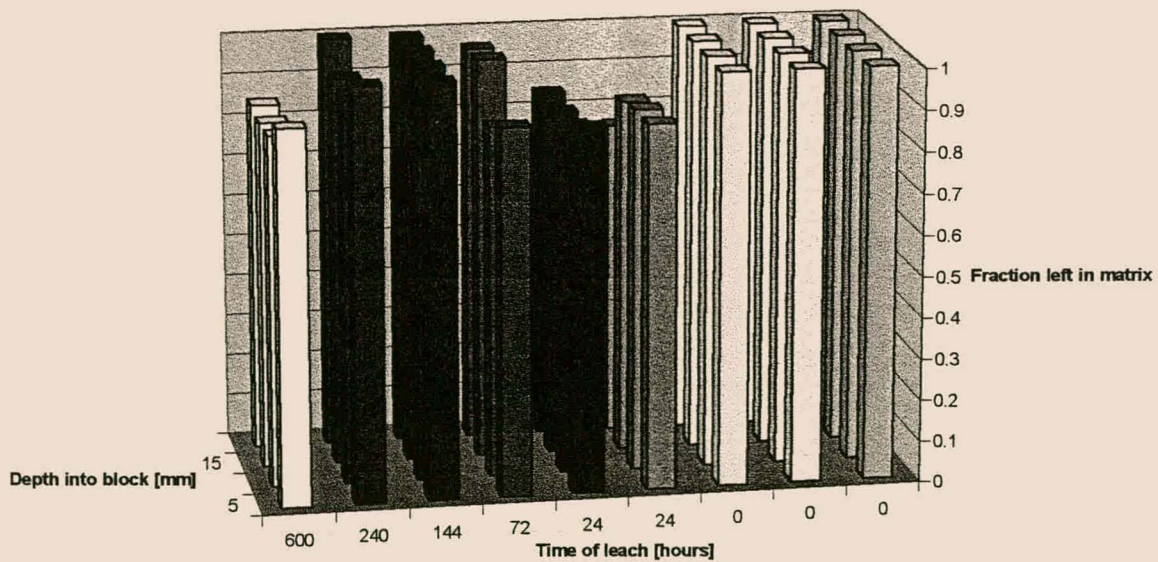


Figure 5.31: Iron left in the different layers after different leaching times.

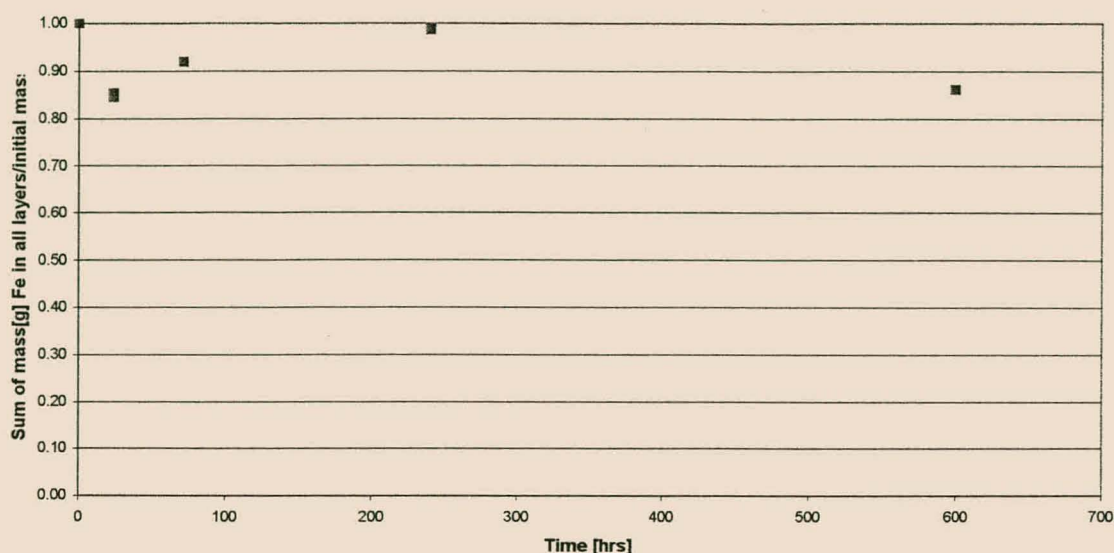


Figure 5.32: Iron fractions left in the entire sample after different leaching times.

In figures 5.31 and 5.32, it is shown that about 14% of the iron leaches from the matrix after a leaching time of 600 hours and during the first 240 hours the iron is still suspected to be rather stable in the matrix. The lower concentrations after 24 hours, does not seem to be characteristic of the behaviour of the matrix and fluctuations or severe failure in the matrix might be responsible for this fluctuation. The results seem to be closely related to the leaching of silica, but also especially to the aluminium. The iron and aluminium are very likely to be similarly bound into the matrix, possibly as part of the same substances such as hematite. Once again the reaction front is not evident in the layers (figure 5.31) and the rate of leaching is possibly controlled by the rate of dissolution or degradation (or slow mobilising reactions).

#### □ Sodium

It is evident that virtually all sodium leaches from the matrix within 72 hours (figures 5.33 and 5.34). This is due to the high solubility of sodium. This fast leaching behaviour was also found in the pozzolanic samples, but perhaps to a lesser extent. When evaluating figures 5.33 and 5.34, the one sample, which was leached for 24 hours, once again gave results that do not follow the general trend. It is however clear that this specific sample showed more drastic leaching for all previously discussed elements, i.e. Si, Al, Ca and Fe and it can be assumed that this matrix was originally less stable than the others. In normal circumstances the sodium will leach very fast, according to a moving reaction front into the matrix as can be seen after 24 hours in figure 5.33, and the matrix will be completely depleted of sodium in less than 72 hours, during an acetic acid leaching test.



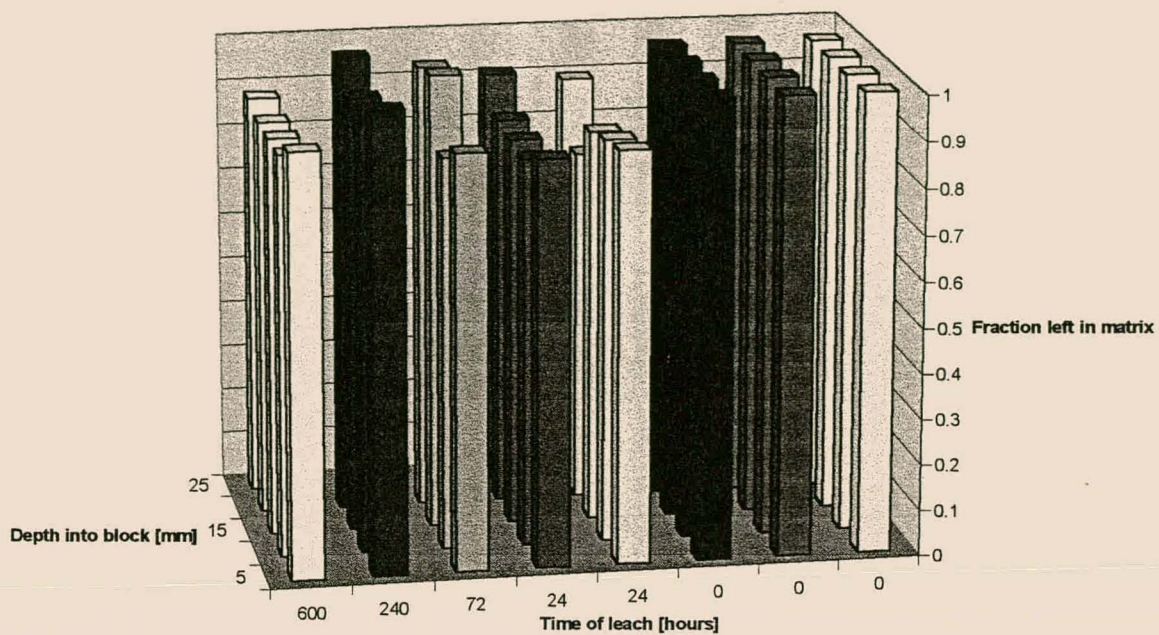


Figure 5.33: Sodium left in different layers after the leaching tests.

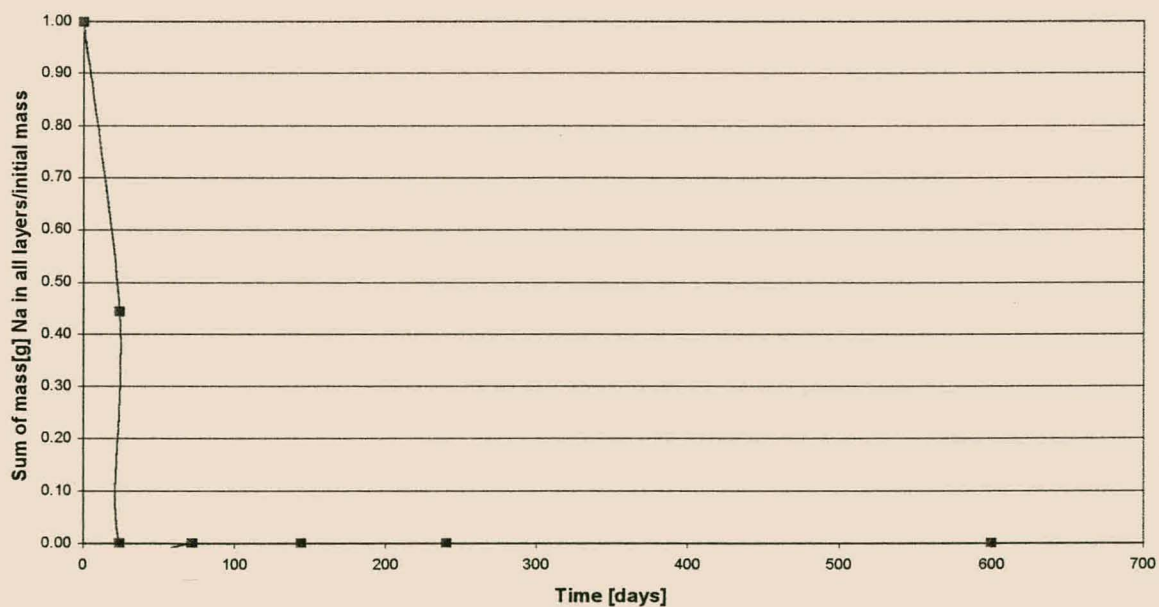


Figure 5.34: Na fractions left in the whole sample after tests

#### 5.2.2.2. Minor matrix components

Less than 1% of the rest of the elements were present in matrix and they are assumed to be the minor matrix components. Due to the low concentrations, analysis results are expected to

be less accurate, and some degree of fluctuations would necessarily be found. The following elements of the geopolymeric samples were analysed from the solids left after leaching tests.

#### □ Titanium

From figures 5.35 and 5.36, 13% of titanium was leached out after 600 hours and the performance was similar to the leaching of iron, aluminium and silica (also showing that the samples that were leached for 24 hours was less stable). In general, titanium seems to be rather stable in the matrix and even in this highly corrosive environment only a small percentage was leached. This leaching seemed to only start after 240 hours (from figure 5.36).

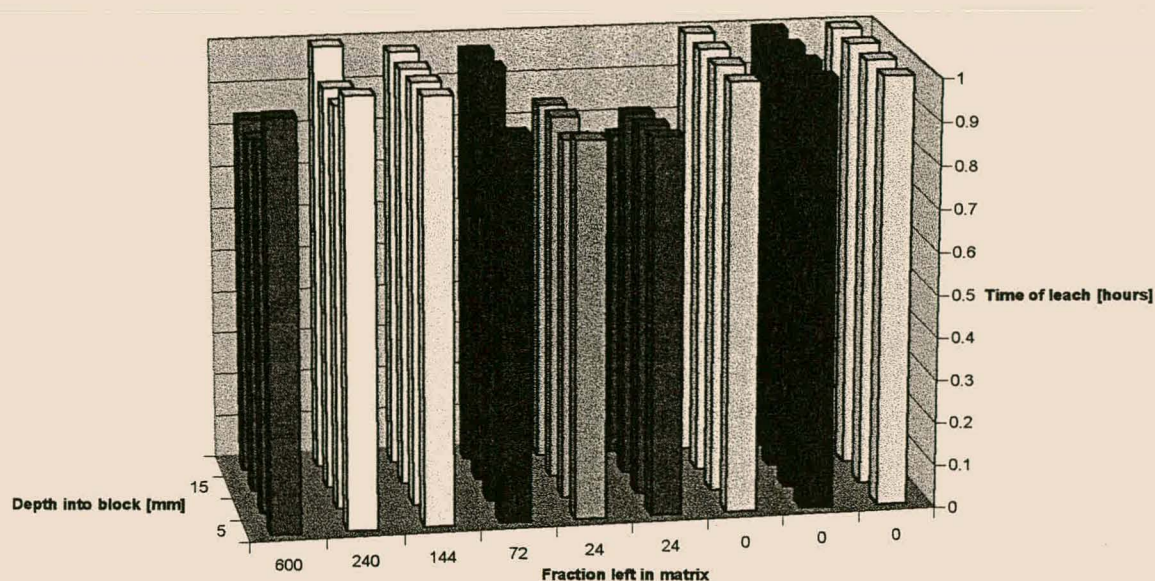


Figure 5.35: Titanium left in the pozzolanic matrix after acetic acid leaching tests.



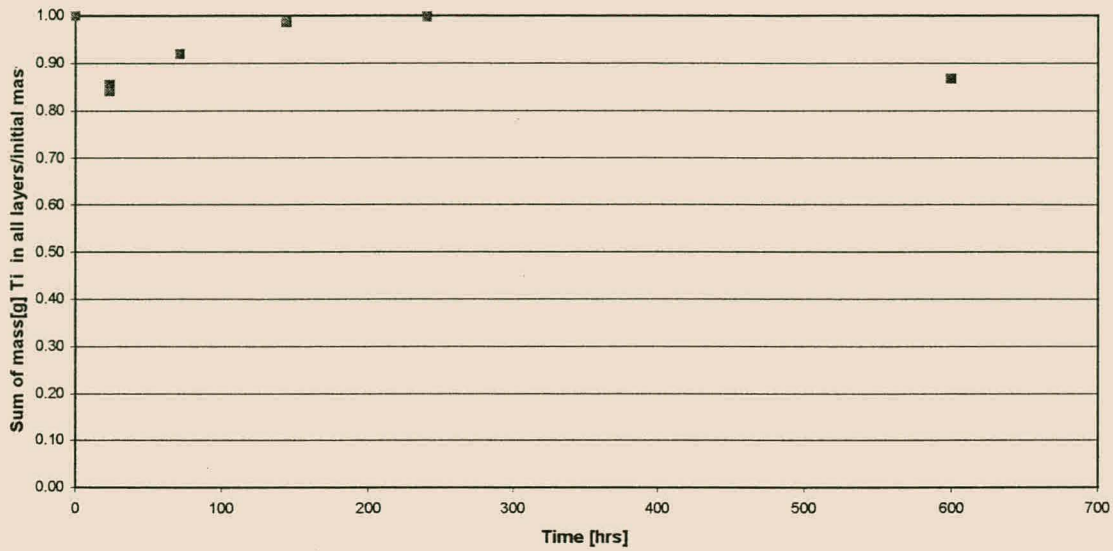


Figure 5.36: Fraction of Titanium left in the solid matrix after leaching tests.

#### □ Manganese

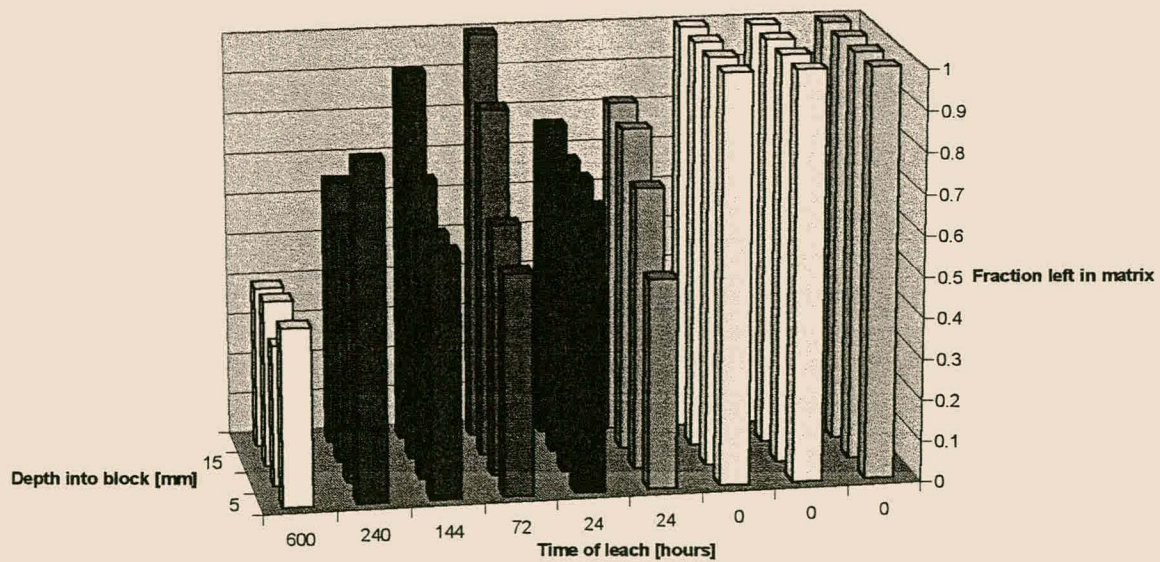
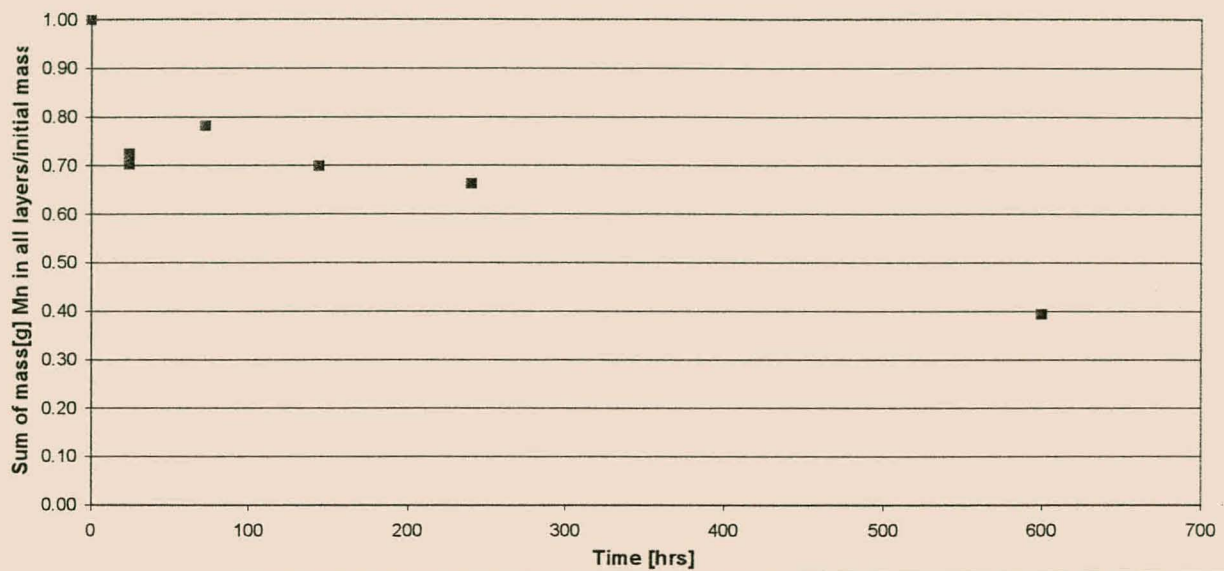


Figure 5.37: Manganese left in the pozzolanic matrix after acetic acid leaching tests.



*Figure 5.38: Fraction of Manganese left in the solid matrix after leaching tests.*

The matrix becomes gradually depleted of manganese, suggesting a possible influence of diffusion from the deeper parts of the sample towards the bulk solution. After 600 hours, 61% of the manganese was leached from the matrix. The behaviour shows similarities to the leaching of calcium and sodium and the mechanisms of leaching might be similar. (See figures 5.37 and 5.38).



## □ Magnesium

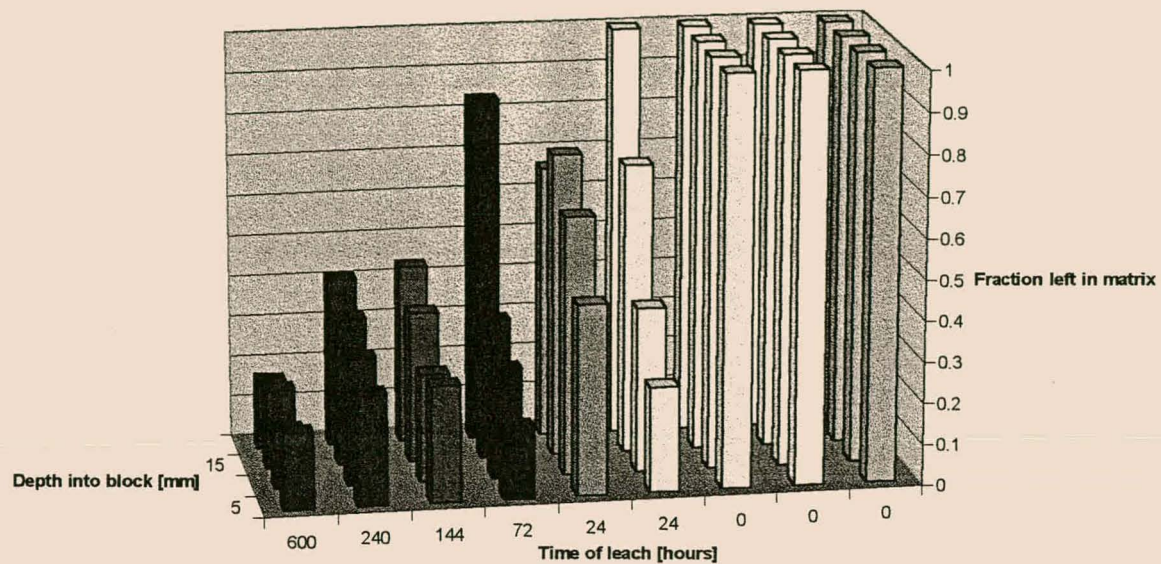


Figure 5.39: Magnesium left in the pozzolanic matrix after acetic acid leaching tests.

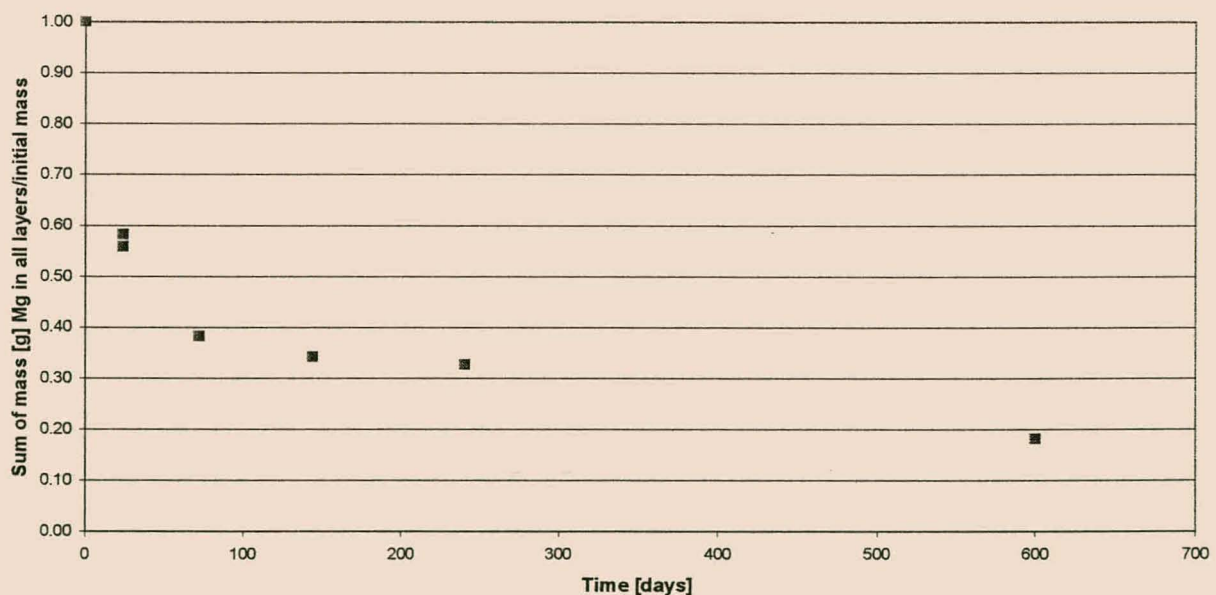


Figure 5.40: Magnesium fraction left in the sample after different leaching time.

Magnesium decreases until only about 18% of the initial amount are left in the solid matrix after 600 hours (figure 5.40). A clear reaction front can be seen in figure 5.39, as the outer layers leached faster than the inner layers of the block, as the front moved into the matrix.

layers leached faster than the inner layers of the block, as the front moved into the matrix. This can be an indication that the diffusion of acid into the matrix might limit the leaching rate.

#### □ Potassium

About 25% were leached from the sample after 600 hours, but a maximum of about 60% was leached from the sample after 72 hours (see figure 5.42). Consequently, no trend for the leaching of potassium could be obtained with only a few data points available. Furthermore, from figure 5.41, leaching appears to be random and no specific behaviour could be identified when evaluating the different layers in these leached samples. Some samples even had more potassium present than the assumed average initial concentrations. This could be due to insensitive analysing methods, or due to uneven distribution of potassium in the initial samples. For a more reliable study of the leaching behaviour of potassium, the samples need to be enhanced with additional potassium to increase the concentrations, and allow more accurate analysis.

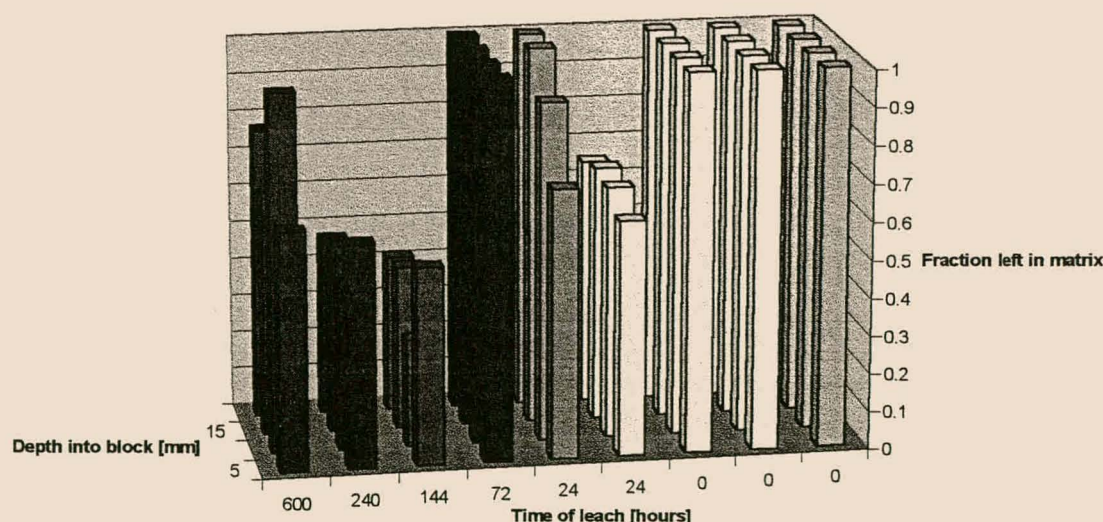


*Figure 5.41: Potassium left in the pozzolanic matrix after acetic acid leaching tests.*



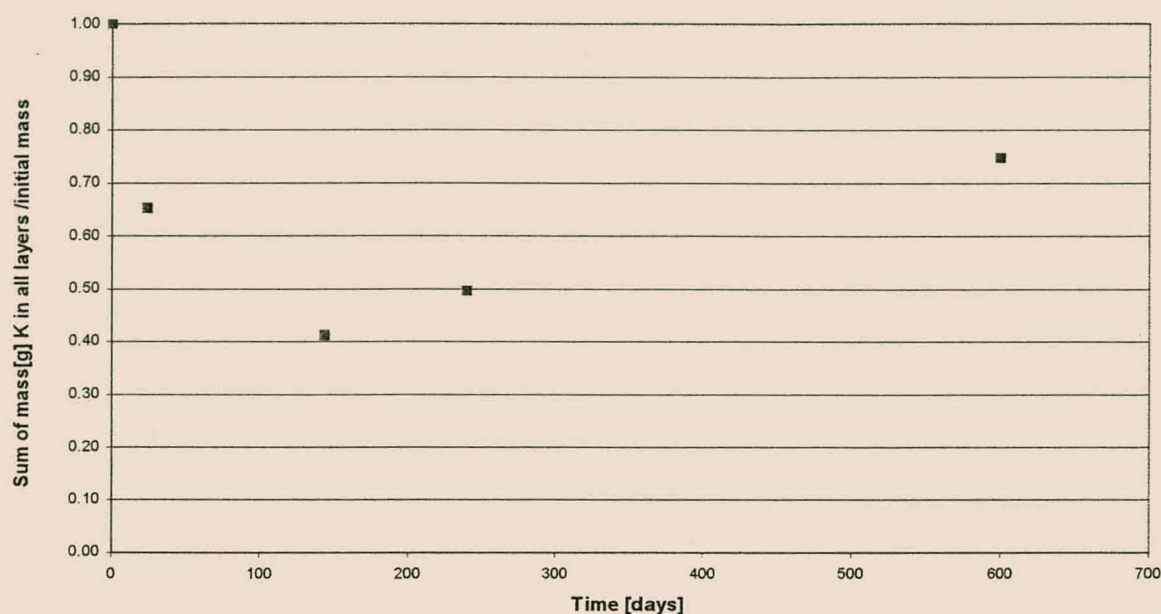


Figure 5.42: Potassium (K) fraction left in the sample after different leaching times.

#### □ Phosphor

After 600 hours of leaching about 55% of the phosphor in the matrix was leached out, but the rate of leaching seems almost constant from 24 until 240 hours, after which the leaching continues. From figure 5.43 the initially leaching of phosphor are faster from the surface layers than from the rest of the sample and as the phosphor in the inner layers are leached by the attacking acid, they also become depleted of phosphor. Once again this rate might be limited by the diffusion of the acetic acid leaching solution into the block or the diffusion of dissolved species from the inside of the sample towards the bulk solution, and the presence of a moving reaction front for the leaching of phosphor, as was found primarily for calcium, and sodium and also for manganese and magnesium. (See figures 5.43 and 5.44).

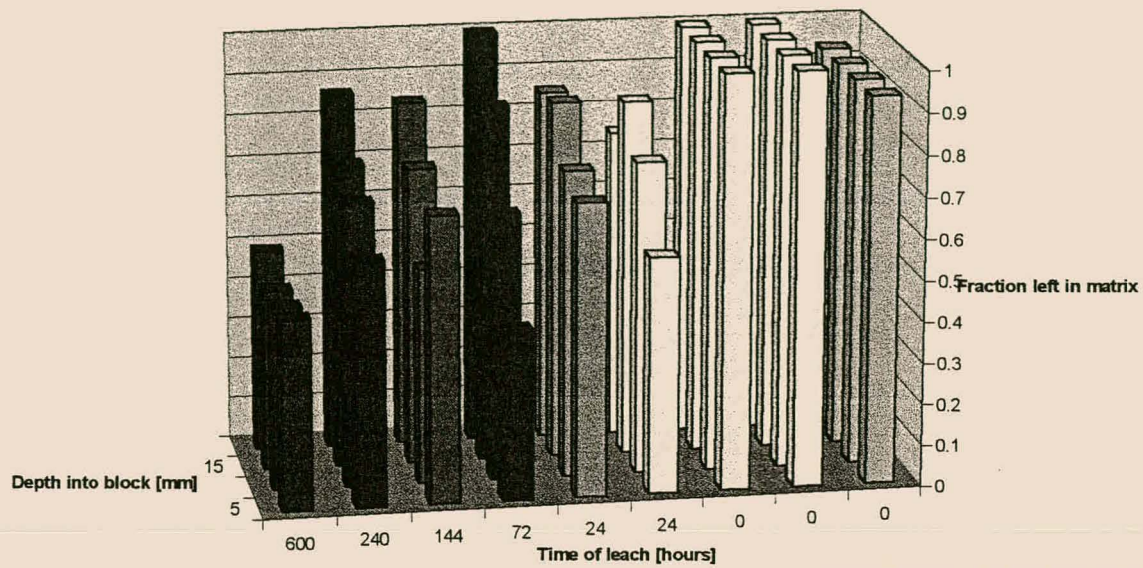


Figure 5.43: P left in pozzolanic matrix after acetic acid leaching tests.

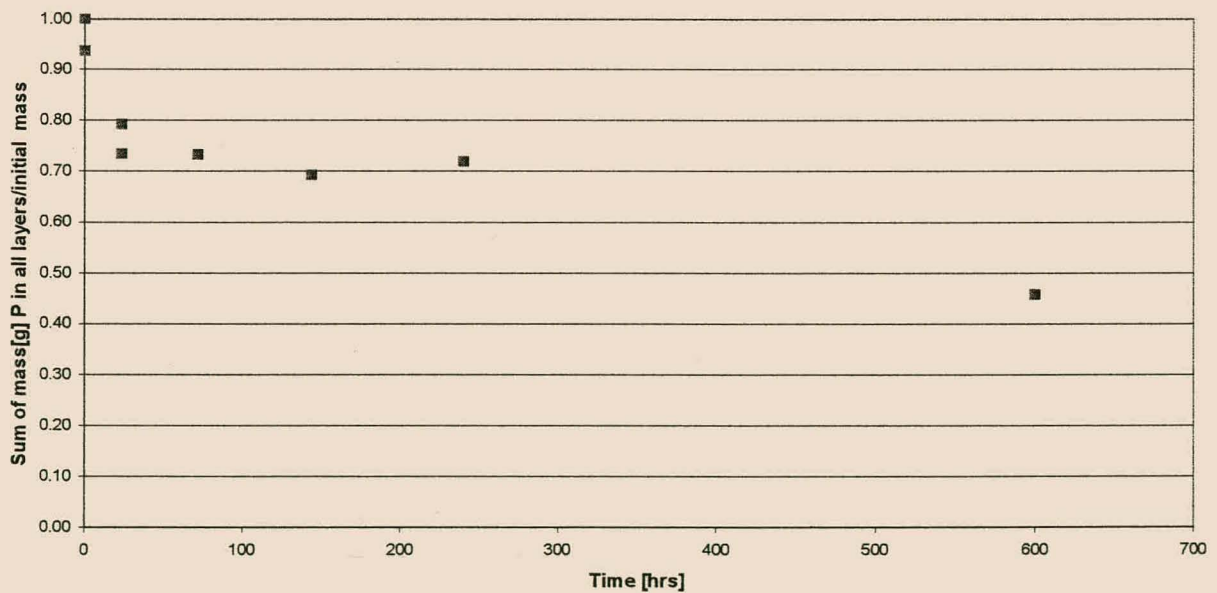


Figure 5.44: P fraction left in the whole sample after different leaching times



### 5.2.3. Conclusions (Geopolymeric vs. Pozzolanic materials)

In table 5.1 the leachability of the different elements in the pozzolanic and geopolymeric samples are summarised. The initial average mass percentages of the elements are also presented.

*Table 5.1: Summary of the leaching behaviour of different elements of the pozzolanic and geopolymeric matrix (leaching times > 600 hours).*

<i>Element</i>	<i>% Initially in the pozzolanic matrix</i>	<i>% Initially in the geopolymeric matrix</i>	<i>% Leached from the pozzolanic matrix (after 670 hours)</i>	<i>% Leached from the geopolymeric matrix (after 600 hours)</i>
Silica (Si)	69	72	20	20
Aluminium (Al)	6	6	27	20
Iron (Fe)	4	5	22	14
Sodium (Na)	2	4	100 (after 670 hrs)	100 (after 72 hrs)
Calcium (Ca)	8	2	95	85
Titanium (Ti)	<1	<1	25	13
Manganese (Mn)	<1	<1	95	61
Magnesium (Mg)	<1	<1	80	82
Potassium (K)	<1	<1	40	25
Phosphor (P)	<1	<1	42	55

From table 5.1 all the elements seem to be more or less equally stabilised for the pozzolanic and geopolymeric matrices at leaching times greater than 600 hours. This implies that during long-term leaching in the environment the specific pozzolanic and geopolymeric matrices would leach out similarly, except for sodium that clearly leaches out faster from the geopolymeric samples. However, of the major matrix components the Si, Al, Ca and Fe did appear slightly more leachable for the pozzolanic case, while more Na and Mg were leached from the geopolymeric samples after 600 hours. The Si, Al, Ca and Fe will add up to the greatest percentage of the materials and it can be concluded that the degradation experienced by the pozzolanic samples were slightly more extreme.

In the results obtained in section 5.2 and 5.3, Si, the main matrix component, seem to be rather stable. This is probably because silica is present in the matrix as insoluble silica oxides and silica hydroxides in silica sand. The calcium-silica-hydrates, which are also present, will however leach much easier, especially because the calcium leaches out fast and silica will, as a result, also be released from the compound. After leaching the matrices for longer than 600 hours, more or less 20% are leached from both matrix types.

Decalcification of both matrices occurs in such a way that 95% of the calcium in the pozzolanic matrix leach out after 670 hours and 85% are leached from the geopolymeric matrix in 600 hours. The behaviour of calcium in the two matrices is rather similar and a moving reaction front was observed for the leaching in both cases. This front moved from the outside of the matrix towards the core, and the surface layers subsequently became depleted of calcium before the inner layers.

All sodium leached completely from both matrices at longer leaching times. The fast leaching rates of sodium are due to the high solubility of the element. The sodium does however leach faster from the geopolymeric samples than from the pozzolanic samples, implying that sodium are better immobilised inside of the pozzolanic structure.

This moving reaction front behaviour of the leaching of Ca was also observed for Na, Mn, Mg, and P in both the pozzolanic and the geopolymeric materials and the leaching behaviour of these elements were very closely related, even though Na and Ca are a bit more soluble and were leached out faster than Mn, Mg and P. These elements are likely to be bound similarly into the matrix.

No significant reaction front (difference in leaching rate of deeper layers of sample than from surface samples) was observed for Si, Fe, Al and Ti in either of the matrices. The leaching behaviour of these elements are also analogous and they are probably also bound into the matrix structure in the same way. Al and Fe are both likely to be part of hematite, which are supposed to form from the jarosite when it reacts with NaOH.

In both cases the behaviour of potassium did not emit any particular trend and the fluctuating results are likely to be owing to the insensitivity of the analysis at low potassium concentrations. Exponential curves with good correlation could be fitted onto the Na and Ca of the pozzolanic matrix ( $R\text{-square} > 0.9$ ), while the fit for the P and Mn was not as good ( $0.7 < R\text{-square} < 0.75$ ), while an exponential fit for Fe, Al, Ti and Si did not give very satisfying correlation ( $0.59 < R\text{-square} < 0.67$ ). For the geopolymeric matrix, exponential curves were also fitted on the data from the different elements. Large fluctuations in data made this difficult, and the best correlation were for Mn (0.74) and Ca (0.68). R-square values for Mg and P, were 0.58 and 0.66 respectively while the rest of the elements, Al, Si, Fe, Ti and K clearly did not exhibit this trend in leaching behaviour.

In general, the main matrix elements seem to be somewhat more stable in the geopolymeric samples than in the pozzolanic samples, but the results were relatively similar. Still, when choosing a feasible matrix structure for use in a landfill, it is perhaps better to select the geopolymeric material.

## CHAPTER 6

# EXPERIMENTAL RESULTS: CONCENTRATION OF LEACHING SOLUTION

*The cumulative concentrations of the leaching solution for different elements were obtained by means of ICP analysis. These results were expressed as percentages of the initial mass of the elements present in the sample to determine the leachability of the elements. A semi-empirical model was fitted on these curves to describe the leaching process and the different curves for the elements in the pozzolanic as well as the geopolymeric matrix were discussed to describe the typical leaching behaviour of all elements in the matrix.*

### 6.1. INTRODUCTION

As was explained earlier (Chapter 3), samples of the leaching solutions were taken at different time intervals during each leaching test. These solution samples were analysed by means of ICP to determine the concentrations of elements present in the leaching vessel at a specific time interval during the experiment. As the leaching process continues, these concentrations are expected to increase as more of the elements leached from the solid sample into the solution.

*Table 6.1: Leaching tests performed to evaluate the leaching of a pozzolanic as well as a geopolymeric matrix.*

Leach run number	Duration of the test	
	[hours]	[days]
POZZOLANIC MATRICES		
L#14	6	0.3
L#15	18	0.8
L#13	48	2
L#17	52	2.2
L#12	96	4



L#18	144	6
L#19	144	6
L#16	168	7
L#9	407	17
L#11	672	28
GEOPOLYMERIC MATRICES		
G5	24	1
G6	24	1
G2	72	3
G3	144	6
G7	145	6
G4	240	10
G1	600	25

The different leaching tests performed on the two matrix types, i.e. the pozzolanic and geopolymeric matrices, are presented in *table 6.1* together with the times at which the experiments were stopped. At the end of the experiments the solids left were analysed (XRF, see chapter 5). We may refer to these test numbers throughout the rest of the chapter(s). Apart from testing the reproducibility of the ICP results, the main reason for the number of test runs, was to analyse the leached solids. The destructivity of the solid analysis method demanded the use of different test-runs to obtain samples leached for different times.

The data obtained from ICP were initially expressed in ppm after which it was divided by the average amount of the specific element in the block (should it all go into the 3 litres of solution) and expressed as a percentage. This maximum was obtained by calculating the average percentage of the element present in a few unleached solid samples. These initial element concentrations of the solids were also expressed in mg/l, i.e. ppm.

Throughout the tests various samples were extracted from the vessel, while acid was added. The volumes of these samples were kept at a minimum, but could have had an influence on the solution concentration during the tests. Correction factors were determined; to establish what effect this volume differences would have on the solution concentrations. The concentrations measured in the samples were multiplied by these values as compensation for this effect. The volumes of acid added as well as the sample volumes were recorded during each sampling period and different factors for the different tests were determined.

## 6.2. MODELLING

In predicting the leaching behaviour of immobilised materials, various models have been proposed. Generally the material consist of a porous solid matrix, in which several solid phases are encapsulated or bound, as well as air voids, which can be filled, or partly filled, with liquid (pore solution). When such a material is placed in a leaching solution, the aggressive solution

has to move into the solid, react with the immobilised species and the resultant dissolved species have to move from the solid into the bulk solution. A subsequent change in the leaching solution concentration will be detected. The transport of contaminants are assumed to occur due to diffusion through the pore solution, rather than the solid matrix itself, since true solid-state diffusion is slow compared to diffusion through the solution in the interconnected pores. There are generally two sources of leaching, i.e. from the surface exposed to the solution as a result of size reduction, and also from the inside of the solids resulting from crack formation and/or existing pores. The mobilisation, or leaching, of species is normally expressed as a leaching rate  $L(t)$  or as the cumulative fraction leached  $F(t)$ , which is obtained from analysing the bulk solution.

To find this rate, several mathematical models have been under consideration for various leaching conditions. A general approach to characterising the leaching phenomenon has been considered by combining three basic models, that is a;

- leaching model based on bulk diffusion,
- leaching model based on bulk diffusion and chemical reaction, and
- leaching model based on interface mass resistance.

The general form for these three models have been combined and led to a semi-empirical expression (as was used by Jansen van Rensburg, 1997) to describe the cumulative amount leached into the bulk solution (CAL) of a contaminant from a stabilised matrix.

The equation is given by:

$$CAL(t) = K_1(1 - e^{-k_2 t}) + K_3 t^{\frac{1}{2}} + K_4 t \quad (6.1)$$

The first term,  $K_1(1 - e^{-k_2 t})$  is the general form of the leaching model based on mass resistance and is based on the kinetics of exchanges of species between the surface of the waste and the aqueous solution (see equation 2.25).

The second term,  $K_3 t^{\frac{1}{2}}$ , is the general form of a bulk diffusion model developed from Fick's second law of diffusion (see equation 2.13). It represents the transport of species by diffusion, while the third term,  $K_4 t$ , represents leaching through slow mobilising chemical reaction and/or to corrosion or structural breakdown of the waste matrix and is the general form of the kinetically controlled chemical reaction model (see equation 2.31).

From the results it was evident that not all the elements that leaches from the solids can be found in the solution, and another term was added to equation 6.1 to represent the amount that seems to precipitate during the leaching tests. By calculating the precipitate concentrations from the differences in solid and solution concentrations, an indication of the nature of this term could be obtained for each element. In some cases this term was assumed to be linear and in some cases a power term. This led to equations 6.2 and 6.3.

$$CAL(t) = K_1(1 - e^{-k_2 t}) + K_3 t^{\frac{1}{2}} + K_4 t - (K_5 t + K_6) \quad (6.2)$$

$$CAL(t) = K_1(1 - e^{-k_2 t}) + K_3 t^{\frac{1}{2}} + K_4 t - K_5 t^{K_6} \quad (6.3)$$

This semi-empirical model was fitted on the cumulative amounts of the elements leached from the matrix as obtained from the leaching test experiments and the parameters  $K_1$ ,  $K_2$ ,  $K_3$ ,  $K_4$ ,  $K_5$  and  $K_6$  were obtained through regression analysis.

Equation 6.2 was mostly used, except for Al, Fe and Si of the pozzolanic matrix, where equation 6.3 was applied.

By evaluating the four terms the contribution of the surface phenomenon, diffusion and the chemical reaction can be expressed as a percentage of the sum of the total amount leached from the matrix (eq. 6.4) at a certain time and from this we can assume that the rate limiting mechanisms of leaching during the tests, is the largest contributors to the leaching solution concentration at the specific time. The precipitation does not contribute to leaching, but only decreases the amount of the element in the solution and was also expressed as a percentage of the first three terms of equations 6.2 or 6.3.

$$\text{The sum of all terms} = K_1(1 - e^{-k_2 t}) + K_3 t^{\frac{1}{2}} + K_4 t \quad (6.4)$$

### 6.2.1 Pozzolanic matrix

*Table 6.2 Table with the mean square differences between the fitted semi-empirical model (equations 6.2 or 6.3) and the data of L#18, for the different elements.*

Element	RSQ
Si	0.97
Ca	0.89
Al	0.91
Na	0.98
Fe	0.97
Mg	0.97
K	0.65
Cu	0.90
Pb	0.78

In table 6.2 the R-square values are given as an indication of the accuracy of the regression curve that was fitted on the data of experiment L#18. L#18 is assumed to be the leaching test that represents the general leaching phenomena during an acetic acid leaching test on the specific pozzolanic matrix and variation from these curves (as was found in some of the other leaching runs) are assumed to be due to either probe failure, ageing of samples, inaccuracies in the analysis, possible differences in initial sample concentrations, or a combination of these factors. In the discussion of the behaviour of the different elements, there will be constantly referred to the data obtained from L#18 of the leaching tests on the pozzolanic samples and to G5 when evaluating the leaching of the geopolymeric matrix. The R-square values (Table 6.2) indicate a good correlation to the data for all the elements, except for potassium (K), where the data points were more scattered than in the other series (due to analysis insensitivity at these low concentrations).

*Table 6.3 Values of constants ( $K_1$  to  $K_6$ ) after regression analysis of either equation 6.2 or 6.3, depending on formation of precipitate with time.*

Element	K1	K2	K3	K4	K5	K6
Si	0.036	1.057	0.002	0.060	0.060	0.000
Ca	607.354	0.000	4.832	0.000	0.313	0.911
Al	607.423	0.000	0.031	0.000	0.046	0.000
Na	38.472	0.093	0.000	0.375	0.000	2.608
Fe	0.000	0.937	0.098	0.036	0.035	0.881
Mg	9.275	0.250	1.669	0.148	0.590	0.729
K	27.339	0.113	4.099	0.000	8.245	0.397
Cu	6.552	0.000	0.068	0.011	0.000	0.000
Pb	4.570	1.685	0.034	0.050	0.000	0.000



From table 6.3 very large  $K_1$  values are observed for Ca and Al indicating a dependence upon the surface reaction, as for Na and K that also have rather large  $K_1$  values. Diffusion seems to be more pronounced in Ca and K than for the other elements due to the larger  $K_3$  values. The largest  $K_4$  value is calculated for Na and Mg, indicating possible dependence on the degradation phenomenon for these elements. Virtually no precipitate was found in the Na solution due to its great solubility and the  $K_5$  and  $K_6$  values of zero supported this observation. Furthermore, it was assumed that no precipitate is formed in the Cu and Pb solutions and  $K_5$  and  $K_6$  is also assumed to be zero. The contribution of each term as the leaching tests proceed, will be discussed later in this chapter.

### 6.2.2. Geopolymeric matrix

*Table 6.4 Table with the mean square differences between the fitted semi-empirical model (equations 6.2 or 6.3) and the data of G5, for the different elements.*

Element	RSQ
Si	0.96
Ca	0.98
Al	0.97
Na	0.98
Fe	0.94
Mg	0.93
K	0.65
Cu	0.97
Pb	0.38

*Table 6.5 Values of constants ( $K_1$  to  $K_6$ ) for the leaching test run G5 (on the geopolymeric matrix) after regression analysis of either equation 6.2 or 6.3, depending on formation of precipitate with time.*

Element	$K_1$	$K_2$	$K_3$	$K_4$	$K_5$	$K_6$
Si	3.668	0.007	0.040	0.000	0.036	0.891
Ca	4.468	0.086	11.581	0.000	0.653	99.514
Al	2.284	0.101	0.765	0.260	0.737	166.174
Na	28.451	0.239	2.734	0.000	0.000	0.000
Fe	5.126	23.352	0.111	0.000	0.003	0.000
Mg	33.177	0.000	10.747	0.281	4.691	0.695
K	0.000	0.101	9.694	0.000	2.552	0.705
Cu	0.000	10.989	0.676	0.000	0.676	0.500
Pb	7.306	1000.000	0.150	0.000	0.132	0.000

According to table 6.4, good R-square correlations were obtained for most of the elements when equations 6.2 or 6.3 were fitted on the data, except for Pb and K, which presented unsatisfactory R-square values of 0.38 and 0.65 respectively.

In table 6.5 the largest  $K_1$  values are for Na and Mg, indicating that the surface reaction might play a large role in leaching of these elements. The  $K_1$  values of Ca and Al are about two orders of magnitude smaller than for the pozzolanic matrix (table 6.3) and the surface dissolution of Ca and Al are probably less pronounced for the geopolymeric matrices than for the pozzolanic matrices. The larger  $K_3$  value for Ca might serve as an indication that the leaching of Ca is rather due to diffusion than the surface reactions, when bound into a geopolymeric matrix. The  $K_3$  value of Mg also exhibits diffusion involvement during the leaching of Mg from the geopolymer. Furthermore,  $K_4$  values appear only significant for Mg and Al, where degradation will subsequently be expected. When evaluating the values of  $K_5$  and  $K_6$ , precipitation effected the leachate concentrations of Ca and Al, to the greatest degree. Precipitation of Mg also seemed significant and these precipitation constants were higher than for the pozzolanic matrix.

### 6.3. LEACHING RESULTS

#### 6.3.1 Pozzolanic matrix results

The following figures represent the data collected by analysing the leaching solution (ICP-analysis) at different times during the acetic acid leaching tests. The different test runs performed on the pozzolanic samples (L#9 to L#18), were done in the same way on the other samples and liquid samples were taken during the tests runs at various time intervals, and analysed. The only variable in these runs is, supposedly, the time before the test runs were stopped. Similar concentrations are therefore expected during these tests. However, some deviation in either the test run conditions, the matrix constituency or the analysis circumstances caused the results to differ somewhat for the different runs and L#18 was assumed to be the test which most accurately represent the leaching behaviour of the pozzolanic matrix. Thus, curves, according to equations 6.2 or 6.3, were fitted on the data-points of L#18 and the resulting curves are plotted, together with the data obtained during tests L#9 to L#18, in the following figures:

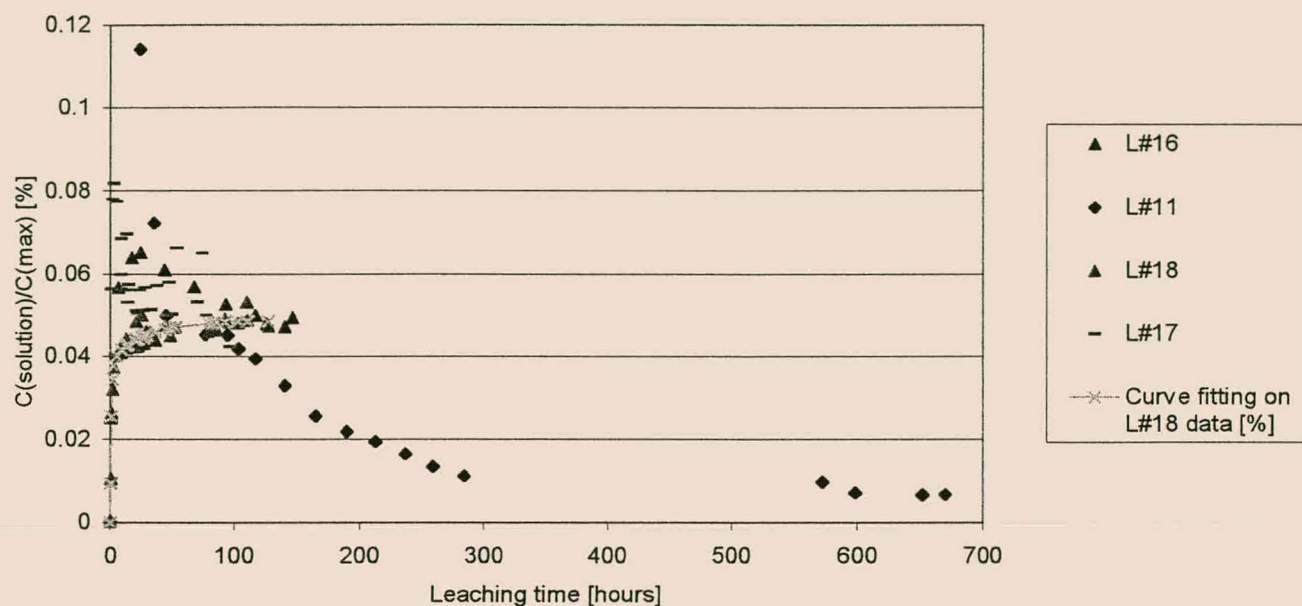


Figure 6.1(a): Leaching solution data and leaching curve for silica (pozzolanic matrix)[0-700 hours]

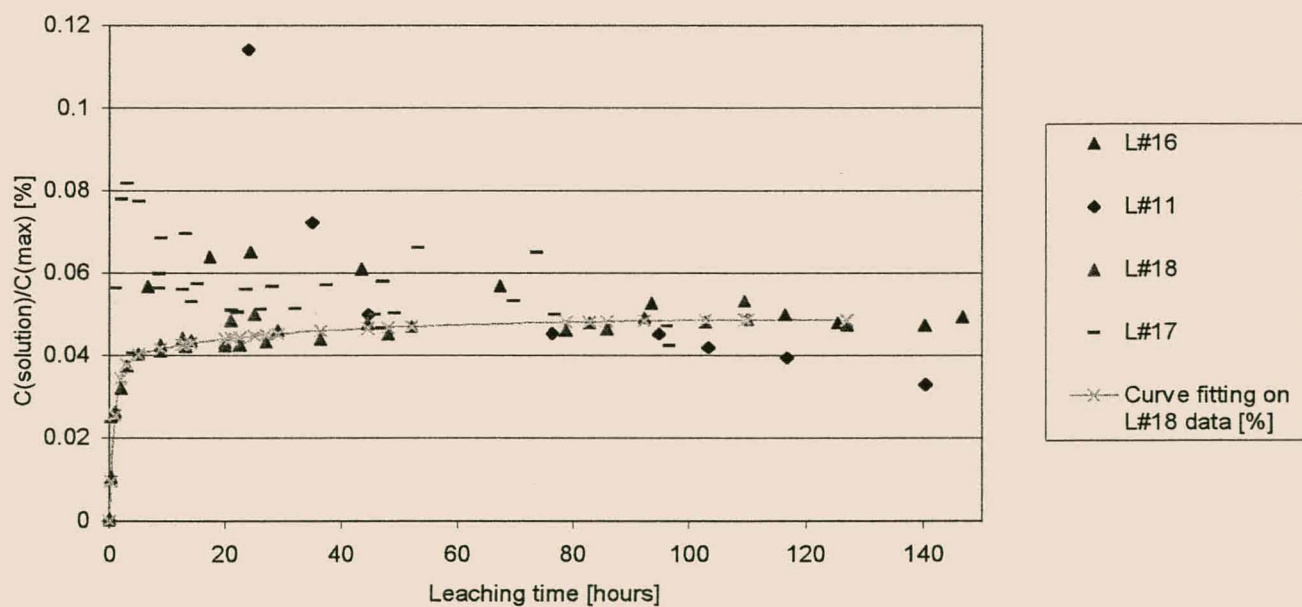


Figure 6.1(b): Leaching solution data and leaching curve for silica (pozzolanic matrix)[0-150 hours]

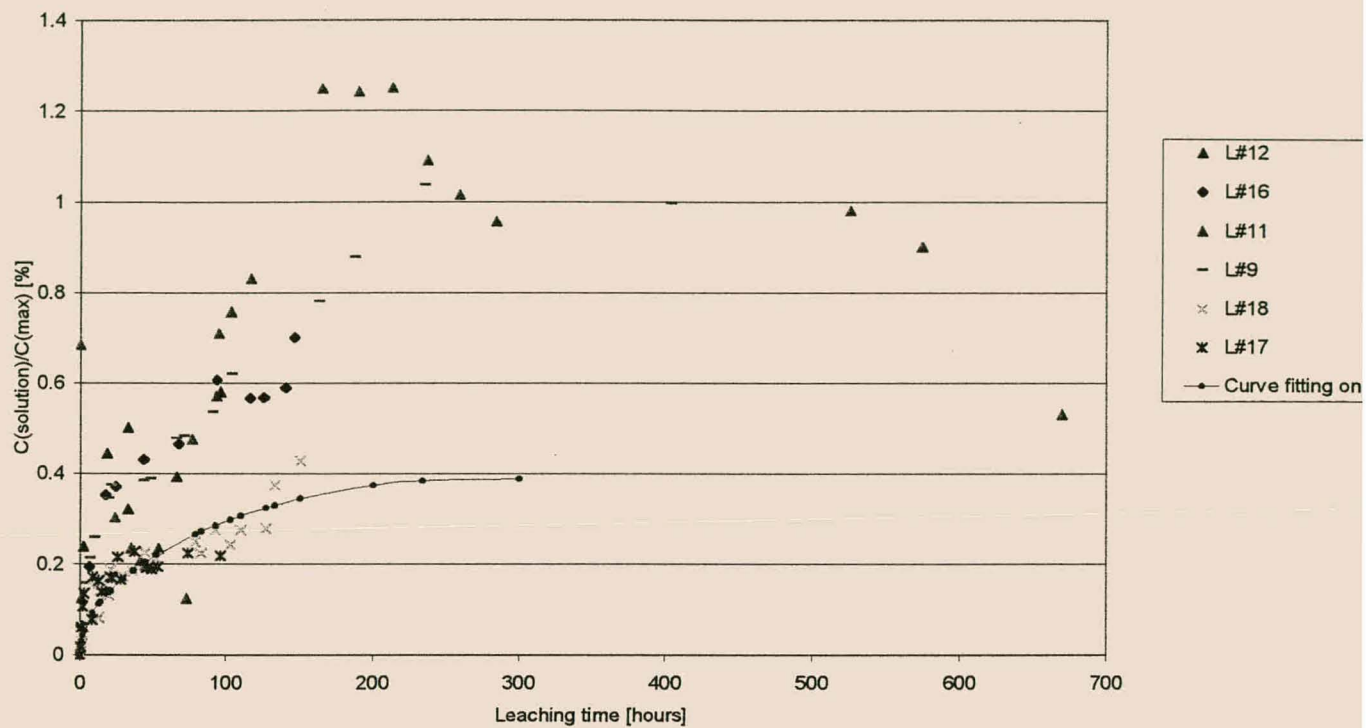


Figure 6.2(a): Leaching solution data and leaching curve for aluminium (pozzolanic matrix)[0-700 hours]



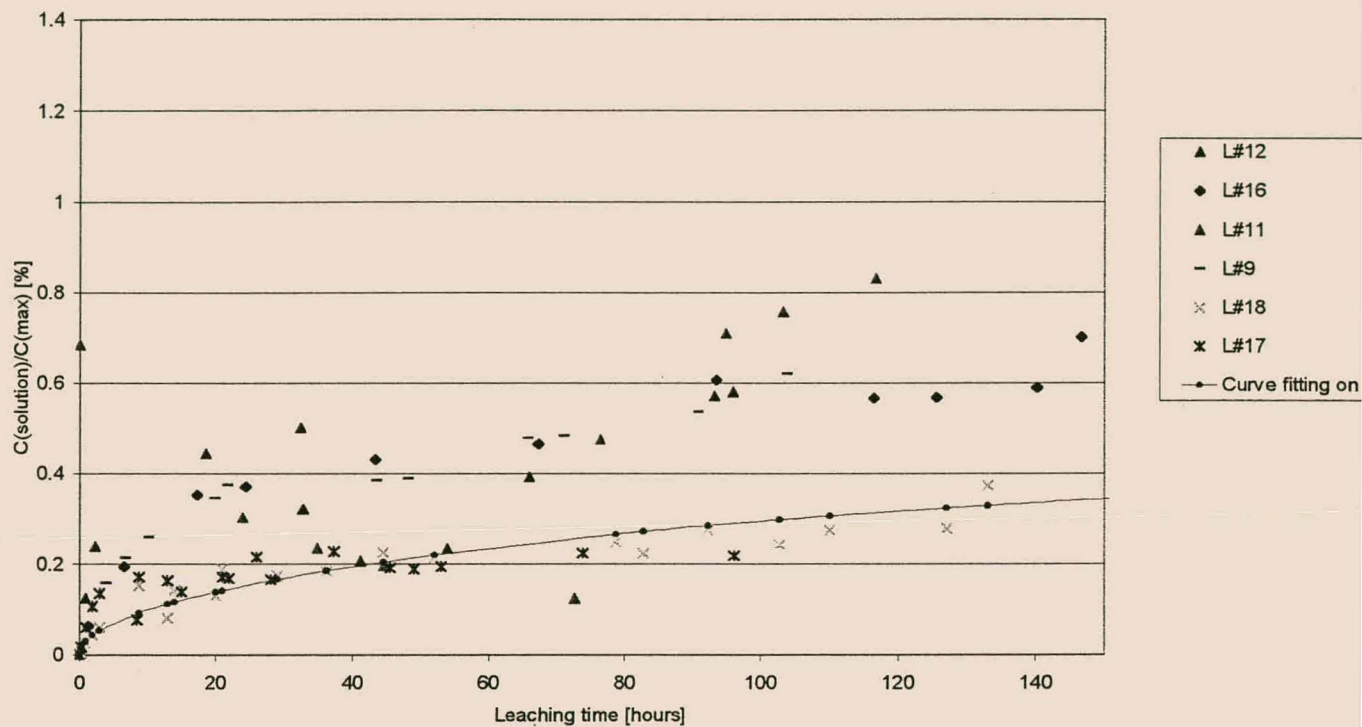


Figure 6.2(b): Leaching solution data and leaching curve for aluminium (pozzolanic matrix)[0-150 hours]

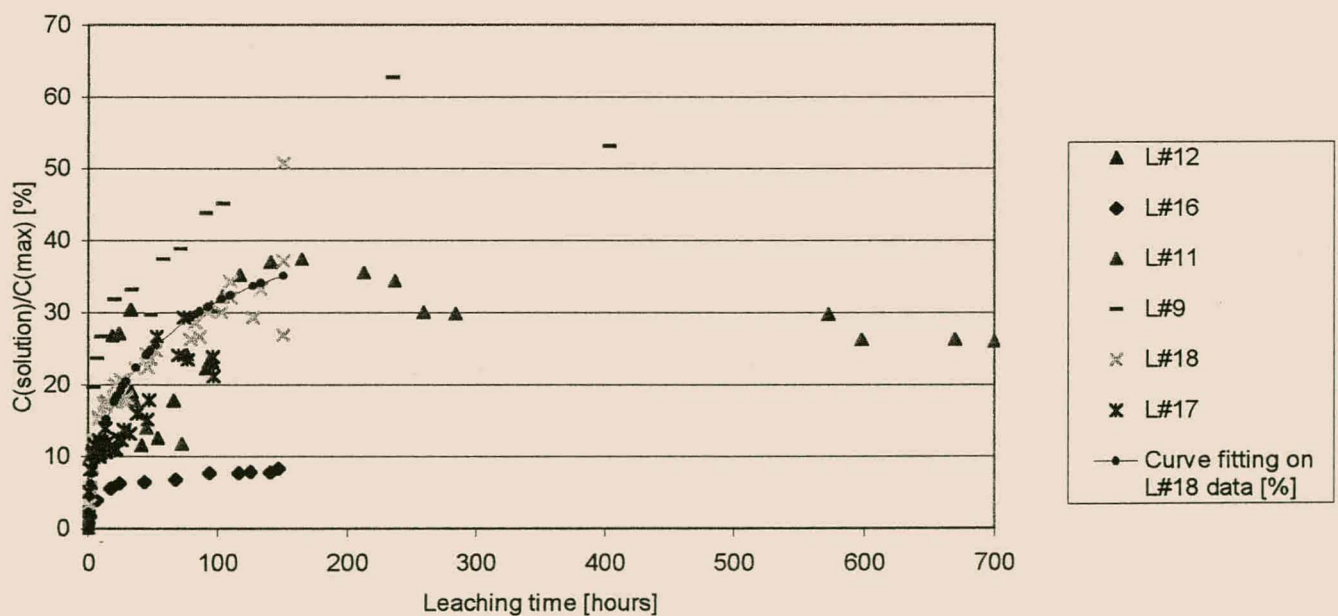


Figure 6.3(a): Leaching solution data and leaching curve for calcium (pozzolanic matrix)[0-700 hours]

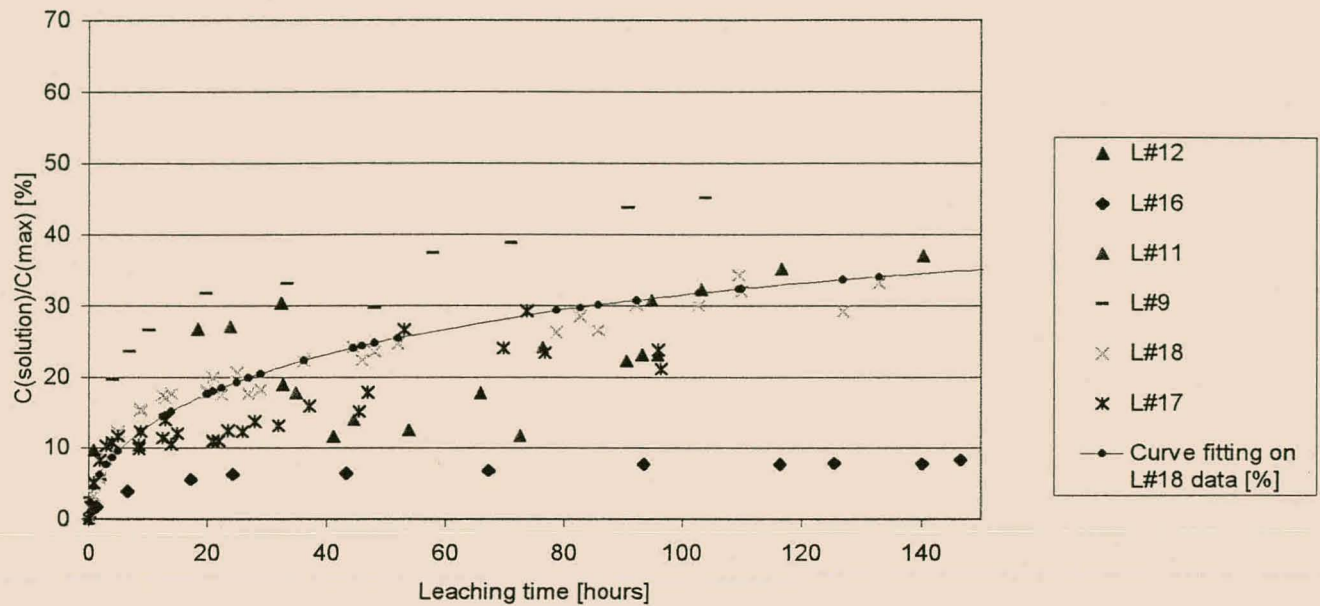


Figure 6.3(b): Leaching solution data and leaching curve for calcium (pozzolanic matrix) [0-150 hours]

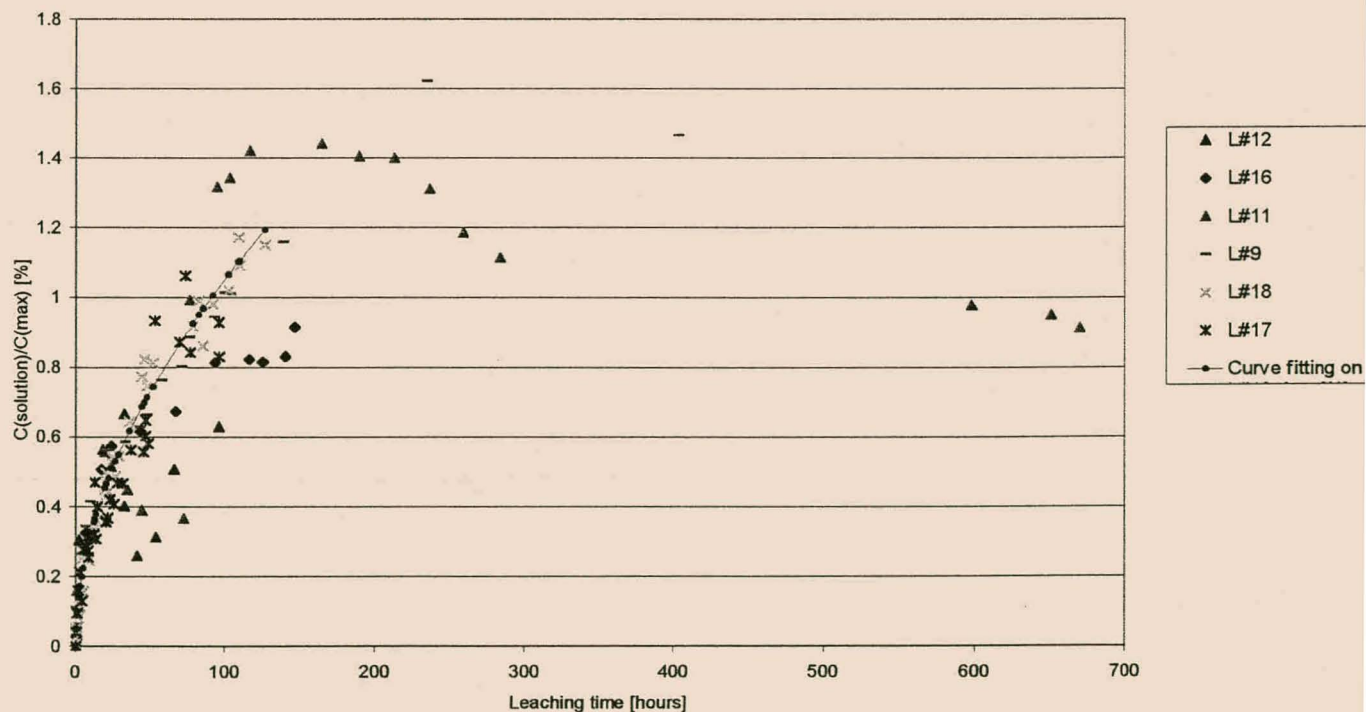


Figure 6.4(a): Leaching solution data and leaching curve for iron (pozzolanic matrix) [0-700 hours]

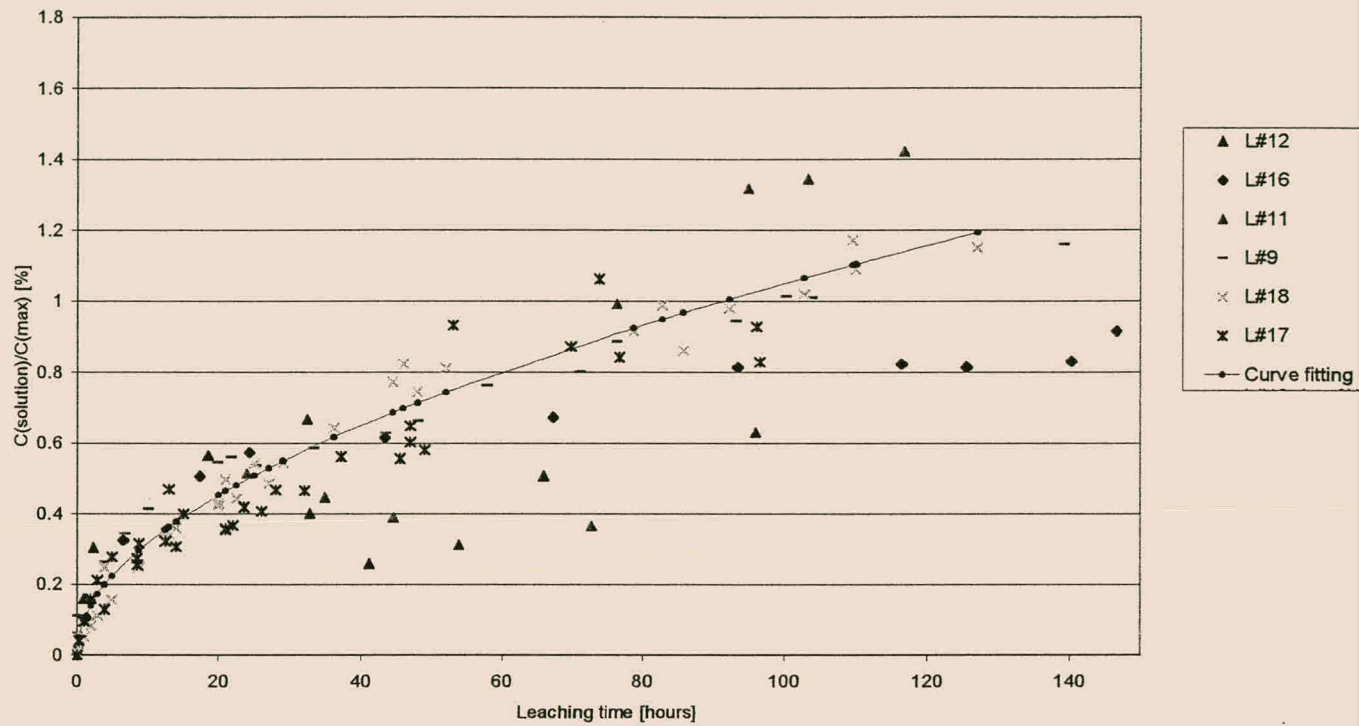


Figure 6.4(b): Leaching solution data and leaching curve for iron (pozzolanic matrix)[0-150 hours]

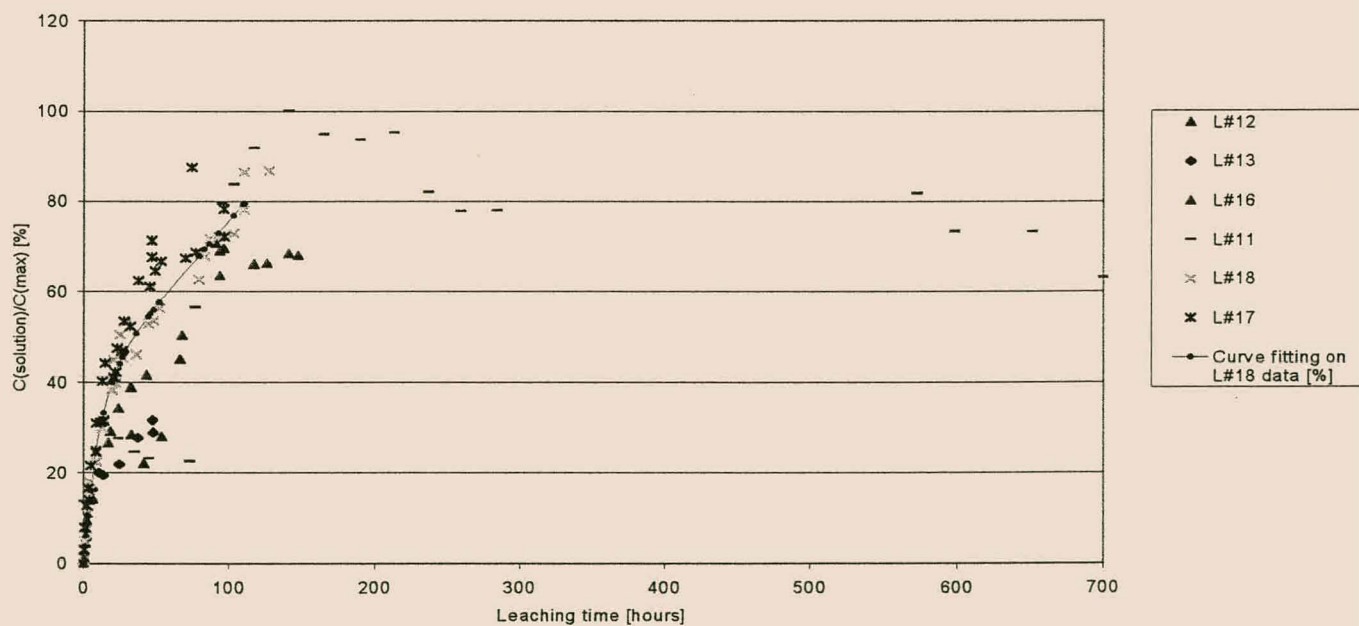


Figure 6.5(a): Leaching solution data and leaching curve for sodium (pozzolanic matrix)[0-700 hours]

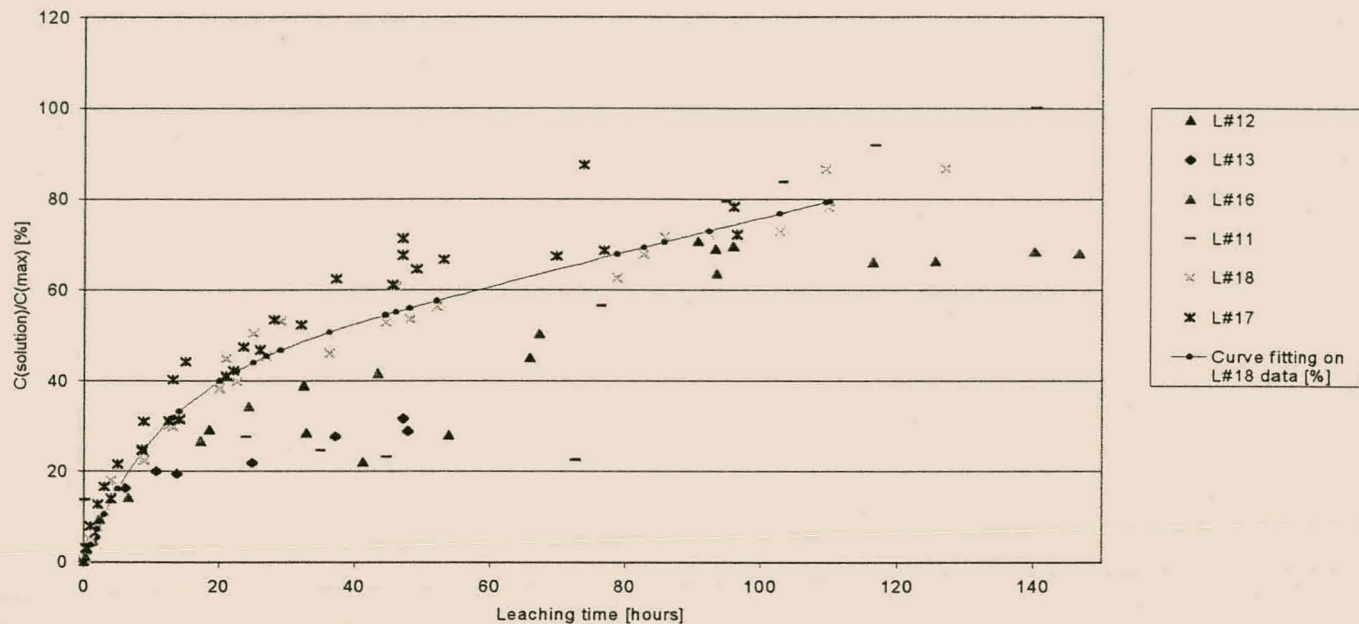


Figure 6.5(b): Leaching solution data and leaching curve for sodium (pozzolanic matrix)[0-150 hours]

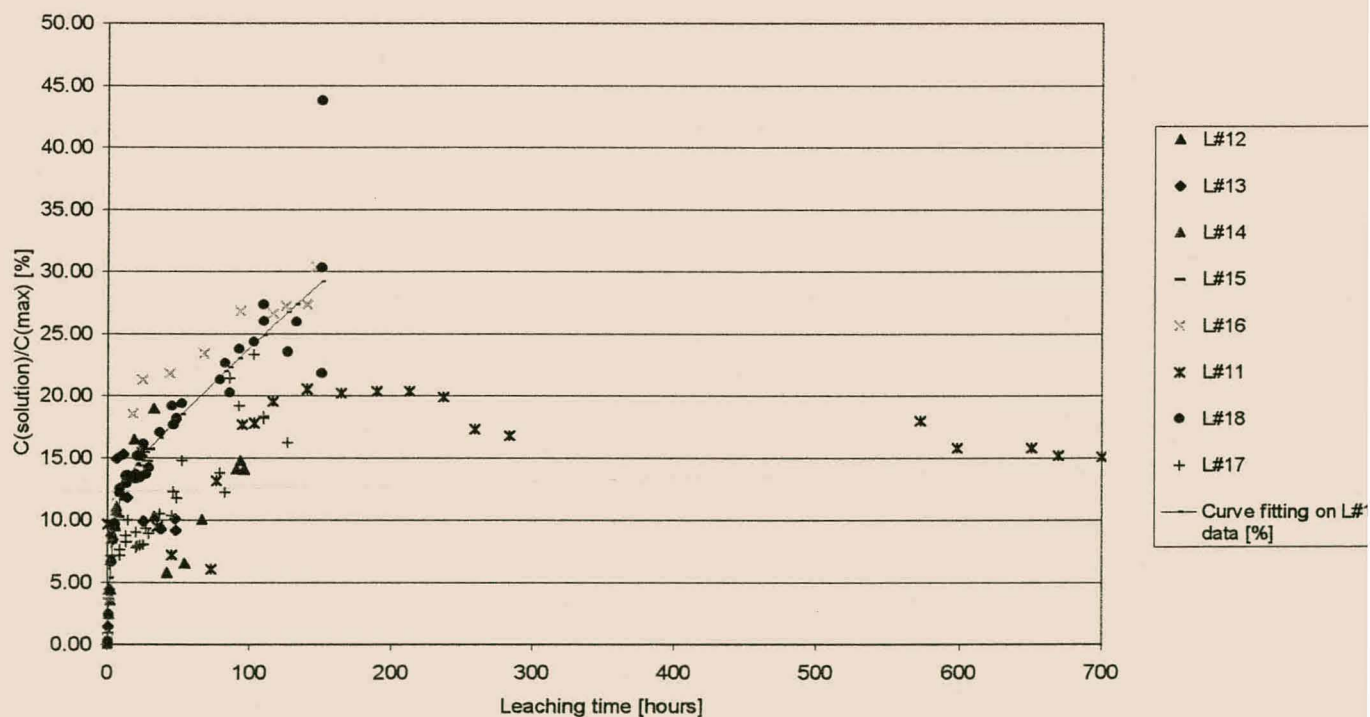


Figure 6.6(a): Leaching solution data and leaching curve for magnesium (pozzolanic matrix)[0-700 hours]



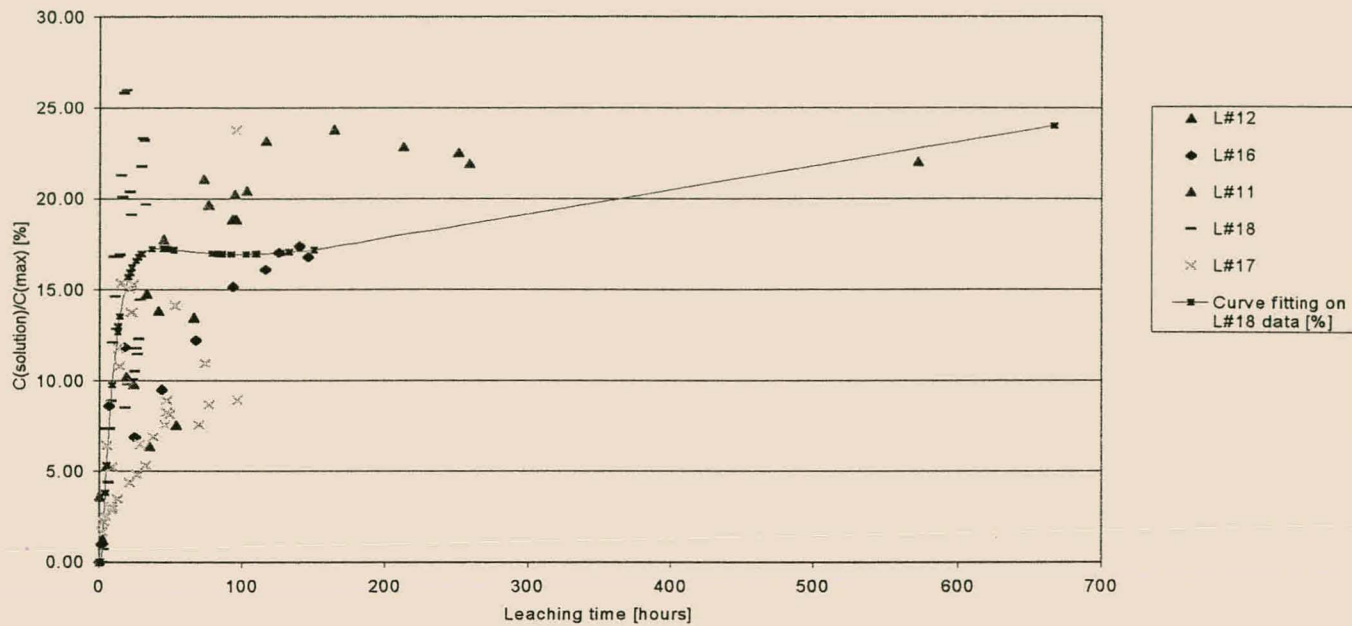


Figure 6.7(a): Leaching solution data and leaching curve for potassium (pozzolanic matrix)[0-700 hours]

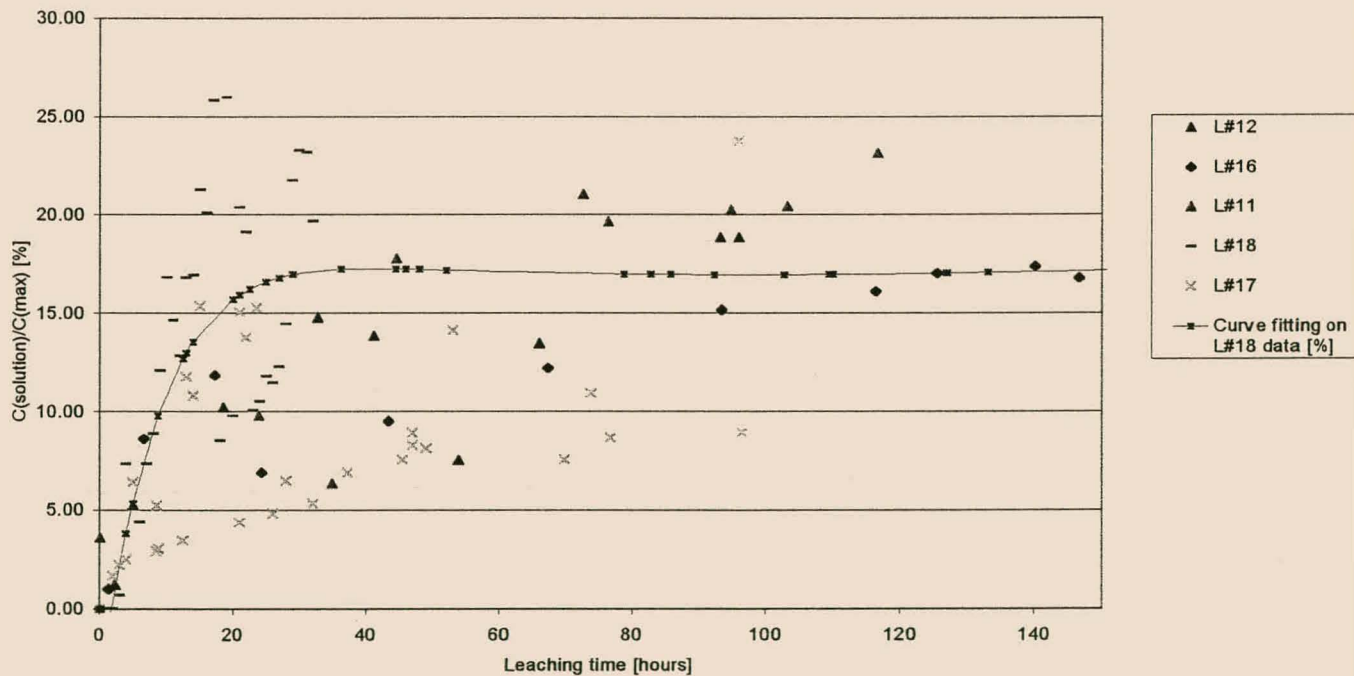


Figure 6.7(b): Leaching solution data and leaching curve for potassium (pozzolanic matrix)[0-150 hours]

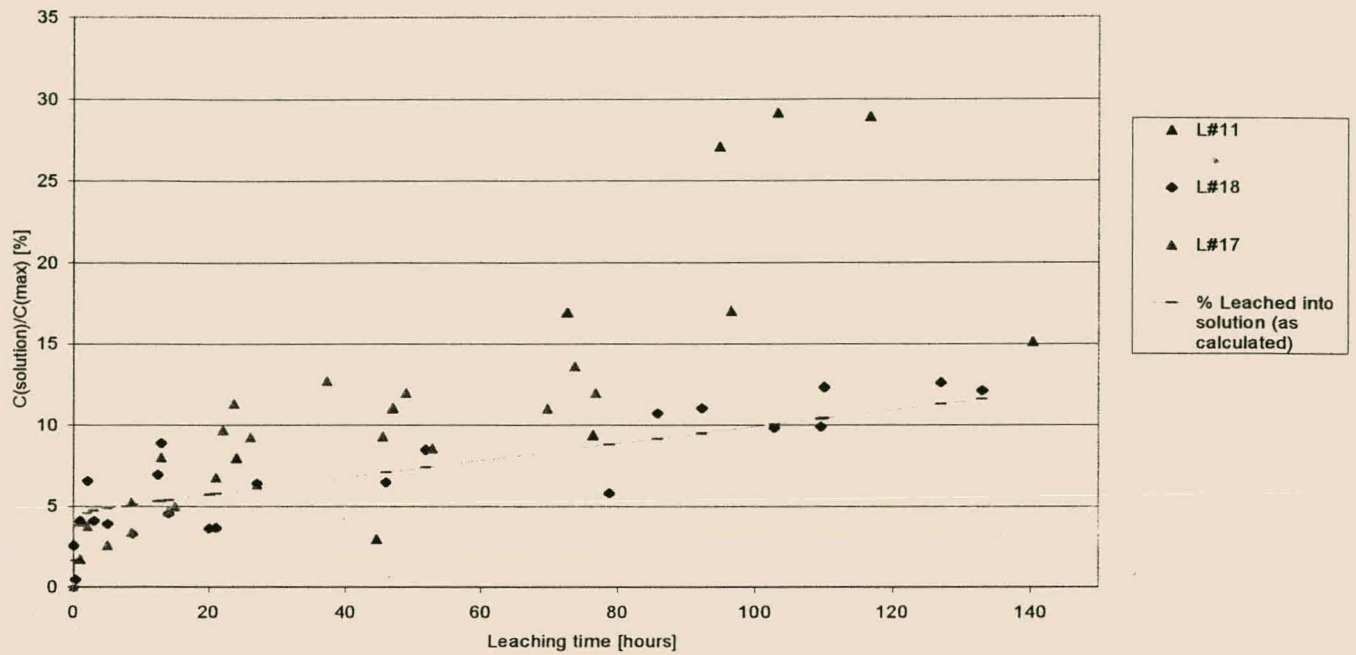


Figure 6.8: Leaching solution data and leaching curve for lead (pozzolanic matrix)[0-150 hours]- assuming no precipitation

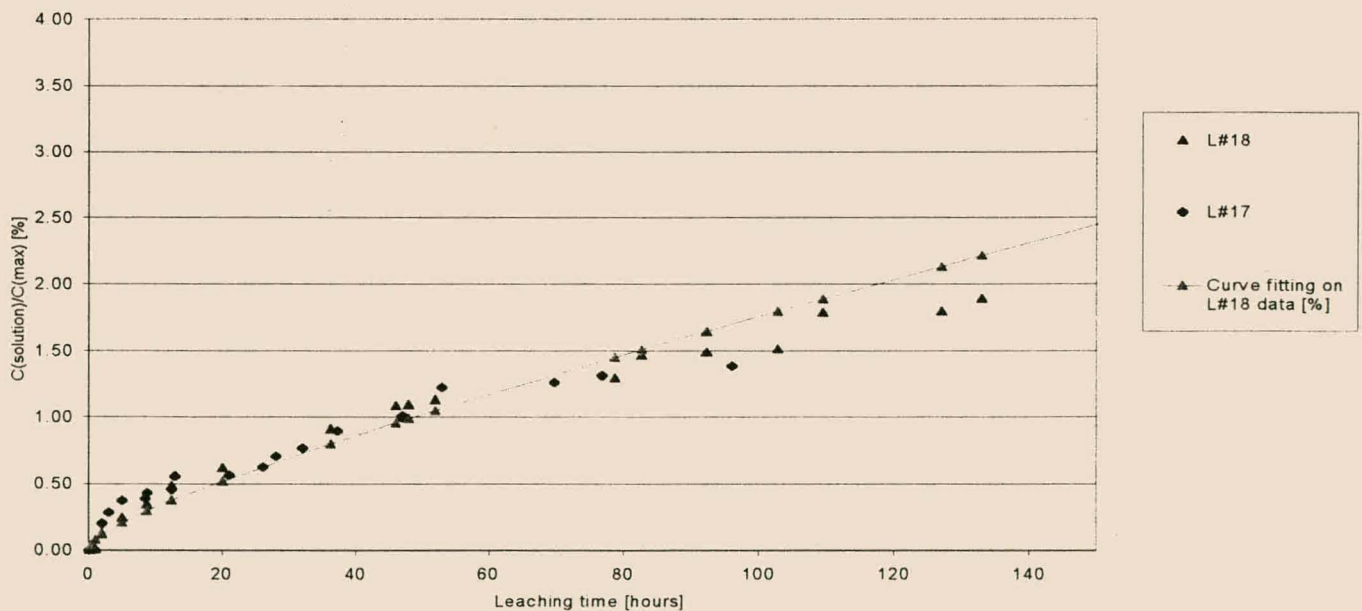


Figure 6.9: Leaching solution data and leaching curve for copper (pozzolanic matrix)[0-150 hours] – assuming no precipitation

- The figures in appendix B (B1 – B7) are representing the elements leached from the pozzolanic solid matrix after leaching tests of different duration. These results are expressed as percentages of the concentrations of the elements, originally present in matrix. Curves according to equation 6.1 (cumulative amount leached – no precipitation), were fitted on the solid data. The leaching curves of the increase in solution concentrations are also plotted on these graphs to point out the differences in the amounts of elements leached from the solid matrix and the amount of those elements found in solution. Both of the solid and solution concentrations are expressed as a percentage of the initial amount of the element in the matrix. The leaching phenomena can mostly be divided into two parts, i.e. the initial stage (little or no precipitation) or the precipitation stage, when the solution concentration starts to decrease.
- The values obtained for the constants of equations 6.2 and 6.3 for the different elements are given in table 6.2. When each term of the equation is considered separately against time, the % contribution of each mechanism (i.e. surface reaction, diffusion, degradation and precipitation) can be calculated and the following curves represent the contribution of each term to the overall amount leached from the matrix, as the duration of the tests increase.

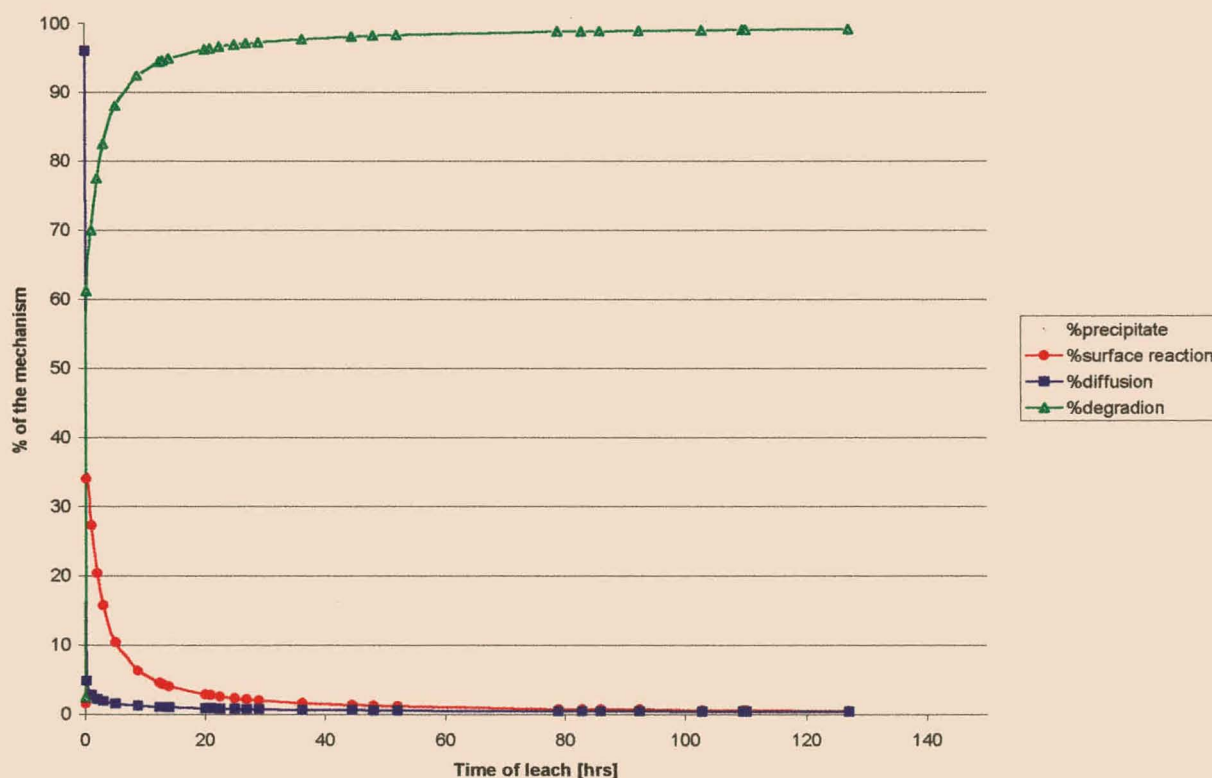


Figure 6.10: % Contributions of each mechanism for silica

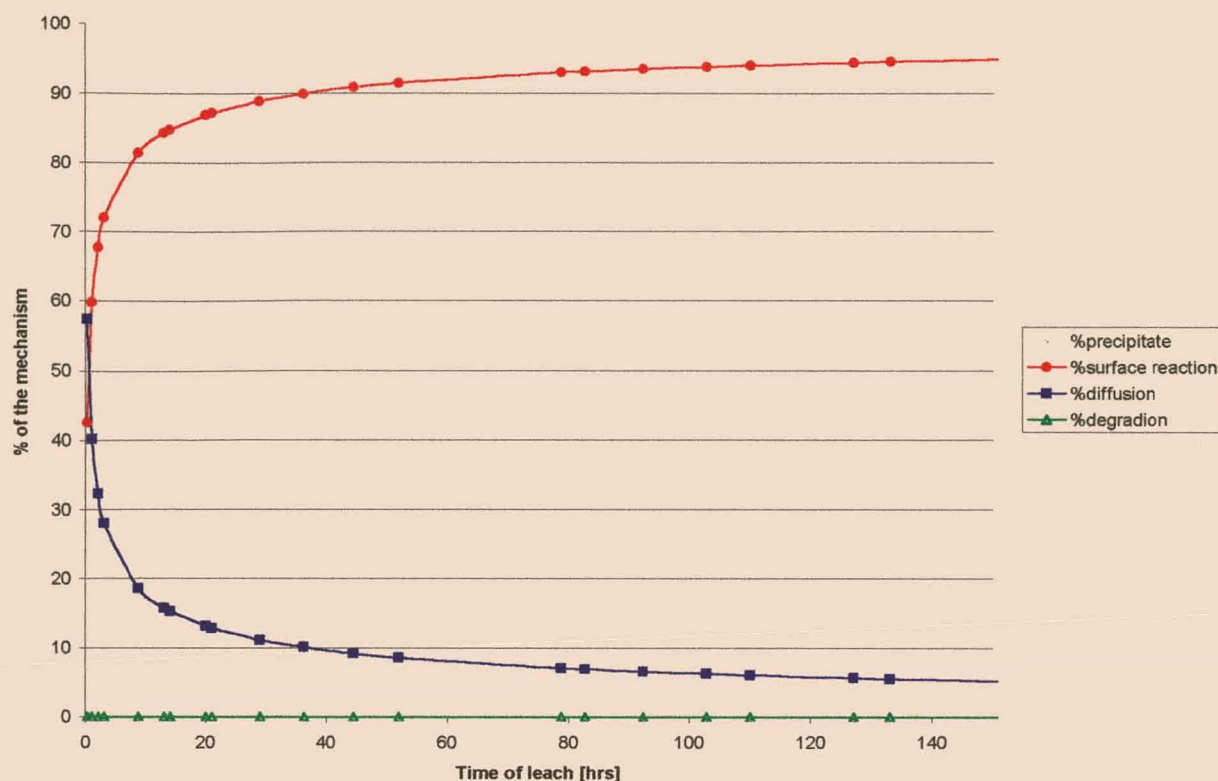


Figure 6.11: % Contributions of each mechanism for aluminium

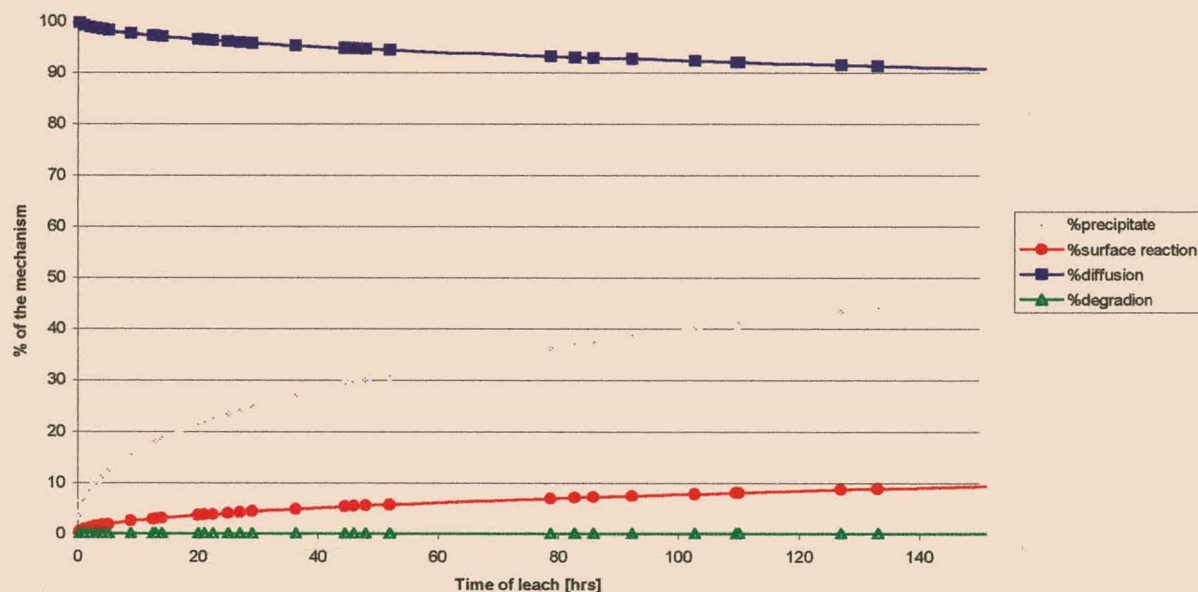


Figure 6.12: % Contributions of each mechanism for calcium



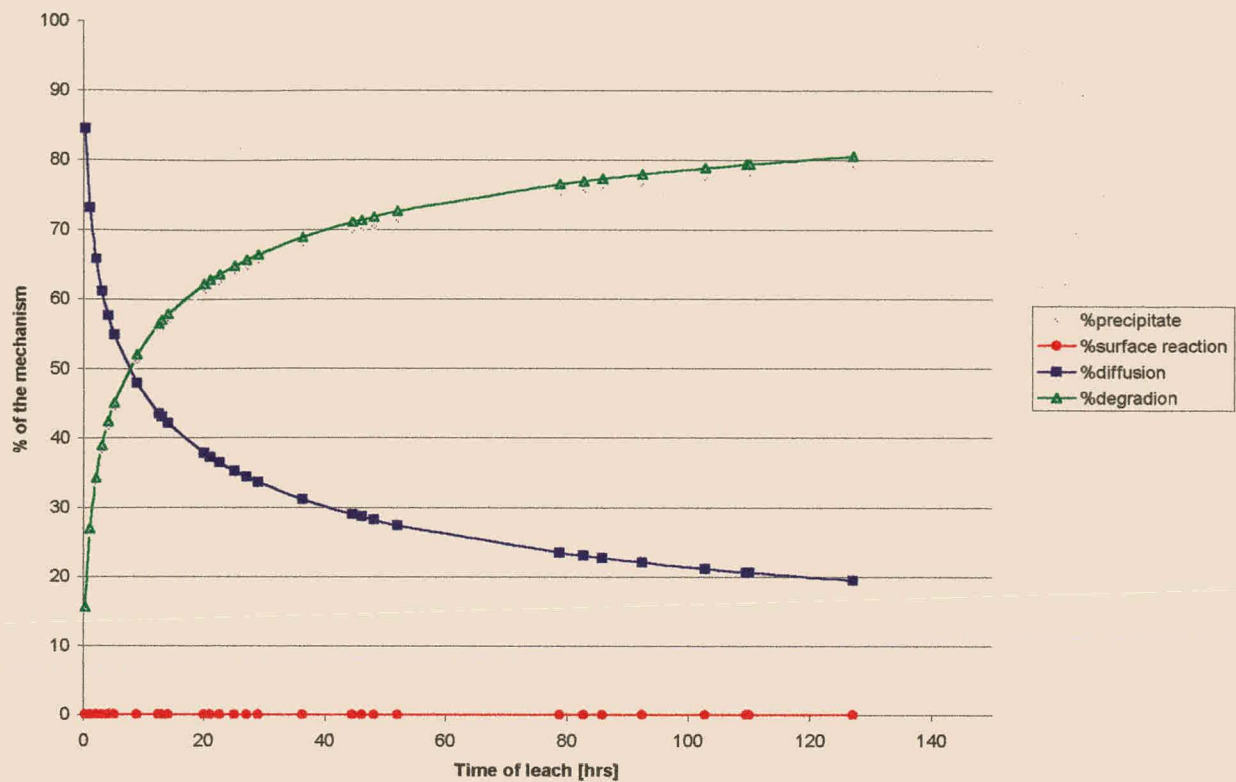


Figure 6.13: % Contributions of each mechanism for iron (Fe)

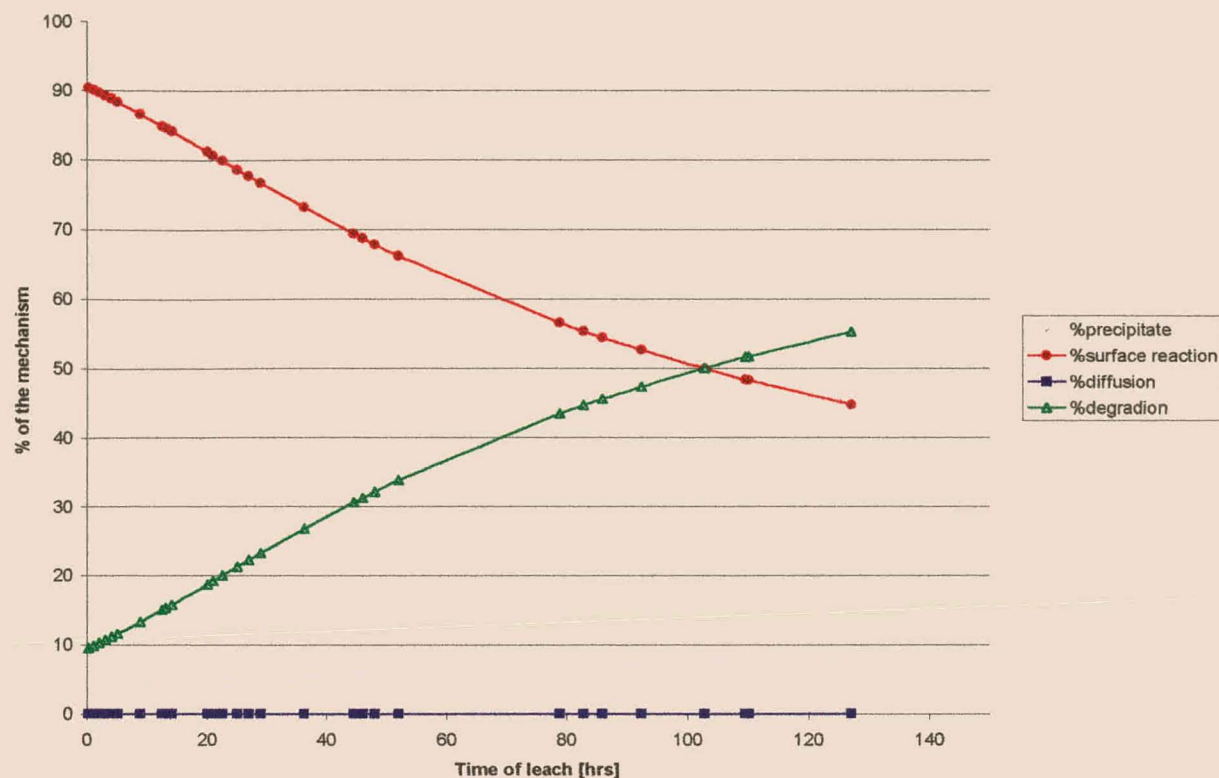


Figure 6.14: % Contributions of each mechanism for sodium

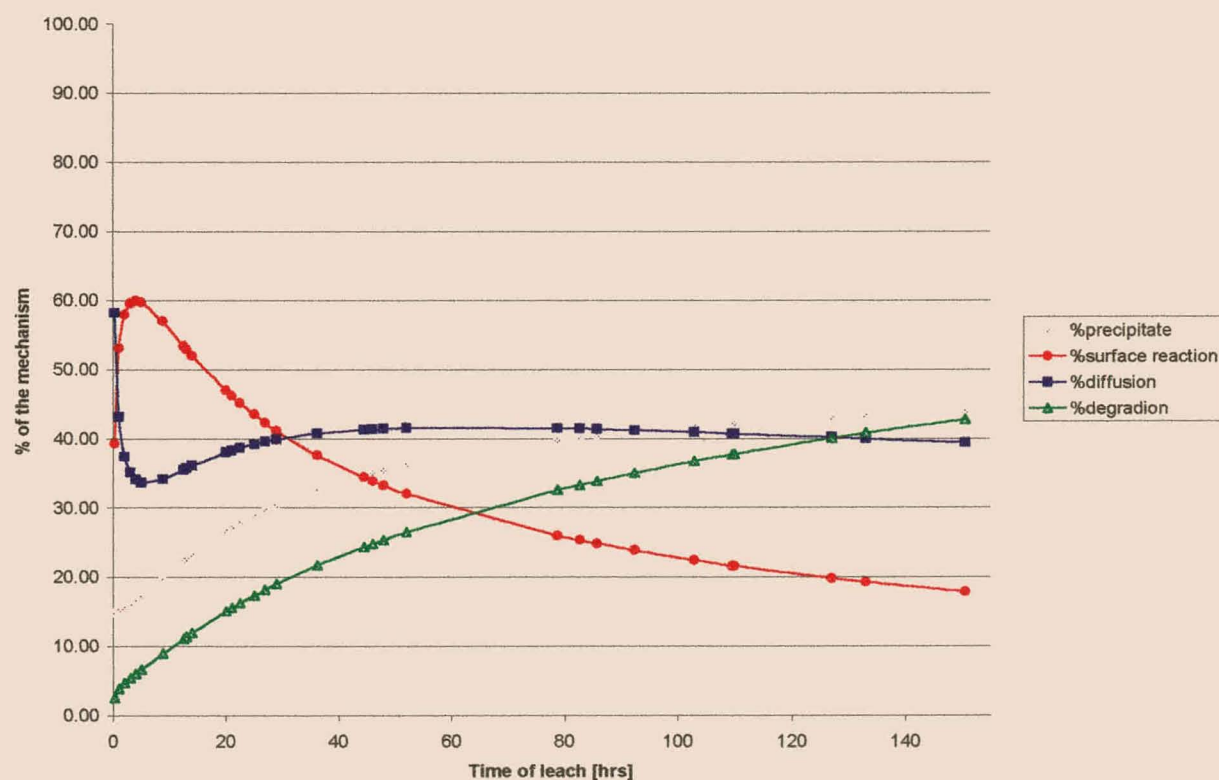


Figure 6.15: % Contributions of each mechanism for magnesium (Mg)

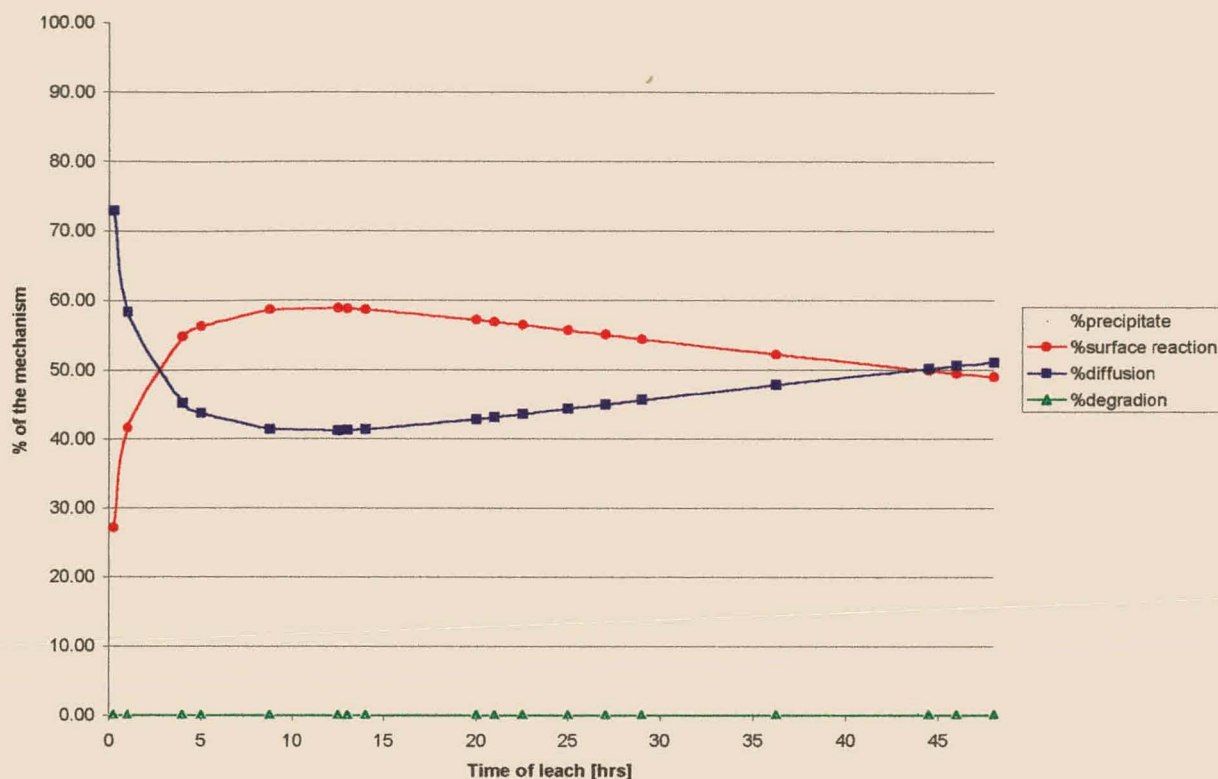


Figure 6.16(a): % Contributions of each mechanism for potassium (K) [0-48 hours]

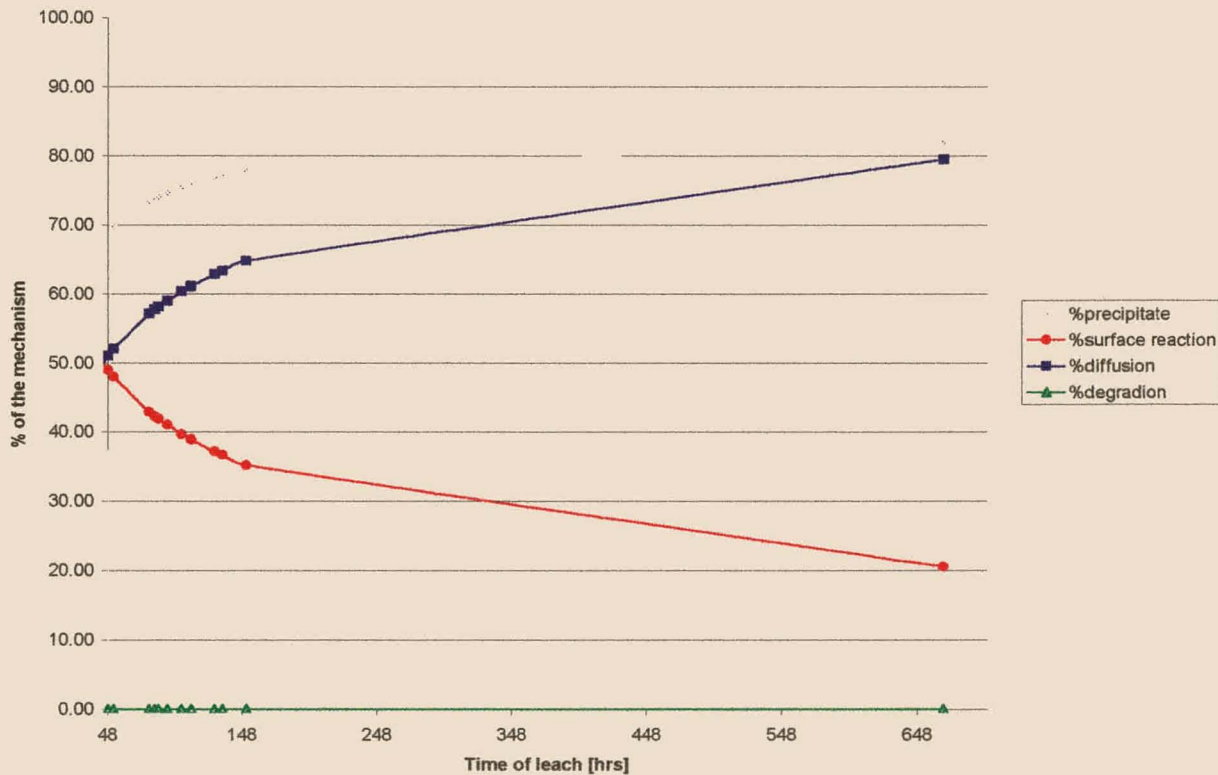


Figure 6.16(b): % Contributions of each mechanism for potassium (K) [48-600 hours]

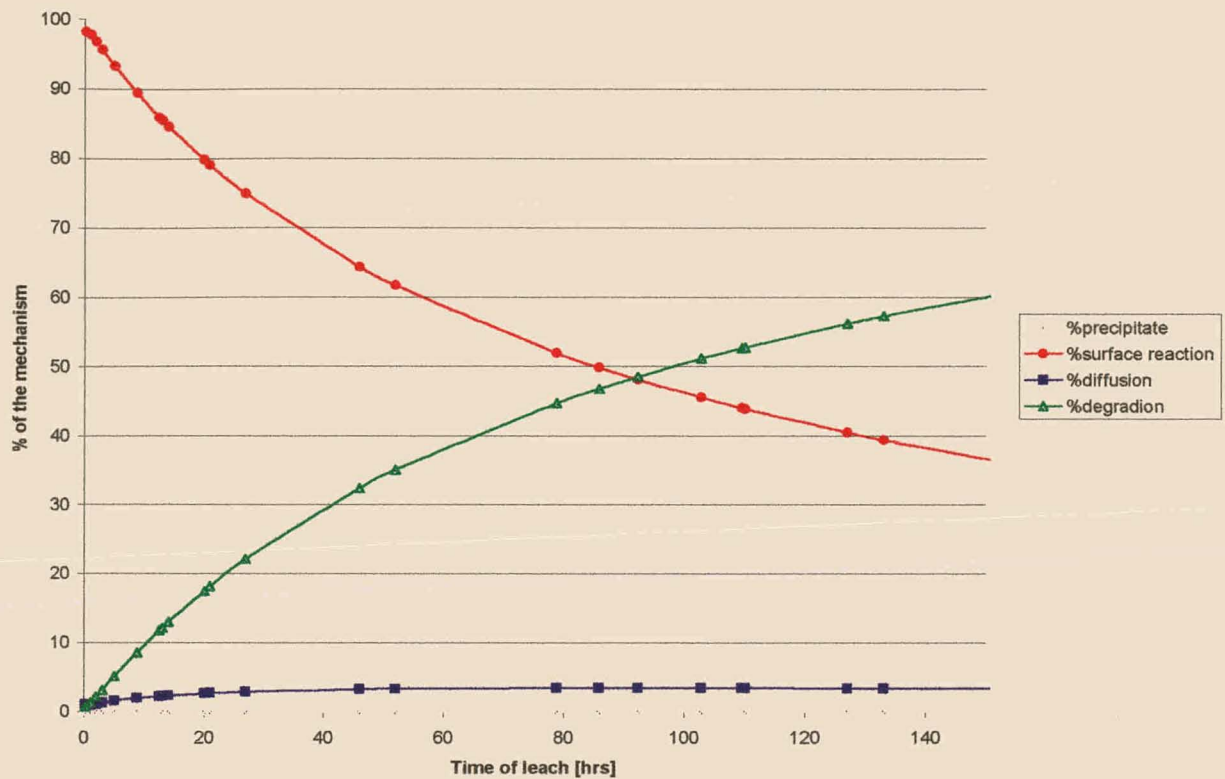


Figure 6.17: % Contributions of each mechanism for lead (Pb)



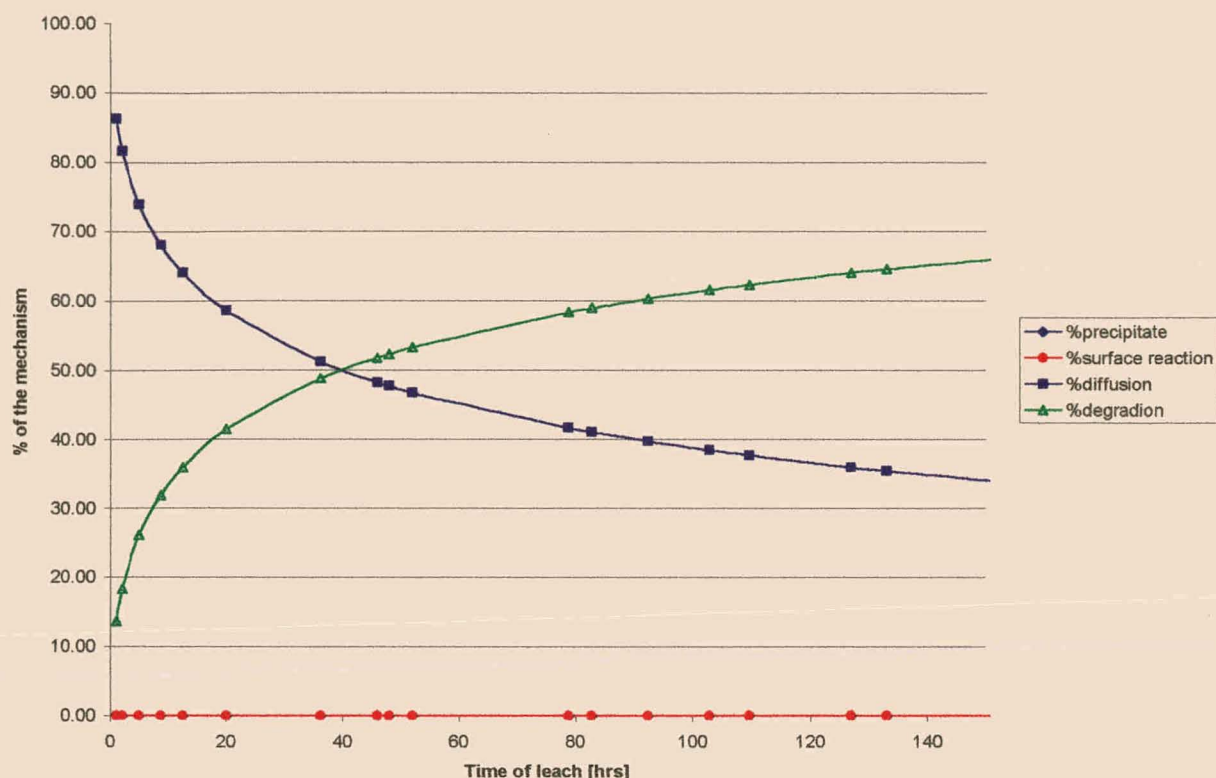


Figure 6.18: % Contributions of each mechanism for copper (Cu)

### 6.3.2. Geopolymeric matrix results

- The following figures represent the data collected from the leaching test runs done on the geopolymeric samples (G1 to G7). Once again similar concentrations were expected during these tests, but some deviation in the results of the different runs were observed (probably due to analysis inaccuracies). From observation the data from G5 was chosen to be the most reliable and to most accurately represent the leaching behaviour of the geopolymeric matrix. Curves, according to equations 6.2 or 6.3, were fitted on the data-points of G5 and the resulting curves are plotted together with the data obtained during tests G1 to G7, in the following figures:

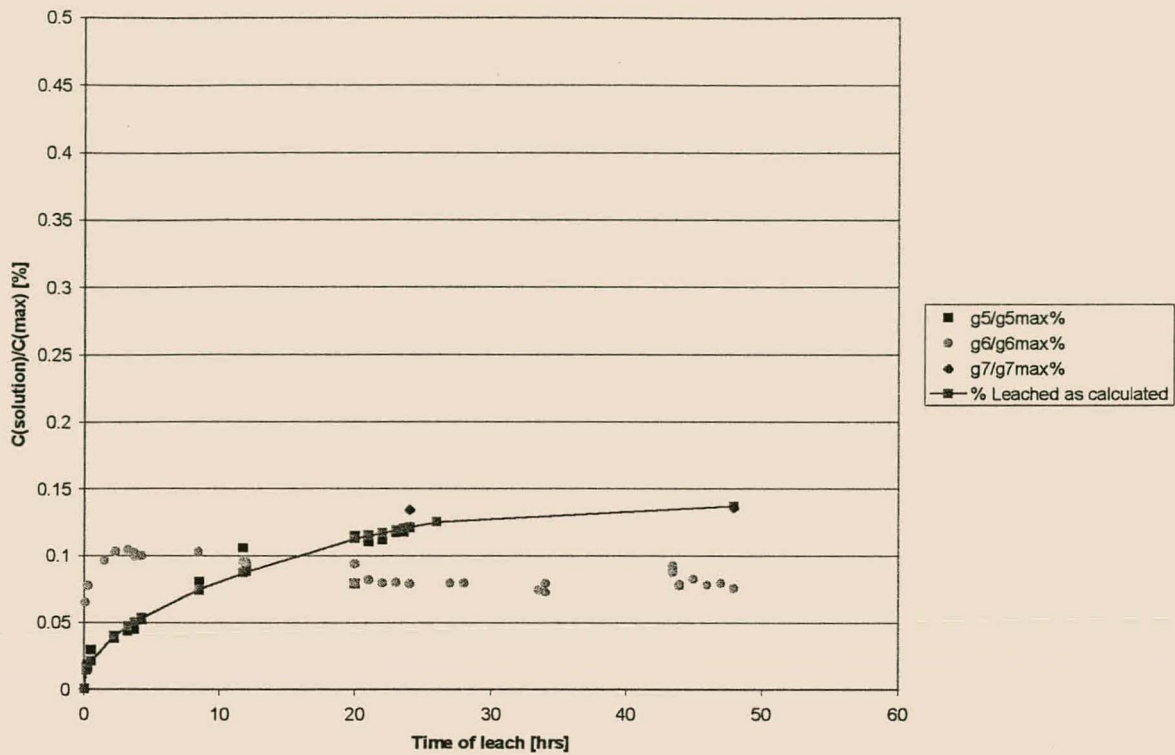


Figure 6.19: Silica leaching trends [0-48 hours]

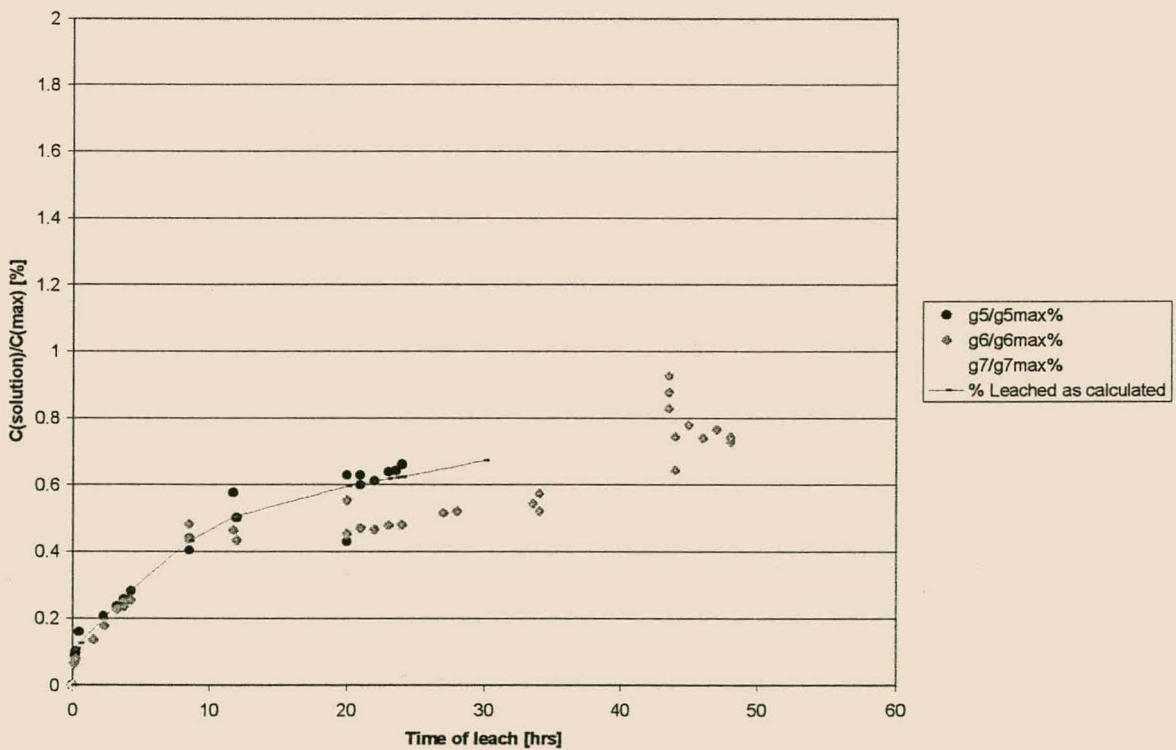


Figure 6.20: Aluminium leaching trends [0-48 hours]

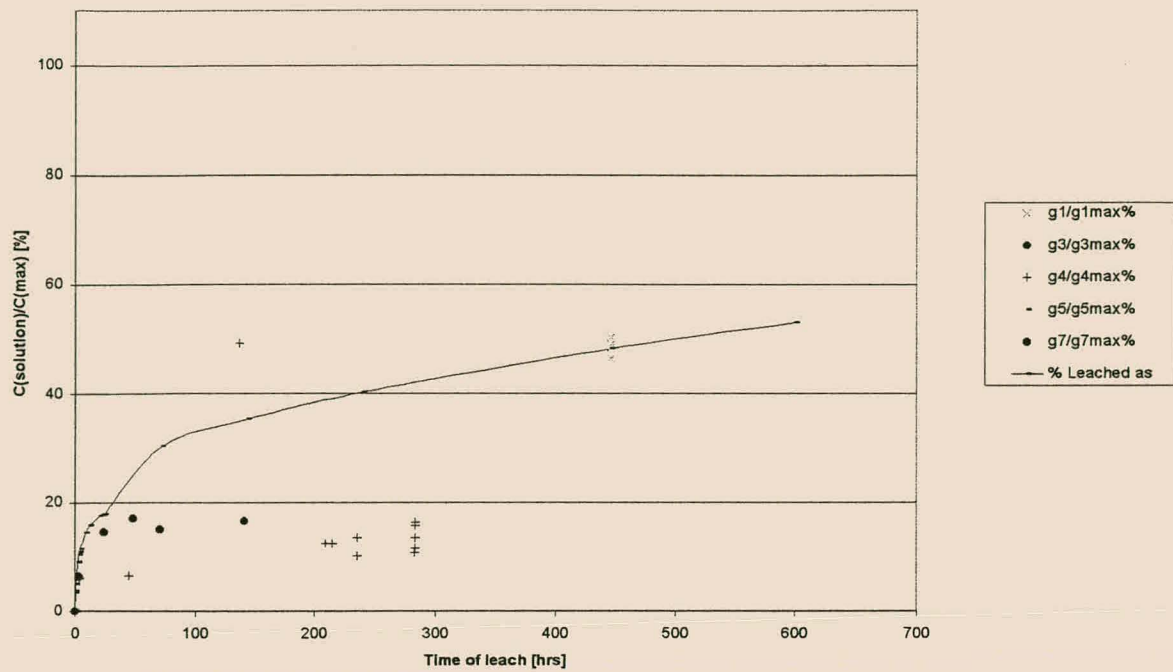


Figure 6.21: Calcium leaching trends [0-600 hours]

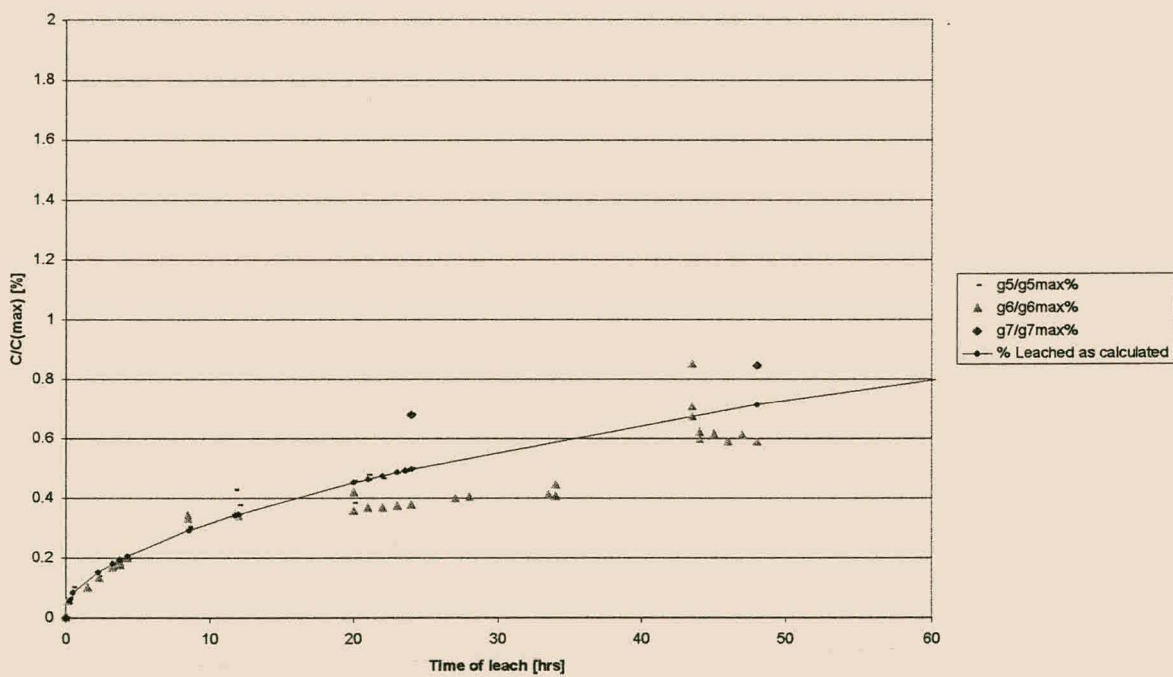


Figure 6.22: Iron leaching trends [0-60 hours]

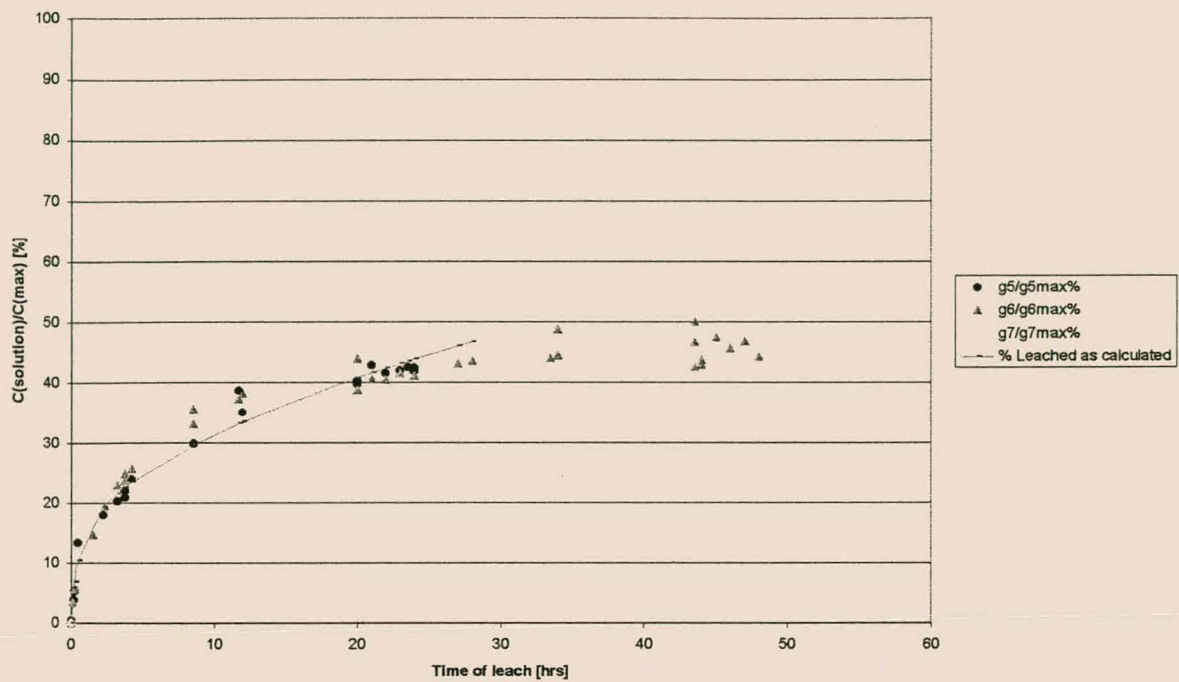


Figure 6.23: Sodium leaching trends [0-40 hours]

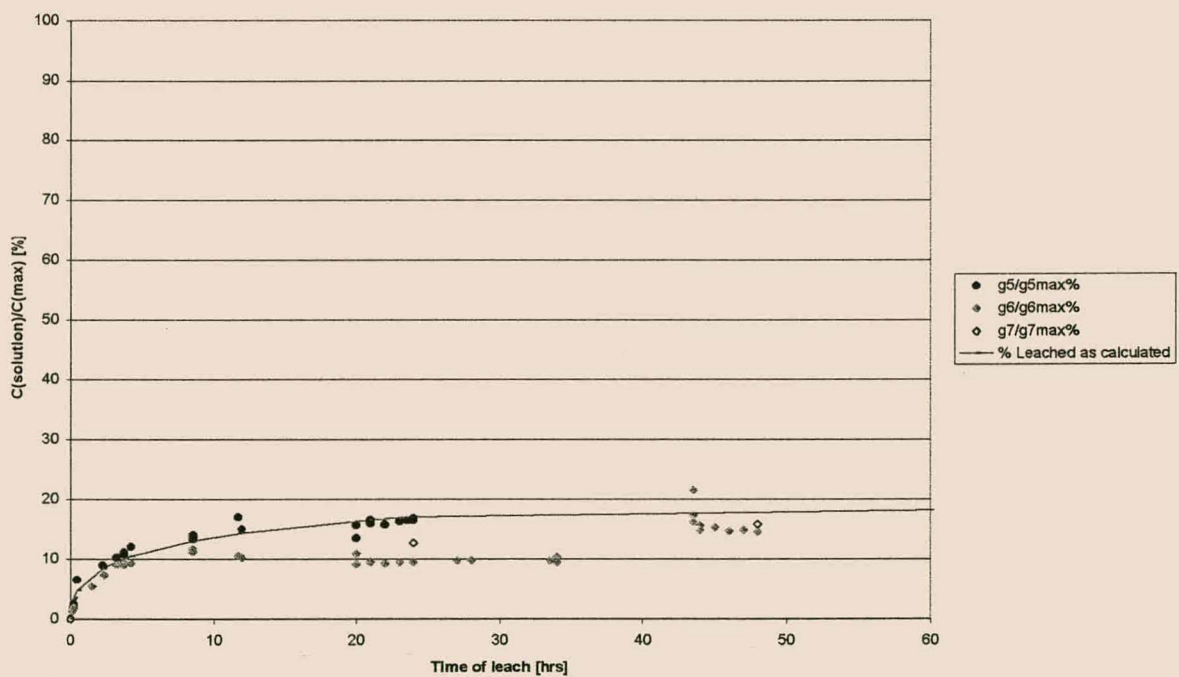


Figure 6.24: Magnesium leaching trends [0-60 hours]



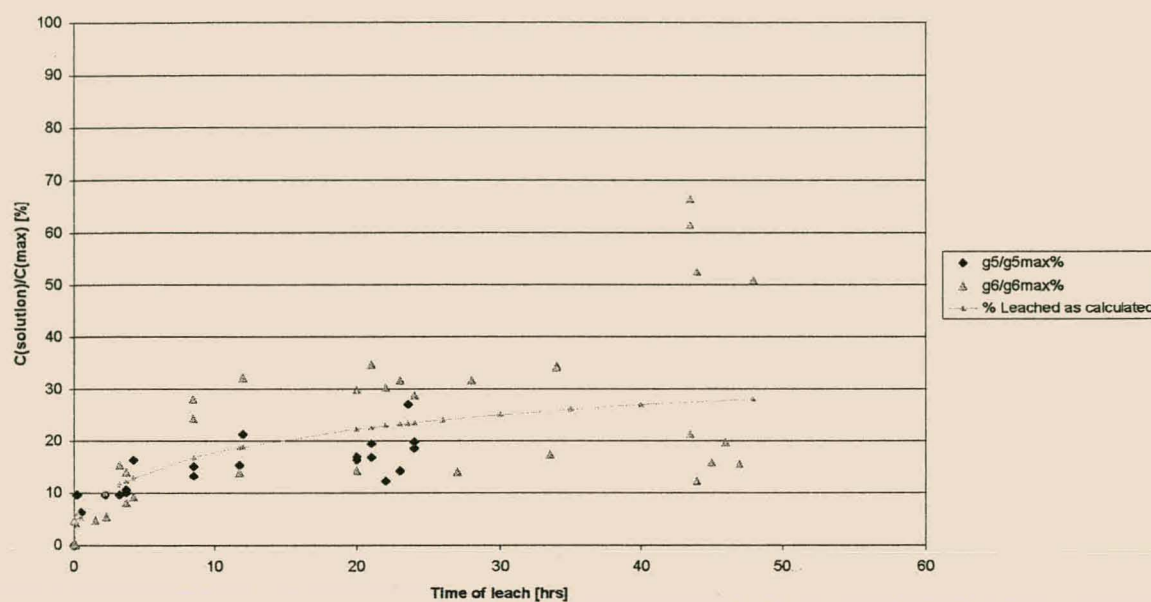


Figure 6.25: Potassium leaching trends [0-48 hours]

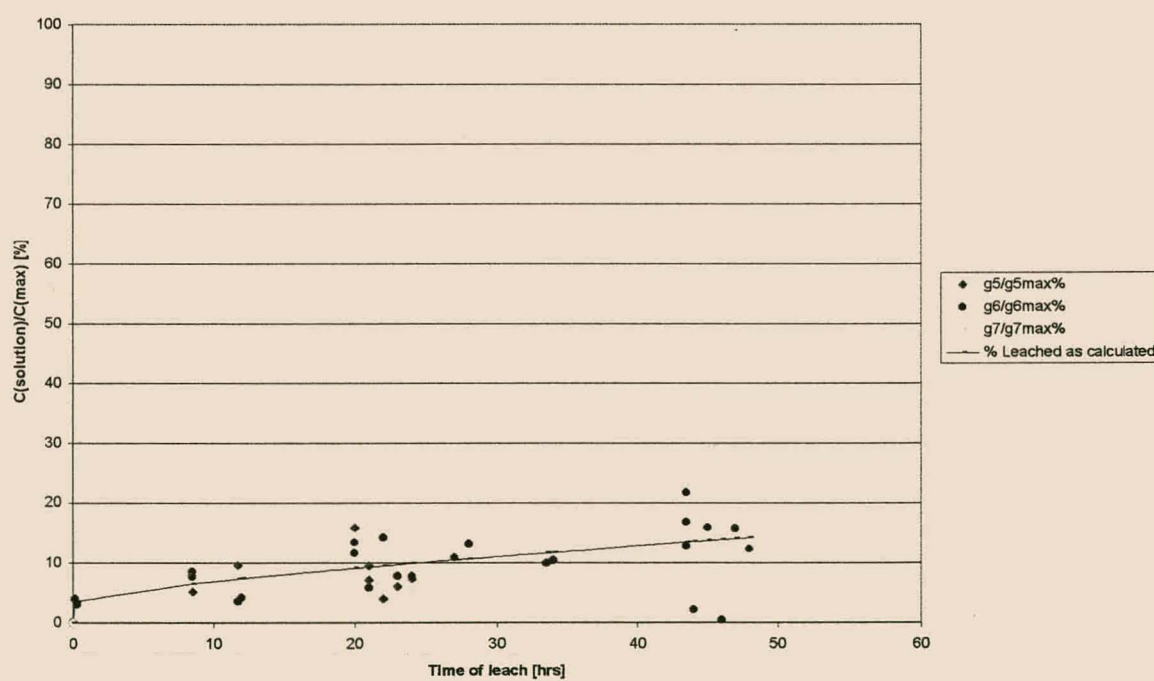


Figure 6.26: Lead leaching trends [0-48 hours]

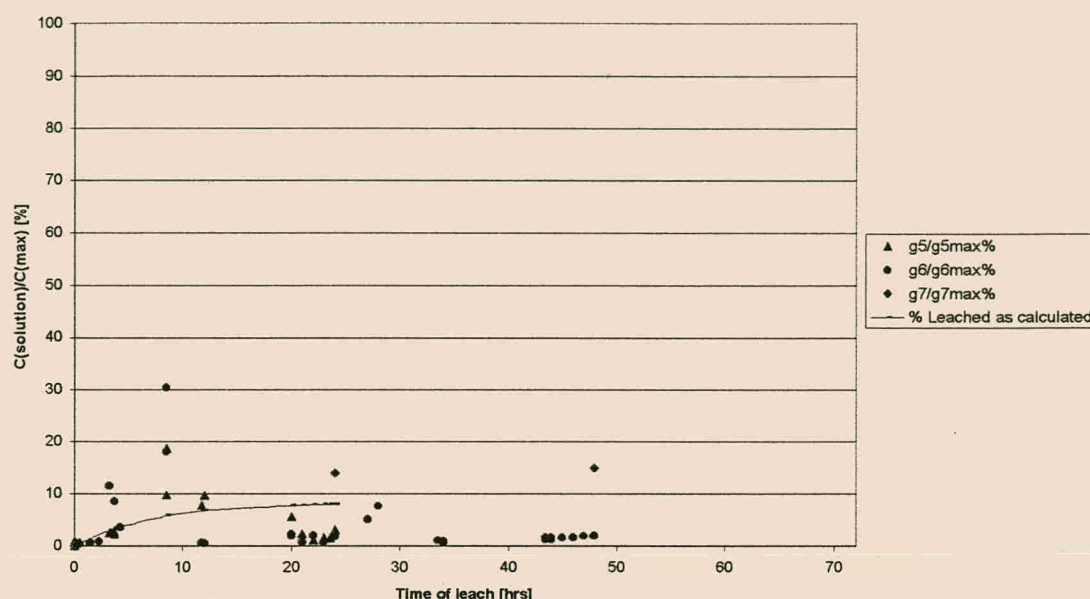


Figure 6.27: Zinc leaching trends [0-48 hours]

Figures B8 to B14 in appendix B represent the elements leached from the solid matrix of the geopolymeric matrix. The results are again expressed as percentages of the concentrations of the elements, originally present in the matrix. Curves according to equation 6.1 were fitted on the solid data and plotted with the data (from XRF –analysis on solids), to exhibit the leaching trends from the solid. The percentages of the solution concentrations were also plotted on the graph to show the differences in the percentages expected in solution and the actual percentages found in solution.

- The percentage contribution of each mechanism (i.e. surface reaction, diffusion, degradation and precipitation) during the leaching tests on the geopolymeric matrices can be seen in figures 6.28 to 6.36.

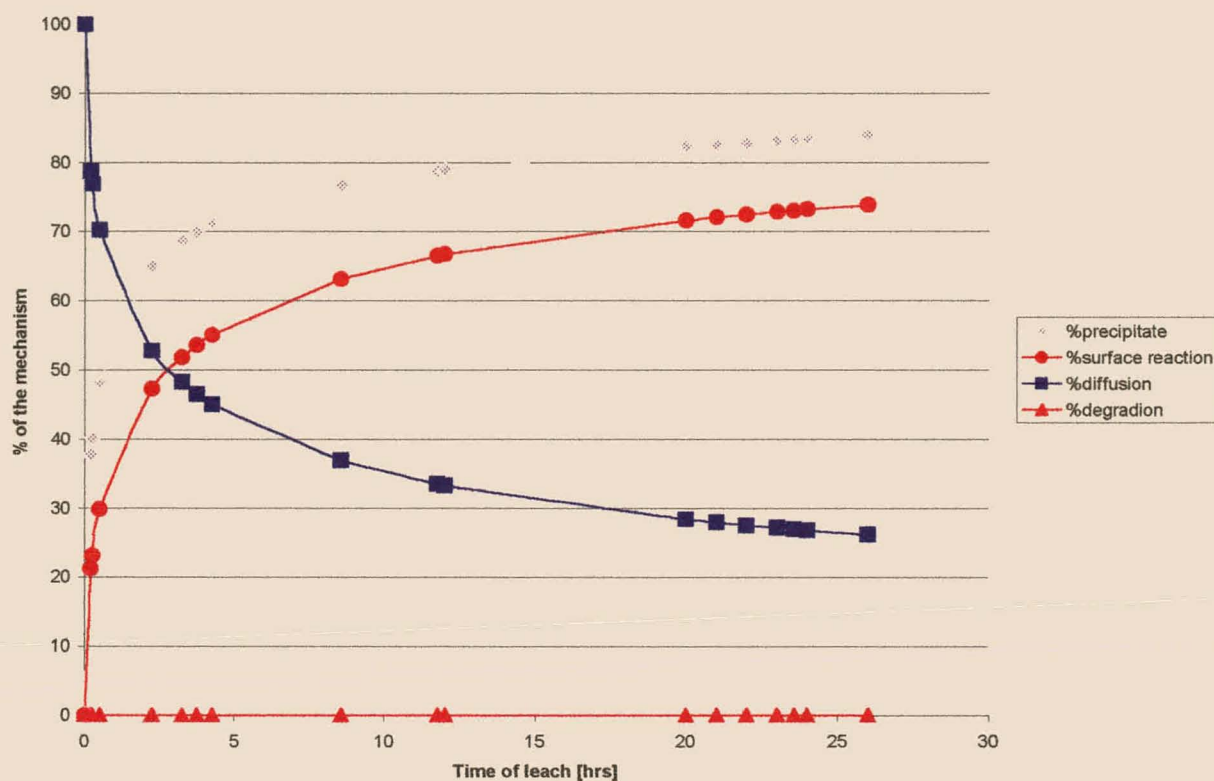


Figure 6.28: % Contributions of each mechanism for silica [0-600 hours] – Geopolymeric matrix

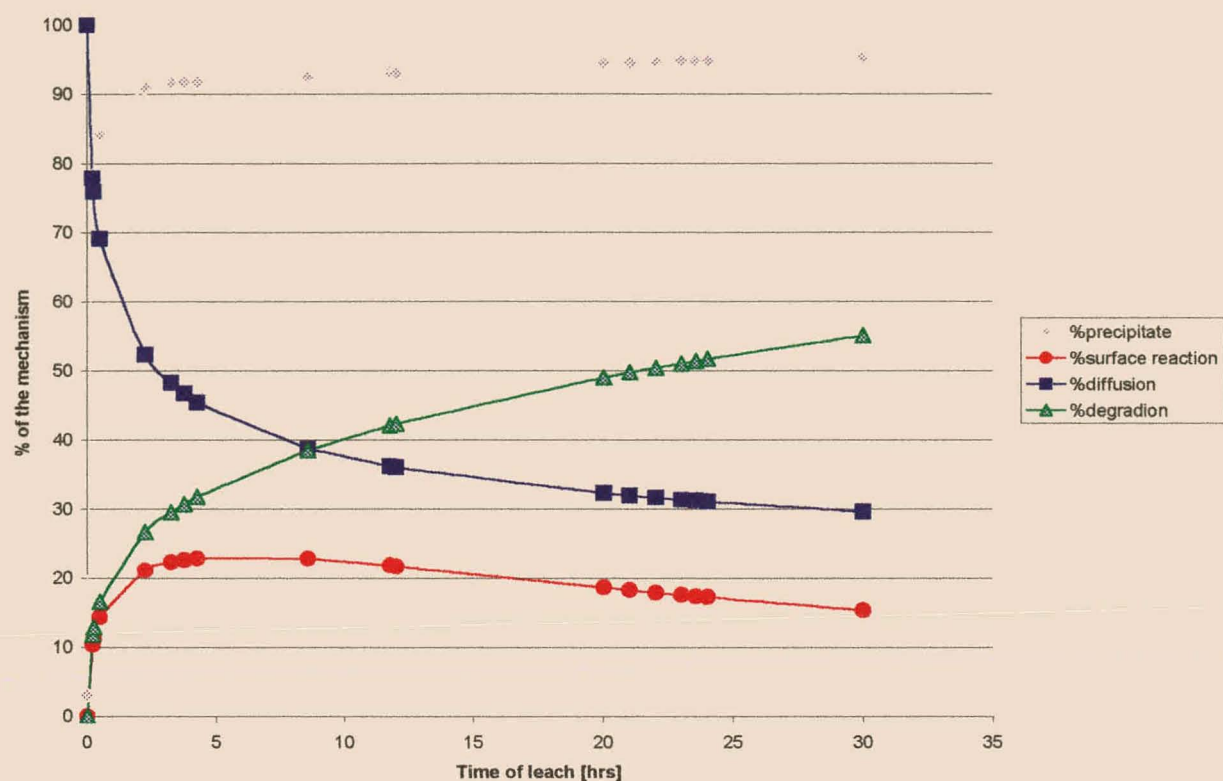


Figure 6.29: % Contributions of each mechanism for aluminium [0-600 hours] – Geopolymeric matrix



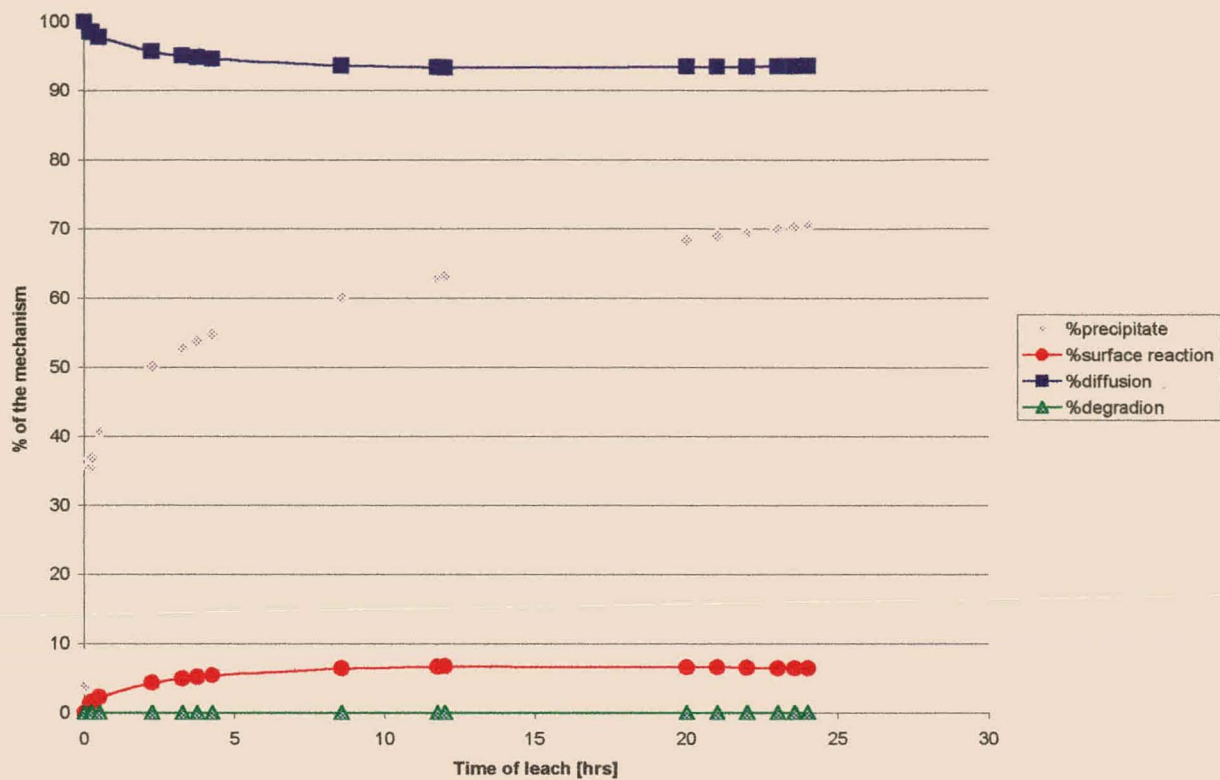


Figure 6.30: % Contributions of each mechanism for calcium [0-600 hours] – Geopolymeric matrix

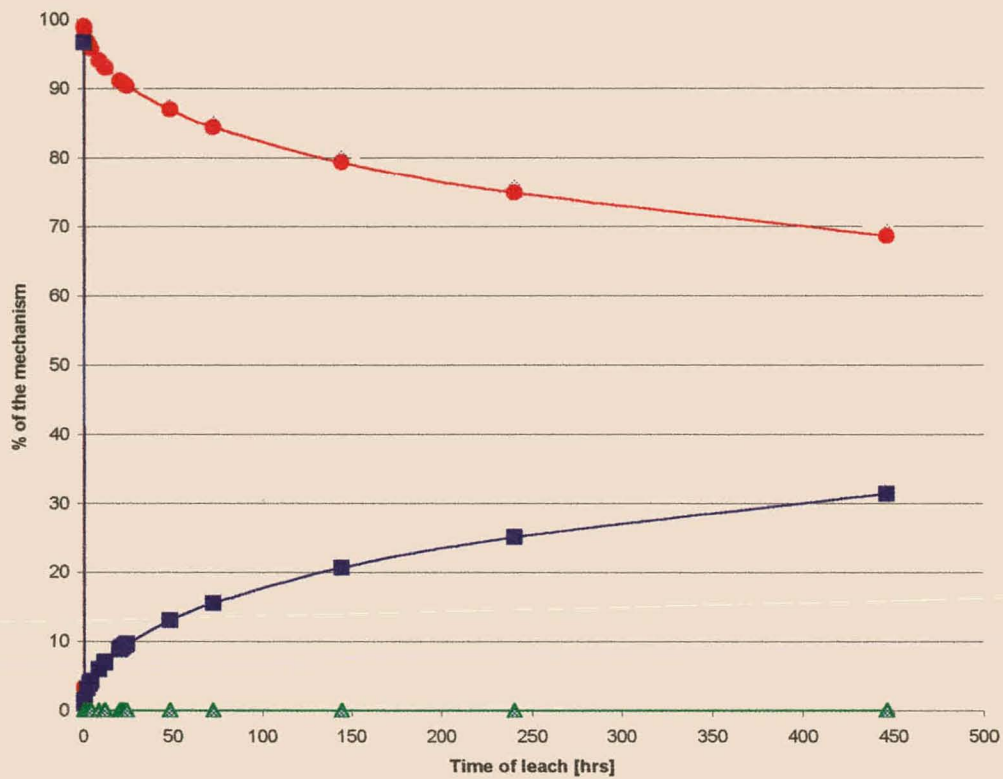


Figure 6.31: % Contributions of each mechanism for iron (Fe) [0-600 hours] – Geopolymeric matrix

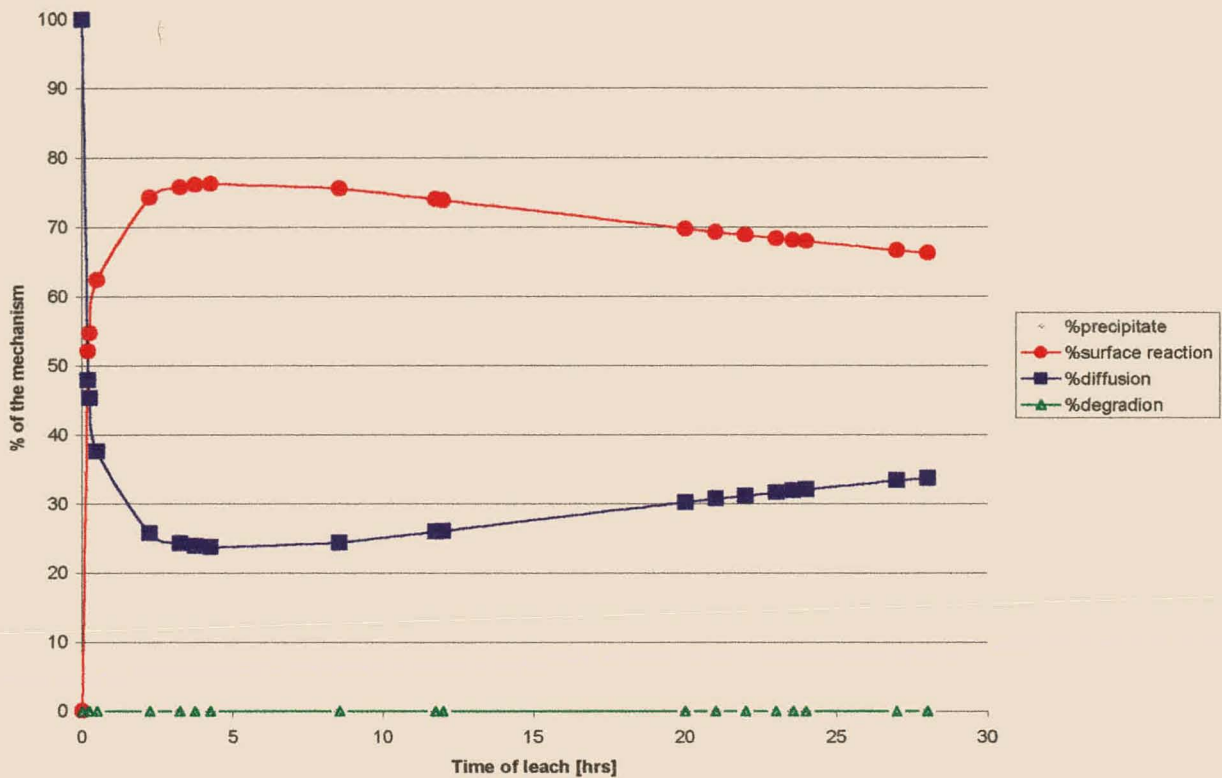


Figure 6.32: % Contributions of each mechanism for sodium (Na) [0-40 hours] – Geopolymeric matrix

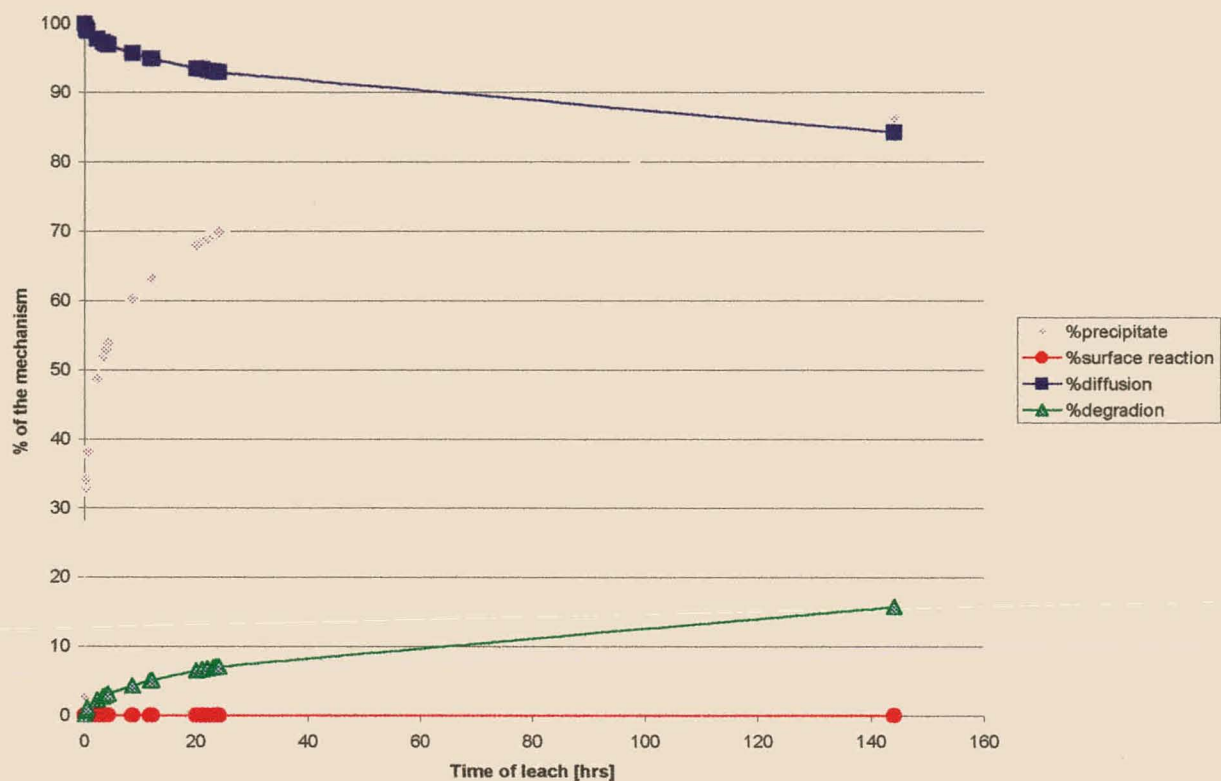


Figure 6.33: % Contributions of each mechanism for magnesium (Mg) [0-600 hours] – Geopolymeric matrix



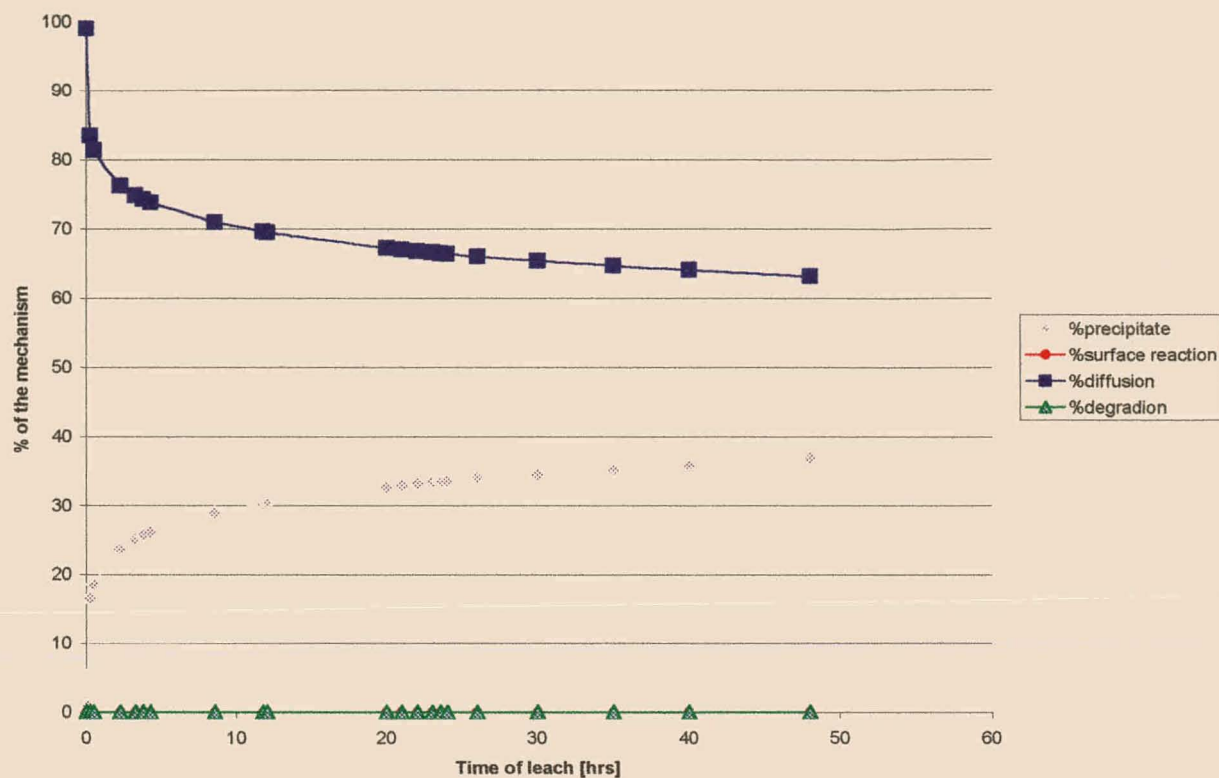


Figure 6.34: % Contributions of each mechanism for potassium (K) [0-600 hours] – Geopolymeric matrix

### 6.3.3. Comparison between different elements

#### 6.3.3.1 Pozzolanic matrix

The concentrations of the different elements in solution against leaching times are presented in figure 6.35 and 6.37 for the of the pozzolanic and geopolymeric materials respectively. A discussion of this results follows in section 6.4.3. Figures 6.36 and 6.38 represent the leaching behaviour of the differents elements from the solid materials of the pozzolanic and geopolymeric materials respectively. This concentrations were not obtained from the analysis of the leaching solutions, but from the XRF-analysis of the remaining solids after leaching tests, instead.

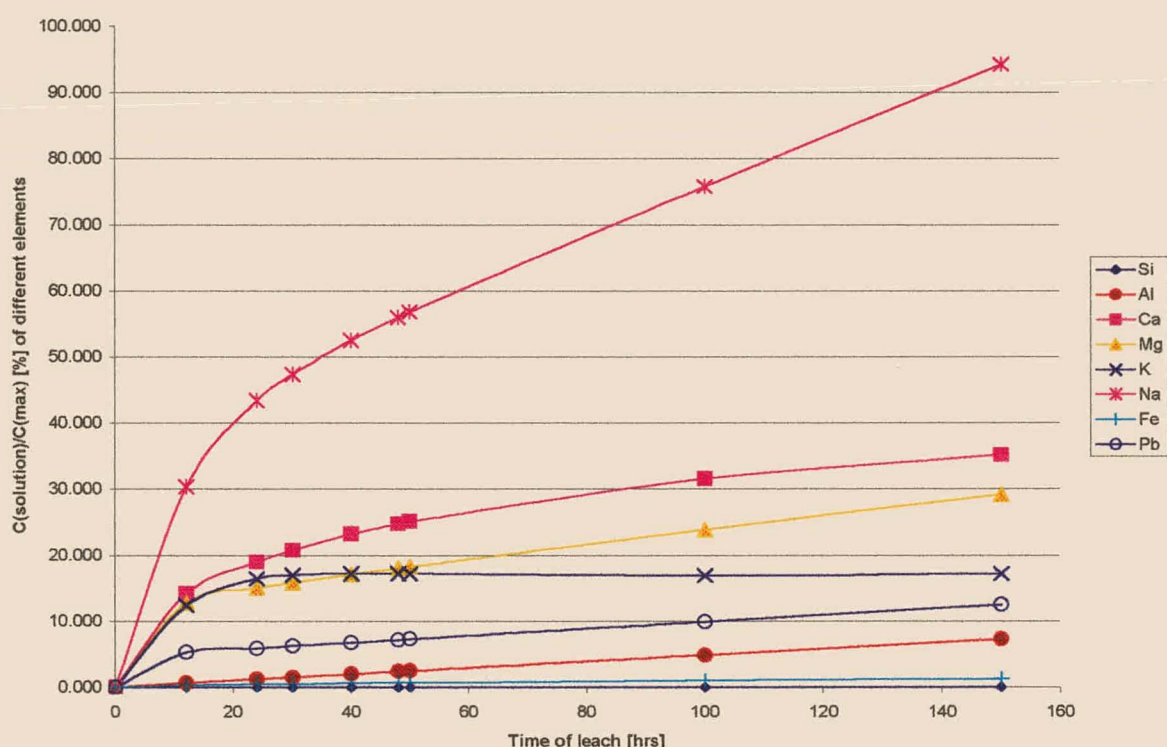


Figure 6.35: Solution concentrations for the different elements in solution (pozzolanic matrix)

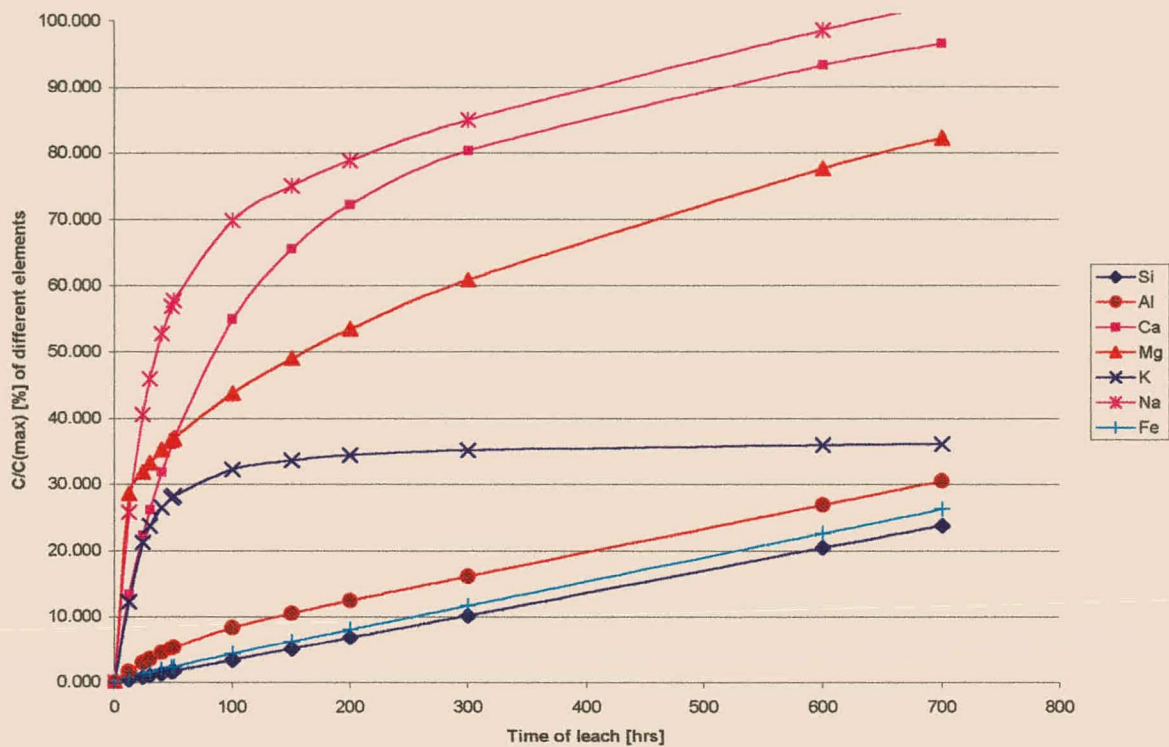


Figure 6.36: Concentrations of the different elements that leached from the (pozzolanic) solids

The behaviour of the pozzolanic matrix (as in figures 6.35 and 6.36) are discussed in more detail in section 6.4.3.1.

### 6.3.3.2. Geopolymeric matrix

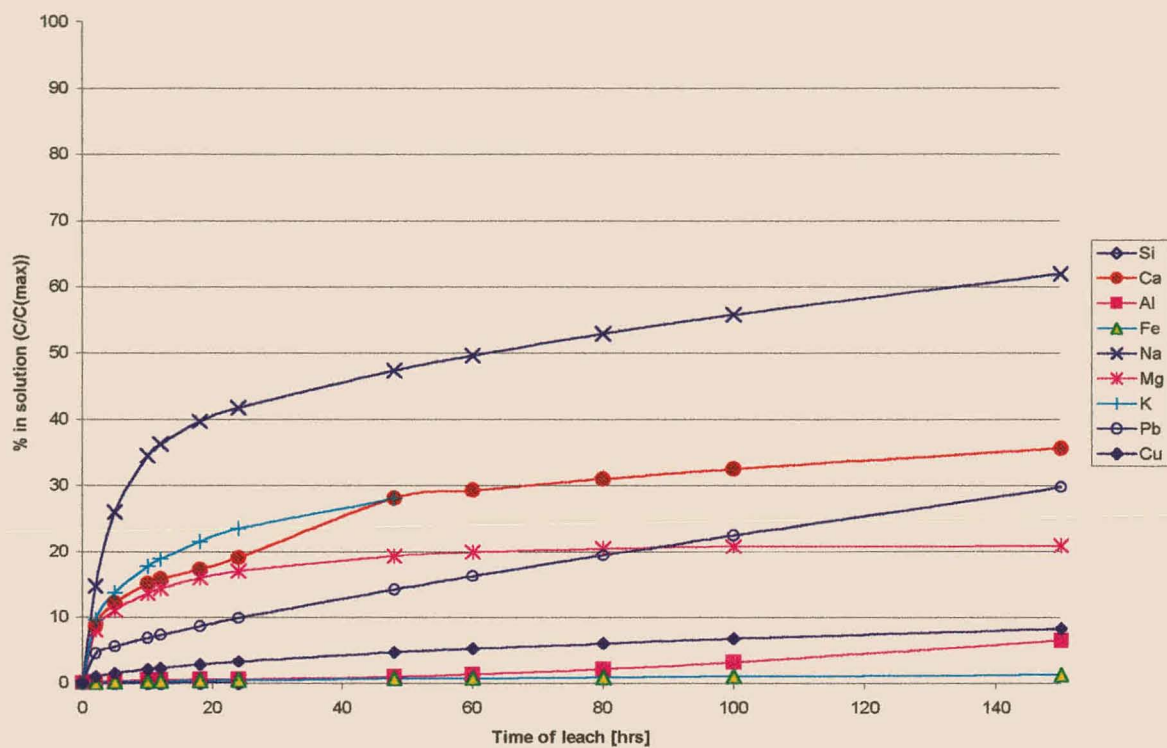


Figure 6.37: Solution concentrations for the different elements (geopolymeric matrix)

A discussion of the results of the different elements of the geopolymeric matrix follows in section 6.4.3.2.



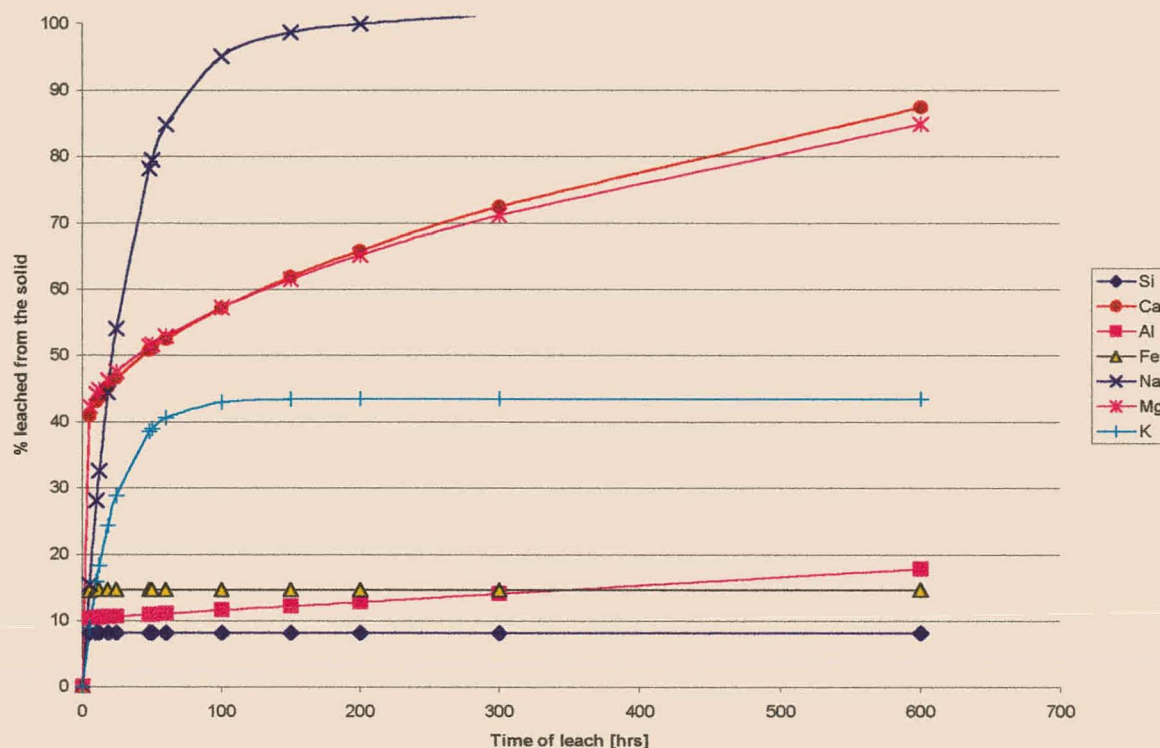


Figure 6.38: Percentages that leached from the (geopolymeric) solids for different elements.

## 6.4 DISCUSSION OF RESULTS (AS GIVEN IN 6.3)

### 6.4.1. Pozzolanic matrix

#### □ Silica

Si is the main matrix component and, according to the XRF analysis, makes out about 77% of the prepared pozzolanic matrix. It can be present in cement as calcium silica hydrate  $((\text{CaO})_3(\text{SiO})_2(\text{H}_2\text{O})_3)$  or in silica sand as an insoluble oxide ( $\text{SiO}_2$ ) (Jansen van Rensburg, 1997). Silica sand makes up 2/3 of the total mass of the matrix and a large part of the silica is thus expected to be present as  $\text{SiO}_2$ . During the preparation of the matrix NaOH was added to the ingredients and, due to the alkaline conditions, some of the silica in the silica sand is expected to dissolve as silicates,  $\text{SiO}_3^{--}$ . The silicates are almost all insoluble, except for those of the alkali metals (Na and K) (Pourbaix, 1966). Although we are not dealing with a typical cementitious matrix, calcium silica hydrate is also expected to be one of the main silica sources in the pozzolanic matrix.

From the R-square value (table 6.4), the fit to the data from L#18, in figures 6.1(a and b), seems rather good. In figure 6.1(a) it is clear that the concentrations of L#11 appear to decrease with an increase in leaching time. This behaviour is probably due to the formation of

less soluble Si-compounds as the concentrations of all elements in the solution increase. In the region of 0.05% of the silica is in solution after about 150 hours of leaching.

Since most of the silica is present as stable  $\text{SiO}_2$  and will not leach, the leaching can be due to the decomposition of calcium silica hydrate (C-S-H), which can be decomposed by an acid medium. Acetic acid is particularly corrosive and leaches about 2.2 times the amount of silica under the same conditions as an acid rain leachate. This is due to the formation of silica acetate, which is completely soluble, because silica acetate will decompose in cold water. This may explain instantaneous leaching of the silica in the acetic acid medium and may have a direct influence on the leaching of the other elements, which may form compounds with silica during the cement hydration process (Jansen van Rensburg, 1997). Apart from C-S-H, nickel silica complexes may also be present in the matrix. In fact, during the hydration of cement, nickel competes with calcium to form complexes with the silica. Therefore, it is reasonable to assume that by leaching either the nickel or calcium from the matrix, the silica would be free to form other compounds and that the leaching of Ca and Ni would be related to the amount of silica leached. Silica may also go into solution as a compound with aluminium, which has a strong affinity for silica. Such alumino-silicates are sparingly soluble in aqueous solutions (Jansen van Rensburg, 1997).

From figure B1 (Appendix B) it is clear that only a very small percentage of the overall amount of silica in the matrix, is found in the leaching solution (about 0.05 % after 127 hours). However, when evaluating the solids left after each leaching test, a substantially larger percentage of the silica seems to leach from the matrix. After 127 hours, about 4.3% of the solid have leached out, that is almost 100 times the amount found in solution. After longer leaching times (400 hours) about 25% of the silica seems to leach from the solid. It is therefore, evident that as the silica leach from the matrix, it does not stay in solution and probably reprecipitate in the bottom of the leaching vessel as sparingly soluble silica complexes or salts, such as alumino- silicates or also possibly as gels of hydrated oxides, which is usually formed during the leaching of C-S-H. These gels are not very soluble in aqueous solutions, which may explain the small leaching rate of the silica, in comparison with the amount in the matrix, when evaluating the solution concentrations (Jansen van Rensburg, 1996).

A regression analysis was done to fit the data of L#18 to equation 6.3 for the cumulative amount leached into the leaching solution. Values for the constants  $K_1$ ,  $K_2$ ,  $K_3$ ,  $K_4$ ,  $K_5$  and  $K_6$  were obtained and are summarised in table 6.3. In figure 6.10, these constants were used to determine the contribution of each term of the equation to the overall cumulative amount leached, as the leaching test proceeds. From this graph, the surface reaction initially seems to be of the most importance and decreases up to about 40 hours, after which it does not seem to have any controlling influence on the amount in solution anymore. About 96% of the silica that leaches out at 20 hours appear to precipitate out again. At 600 hours, almost all additional silica that leaches, according to this model, precipitates. The degradation term

seems to have a similar influence on the leaching mechanism as the precipitation term. The values of the diffusion term are rather low and do not seem to have a great influence on the leaching mechanism. From these results, it appears though that as silica dissolves at a fast rate initially and silica acetates form with the silica on the surface. After about 0.05% of the silica is leached, a maximum solution concentration is obtained and the rest of the silica forms insoluble compounds, which precipitates in the bottom of the leaching vessel. The main leaching mechanism at this stage seems to be degradation. This term increases until all leaching seem to be due to degradation and all the leached silica precipitates back at this stage.

#### □ *Aluminium*

The aluminium is the second largest quantity present in the matrix, and according to the XRF results; about 6% of the matrix consist of  $Al_2O_3$ . Aluminium can also be present as other compounds. Pourbaix (1966) discussed the solubility of aluminium oxide and its hydrates and stated that aluminium oxide, or alumina,  $Al_2O_3$ , occurs in various forms,  $\alpha$ -,  $\beta$ -,  $\gamma$ -, and  $\delta$ -alumina, which differ in crystal structure. The physical and chemical properties of alumina depend to a large extend on the temperature reached during its preparation. When alkali is added to a solution of an aluminium salt, or acid is added to aluminate, a precipitate is obtained which is a hydroxide gel, amphoteric in nature, and corresponds practically to the composition of  $Al(OH)_3$ . This aluminium hydroxide gel is not stable, but will crystallise in the course of time to first give the monohydrate  $\gamma-Al_2O_3 \cdot H_2O$  or böhmite, when crystallising in the rhombohedral system and then the trihydrate  $Al_2O_3 \cdot 3H_2O$  or bayerite, when crystallising in the monoclinic system, and finally gives another trihydrate, hydrargillite, crystallising in the same system. This development of aluminium hydroxide is known as "ageing". The various hydrates formed during the ageing are characterised by an increasing stability and an accompanying variation in all their properties, in particular their solubility in acids, bases and pure waste.

Jansen van Rensburg (1997), mentioned that aluminium is present in the cement matrix as ettringite  $(Ca_3(Al_2O_3)_2(CaSO_3)(H_2O)_{32})$ , calcium monosulphoaluminate hydrate  $(Ca_3(Al_2O_3)_2(CaSO_3)(H_2O)_{12})$  and calcium aluminate hydrate  $(Ca_4Al_2O_3(H_2O)_{19})$ . These products may also possibly be formed, in the case of pozzolanic and geopolymeric matrices. When the matrix comes into contact with acids, the attacking acid will decompose the cement paste. According to the solubility of calcium aluminium hydrate, this compound will decompose in a water medium, which may result in the leaching of the aluminium. In an acid medium the destruction of this compound, and consequently the leaching, will be much faster. Most of the aluminium is present as gels of hydrated aluminium oxide, which is sparingly soluble in acids, thus limiting the dissolution of aluminium into the solution. Once again acetic acid seems to leach more Al from the matrix than acid rain (pH =2), which can also be attributed to the dissolution of the calcium aluminium hydrate compound and the ability of aluminium to form complexes in the acetic acid solution (Jansen van Rensburg,

1997). The large stability constants of aluminium acetate and aluminium hydroxide acetate and also the solubility of the aluminium salts play a significant role in the leaching result of this element. In water media only a very small amount of aluminium is leached, which can mainly be attributed to the decomposition of the calcium aluminate hydrate, resulting in the release of some of the aluminium, although it is mostly present in the matrix as aluminium oxide ( $\text{Al}_2\text{O}_3$ ), which is insoluble in water and will settle out of solution or remain in the matrix. The aluminium hydroxide ( $\text{Al}(\text{OH})_3$ ) that may form in a water medium is insoluble at pH values above 4. The leaching results in figure 6.2 (a and b), shows that after initial fast leaching, about 0.4% of the aluminium are found in the solution at about 150 hours. After this, aluminium would rather precipitate from the solution, than any further leaching. The curve in the figures was once again fitted on the data from L#18 and the higher concentrations obtained in the other test runs are possibly due to inaccurate analysis, ageing of the samples prior to analysis or the initial higher aluminium concentrations in the samples.

From figures B2 (Appendix B), the concentrations in the leaching solution, compared to the amount of aluminium leached from the solid, are once again much lower. About 0.4 % of the total amount of aluminium originally in the matrix are found in solution after 150 hours of leaching, whereas the percentage of the aluminium leached from the solid, are about 13% after 150 hours, which is substantially more. After about 700 hours about 30% of the aluminium will be expected to leach from the solids. Once again the insoluble compounds in the leaching solution are expected to precipitate in the bottom of the leaching vessel as soon as the solution reaches a certain concentration (about 30 ppm). It can be assumed that the 0.4% of the matrix that is found in solution can be attributed to the dissolution of calcium alumina hydrates, which probably forms alumina acetates in solution, whereas the rest of the aluminium that leaches from the solid is most probably insoluble alumina oxides which are released from the surface and simply settles in the solution without dissolving in the leachate.

From figure 6.11 the governing mechanism appears to be the surface reaction. Although diffusion also attributes to the leaching phenomenon, especially at times < 40 hours, after which the contribution of this term stays rather constant. Therefore, for the first 150 hours the rate of leaching is determined by the dissolution of aluminium compounds, such as calcium aluminium hydrates and possibly the release of insoluble alumina oxides from the surface. This would continue for the duration of the leaching test (up to 670 hours), but after the maximum solution concentration is reached, all the aluminium that leaches from the solid seems to precipitate. That is only if all leaching from the solid is not due to the insoluble alumina oxides that are released straight from the matrix to settle in the solution. Diffusion has a small effect on the leaching according to this model, especially in the beginning of the test after which it decreases and reaches a minimum after about 40 hours. This initial contribution might be due to diffusion of acid into the matrix, which dissolves C-A-H, or due to the diffusion of the dissolved aluminium into the solution



## □ Calcium

Another of the primary matrix constituents is calcium, which makes out about 5% of the matrix according to the XRF results (expressed as CaO) of samples of the matrix prior to any leaching tests. Alkaline earth metals, such as calcium, exert an extremely low solution potential and as a whole their domain of stability lies well below that of water, these materials are very unstable in the presence of aqueous solutions of any pH. They are extremely base metals and powerful reducing agents, and have a large affinity to react with water, which they decompose with the evolution of hydrogen (Pourbaix, 1966).

Jansen van Rensburg (1997) mentioned that CaO is believed to be a favourable site for acid attack during the leaching process leading to the polymerisation of the silicates (calcium silicate hydrate). The following polymerisation mechanisms have been proposed, i.e.:



Where X = calcium, potassium, sodium or toxic metal ions. This exposes silica to the acid solution leading to an increased branching and cross-linking of silicates to produce a crumbly porous solid with very little mechanical strength. It is evident that the leaching will increase with an increase in acid strength and subsequently a decrease in leaching medium pH. Baker and Bishop (1997) used the leaching behaviour of calcium to demonstrate the acid neutralisation capacity, due to the linearity between the two functions. The release of the latter determined the potential leach ability of the material and the resulting mobilisation of contaminants. Leaching of calcium might thus represent the leach ability of the entire matrix.

From figure 6.3(a and b) leaching seems to be rather fast initially, but slows down beyond 24 hours until a maximum of about 35% of the calcium is in solution. Variation of data from the leaching curve, which was fitted according to data from L#18, is once again probably due to inaccuracies of the analysis. The higher concentration of data from L#9 may be due to an initial higher concentration of calcium in the matrix, incorrect analysis or possibly due to the use of a different pH probe during the test and a possible higher acid concentration. Once again, after longer leaching times a slight decrease in the concentration seem to occur (see data from L#11). This might be due to the precipitation in the samples at the higher concentrations, where different elements in solution can react with each other and form insoluble compounds or salts.

When evaluating figure B3 (Appendix B), the difference between the percentage of calcium in solution and the percentage of the calcium leaving the solid matrix, does not seem to differ quite as much as for Al and Si. But after about 670 hours all calcium seemed to have leached

from the matrix while a maximum of 35% stayed in the solution. The difference seems to precipitate after this solution concentration is reached.

From the XRF results it was clear that the leaching of calcium from the solid occurs through a reaction front that moves from the surface towards the core of the sample. Due to this observed behaviour, diffusion of the dissolved calcium ions is expected to have an effect on the leaching mechanism. The model agreed with this assumption and about 100% of the leaching were initially due to this diffusion, after which it decreased somewhat and the surface reaction term seemed to have a larger influence on the mechanism. The dissolution reaction is rather fast and is expected to contribute largely (especially in the beginning of the test) to the concentration of the solution. However, if the diffusion from the inside of the matrix is rather fast, it will cause a large amount of calcium to go into solution and this contribution might be larger than the surface reaction contribution, which might explain the results of figure 6.12: From the model, the degradation seems to have a very small contribution throughout this test, which could mean that the calcium is not physically encapsulated in the matrix and leaches into the bulk and pore solution by normal dissolution kinetics.

#### □ *Iron*

About 4% of the matrix consist of Fe, which is mainly originating from the jarosite, added to the matrix.

The behaviour of Fe closely relates to that of aluminium. From figure 6.4 (a and b), a maximum concentration of 1.2% of the iron is found in solution. The leach is also characterised by initial fast leaching which is slowing down until the solution concentration stays more or less constant. Once again a decrease in the solution concentration is observed at longer leaching times, possibly due to the reaction between the elements in solution to form less soluble compounds or precipitates. From figure B4 (Appendix B) it is once again clear that a substantially larger amount of the Fe leaches from the matrix, than the amount found in the solution. After about 150 hours about 1.2% are in solution, while about 6% seemed to have leached from the matrix. After 670 hours, about 25% have leached from the matrix and precipitation could also in this instance, be the reason for this.

From figure 6.13 the diffusion reaction initially contributes to a large portion of the leaching, but decreases as the test proceeds, while the influence of degradation increases, until the latter is the governing leaching mechanism (after about 12 hours). This might be an indication that Fe does not occur near the surface in great quantities and needs to be diffused from the inner parts of the sample towards the bulk solution. The significant influence of degradation can be an indication that Fe is physically encapsulated inside of the matrix and that as corrosion of the matrix increases, more of the iron is exposed and can be leached into the bulk solution.

The influence of the surface reaction is very small. This would mean that the initial leaching of iron would not be due to the fast dissolution of the elements on the surface.

#### □ *Sodium*

From XRF analysis, about 1% of the matrix consists of Na, expressed as sodium oxide. According to Pourbaix (1966), sodium will go into solution as the  $\text{Na}^+$  ion, but can exist as different solid substances such as, NaH, Na,  $\text{Na}_2\text{O}$ , NaOH and  $\text{Na}_2\text{O}_2$ . As the whole domain of stability is once again well below the stability of water, these metals are extremely unstable in the presence of aqueous solutions of any pH. The oxides, being very soluble, cannot produce any passivation, and the metals decompose aqueous solutions very vigorously, with the evolution of hydrogen. Alkali metal hydrides are much less unstable in the presence of water than are the alkali metals themselves. Although they react vigorously with water forming hydrogen, the alkali metal hydrides are perfectly stable in the absence of water and oxygen.

From the figures 6.5(a and b), the solubility of the sodium is evident and the sodium leaches from the matrix until the whole matrix is depleted of Na as was found when analysing the remainder of the matrix after about 670 hours. After 150 hours of leaching, about 80% of the sodium were found in solution. L#11 exhibited slightly faster leaching and after 200 hours all of the sodium was leached out (100% in solution) of this matrix. The concentrations of this solution (L#11) did, once again, decrease after all the Na was leached out, until more or less 80% were left in solution at 600 hours. The solid was totally depleted from sodium after about 600 hours and the leaching trends from the solid and the solution phenomena appeared similar (figure B5, Appendix B). This indicates that no substantial precipitation occurred during the test and that all Na that leached from the solid stayed in solution, except for the solution of L#11 at longer leaching times. This might be due to analysis problems, or possibly the binding into compounds with other elements that might settle in the solution and cause the sodium concentration to decrease somewhat.

From figure 6.14 the surface reaction is the largest contributor to the cumulative amount leached, up to about 100 hours of leaching. The contribution of the surface reaction decreases as the outer layers becomes depleted of Na. Diffusion does not have an effect to the leaching phenomenon in the solution according to this model, but the effect of degradation increases as the test proceeds until it is the main mechanism after about 100 hours. This implies that that little or no diffusion through the porous matrix occurs during the test and that the inner layers are reached by means of physical degradation, which exposes these parts. The latter is not very likely because all the sodium in the matrix are leached into solution and as the matrix does not completely disintegrate after about 100 hours, all the sodium cannot be exposed to the leaching solution and some diffusion are expected to occur, but at a rather fast rate. The increase in the contribution of the degradation mechanism might indicate that as

more aggregates are exposed, the leaching rate increases. This can also be an indication of physical containment inside of the matrix

#### □ *Potassium*

According to Pourbaix (1966), Na and K form practically no complexes and very few insoluble compounds and the metals are greatly unstable in the presence of water and oxygen, with which they react vigorously. The potassium is thus expected to go into solution rather fast, unless it is substantially stabilised (by physical containment for example).

From figure 6.7(a and b), the percentage of potassium leached from the solid, are more or less in the same region than the potassium found in the solution, but at leaching times exceeding 100 hours the concentration stabilises at about 18-20% of the maximum obtainable concentration, where the solution seems to be satisfied. However, leaching from the solid continues beyond this point in the test and about 45% of the K in the matrix were leached out after the 670-hour leach. (See figure B6 in Appendix B). It is thus evident that K continues to be leached from the matrix, but does not stay in solution and may form precipitates in the bottom of the leaching vessel as K salts or may form compounds with other elements that would precipitate when about 20% of the K in the matrix has gone into solution. The lower concentrations in some of the other test runs are possibly also due to ageing of the samples, fluctuations in the analysis results, or also possibly due to unstable pH due to failure of the pH-probes as they become dirty and inaccurate during some of the tests. This problem was particularly found in L#12 and could explain the significant drop in concentration after about 24 hours.

Figure 6.16 (a), shows that for the first 48 hours, diffusion and the surface reaction govern the leaching mechanism, while degradation does not have any significant influence. After 48 hours precipitation was also included in the model and figure 6.16 (b) shows that the surface reaction decreases, after the initial fast leach, while the diffusion reaction becomes more pronounced. This is possibly due the depletion of K from the surface sites, while leaching from the inner parts of the matrix and diffusion of these elements through the porous matrix continues.

#### □ *Magnesium*

Magnesium can be present in the solid form as either  $\text{Mg}(\text{OH})_2$  or  $\text{MgO}$  (Pourbaix, 1966) due to the oxidation of magnesium, which would occur, in the alkaline solution when preparing the samples.  $\text{Mg}(\text{OH})_2$  is thermodynamically more stable. Magnesium has a great affinity to react with water at all pH values, and dissolves as  $\text{Mg}^+$  and  $\text{Mg}^{++}$  ions. At pH values above



about 8.5 and up to 11.5, it can cover itself with a protective oxide or hydroxide layer, which inhibits the dissolution reaction.

From figure 6.6(a and b) the magnesium seems to be leached out relatively easily, and about 30% of the solid was leached after 150 hours. Once again the solution concentration decreases somewhat in L#11 after longer leaching times (mostly after 250 hours). From figure B7 Appendix B, about 50% of the Mg in the solid are leached when about 30% are found in solution and after 670 hours about 80% of the magnesium is leached from the solid. This is once again an indication of precipitation in the leaching vessel.

From figure 6.15 the leaching of Mg is initially controlled by the fast surface reaction. This contribution decreases with time as the diffusion as well as degradation effects increase. This can be due to the depletion of the Mg in the surface layers and the leaching of Mg from the inner layers, which need to diffuse through the porous matrix. Degradation might be responsible for the exposure of aggregates for further leaching and will increase the leaching rate in this manner. It is also evident that the effect of precipitation increases towards the end of the test.

#### □ *Lead*

According to Pourbaix (1966), lead generally tends to dissolve in acid solutions as  $Pb^{++}$ , plumbous ions at atmospheric pressure. The ions can be converted by a very powerful oxidising action to lead peroxide,  $PbO_2$ . In the absence of passivating substances (such as carbonates), any oxidising action can cause lead to corrode, except when lead peroxide is stable (high electrode potentials).  $PbO$  is too soluble to provide any protection from corrosion and the lead is therefore, corroded by most soft waters (waters free from passivating substances such as bicarbonates).  $PbO$  is amphoteric and dissolves in acid, neutral and slightly alkaline solutions as plumbous ions  $Pb^{++}$ , and in very alkaline solutions as biplumbite ions.  $PbO_2$  is insoluble in neutral and moderately acid or alkaline solutions, but slightly soluble in very acid solutions to form plumbic ions,  $Pb^{+++}$ . The latter is expected during the leaching tests when the matrix is exposed to the acid leaching solution. Apart from  $PbO_2$  or  $PbO$ , the lead might also be present in the matrix as compounds with other elements, and might also leach from these compounds into solution.

Lead seems to initially leach relatively fast, after which the rate decreases somewhat (see figure 6.8). Within the first few hours, about 5% of the lead were leached into the solution. After 150 hours this percentage increased to about 13%. From this behaviour, the surface reaction is also expected to govern the leaching mechanism initially, while diffusion or degradation becomes more pronounced for longer leaching times. This is verified by figure 6.17, where it is evident that the surface reaction is initially the main mechanism. The contribution of this term decreases, until about 90 hours, where the increasing influence of degradation becomes the governing mechanism. The influence of diffusion stays more or less

constant throughout the test, at about 6% of the sum of the mechanisms. The influence of degradation might be an indication that lead are physically bound inside of the matrix and may be released into the leachate after sufficient degradation and exposure of the aggregates.

#### □ *Copper*

When copper is present as a solid substance it will probably be as Cu, Cu<sub>2</sub>O, CuO, or Cu(OH)<sub>2</sub> and will go into solution at a low pH as Cu<sup>++</sup> or Cu<sup>+</sup>. Copper is also likely to form soluble complexes or insoluble compounds, of which CuP<sub>2</sub>O<sub>7</sub><sup>-</sup> is a possible product in the matrices under consideration. Most cuprous salts are sparingly soluble e.g. CuCN, CuCl, CuSCN, etc. A number of cupric salts are also sparingly soluble of which the least soluble ones seem to be ferrocyanide, K<sub>2</sub>Cu[Fe(CN)<sub>6</sub>], CuS and the carbonate, CuCO<sub>3</sub> (Pourbaix, 1966).

Copper seems to be rather stable in the matrix and only about 2% was found in solution after 100 hours of leaching (figure 6.9). The concentration seems to readily increase towards the end of the test. In the regression analysis of the leaching solution concentrations it was assumed that no precipitation occurred during the test. From figure 6.25, the diffusion of copper seems to be mainly responsible for leaching into the bulk solution during the initial stages, but the effect of degradation increases towards the end of the test and after about 40 hours, the effect of degradation seems to be larger than that of diffusion. According to this model the surface reaction does not contribute to the leaching phenomenon. This could be an indication that the copper is largely physically bound inside of the matrix.

### 6.4.2 Geopolymeric matrix

#### □ *Silica*

Because of the silica sand added to the matrices as bulking agent, silica is bound to be the major matrix component and will make out about 2/3 of the total mass. Due to addition of NaOH during preparation of the matrix, silicates are expected to form. The latter is relatively insoluble, except for Na- and K-silicates. The silica in the matrix is expected to mostly be present as calcium silica hydrates (C-S-H), or as insoluble silica oxides (SiO<sub>2</sub>), inside of the silica sand. C-S-H will be decomposed by the acetic acid to form silica acetates, but the SiO<sub>2</sub> is not expected to leach very fast.

In figure 6.19 a curve was fitted on the data obtained during leaching runs G1 to G7. Due to wide variation in the results for runs done in the same way, the representative curve was fitted on data from leach G5. Samples of the other runs seemed to exhibit incorrect

concentrations due to ageing of the samples prior to analysis and did not present the correct concentrations. This was especially found in the longer leaching tests, such as G1, G4 and G3, where the samples were kept until the end of the tests before it was analysed. From this graph about 0.14% of the silica was in solution after 48 hours.

In figure B8 (Appendix B) the solid silica that left the solid was plotted against time. Due to the scattered data points a typical trend could not be identified for the solid behaviour, and an average of about 8% was assumedly leached after about 24 hours and the silica solution stayed more or less constant at this concentration up to 600 hours of leaching. It is clear that a considerable amount of the silica that left the matrix was not dissolved in the solution and possibly formed insoluble compounds such as alumino-silicates. The silica in solution is possibly due to the decomposition of C-S-H, and some of the silica sand might directly be released from the solid and settle in the solution.

In figure 6.28 the influence of the different terms of equation 6.2 or 6.3, were plotted against time. From this it is clear that a large part of the silica in the solution precipitates. From the model (eq.6.2 or 6.3), the main mechanism is initially diffusion, but this effect decreases as the surface reaction contribution increases and becomes the main mechanism after about 2 hours.

#### □ *Aluminium*

The curves observed in figures 6.20 and B9 (Appendix B) for aluminium seems very similar to that of silica, which can be an indication that the leaching of aluminium is influenced by the leaching of silica. The aluminium is possibly bound to the silicates as alumino-silicates. However, the latter compound is insoluble and not expected to dissolve and leach into the solution, but it is possible that these aggregates become exposed due to degradation of the matrix and settles out into the bulk solution. This might also explain why a large percentage of the amount of aluminium that leaches from the solid, was not found in the solution (expressed as precipitates in figure 6.29).

When evaluating figure 6.20 a very small amount of aluminium appears to be leached after 48 hours (less than 1 %), which can mainly be attributed to the decomposition of the calcium aluminate hydrate, resulting in the release of some of the aluminium. But considering that most of the aluminium in the matrix is present as aluminium oxide ( $\text{Al}_2\text{O}_3$ ), which is insoluble in water, the additional amount leached from the solid might be due to the settling of some of this compound out of solution.

From figure 6.29 it is clear that a large % of the aluminium precipitates in the solution (either directly settles out, or forms insoluble compounds or salts, once in solution). Diffusion seems to govern the mechanism initially, but this effect decreases until degradation are the reigning mechanism after about 9 hours. This is probably due to the physical exposure of some of the

aluminium compounds to leave it free to settle out of the matrix into the bulk solution. The surface reaction also attributes to a lesser extend to the leaching mechanism, possibly in the fast leaching of the aluminium from calcium aluminium hydrates. It is not clear why the diffusion effect starts off as the main mechanism and decreases so rapidly. This might be due to the formation of insoluble oxide layers, or other inhibiting layers inside of the matrix, which might prevent the aluminium from dissolving into the pore solution and would decrease the amount of aluminium that diffuses through the pores to the bulk solution. It can also be owed to the depletion of the soluble aluminium compounds, such as the calcium aluminium hydrates, which might leach out rather fast even from the deeper layers of the matrix.

#### □ *Calcium*

Up to 53% of the calcium is leached after 600 hours (see figure 6.21 and B10 in Appendix B). Calcium silicate hydrates are responsible for the formation of the porous matrix and the leaching of calcium are assumed to have a direct effect on the physical stability of the matrix. The calcium, which are leached from the solid, but not found in the solution, is likely to be precipitated as less soluble calcium salts or compounds. The leaching of calcium are expected to directly influence the leaching of other elements, such as silica, which is left exposed to the acid solution as the calcium is leached out.

From the curves in figure 6.30, where the percentage contributions of the mechanisms is plotted together, precipitation seem to have an increasing effect, which is about 70% after 24 hours. The leaching is mostly due to diffusion, but the surface reaction (fast dissolution of calcium into the solution) also attributes to the leaching to a lesser extent, while the degradation/chemical reaction, does not contribute to the cumulative amount leached, according to the regression results. The reigning diffusion mechanism seems quite possible if we look at the decalcification that occurs in the different layers of the solid (chapter 5). A reaction front, moving from the surface towards the core was observed during the test and this type of reaction would typically be controlled by diffusion of the acid into the block or by the diffusion of the dissolved species towards the solution. The effect of the surface reaction is probably the result of the fast leaching of the relatively soluble substances on the surfaces.

#### □ *Iron*

In figure 6.22 only about 0.7 % of the iron is in the leaching solution after 48 hours. From figure B11 (Appendix B) a maximum of about 15 % of the iron leach out during tests lasting up to 600 hours. The curve calculated from regression analysis for the behaviour of the iron concentration in the solution, fit relatively well on the data ( $R\text{-square} = 0.94$ ), but the data points from the solid analysis were scattered, either due to analysis difficulties, or merely due to small samples which were not necessarily representative. A few more data points will be



needed to establish a more accurate curve for the leaching of iron from the solid. It is once again evident that not all the iron that leaves the solid goes into solution, but that some less soluble iron compounds, either forms in the leaching solution or settles straight from the matrix as a precipitate in the solution.

From the curves in figure 6.31, about half of the iron that leached from the solution seemed to precipitate. The mechanisms that contribute mostly to the leaching are, according to the model used, primarily the surface reaction, which decreases as the diffusion mechanism becomes more pronounced. This might be an indication of the initial fast leach of iron from the surfaces into solution, which slows down, as the available iron becomes less. The effect of diffusion increases as more iron from the inner layers of the matrix reaches the solution.

#### □ *Sodium*

Sodium is very soluble and expected to leach out at a fast rate into the solution. From figure 6.23, this is evident, and about 43% of the sodium is expected in solution after 24 hours. Due to the high solubility, sodium seems to go straight into solution and precipitation does not influence the leaching solution concentration significantly (at least not for the first 40 hours), see figure B12 in Appendix B). In figure 6.32, the semi-empirical model shows that the surface reaction and diffusion mechanisms are responsible for leaching. The surface reaction decreases slightly, as the diffusion contribution increases. The large effect of the surface reaction can be explained by the solubility of sodium that would go into solution rather fast. From chapter 4, we also observed a leaching reaction front for sodium, as for calcium, moving from the surface to the core. This could once again explain the influence of diffusion that was seen from this leaching curves and either the diffusion of the acid into the sample, or the diffusion of the sodium from the sample to the solution, are responsible for this effect.

#### □ *Magnesium*

From figure 6.24, magnesium appears to leach out rather easily, and about 17 % were found in solution after 24 hours (see also B13 in Appendix B). From figure 6.33 diffusion is initially the main mechanism, which decreases somewhat as the effect of degradation increases. More or less 70% of the Mg that leach from the solid, precipitate after 24 hours, and this percentage increases as the leaching continues, implying that all additional Mg that leach precipitates directly. The reaction front phenomenon was also observed in the different layers in the case of magnesium and this is also an indication that diffusion through layers occurs, as the model shows. Degradation also seems to have an influence, instead of the surface reaction, as was seen for the sodium and calcium. Magnesium seems to be less soluble than these two elements and the surface reaction does not contribute to such a degree to the solution concentration. Instead, according to the model, degradation seems to have an increasing influence and the leaching of other elements, such as calcium could lead to exposure of the magnesium ions or weakened bonds of this element to the solid matrix, causing the

magnesium to leave the solid and either dissolve into the solution, or precipitate as a magnesium salt. The possibility that magnesium compounds become physically detached from the matrix and directly settles out into solution should not be ruled out either.

#### □ *Potassium*

Potassium forms very little insoluble compounds as was already mentioned, and should subsequently leach easily. After 48 hours 30% of the K in the matrix is in solution (figure 6.25). And from figure B14 (Appendix B) in the region of 43% has leached from the solid at 600 hours. However, potassium was present in very low concentrations in the matrix, and the results obtained from the XRF-analysis on the solids shows a significant degree of fluctuation and the curve fitted on the leaching behaviour of the solid showed a relatively low R-square value of 0.36. Still, an increasing fraction of the potassium that leaves the solid can be assumed to precipitate in the solution and the solution concentration seem to stabilise after more or less 30% of the potassium is in solution. When evaluating the mechanisms that contribute to the leaching as the semi-empirical model predicts in figure 6.33, the effect of precipitation increases as the leaching times increase and after 48 hours, 36% of the leached calcium precipitates. Also from this figure, diffusion appears to govern the leaching mechanism, while the surface reaction and degradation does not have a mentionable influence. The zero effect of degradation might indicate that K is not physically bound into the matrix. And the large influence of diffusion, could indicate the same moving reaction front effect as was found for Ca, Na, Mg and Mn when evaluation the different layers of the solids left after leaching. This effect was not as clear for potassium in chapter 4, due to insensitivity of the analysis method towards low K-concentrations.

#### □ *Lead*

From figure 6.26 more or less 14% of the lead was leached into solution after 48 hours. The effect of precipitation is not clear, due to difficulty in interpreting the solid data for lead (very low concentrations – mostly less than 30 ppm). Therefore, equation 6.1 was fitted on the solution data (assuming no precipitation).

#### □ *Copper*

Copper did not seem to significantly leach from the matrix, and the analysis showed concentrations of virtually zero in the leaching solutions.

### 6.4.3 Comparison between the leaching behaviour of different elements

#### 6.4.3.1. Pozzolanic matrix

In figure 6.35, the trends for the behaviour of the different elements in solution was plotted on the same graph against time. The results are fitted to data obtained for the first 144 hours as obtained from data in L#18. In figure 6.36, the trends obtained from the analysis of the elements left in the solids after leaching, are plotted for 0 to 600 hours. Unfortunately, no data was obtained for leaching times less than 24 hours.

- As the trends in figure 6.35 exhibit, the percentage of each element found in solution during the tests, from the highest to the lowest, are as follows:

Na>Ca>Mg>K>Pb>Al>Fe>Si

- In figure 6.36 the leachability of the elements from the solids can be organised as follows, once again, from the highest percentage that leached from the solid, to the lowest percentage:

Na>Ca>Mg>K>Al>Fe>Si

The solid analysis of lead was done, but due to low concentrations these data was not considered to be accurate enough to determine the solid behaviour of lead in this matrix.

- Na is very soluble and all the sodium leaches from the matrix after about 600 hours. After only 48 hours about 57 percent was leached from the solid and sodium seems to mostly stay in solution.
- Calcium also gradually leaches out, until the matrix is virtually depleted of calcium after 700 hours (about 45% are leached after 48 hours). However, a large percentage of the leached calcium is not found in solution and is assumed to be present a precipitate in the bottom of the leaching vessel. The precipitate makes out more or less 30% of the total amount leached after 48 hours, and as more calcium leaches from the matrix, more precipitates forms.
- Na, Ca, Mg, K, and Pb, all clearly show a faster leaching rate for the first 12 hours, after which the release of elements slows down somewhat. The main mechanisms of release for these elements are: for Na – mostly a decreasing surface reaction and an increasing diffusion effect; for Ca – mostly diffusion, but also a surface reaction contribution; for Mg – initially mostly the surface reaction, with an increasing influence of diffusion and degradation; for K – mostly increasing diffusion, but also a decreasing surface reaction. It

is evident that diffusion plays a role in the leaching mechanisms of all these elements. This can be explained by the moving reaction fronts that were observed in the solids (chapter 4). It is clear from this behaviour that either diffusion of the acid into the block or diffusion of the dissolved elements towards the solution plays a significant role and is the cause for the faster leaching of these elements from the outer layers of the sample.

- Silica, the major matrix constituent, leaches out until about 26% is leached after 700 hours. About 2% are leached after 48 hours, of which only more or less 0.04% of silica stays in solution. This element is not very soluble and all silica that is leached during the later stages of the tests, precipitate or leach out as insoluble silica oxides or sparingly soluble compounds, such as aluminosilicates. The initial faster leaching, might be due to the leaching of calcium silica hydrates. Degradation governs the mechanism according to the regression results. This is especially so, at longer leaching times, while the surface reaction and diffusion, contributes in a much smaller way to the mechanism.
- Iron and silica show similar trends and iron might be bound to the silica compounds that decompose and leach out. A large percentage of the leached iron also precipitate and degradation is the largest contributor to the mechanism (as for Si), after 8 hours of leaching. Before this, diffusion has a more pronounced effect, which decreases with time. Possibly these substances are both bound to calcium (calcium-silica-hydrates) to some degree, and as the decalcification reaction front moves into the solid. Silica and iron dissolves in the pore solution and diffuses out towards the bulk solution. However, additional silica will leach out and this is most likely to occur from the surface as insoluble silica oxides that might be released from the surfaces and settle out in the solution.
- Aluminium is another one of the major matrix constituents and also shows similar behaviour in solution and in leaching from the solid, as silica. Only slightly higher percentages of aluminium leach out. A large percentage of this aluminium precipitates and the main leaching mechanisms, according to the model, are the surface reaction, and also diffusion to a lesser extent. Aluminium that does not leach out, is probably present as insoluble alumina oxides or hydroxides. All calcium-alumina-hydrates that might be present will leach out when calcium leaches out, and can also attribute to aluminium leaching, while aluminium that is possibly bound to the silicates as insoluble aluminosilicates, might directly come loose from the solid and precipitate in solution
- As for Pb, about 8% are in solution after 48 hours and about 13% after 150 hours. The surface reaction initially governs this mechanism, but decreases as degradation (or chemical reactions) contribute more, to the leaching. This might be an indication that lead is physically bound into the matrix and that matrix degradation will lead to the increased leaching of lead. Still, no data of the true lead concentrations that are leached from the



matrix is obtained, and the curves might not truly represent the behaviour of lead, should significant precipitation occur in the leaching solution.

#### 6.4.3.2. *Geopolymeric matrix*

In figure 6.37, the trends for the behaviour of the different elements in solution were plotted on the same graph against time. The results are fitted to data obtained for the first 48 hours (in the region where reliable solution data was obtained), but extrapolated for 150 hours. In figure 6.38, the trends obtained from the analysis of the elements left in the solids after leaching can also be seen. From these, trends of elements that left the solid matrix can be obtained for 0 to 600 hours. Unfortunately, no data was obtained for less than 24 hours.

A few conclusions can be drawn from these curves:

- The leaching from the solid for the geopolymeric matrix can be summarised from the highest percentages to the lowest (after 600 hours) as follows:

$\text{Na} > \text{Ca} > \text{Mg} > \text{K} > \text{Al} > \text{Fe} > \text{Si}$

- In solution, if the leachability of the different elements compares differently to each other, it is due to different solubility and precipitation. After 48 hours, the highest to the lowest percentages in solution are as followed:

$\text{Na} > \text{K} > \text{Ca} > \text{Mg} > \text{Pb} > \text{Cu} > \text{Al} > \text{Fe} > \text{Si}$

- When evaluation figure 6.38, it is clear that the sodium demonstrates the most drastic leaching behaviour. After 48-72 hours all the sodium is leached from the matrix. Precipitation does however occur, because only about 50% are in solution at this stage.
- Calcium is one of the main matrix components and the gradual decalcification that occurs, are expected to contribute to the degradation of the matrix, by the disintegration of C-S-H. This, as mentioned by Jansen van Rensburg (1997), will leave a porous matrix with less structural stability. Mainly the diffusion, but also to a degree, the surface reactions are responsible for the leaching of calcium (according to the semi-empirical model (eq. 6.2)).
- Silica, the main matrix component, is not as soluble as calcium and only about 8% of the silica are leached from the matrix. After 24 hours about 85% of the leached silica will precipitate and settle out in the solution, leaving only 0.15% in solution. The leaching of silica stays more or less the same after 24 hours when the maximum solution concentration is reached. Precipitation also increases from 0 to 85% after 24 hours.

Leaching seems to be due to the diffusion and surface reaction mechanisms for the first 24 hours (as for calcium). Almost 50% of the calcium in the matrix is leached after 48 hours, which implies that half of the silicates from the C-S-H present, will decompose within 48 hours and silicate ions will diffuse towards the solution. The surface reaction might have a larger influence for silica leaching than for calcium leaching, because apart from C-S-H, silica oxides might also directly be released from the matrix surface and settle in the solution.

- Aluminium is more stable in the matrix than calcium, and a maximum of about 18% was leached after 600 hours, of which a large part precipitates (almost 95% at 24 hours).
- About 15% of iron seems to leach from the matrix after which no more leaching occurred and the iron stayed stable in the matrix, even after a further 600 hours of leaching. Precipitation of the iron did however occur and less than 1% of the iron was in solution after 48 hours.
- Sodium seems to be the most soluble element and after 48 - 72 hrs all the Na was in solution. No precipitations of the sodium that leach from the matrix seem to be present, leaving it to be the most abundant element in solution.
- Ca, Na, K and Mg show similar leaching behaviour, while leaching from the solid and they might be bound into the matrix in the same way (this is also applicable for P and Mn, according to chapter 4). After 48 hours about 50% of the three elements are leached, while after 600 hours 80 – 90% were leached out of the solid. Their solubility do however, differ and while all the sodium stays in solution, the potassium and magnesium precipitates after certain maximum solution concentrations were reached. For all three elements diffusion plays a large roll in the leaching phenomena. For the Na, though, the surface reaction has a larger effect than diffusion.
- 14% of the hazardous heavy metal ion, lead, was found in solution after 48 hours. The mechanism of degradation is not clear, because the concentrations of this element could not be accurately analysed during XRF analysis, and no knowledge of the precipitation behaviour of lead is available to fit this model. If assuming that no precipitation occurs, the surface reaction and degradation seem to rule the leaching behaviour, which might be an indication that lead is physically bound into the matrix.

#### 6.4.3.3. *Comparison between the leaching behaviour and mechanisms of Pozzolanitic and Geopolymeric matrix*

We can compare the leaching behaviour of these two matrices to see what differences in leachability and general leaching behaviour of the main matrix components, we can expect for long-term exposure of the matrices to corrosive environments. We need to consider both the

leaching solution concentrations, as well as the concentrations of elements that leave the solids during the leaching tests.

- Silica, the primary component (70 –80% of the matrix) does not leach out in great percentages, due to the insoluble silica oxides and –hydroxides, which are present in the silica sand. The latter was added as bulking agent and is thus present in large quantities. In solution most of the silica precipitated, in the pozzolanic as well as geopolymeric cases, and the percentages of silica in solution was below 1%. However, if we consider the amount of silica that was left in the solid matrices after the leaching tests, it seems as if, on average, more silica left the pozzolanic matrix than the geopolymeric matrix after 600 hours. About 8% of the silica were leached from the latter, while about 20% were leached from the pozzolanic matrix after this time of exposure to the leachate. This might be an indication of faster degradation of the pozzolanic matrix. The mechanisms of release from the solid (figures 6.10 and 6.28) initially seem to be mainly the surface reaction for both matrix types, this is possibly due to the fast dissolution of silica-acetates from soluble silicates, such as Na- and K-silicates, or from the calcium-silica-hydrates or nickel-silica-hydrates. For the pozzolanic matrix, the surface reaction contribution to leaching decreases and leaching from the surface seem to become less important with respect to the increasing effect of degradation on the leaching at later stages. The leaching from the geopolymeric matrix also stops after the initial fast leaching, possibly due to insoluble silica oxide layers that forms on the structure. Almost all leaching that occurred in this material seems to have been due to surface leaching and to a lesser degree some diffusion of silica from the inside of the material. The degradation effect in the pozzolanic samples can be due to release of physically bound silica, as the matrix is degraded by decalcification. The silica oxide particles might even directly be released from the structure and settle out into solution. This further leaching, due to degradation, does not occur in the geopolymeric case, which can be an indication that the geopolymer is a more stable matrix.
- For aluminium the stability in the geopolymeric matrix seems more than in the pozzolanic matrix and after 600 hours, 27% of the pozzolanic matrix and 18% of the geopolymeric sample were leached. Aluminium, present as oxide or hydroxide gels are sparingly soluble and the surface reactions, that seems to initially control the leaching of aluminium from the pozzolanic matrix, are more likely due to the dissolution of more soluble substances such as calcium-aluminium-hydrates, or as alumino-silicates. The dissolution of this compound might explain the similar leaching behaviour of silica and aluminium from the geopolymeric matrix, where diffusion and degradation seemed to play a primary roll. The release mechanisms of the two matrix types seem to differ somewhat, and the aluminium that leaches out are probably bound to the matrices in different ways. In the pozzolanic matrix, for example, mainly as calcium-alumina-hydrates (explaining the similarity in leaching mechanisms shown by calcium and aluminium for the pozzolanic matrix) and alumino-silicates for the geopolymeric matrix (due to the similarity in

leaching of silica and aluminium for this matrix). Diffusion and degradation are the mechanism responsible for leaching of aluminium from the geopolymeric matrix and the surface reaction, for leaching of the pozzolanic matrix. This surface reaction implies that there must be aluminium substances in the pozzolanic matrix that are more susceptible for dissolution into the solution, or that more of the insoluble silica-oxides or hydroxides are directly released from the solids to settle out in the solution, than for the geopolymeric matrix.

- Iron, which mostly originates from the jarosite waste, is more stable in the geopolymeric matrix than the pozzolanic matrix, if we compare the percentages that leached out after 600 hours (15% leach from the geopolymeric samples and 26% from the pozzolanic samples). The behaviour of iron appears to be very similar to that of silica during leaching of both the matrix types and silica and iron are probably bound to the structures in similar ways. In the pozzolanic case the leaching seem to be due to diffusion and degradation and for the geopolymeric matrix mainly as the surface reaction and diffusion, according to the semi-empirical model. The degradation influence in the leaching of the pozzolanic sample might be responsible for the larger amounts of iron that was leached from this matrix, because due to degradation, the leaching effect might be enhanced by more exposure to the leachate.
- Calcium also leached from the pozzolanic matrix to slightly greater extends. Calcium, being rather soluble, exhibits the mechanisms of leaching, diffusion and the surface reaction for both the matrices. This element appears to be bound into the different matrices similarly and also leach out similarly.
- Sodium (Na) leaches out very fast, particularly from the geopolymeric matrix. The same mechanisms were responsible for the leaching of sodium from both the matrix types and, according to the model, the surface reaction and diffusion are in both cases responsible for leaching, which is also similar to the behaviour of calcium. It can be concluded that Na and Ca are bound to both the matrices similarly and leach out by similar mechanisms, but Na seem to be more stable in the pozzolanic matrix and Ca slightly more stable in the geopolymeric matrix.
- Magnesium behaves very similar to calcium and sodium in both cases and seems slightly less stable in the geopolymeric matrix.
- Overall, as was already concluded in chapter 5, if one considers the main elements after 600 hours for the two matrix types, Si, Al, Ca and Fe are more stable in the geopolymeric matrix, while Na and Mg are more stable in the pozzolanic matrix. But the Si, Al, Ca and Fe will contribute to a larger part of the matrix and the degradation phenomenon therefore seem to be larger in pozzolanic material than in the geopolymeric material and the



geopolymeric material might, in the long run, be structurally more sound than the pozzolan.

- In solution, most of the elements partly precipitate as the elements are leached from the solid into the solution, and a maximum concentration of most elements is reached after a certain period of time. Leaching from the solids do however continue and all elements seem to either precipitate as insoluble salts or compounds as soon as it goes into solution, or insoluble substances directly settle out from the matrix into the solution. The concentrations of the different elements in solution are more or less similar for the different matrices, except for sodium where larger amounts were in solution during leaching of a pozzolanic matrix than during leaching of the geopolymeric type. In the latter case a considerable percentage of the sodium precipitated, which was not the case in the pozzolanic solution.

## CHAPTER 7

# CONCLUSIONS

*Conclusions on chapters 1 to 6 on the degradation behaviour during leaching tests on pozzolanic and geopolymeric matrices, produced to stabilise hazardous components in fly ash and jarosite.*

---

In the manufacturing of almost all products, from preparing dinner to refining oil, it is a common experience to have waste produced in collaboration with the desired product. Reducing, reusing, or recycling practices only provide partial solutions to most of these problems, and only as far as economically permitted. In addition to this problem, industrial wastes also have the tendency to be hazardous of nature and cannot be disposed into the environment without consideration of the long-term pollution implications. As environmental awareness and regulations increase, solid waste disposal becomes an escalating problem and waste disposal companies increasingly take interest in the hazardous waste treatment technology.

**Chapter 1** discussed industrial waste disposal problems and stabilisation as a possible treatment for wastes, to immobilise hazardous components and thereby prevent potentially harmful interaction with the biosphere. This involves additives being mixed with wastes, resulting in a product where the hazardous elements/compounds are trapped inside a stable matrix and the rate of contaminant migration from the waste is minimised, to reduce toxicity. This makes the waste more suitable for disposal, typically in landfills. The reduction in leaching rates may result from physical and chemical retention in the solid matrix and the high pH of the products. However, in waste disposal sites, water infiltration through the waste can become contaminated with waste constituents, leading to instability of the immobilised matter and increased leaching of hazardous contaminants into ground or surface waters. Standardised leaching tests, for testing the stability of such materials were considered to determine measures of stability for the classification of waste streams as either hazardous or non-hazardous. Jansen van Rensburg (1997) developed a suitable leaching strategy to simulate environmental conditions at a waste disposal site. Typically during leaching tests the behaviour is governed by initial fast surface reactions, followed by much slower diffusion, but leaching rates can also be increased due to a slow mobilising chemical reaction and/or corrosion or structural breakdown of the waste matrix.

The objective of this thesis is to study and characterise this degradation during leaching tests on immobilised matrices (consisting of fly ash and jarosite)

In **chapter 2** a brief look into the history of this technology can explain why little research has been done in this field, in particular the long-term leaching behaviour of the immobilised materials. Even though, today immobilisation (or stabilisation) of toxic or hazardous components of a waste is a widely acceptable technology and a solution to many waste disposal problems, no published work was done on leachability, environmental degradation, or any other performance characteristics of solidified waste, until the early 1970's (other than internal studies by nuclear installations). Only in recent years, after 1975, when legislation on environmental matters started to limit the disposal methods, did research and development in this field start to bloom and today regulations and legislation still keeps this technology alive. Chapter 2 presented some background on the basic outlay of the immobilisation technology and the chemistry behind it, as well as a few proposed models for the characterisation of leaching from the stabilised matrices, during standardised leaching tests.

In **chapter 3**, the basic materials, and methods of preparation, leaching and analysis were discussed. The waste forms under consideration were fly ash and jarosite, which were combined with additives to form two different kinds of matrices, pozzolanic and geopolymeric in geo-chemical structure. Samples were prepared and cured in exactly the same way and the same leaching test was done on every sample, only differing in the time that the experiments lasted. Acetic acid was chosen as leaching solution during the tests to simulate the intensified behaviour in a landfill. Other variables that could effect the leaching behaviour, such as temperature, pH, stirring speed and sample sizes, were held as constant as possible throughout the leaching tests.

In **chapter 4** the observations of physical and microcrystalline behaviour of the different matrices during testing were discussed. A specific crack pattern, similar to the effect of peeling an onion, was observed in leaching of some of the pozzolanic samples. Large cracks seem to form about 5mm from the sample surfaces and the whole layer seemed to become detached from the sample, due to these large cracks, and with longer exposure to the leachate, this also happened to a second layer. This was not observed for all the samples, due to evident variation in behaviour during the different tests, which can be attributed to differences during the complex reactions in the samples, which led to samples that slightly vary in strength and would degrade to different degrees. This "onion effect" was not observed in the leaching of the geopolymeric matrix and the outer layers seemed to rather flake off than the large cracks that were seen in the pozzolanic samples.

When considering the scanning electron microscopic (SEM) analysis and crack patterns, the main mechanisms of degradation seem to be acid attack and also possibly the alkali silica reaction for both the pozzolanic and geopolymeric matrices. We concluded in chapter 4 that the acid attack was most likely responsible for the corrosion of the surfaces as we observed

for both the matrices during the tests. The alkali silica reaction, in turn, might be the source of cracks due to the hydration and subsequent swelling of the alkali-silica gels that are likely to form in both structures. Additional to these reactions, larger cracks in the pozzolanic matrix, might also be due to crystals (containing Ca, P, Si, and little Al), which could expand and lead to the large cracks in some of these samples.

No trends could be fitted with certain accuracy onto either the porosity changes or the mass loss during leaching of the pozzolanic and the geopolymeric samples. The variation in the calculated values, are assumed to be due to natural variation in sample consistencies, which would cause more substantial degradation in some cases than in others. There is however signs that both the porosity and mass loss might show an exponential trend when expressed as a function of leaching time, but more experiments are needed to confirm this.

In **chapter 5** the degradation phenomena were characterised by evaluating the results obtained from analysing the solids that were left after each leaching test. From cutting these remaining samples into layers, an indication of the leaching behaviour of different elements with respect to depth into the block was obtained.

Si, the main matrix component is rather stable in both matrices, probably because of the presence of silica as insoluble silica-oxides and -hydroxides in silica sand. Release of silica into the solution, are probably due to the dissolution of calcium silica hydrates, which will leach much easier. The leaching of calcium from the structure will especially contribute to this effect, because the calcium leaches out relatively fast, entailing that the compound might break up and release silica into the leachate. About 8% of the silica was leached from the geopolymeric samples after 600 hours, while about 20% were leached from the pozzolanic matrix after this time.

Decalcification of both matrices occurs in such a way that 95% of the calcium in the pozzolanic matrix leach out after 670 hours and 85% are leached from the geopolymeric matrix in 600 hours. The behaviour of calcium in the two matrices is rather similar and a moving leaching reaction front was observed in both cases. This front moved from the outside of the matrix towards the core, and the surface layers subsequently became depleted from calcium before the inner layers.

All sodium completely leached from both matrices at longer leaching times. The fast leaching rates of sodium are due to the high solubility of this element. The sodium does however leach faster from the geopolymeric samples than from the pozzolanic samples, implying that sodium are more sufficiently immobilised in the pozzolanic structure.

This moving reaction front behaviour for the leaching of Ca was also observed for Na, Mn, Mg, and P in both the pozzolanic and the geopolymeric materials. The leaching behaviour of these elements was very closely related, even though Na and Ca are a bit more soluble and



was leached out faster than Mn, Mg and P. These elements are all likely to be bound into the matrix in the same way.

For aluminium, 27% of the pozzolanic matrix and 18% of the geopolymeric sample were leached after 600 hours and 15% of the iron, another primary matrix component, leached from the geopolymeric matrix, while 26% left the pozzolanic samples, after this leaching time. No clear reaction fronts (difference in leaching rate from the deeper layers of the samples than from surface samples) were observed for Si, Fe, Al and Ti during leaching tests on both matrix types. The leaching behaviour of these elements were alike and they were probably also bound into the matrix structure similarly. Al and Fe are apt to both be part of hematite, a reaction product of jarosite and NaOH, in both matrices.

When comparing the leaching behaviour of the two matrices after 600 hours, the main matrix components Si, Al, Ca, and Fe are more stable in the geopolymeric matrix, while Na and Mg are more stable in the pozzolanic matrix. The Si, Al, Ca and Fe will however, add up to a larger part of the matrix. The degradation phenomenon therefore appears to be greater in the pozzolanic material than in the geopolymeric material. This indicates that the geopolymeric material might, in the long run, be structurally more stable than the pozzolan.

**Chapter 6** focussed on the results that were obtained from analysing the leaching solutions. By comparing the solution concentrations with the expected percentages of elements in solution  $\{(\text{amount initially in solid} - \text{amount left in solid})/\text{amount initially in solid} \times 100\}$ , it was clear that some precipitation occurred in the solution. A semi-empirical model was fitted on the cumulative amounts of the elements in the solution during the leaching tests and the parameters  $K_1$ ,  $K_2$ ,  $K_3$ ,  $K_4$ ,  $K_5$  and  $K_6$  were obtained through regression analysis. Two forms of this model are given in equations 6.2 and 6.3 and the separate terms represent leaching by a surface reaction, diffusion, degradation/chemical reaction and another term was also added to represent the precipitation that occurred in the solution. For some elements the precipitation was assumed to be linear with respect to leaching time (eq. 6.2) and for other elements this term was regarded as a power term (eq. 6.3).

$$\text{CAL}(t) = K_1(1 - e^{-k_2 t}) + K_3 t^{\frac{1}{2}} + K_4 t - (K_5 t + K_6) \quad 6.2$$

$$\text{CAL}(t) = K_1(1 - e^{-k_2 t}) + K_3 t^{\frac{1}{2}} + K_4 t - K_5 t^{K_6} \quad 6.3$$

Silica does not leach out in great percentages, due to the insoluble silica oxides and hydroxides, which are present in great quantities in the silica sand. The mechanisms of release from the solid seem to be mainly the surface reaction for both matrix types, and also degradation for the pozzolanic matrix at later stages.

Similar behaviour was found for the leaching of silica and aluminium from the geopolymeric matrix, where diffusion and degradation seemed to play primary rolls. The release mechanisms of the aluminium seem to be somewhat different for the two matrix types, which might be an indication that aluminium is not bound by the same mechanisms in the different matrix types.

The similar behaviour of iron and silica, during leaching tests on both the matrix types, might indicate that silica and iron, too, are combined in the structures in similar ways. Calcium, sodium and magnesium, which are all rather soluble ( $\text{Na} > \text{Ca} > \text{Mg}$ ) also exhibits closely related leaching behaviour and are probably constrained in the matrices in the same way.

In conclusion, this study contributes to the understanding of the degradation phenomenon of immobilised matrices during leaching tests. When the leaching tests can accurately be characterised, these results can be used for further predictions on the long-term behaviour of the stabilised wastes in disposal sites, and the resulting effect they might have on the environment. It is clear that during these tests different matrices might physically break down due to different degradation mechanisms and crack formations. And this might affect the leaching behaviour. In this study, the concentrations of the main matrix components in the leaching solution were considered as a way to characterise this corrosion behaviour and a semi-empirical model gives an indication of what mechanisms are mainly responsible for the mobilisation of the elements. The depletion of these elements from the matrices, with respect to depth into the samples and time of exposure to the leaching solution, also gives an indication of how the different elements typically becomes detached from the samples and leach into the bulk solution. This data can present concentration profiles for the different elements as a function of time and position in the matrix and can perhaps later be used in refining models for the prediction of leachate concentration. No direct relationship between the physically observed degradation (crack formation etc.) and the leaching solution concentrations could be obtained, because it cannot be ascertained exactly when the cracks appear. This observed behaviour does however give an indication of what mechanisms of attack and corrosion are expected to occur during the tests.

## REFERENCES

- ◆ Adenot, F. and Buil, M., *Modelling of the corrosion of the cement paste by deionized water*, Cement and Concrete Research, 1992, Vol 22, pp. 489-496.
- ◆ Al-Amoudi, O.S.B., Maslehuddin, M. and Asi, I.M., *Performance and correlation of the Properties of Fly Ash*, Cement Concrete, and aggregates, December 1996, Vol 18(2), pp. 71-77.
- ◆ Albino, V., Cioffi, R., de Vito, B. and Santoro, L., *Evaluation of solid waste stabilization processes by means of leaching tests*, Environmental Technology, 1995, Vol. 17, pp. 309-315.
- ◆ Baker, P.G. and Bishop, P.L., *Prediction of metal leaching rates from solidified/stabilised wastes using the shrinking unreacted core leaching procedure*, Journal of Hazardous Materials, 1997, 52, pp. 311-333.
- ◆ Barham, J.R., *Schertmannite: A unique mineral, contains a replaceable ligand, transforms to jarosites, hematites, and/or basic iron sulfate*, Journal of materials research, 1997, Vol 13, no.10, pp. 2751-2757.
- ◆ Barna, R., Sanchez, F., Moszkowicz, P., Mèhu, J., *Leaching behavior of pollutants in stabilized/solidified wastes*, Journal of Hazardous Materials, 52, 1997, pp.287-310.
- ◆ Batchelor, B., *A Numerical Leaching Model For Solidified/Stabilized Wastes*, Wat. Sci. Tech., 1992, Vol. 26, No. 1-2, pp.107-115.
- ◆ Bonen, D, Tennis, P.D., Olson, R.A., Jennings, H.M. and Mason, T.O., *Stabilization of Simulated alkaline Non-vitrifiable low-level radioactive waste by carbonate-bearing Afm and Aft phases*, Mechanisms of Chemical Degradation of Cement-based Systems, Ed. Scrivener, K.L. and Young, J.F., 1997, E & Fn Spon, London, pp.374-383.
- ◆ Boy, J.H., Race, T.D. and Reinbold, K.A., Bukowski, J.M., Brough, A.R. and Zhu, X., *Response of Pb in Cement Waste Forms During TCLP Testing*, Mechanisms of Chemical Degradation of Cement-based Systems, Ed. Scrivener, K.L. and Young, J.F., 1997, E & Fn Spon, London, pp. 444-452.
- ◆ Buckle, R.L. and Lorenzen, L., *The Stabilisation and disposal of jarosite*, Second International Symposium on Iron Control in Hydrometallurgy, Editors: Dutrizac, J. and Harris, R., 20-23 Oct (1996), pp. 597-611, Ottawa, Canada.

- ♦ Carde, C., François. R., and Olivier, J.P., *Microstructural changes and mechanical effects due to the leaching of calcium hydroxide from cement paste*, Mechanisms of Chemical Degradation of Cement-based Systems, Ed. Scrivener, K.L. and Young, J.F., 1997, E & Fn Spon, London, pp.30-37.
- ♦ Chowdhury, M.A., Kunitake, M, and Kondo, F., *Seepage through an Embankment Computed by Grid Research Using FEM*, Proceedings of the Seventh (1997) International Offshore and Polar Engineering Conference, Honolulu, USA, May 25-30, 1997, pp. 887-893.
- ♦ Conner, J, R, *Chemical Fixation and Solidification of Hazardous wastes*, Ed. Van Nostrand Reinhold (1990), New York, pp. 23-57, 61-93, 304-415.
- ♦ Connor, J.R., *Stabilizing hazardous waste*, Chemtech, December 1993, **23**(12), pp. 35-44.
- ♦ Das, G.K., Acharya, S., Andand, S., and Das, R.P., *Jarosites a Review*, OPA (Overseas Publishers Association), Amsterdam, 1996, pp. 185-210.
- ♦ Dixon, D.G. and Hendrix, J.L., *A General Model for Leaching of Ore or more Solid Reactants from Porous Ore Particles*, Metallurgical Transactions B, vol. **24B**, February 1993, pp. 157-168.
- ♦ Drakonaki, S., Diamadopoulos, E., Vamvouka, D., and Lahaniatis, M., *Leaching Behaviour of Lignite Fly Ash*, Journal of Environmental Science and Health. Part A, Toxic/hazardous substances & environmental engineering, 1998, pp.237-248.
- ♦ Englehardt and Peng, *Pozzolanic Filtrations: Solidification of radionuclides in nuclear reactor cooling water*, Waste Management, 1996, Vol **15**, no.8, pp. 585-592.
- ♦ Farah, A., Hmidi, N., Moskalyk, R., Amaratunga, L.M., and Tambalakian, A.S., *Numerical Modelling of the effectiveness of sealants in retarding acid mine drainage from mine waste rock*, Canadian Metallurgical Quarterly, 1997, vol.**36**, nr 4, pp241-250.
- ♦ Ferraris C.F., Clifton, J.R., Garboczi, E.J. and Davis, F.L., *Stress due to alkali-silica reactions in mortars*, Mechanisms of Chemical Degradation of Cement-based Systems, Ed. Scrivener, K.L. and Young, J.F., 1997, E & Fn Spon, London, pp. 75-82.
- ♦ Ferraris, C.F., Clifton, J.R., Garboczi, E.J. and Davis, F.L., *Mechanisms of Degradation of Portland Cement-Based Systems by Sulfate attack*, Mechanisms of Chemical



Degradation of Cement-based Systems, Ed. Scrivener, K.L. and Young, J.F., 1997, E & Fn Spon, London, pp. 185-192.

- ◆ Fredrich, J.T. and Lindquist, W.B., *Statistical Characterization of the Three-dimensional Microgeometry of Porous Media and Correlation with Macroscopic Transport Properties*, International journal of rock mechanisms and mining sciences, 1997, vol. 34, no 314, p. 368.
- ◆ Gavasci, R., Lombardi, F., Polettini, A. and Sirini, P., *Leaching tests on solidified products*, Faculty of engineering, University of Rome, Rome, Italy.
- ◆ Giesekke, E., *Mineral-based treatment strategies for local waste and effluents*, Presented at The Science of Minerals Conference, Muldersdrift, May 8<sup>th</sup> (1998)-Mintek Randburg, South Africa, 1998.
- ◆ Glasser, F.P., *Chemical attack on cement in nuclear repositories*, Mechanisms of Chemical Degradation of Cement-based Systems, Ed. Scrivener, K.L. and Young, J.F., 1997, E & Fn Spon, London, pp. 324-330.
- ◆ Herbert, R.B. Jr., *Partitioning of heavy metals in Podzol soils contaminated by mine drainage waters*, Water, air, and soil pollution, vol 96, 1997, part 1-4, pp. 39-59.
- ◆ Hinsenveld, M., *A Shrinking Core Model as a Fundamental Representation of Leaching Mechanisms in Cement Stabilized Waste*, PhD. Dissertation, University of Cincinnati, Cincinnati, OH, 1992.
- ◆ Jansen van Rensburg, A.E., *The Development of a Leaching Procedure to Determine the Effectiveness of Immobilising Nickel as a Heavy Metal in Solid Wastes*, M.Eng. Thesis, Department of Chemical Engineering, University of Stellenbosch, Stellenbosch, South Africa, 1997.
- ◆ Jiang, W., Silsbee, M.R., Breval, E. and Roy, D.M., *Alkali activated cementitious materials in chemically aggressive environments*, Mechanisms of Chemical Degradation of Cement-based Systems, Ed. Scrivener, K.L. and Young, J.F., 1997, E & Fn Spon, London, pp. 289-295.
- ◆ Khalil, M.Y. and Merz, E., *Immobilization of intermediate-level wastes in geopolymers*, Journal of Nuclear Materials, 1994, 211, pp. 141-148.

- ◆ Malek, R and Roy, D; *Durability of alkali activated cementitious materials*, Mechanisms of Chemical Degradation of Cement-based Systems, Ed. Scrivener, K.L. and Young, J.F., 1997, E & Fn Spon, London, 1997, pp. 83-89.
- ◆ Medici F, Merli, C., Scoccia, G. and Volpe, R., *Release of Toxic Elements from Solidified Wastes: A Mathematical Model*, Stabilization and Solidification of Hazardous Radioactive, and Mixed Wastes, 1992, Vol 2, pp.171-181.
- ◆ Monteiro P.J.M., Wang, K., Sposito, G., dos Santos, M.C. and de Andrade, W.P., *Influence of Mineral admixtures on the alkali-aggregate reaction*, Cement and Concrete Research, 1997, Vol 27, Nr. 12, pp. 1899-1909.
- ◆ Naiqian, F. and Tingyu, H., *Mechanism of natural zeolite powder in preventing alkali-silica reaction in concrete*, Advances in cement research, July (1998), Vol 10(3), pp.101-108.
- ◆ Pourbaix, M., *Atlas of Electrochemical Equilibria in Aqueous Solutions*, Great Britain (1966), Pergamon Press Ltd.
- ◆ Rosato, L.I. and Agnew, M.J., *Iron disposal options at Canadian Electrolytic Zinc*, Iron Control and Disposal, pp. 77-89.
- ◆ Seidel, A., Sluzny, A., Shelef, G. and Zimmels, Y., *Self inhibition of Aluminum leaching from Coal Fly ash by Sulfuric acid*, Chemical Engineering Journal, 1999, Vol 72, pp. 195-207.
- ◆ Subbarao, C. and Ghosh, A., *Fly ash management by stabilization*, India, Journal of Solid Waste Technology and Management, August (1997), Vol. 24(3), pp.126-130.
- ◆ Taylor, H.F.W. and Gollop, R.S., *Some Chemical and Microstructural aspects of concrete durability*, Mechanisms of Chemical Degradation of Cement-based Systems, Ed. Scrivener, K.L. and Young, J.F., 1997, E & Fn Spon, London, pp. 177-183.
- ◆ Taylor, H.F.W. and Gollop, R.S., *Some Chemical and Microstructural Aspects of Concrete Durability*, Mechanisms of Chemical Degradation of Cement-based Systems, Ed. Scrivener, K.L. and Young, J.F., 1997, E & Fn Spon, London, pp. 178-181.
- ◆ Thaulow, N. and Jakobsen, U.H., *The Diagnosis of Chemical deterioration of concrete by optical microscopy*, Mechanisms of Chemical Degradation of Cement-based Systems, Ed. Scrivener, K.L. and Young, J.F., 1997, E & Fn Spon, London, pp. 3-13.

- ♦ Van Breugel, K. and Koenders, E.A.B., *Numerical Simulation of the effect of elevated temperature curing on porosity of cement based systems*, Mechanisms of Chemical Degradation of Cement-based Systems, Ed. Scrivener, K.L. and Young, J.F., 1997, E & Fn Spon, London, pp. 236-249.
- ♦ Van Deventer, J.S.J. and van der Merwe, P.F., *Kinetic Model for the Decomposition of Cyanide during the Elution of Gold from Activated Carbon*, Separation Science and Technology, **30**(6), 1995, pp. 883-898.
- ♦ Van Jaarsveld, J.G.S, Van Deventer, J.S.J, and Lorenzen, L., *Factors Affecting the Immobilization of Metals in Geopolymerized Flyash*, Metallurgical and Materials Transactions B, 1996, Volume 29B, pp. 283-291.
- ♦ Van Zyl, R.L, *The Immobilisation of Heavy Metal Ions in Metallurgical Waste*, M.Eng. thesis, Departement of Chemical Engineering, University of Stellenbosch, Stellenbosch, South Africa, 1997.
- ♦ Wang, K. and Chiang, K., *Metal Leachability and Species Analysis in Municipal Solid Waste Incinerator Ashes*, Proceedings of the International Conference in Solid Waste Technology and Management, Taiwan, 1996.
- ♦ Weng, C.H. and Huang, C.P., *Treatment of Industrial Wastewater by Fly Ash and Cement Fixation*, Journal of Environmental Engineering, Nov./Dec. 1994, **120**(6), pp. 1470-1485.
- ♦ Yousuf et. al., *An FTIR and XPS Investigation of the Effects of Carbonation on the Solidification/Stabilization of Cement based systems -Portland type v- with Zinc*, Lamar University Beaumont, Cement and Concrete Research, Vol **23**, pp.773-784, USA, 1993.
- ♦ Zinck J.M.and Dutrizac, J.E, *The behaviour of zinc, cadmium, thallium, tin and selenium during ferrihydrite precipitation from sulphate media*, CIM Bulletin, April 1998, Vol **91**, part 1019, pp. 94-101.

## APPENDIX A

---

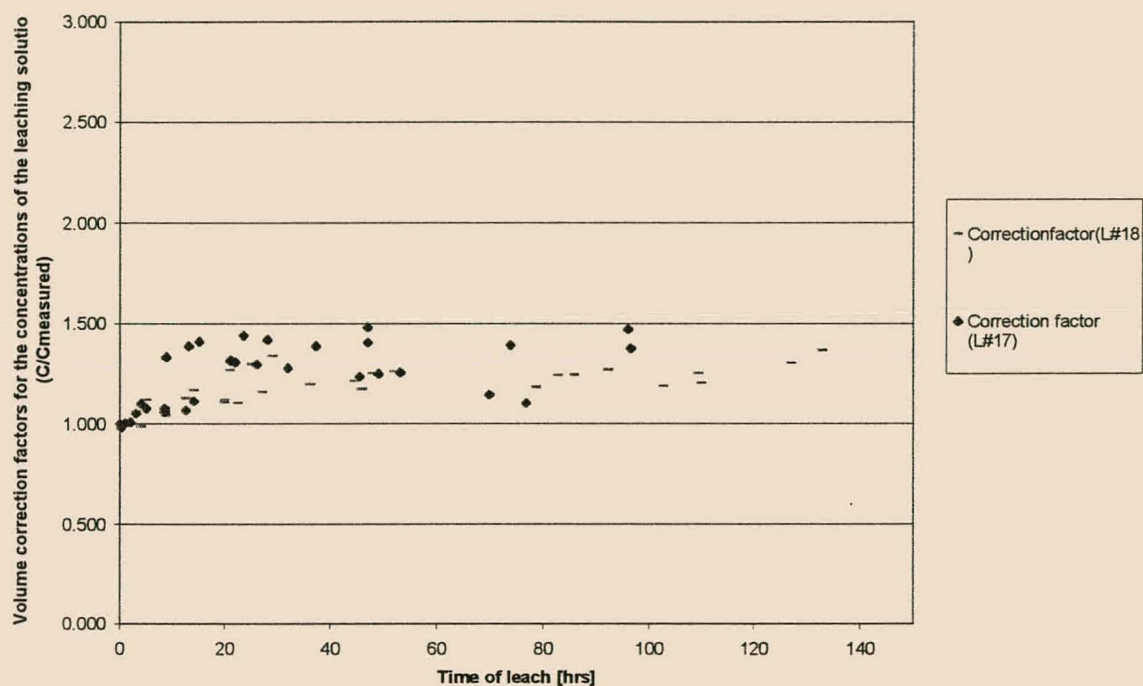


*Figure A1 Correction factors for the concentrations of the leaching solutions (L#17 and L#18 of the pozzolanic matrix):*



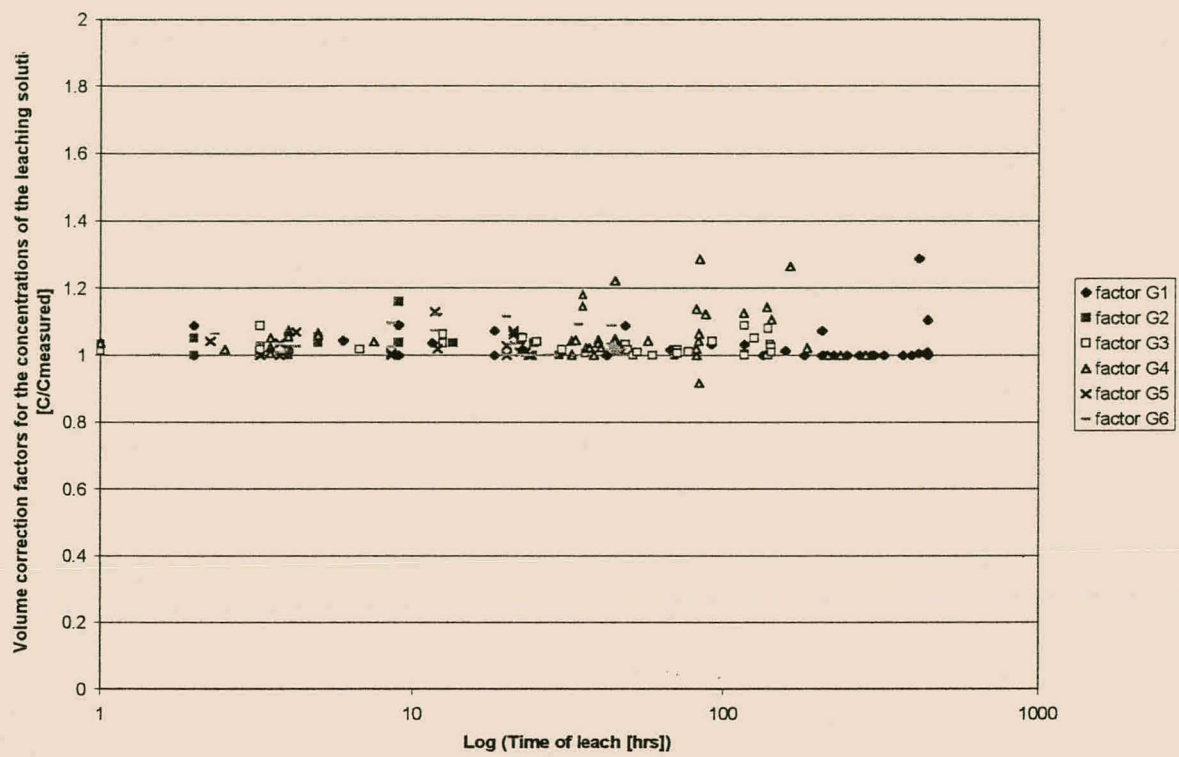


*Figure A2 Correction factors for the concentrations of the leaching solutions G1 to G6 (Geopolymeric matrix):*

## APPENDIX B

Results of leaching tests:

➤ **Pozzolanic**

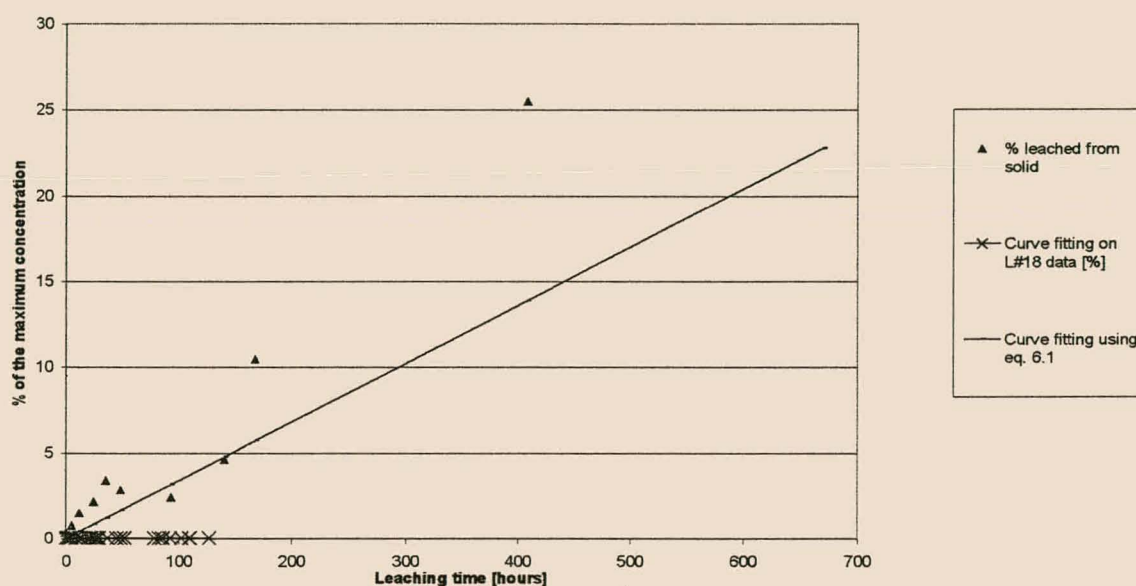


Figure B1: Trends followed by silica when leached from the solid as well as leaching trends of solution (pozzolanic matrix)

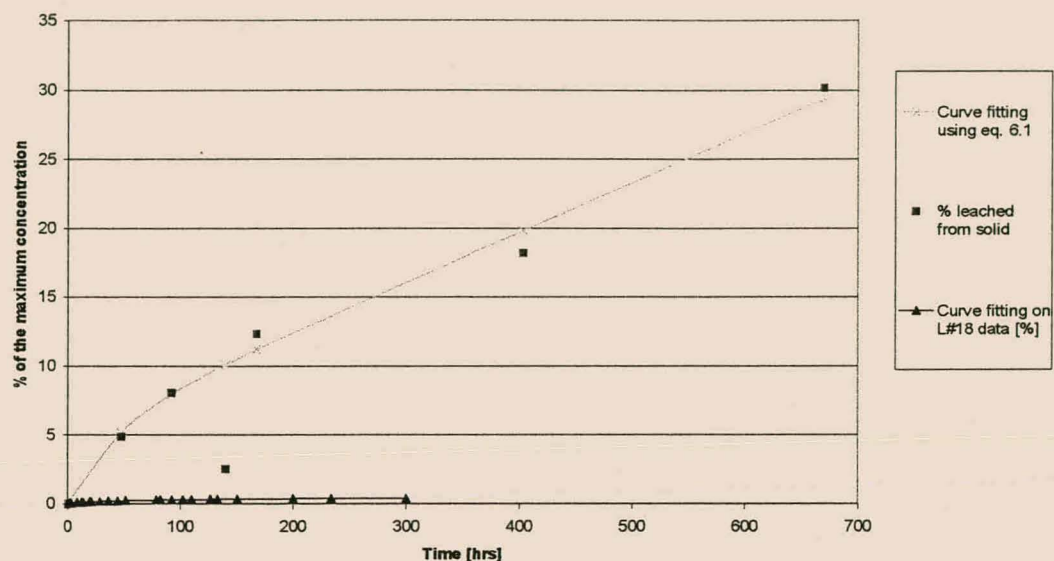


Figure B2: Trends followed by aluminium when leached from the solid as well as leaching trends of solution (pozzolanic matrix)

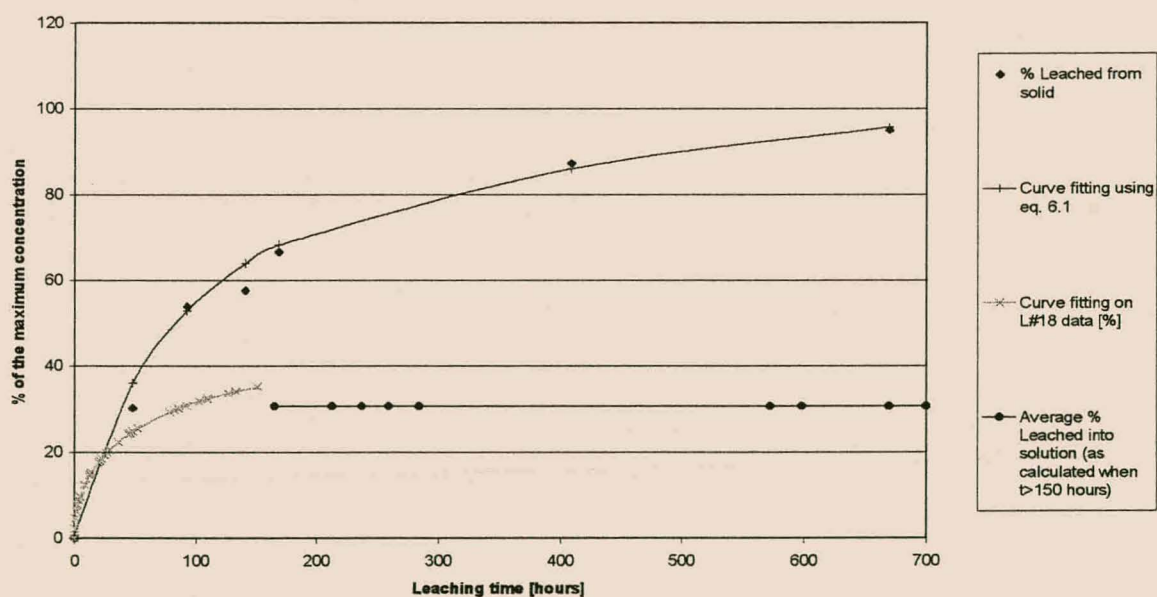


Figure B3: Trends followed by calcium when leached from the solid as well as leaching trends of solution (pozzolanic matrix)

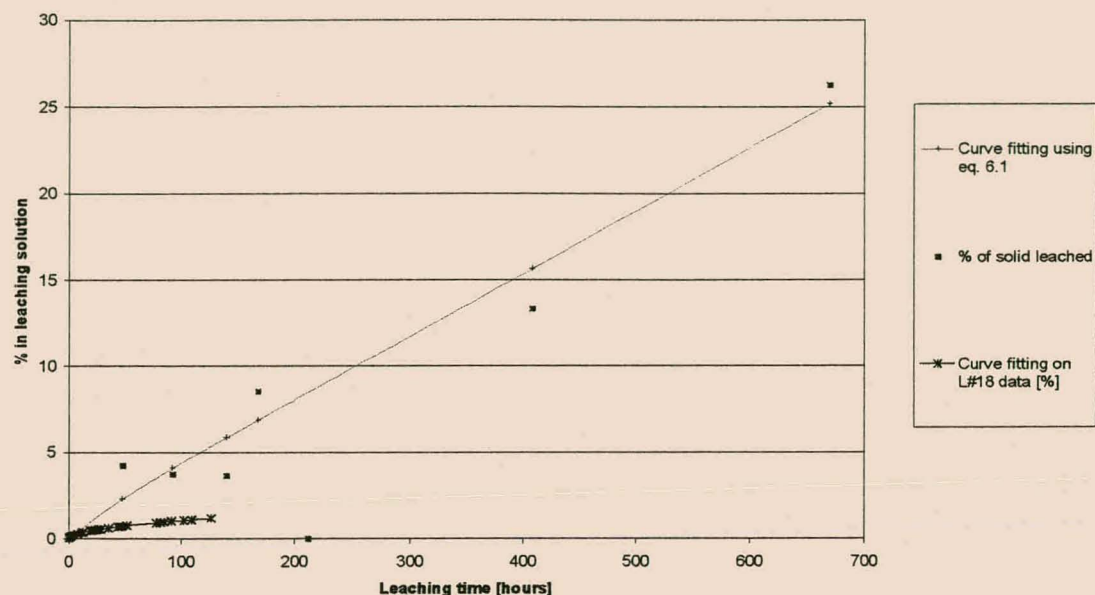


Figure B4: Trends followed by iron when leached from the solid as well as leaching trends of solution (pozzolanic matrix)

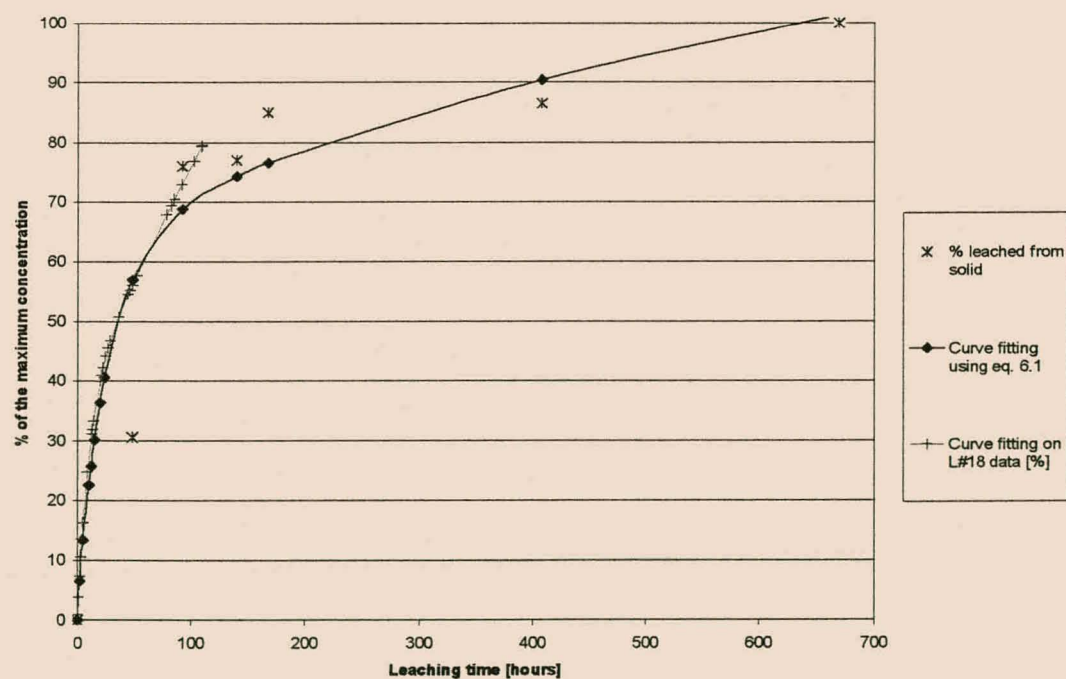


Figure B5: Trends followed by sodium when leached from the solid as well as leaching trends of solution (pozzolanic matrix)



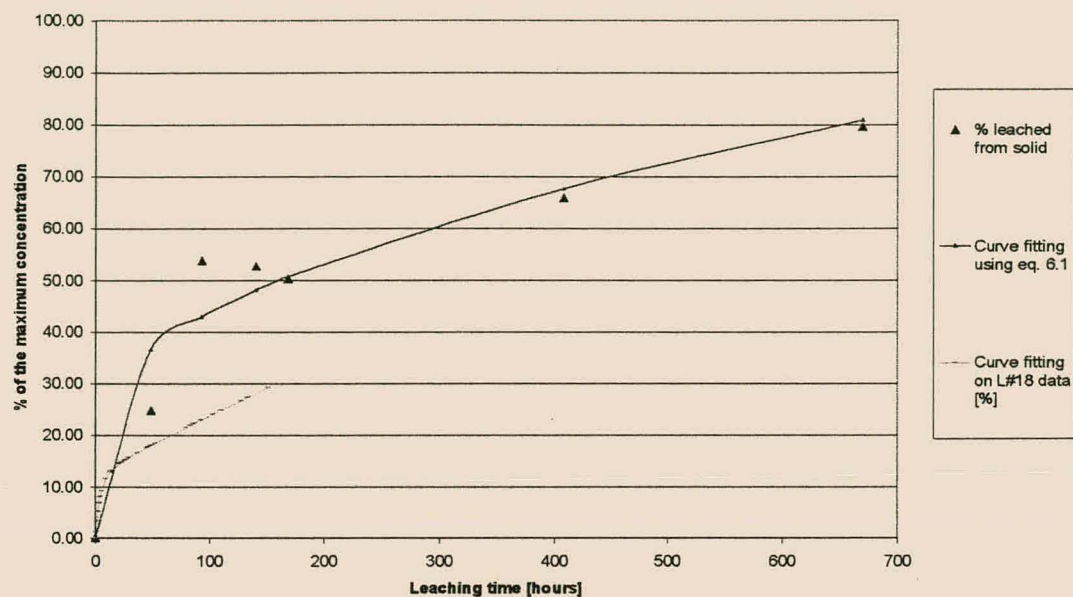


Figure B6: Trends followed by magnesium when leached from the solid as well as leaching trends of solution (pozzolanic matrix)

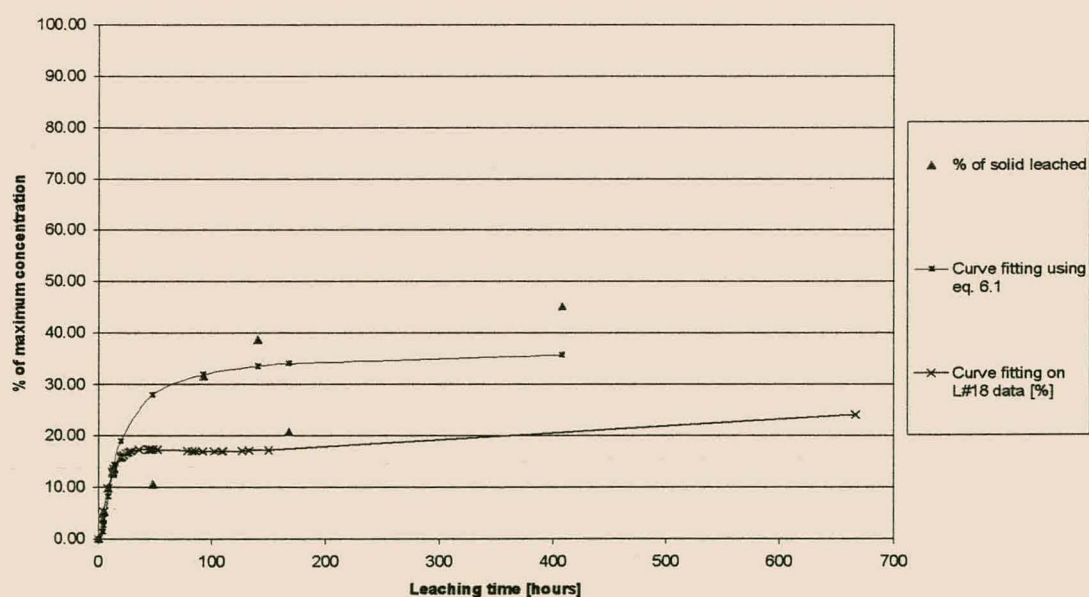


Figure B7: Trends followed by potassium when leached from the solid as well as leaching trends of solution (pozzolanic matrix)

➤ **Geopolymeric:**

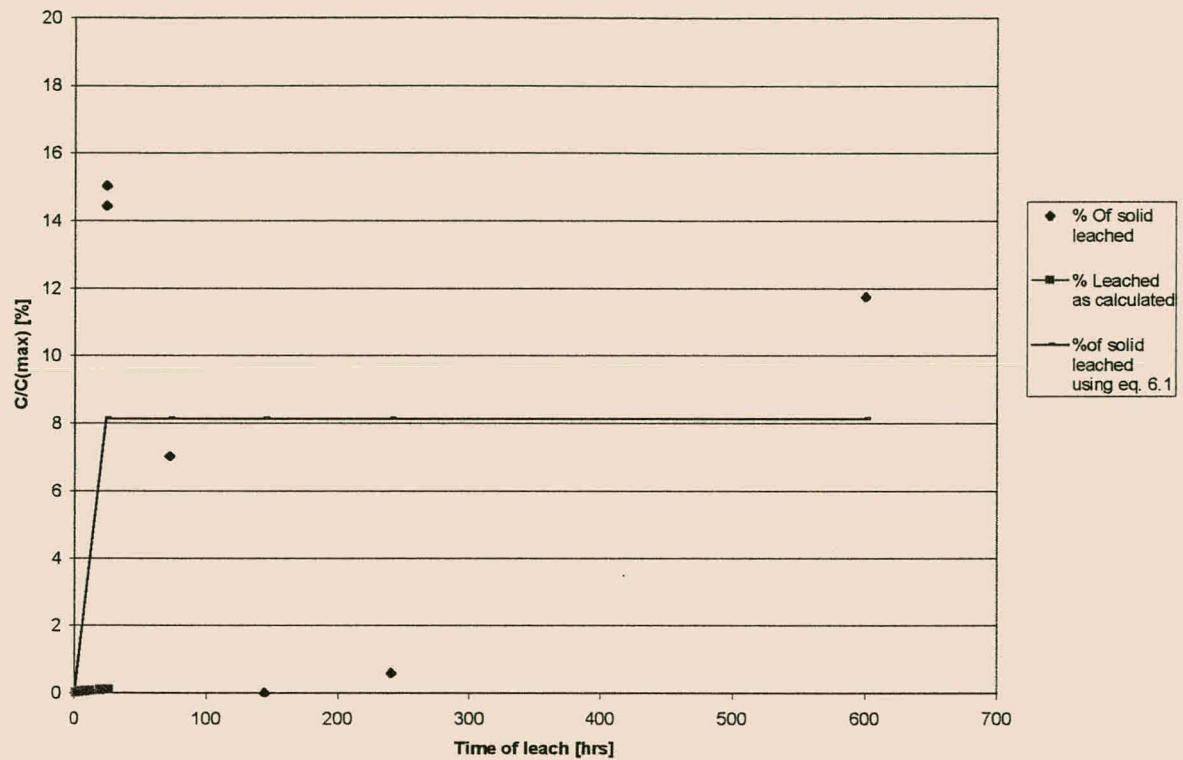


Figure B8: Trends of leaching from the solid for silica [0-600 hours] – Geopolymeric matrix

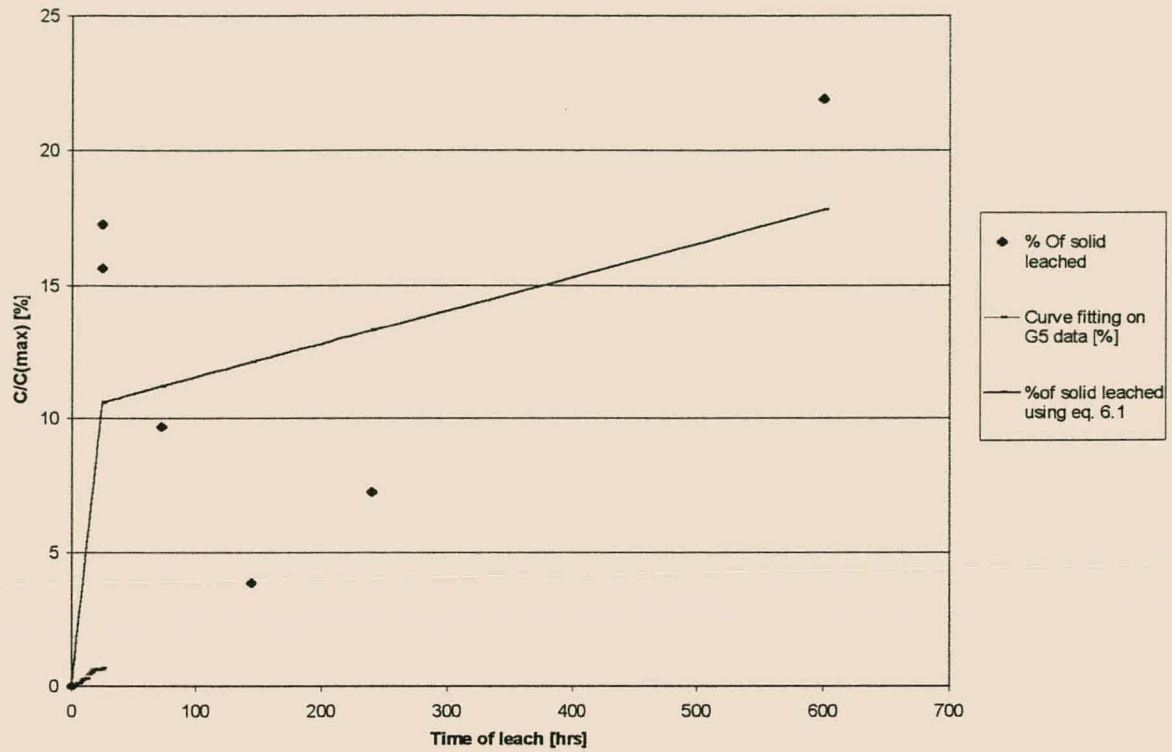


Figure B9: Trends of leaching from the solid for aluminium [0-600 hours] – Geopolymeric matrix

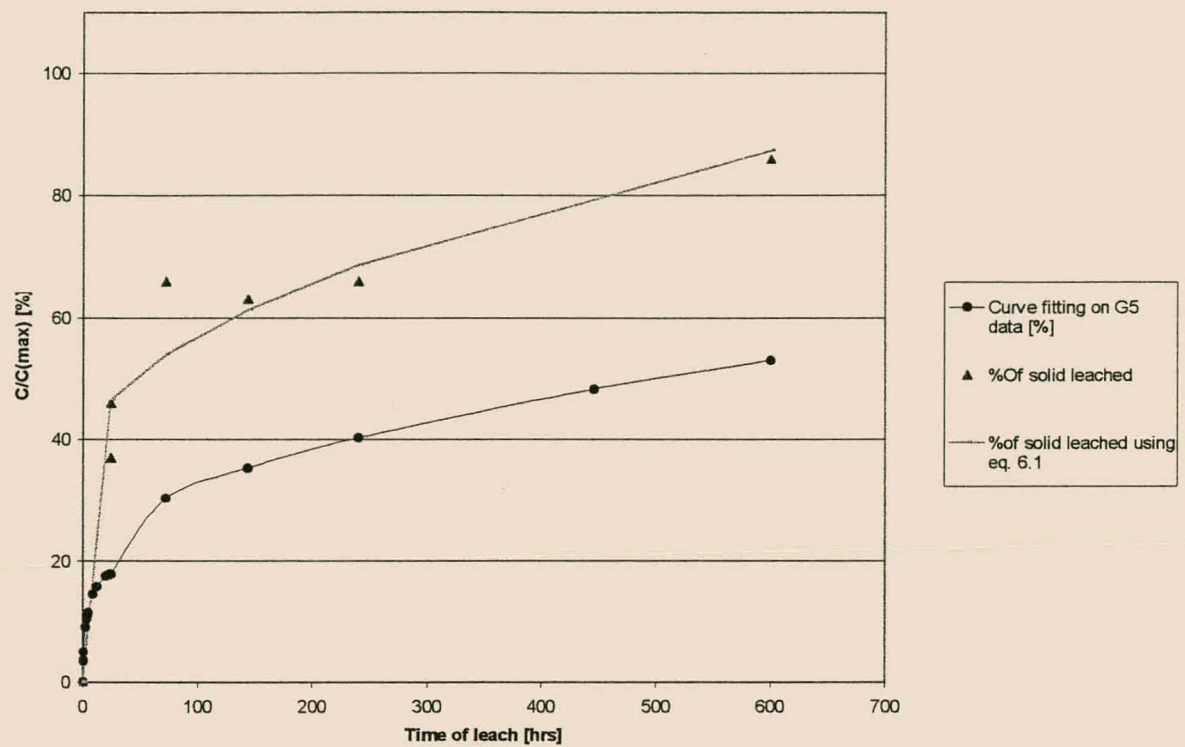


Figure B10: Trends of leaching from the solid for calcium [0-600 hours] – Geopolymeric matrix



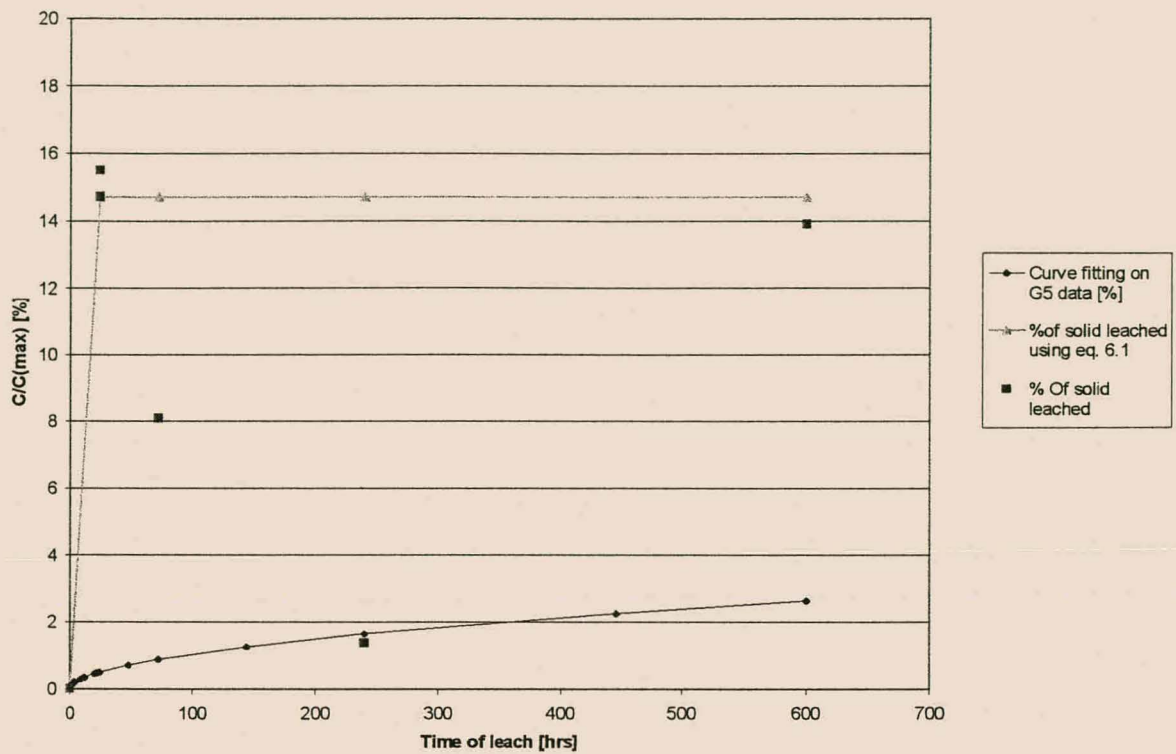


Figure B11: Trends of leaching from the solid for iron [0-600 hours] – Geopolymeric matrix

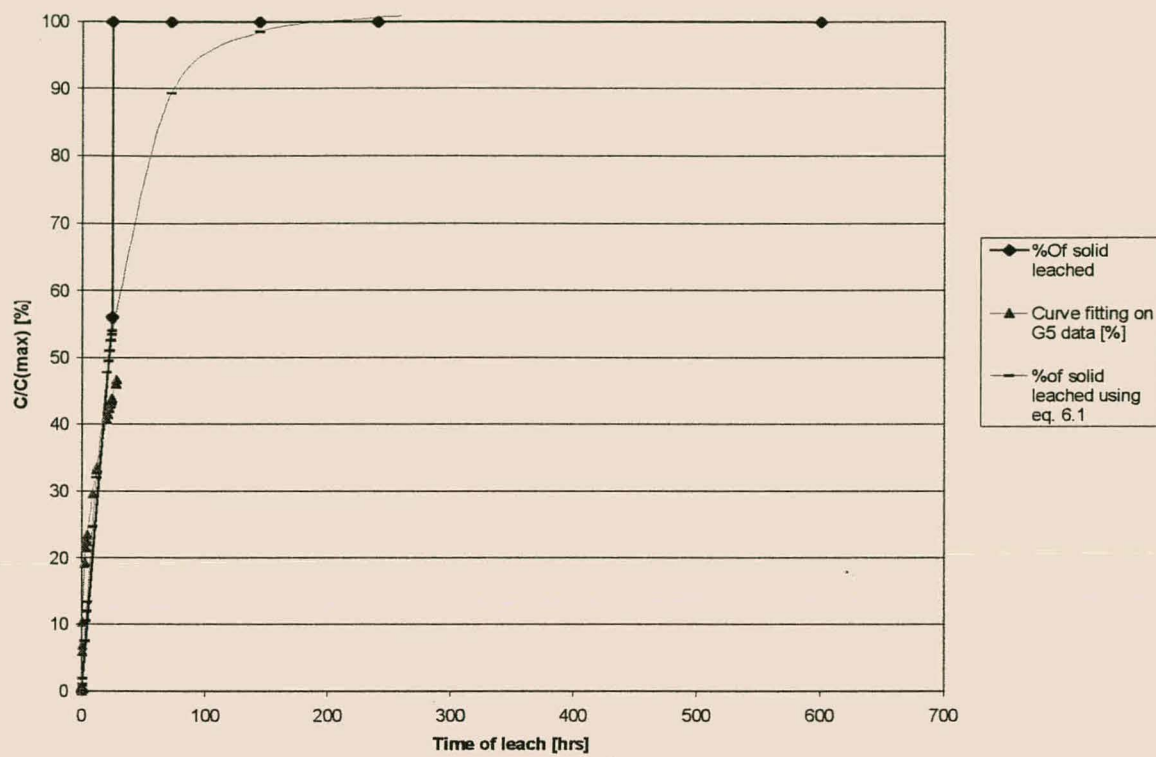


Figure B12: Trends of leaching from the solid for sodium (Na) [0-600 hours] – Geopolymeric matrix

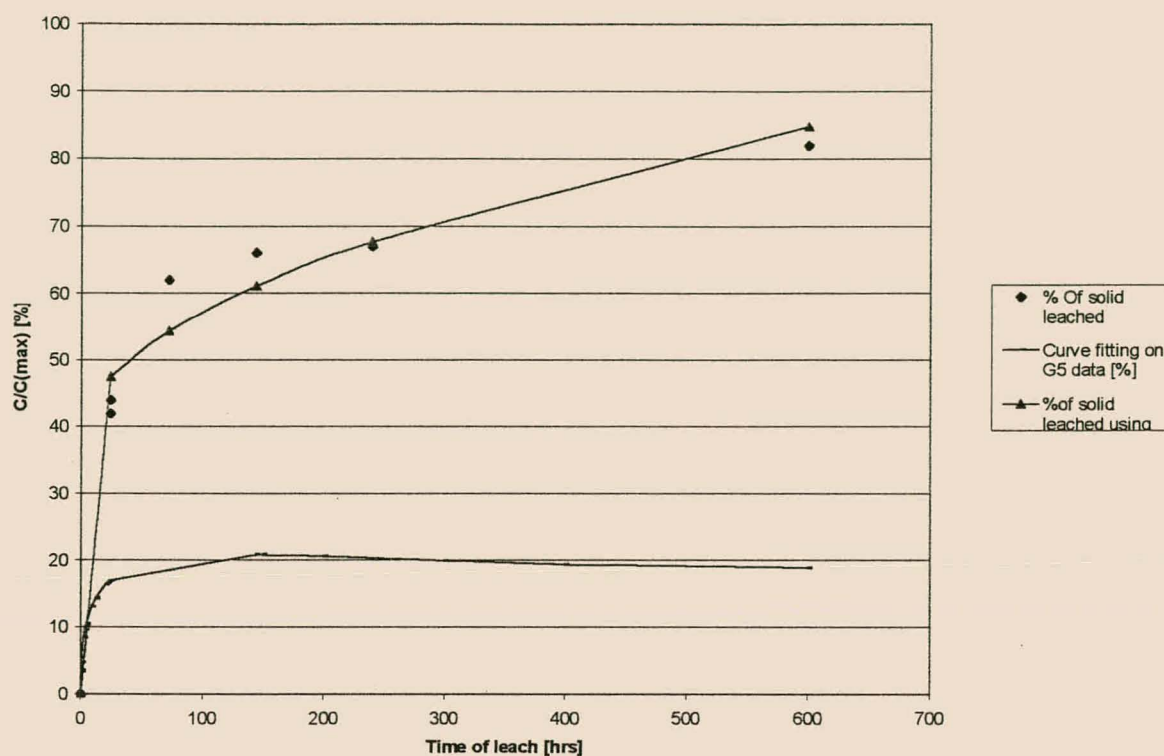


Figure B13: Trends of leaching from the solid for magnesium [0-600 hours] – Geopolymeric matrix

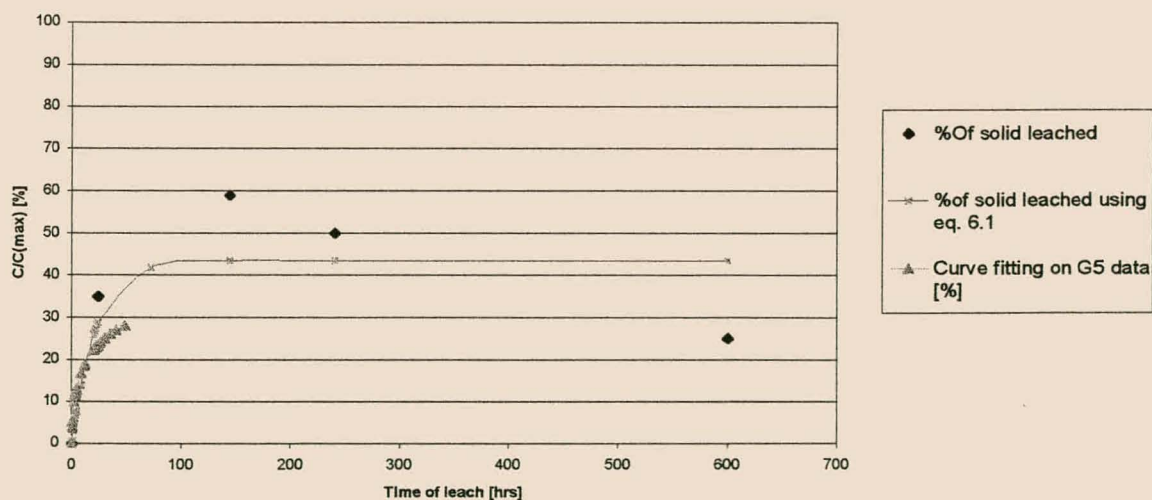


Figure B14: Trends of leaching from the solid for potassium [0-600 hours] – Geopolymeric matrix